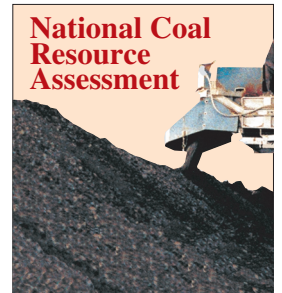


Chapter Q

Geology and Coal Resources of the Upper Cretaceous Fruitland Formation, San Juan Basin, New Mexico and Colorado

By James E. Fassett¹



[Click here to return to Disc 1
Volume Table of Contents](#)

Chapter Q of

Geologic Assessment of Coal in the Colorado Plateau: Arizona, Colorado, New Mexico, and Utah

Edited by M.A. Kirschbaum, L.N.R. Roberts, and L.R.H. Biewick

U.S. Geological Survey Professional Paper 1625–B*

¹ U.S. Geological Survey, Denver, Colorado 80225

* This report, although in the USGS Professional Paper series, is available only on CD-ROM and is not available separately

Contents

Abstract.....	Q1
Introduction	2
Purpose and Scope	2
Location and Extent of Area.....	2
Earlier Investigations	2
Geography.....	4
Drainage.....	4
Landforms	5
Access.....	5
General Geology	5
Regional Structure.....	8
Energy Minerals.....	8
Oil and Gas.....	8
Upper Cretaceous Coal.....	8
Acknowledgments.....	9
Geology of the Fruitland Formation and Related Rocks	9
Depositional History	9
Lewis Shale.....	9
Huerfanito Bentonite Bed of the Lewis Shale.....	9
History and Definition.....	9
Subsequent Developments	10
Distribution and Character	11
Pictured Cliffs Sandstone.....	12
General Discussion	12
Shoreline Trends	13
Rate of Regression	15
Fruitland Formation.....	15
Kirtland Formation	16
McDermott Member of the Animas Formation.....	16
Upper Cretaceous Chronostratigraphy of the San Juan Basin	16
Earlier Publications	16
Hunter Wash Study Area.....	16
Ash Beds	16
Ash-Bed Ages	19
Magnetic Polarity	19
Paleontology.....	19
Chimney Rock Study Area.....	24
Ash Beds	24
Age of Ash Bed CR	25

La Plata Mine Ash Bed	25
Ammonite Zonation of Lewis Shale at Chimney Rock Site	25
Magnetic Polarity	26
Summary of Chronostratigraphy	26
Ammonite Zones in Upper Lewis Shale	26
Ash-Bed Ages	27
Age of Magnetic Polarity Reversal from C33n to C32r	27
Rates of Sediment Accumulation and Pictured Cliffs Shoreline Regression	29
Rate of Subsidence of San Juan Basin Area During Pictured Cliffs Time	32
Depositional Model for Lewis/Pictured Cliffs/Fruitland System	34
This Report	34
Ayers Model	34
Basin Structure	37
Huerfanito Bentonite Bed Structure	37
Pictured Cliffs Sandstone Structure	40
Assessment of Fruitland Formation Coal Resources	40
Methodology	40
Base Map Preparation	40
Geophysical Logs	42
Distribution of Data Points	44
Core Data	46
Coal Outcrop Measurements	46
Database	46
Data Point Locations	46
Geophysical Log Data	46
Contour Map Preparation	48
Data Screening for Errors	48
Geographic Distribution of Fruitland Formation Coal	48
Net-Coal Isopach Map	48
Fruitland Coal Distribution	48
Map View	48
Coal-Bed Geometry	49
Map–Cross Section Comparison	50
Comparison with Earlier Studies	50
Basin-Wide Studies	50
Other Studies	52
Fruitland Coal-Bed Correlations—Earlier Studies	54
Surface Mapping	54
Subsurface Studies	54
Local Studies	54
Basin-Wide Studies	64
Fruitland Coal-Bed Correlations—This Report	64

Cross Section A-A'	64
Computer Correlations	65
Altered Volcanic Ash Beds as Markers	65
Fruitland Coal Character	66
Coal Quality	66
Maceral Content	67
Vitrinite Reflectance	69
Fruitland Coal Resources	72
Coal Density	72
Procedures, Categories, and Maps Used	73
Coal Tonnage	73
Strippable Coal Resources	75
Fruitland Coal Mining	77
References Cited	77
Appendix 1—ArcView Files for Coal Assessment of the San Juan Basin, New Mexico and Colorado	
[The digital files used for the coal resource assessment of the San Juan Basin assessment unit are presented as views in the ArcView project. The ArcView project and the digital files are stored on both discs of this CD-ROM set—Appendix 1 of chapter Q resides on both discs. Persons who do not have ArcView 3.1 may query the data by means of the ArcView Data Publisher on disc 1. Persons who do have ArcView 3.1 may utilize the full functionality of the software by accessing the data that reside on disc 2. An explanation of the ArcView project and data library —and how to get started using the software—is given by Biewick and Mercier (chap. D, this CD-ROM). Metadata for all digital files are also accessible through the ArcView project]	
Appendix 2—Database for Fruitland Formation Coal Assessment	
[Location, lithologic, and stratigraphic data are available in ASCII format, DBF, and Excel spreadsheets on disc 2 of this CD-ROM set]	
Appendix 3—Figures and Tables from Fassett and Hinds (1971).....	83
Appendix 4—Mean Vitrinite Reflectance Values for Fruitland Formation Coal Samples in the San Juan Basin.....	100
Appendix 5—Gravity Anomaly Map with Thermal-Maturity Overlay	116
Appendix 6—Fruitland Formation Coal Resources in Various Categories.....	117

Plate

1. List of wells and stratigraphic cross section showing the interval from the Huerfanito Bentonite Bed of the Lewis Shale to the top of the Ojo Alamo Sandstone, San Juan Basin, New Mexico and Colorado Q132

Figures

1. Index map—Colorado Plateau coal assessment areas	Q3
2. Index map of San Juan Basin area	4
3. Structural elements of San Juan Basin	6
4. Late Cretaceous stratigraphic section, San Juan Basin area	7
5. Paleogeographic map showing Western Interior Seaway in Late Cretaceous time	8
6. Map of Regina Site area—outcrop of Huerfanito Bentonite Bed	10
7. Stratigraphic column from drill hole near Huerfanito Regina site	11
8. Isopach map of interval between Huerfanito Bed and top of Pictured Cliffs Sandstone	14
9. Geologic map of Hunter Wash study area	17
10. Structural cross section in Hunter Wash area	18
11. Magnetostratigraphic column in Hunter Wash area	24
12. Magnetostratigraphic column in Chimney Rock area	25
13. Stratigraphic cross section from Hunter Wash area to Chimney Rock area	26
14. Bio-isochrone map showing Pictured Cliffs shorelines/ Western Interior ammonite zones	27
15. Uncertainty-range chart for radiometric dates from Hunter Wash and Chimney Rock areas	28
16. Chart showing interpolated ages for C33n–C32r paleomagnetic reversal in Hunter Wash area	29
17. Chronostratigraphic charts showing ash-bed ages, rock thicknesses, rates of deposition	30
18. Map showing Pictured Cliffs shorelines and ages at times dated ash beds were deposited	31
19. Paleogeographic map, Western Interior Seaway, showing San Juan Basin location	33
20. Time-sequence diagram showing mode of regression of Pictured Cliffs Sandstone shoreline	35
21. Stratigraphic cross section from Ayers and others (1994)	36
22. Contour map of Huerfanito Bentonite Bed	38
23. Structural profiles for Huerfanito Bed and top of Pictured Cliffs Sandstone across San Juan Basin	39
24. Contour map of top of Pictured Cliffs Sandstone	41
25. Density log showing the response of coal beds	43
26. Map showing ideal spacing for control points in San Juan Basin	44
27. Coal reliability categories map for San Juan Basin	45
28. Net-coal isopach map for Fruitland Formation coal beds	47
29. Comparison of three published net-coal isopach maps with net-coal map of this report	51

30. Density log of caved drill hole showing how caved areas look like coal on bulk-density log.....	53
31. Map showing locations of local subsurface studies of Fruitland coals.....	54
32. Stratigraphic cross section from Ayers and Zellers (1994) and a revised interpretation	57
33. Coal-bed correlation diagram from Ayers and Zellers (1994) and revised interpretation.....	59
34. Comparison of stratigraphic interpretations of Fruitland in Ayers and Zellers (1994) and this report.....	60
35. Fruitland coal-bed correlations near the Pine River gas seep area	62
36. Fruitland coal-bed correlations near the Durango gas seep areas.....	63
37. Vitrinite-reflectance contour map of San Juan Basin.....	68
38. Type bulk-density log showing densities for each coal bed in drill hole.....	72
39. Map of overburden thickness on top of Pictured Cliffs Sandstone (base of Fruitland Formation).....	74

Tables

1. Analytical data for $^{40}\text{Ar}/^{39}\text{Ar}$ age determinations for sanidine crystals from outcrop samples of the Huerfanito Bentonite Bed.....	Q12
2. Localities and stratigraphic positions, relative to the Huerfanito Bentonite Bed, of known <i>Didymoceras nebrascense</i> and <i>Baculites scotti</i> fossil collections in the San Juan Basin, New Mexico	13
3. List of drill holes shown on figure 9; holes on cross section H-H' (fig. 10)	18
4. Analytical data for $^{40}\text{Ar}/^{39}\text{Ar}$ age determinations for six San Juan Basin altered volcanic ash beds from the Hunter Wash area in New Mexico and the Chimney Rock area in Colorado	20
5. Summary table of estimated coal resources in beds 1.2 ft thick or greater, Fruitland Formation, San Juan Basin, Colorado and New Mexico	75
6. Coal production from Fruitland Formation strip coal mines in the San Juan Basin.....	76

Geology and Coal Resources of the Upper Cretaceous Fruitland Formation, San Juan Basin, New Mexico and Colorado

By James E. Fassett

Abstract

The coal-bearing Fruitland Formation of Upper Cretaceous age is in the San Juan Basin of southwest Colorado and northwest New Mexico. The Fruitland crops out around the periphery of the basin and is a little more than 4,000 ft deep in several areas in the northeast part. The basin is an asymmetric structural feature that formed in early Tertiary time; the area of the basin within the Fruitland outcrop is about 6,500 mi². The basin contains more than 14,000 ft of Cambrian through Holocene sedimentary rock, about 6,000 ft of which are Late Cretaceous in age. Upper Cretaceous rocks consist of a series of intertonguing marine and nonmarine strata deposited on the west side of the epicontinental Western Interior Seaway in Cenomanian through Campanian time. These strata were deposited as the shoreline of the seaway transgressed and regressed several times across the basin area. The final regression of the shoreline occurred in late Campanian time (76–73 Ma), resulting in deposition of the Pictured Cliffs Sandstone and associated rocks. Fruitland Formation coal beds were deposited in backshore swamps on top of Pictured Cliffs Sandstone shoreface deposits. The Kirtland Formation (revised name in this report) and the McDermott Member of the Animas Formation overlie the Fruitland and are the stratigraphically highest Upper Cretaceous rocks in the basin. The Tertiary Ojo Alamo Sandstone and upper part of the Animas Formation unconformably overlie Cretaceous strata across the basin; the hiatus at this contact is > 8 m.y. The youngest Tertiary rocks in the basin are Eocene in age.

Fruitland Formation coal resources assessed in this study total 230 billion short tons. Coal beds are typically concentrated in the lowermost 200 ft of the Fruitland, and they are usually thickest at the base of the coal-bearing interval. Coal beds are generally not continuous for more than a few miles; however, in some areas coal zones are continuous for tens of miles. Coal beds range from paper thin to more than 50 ft thick. Fruitland net-coal thicknesses range from 1.2 ft to more than 90 ft (1.2 ft is the minimum coal thickness for coal-resource calculations in this report). The net-coal distribution pattern is marked by a thick coal band that trends northwest

across the north-central part of the basin and is southwest of a large vertical buildup of the Pictured Cliffs Sandstone. Net-coal values in this band range from 40 to more than 90 ft thick. Thicker coal beds in this area reflect peat swamps that occupied the same area for a sustained period of time as the position of the Pictured Cliffs Sandstone shoreline stabilized and backshore peat deposits built up vertically in tandem with the vertical buildup of the adjacent Pictured Cliffs shoreface sands. Northeast and southwest of this thick coal band are areas of relatively thin net coal. A large area of less than 20 ft of net coal occupies the southwest part of the basin. A small, northwest-trending band of net coal more than 40 ft thick is present in the southwest part of the basin, just downdip from the Fruitland outcrop. Two areas containing no Fruitland coal are present on the eastern edge of the basin. A northeast-trending pattern of relatively narrow and linear thinner net-coal bands cut across the thick northwest-trending thick coal area. These thinner coal bands probably represent fluvial channel systems that cut through the backshore peat swamps to the sea. In cross section, Fruitland coal beds occur in an overlapping, en echelon pattern rising stratigraphically to the northeast; coal beds in the southwest part of the basin are more than 2.5 m.y. older than in the northeast part of the basin.

Fruitland coal is low sulfur (average less than 1 percent) and high ash (averaging about 30 percent). Moisture content is variable, ranging from 5 to 10 percent at shallow depths near the outcrop to less than 3 percent in the deeper parts of the basin. Heating values range from 10,300 Btu (moist mineral-matter-free (mmmf)) along the southwest margin of the basin to nearly 16,000 Btu in the north-central part of the basin. Fixed-carbon percentages (mmmf) range from about 40 percent in the southwest to more than 80 percent in the north-central area. Coal rank ranges from subbituminous A in the south to low-volatile bituminous in the north-central part of the basin. Coal rank generally increases from the southwest edge of the basin to slightly north of the present basin axis and then diminishes northward to the edge of the basin. Fruitland coal is almost all non-agglomerating.

The San Juan Basin is the second largest gas field in North America. Most of the early gas production came from

Upper Cretaceous, fractured shoreface-sandstone reservoirs. In the 1970's, coal-bed methane was found to be present in Fruitland Formation coal beds in commercial quantities. Thousands of Fruitland coal-bed methane wells have been drilled throughout the basin, and yearly gas production from Fruitland coal beds now exceeds gas production from all of the sandstone reservoirs combined (about one trillion ft³ of gas in 1999). Although this report is focused on the Fruitland coal resources, the basic data contained herein should contribute to a better understanding of coal-bed methane in the basin as well.

Bulk-density geophysical logs from oil and gas drill holes were the principal source of data for assessing Fruitland coal resources. Utilizing GIS software, locations of wells used for control points were precisely measured based on reported distances from section lines. (The public land survey system (PLSS) for the San Juan Basin containing township, range, and section boundaries was provided by the Bureau of Land Management in digital form.) Latitude and longitude coordinates for the spotted control points were determined by the GIS program. Maps showing net-coal thicknesses, structure, and overburden thicknesses were generated by a two-dimensional modeling program. Coal tonnages by State, county, township, overburden category, thickness range, and surface and coal ownership were calculated using the same program.

Introduction

Purpose and Scope

The geologic characterization of the Fruitland Formation and the assessment of Fruitland Formation coal resources in the San Juan Basin, New Mexico and Colorado, is part of the U.S. Geological Survey's (USGS) National Coal Resource Assessment Project initiated in 1994. Five major coal-producing regions of the United States are included in the National Coal Assessment: (1) the Appalachian Basin, (2) the Illinois Basin, (3) the Gulf of Mexico Coastal Plain, (4) the Powder River Basin and the Northern Great Plains, and (5) the Colorado Plateau. The San Juan Basin is in the Colorado Plateau region (fig. 1).

The purpose of this report is to illustrate and describe the occurrence of coal in the Fruitland Formation in the San Juan Basin and to assess the total coal resources of the Fruitland. Coal resources were measured and calculated in accordance with standard USGS methods and procedures as specified in Wood and others (1983), except as noted. In addition, the geologic history of the deposition, burial, and subsequent structural deformation of the coal-bearing Fruitland Formation and associated strata is presented. Coal-thickness measurements are mostly based on geophysical log interpretations; a relatively few direct coal-thickness measurements are from drill core descriptions. No outcrop measurements of coal were used

as data points for coal resource calculations. The geologic characterization of the Fruitland is based on direct examination on the outcrop and geophysical-log interpretations in the subsurface.

Published reports relating to the geology and coal resources of the Fruitland Formation are reviewed and discussed. Where there are differences in interpretation between previously published material and the data presented in this report, the differences are described to allow the reader to properly evaluate conflicting interpretations.

Location and Extent of Area

The San Juan Basin is located in what is called the Four Corners area near the common corners of the States of New Mexico, Colorado, Utah, and Arizona (fig. 2). In this report, the basin is defined as the area lying within the outcrop of the base of the Fruitland Formation (top of the Pictured Cliffs Sandstone) as portrayed on figure 2. The basin outline has an elliptical shape and is about 100 mi long (north-south) and about 90 mi wide (east-west). The basin extends over an area of about 6,500 mi².

The basin includes parts of San Juan, Rio Arriba, Sandoval, and McKinley Counties in New Mexico and La Plata and Archuleta Counties in Colorado. Parts of the Navajo, Ute Mountain Ute, Southern Ute, and Jicarilla Apache Indian Reservations are within the basin area (fig. 2). Several developed archaeological sites are present in the San Juan Basin. The two primary sites are Chaco Canyon National Historical Park in New Mexico and Mesa Verde National Park in Colorado (fig. 2). A smaller archaeological site, Aztec National Monument, is located in the northwest part of the basin, in the town of Aztec, N. Mex. The Chimney Rock Archaeological Area is located just north of the Chimney Rock mine (fig. 2) within the San Juan National Forest; the Salmon Ruins site is just west of Bloomfield, N. Mex. Large numbers of smaller, undeveloped archaeological sites dot the basin area, including large numbers of unexcavated sites on the river terraces along the La Plata River valley north of Farmington, N. Mex. The Bisti-De-na-zin Wilderness Area is located in the southwest part of the basin.

Earlier Investigations

The first detailed, basin-wide study of the coal resources of the Fruitland Formation was by Fassett and Hinds (1971). Prior to that report, a large number of publications, principally USGS reports and maps, described the occurrence of Fruitland coal in various parts of the basin; a complete list of those publications is in the Fassett and Hinds (1971) report. A report by the New Mexico Bureau of Mines and Mineral Resources by Shoemaker and others (1971) contained a series of papers on strippable Fruitland coal (maximum depth of 250 ft) in six areas on the western margin of the basin. Papers by Kelso

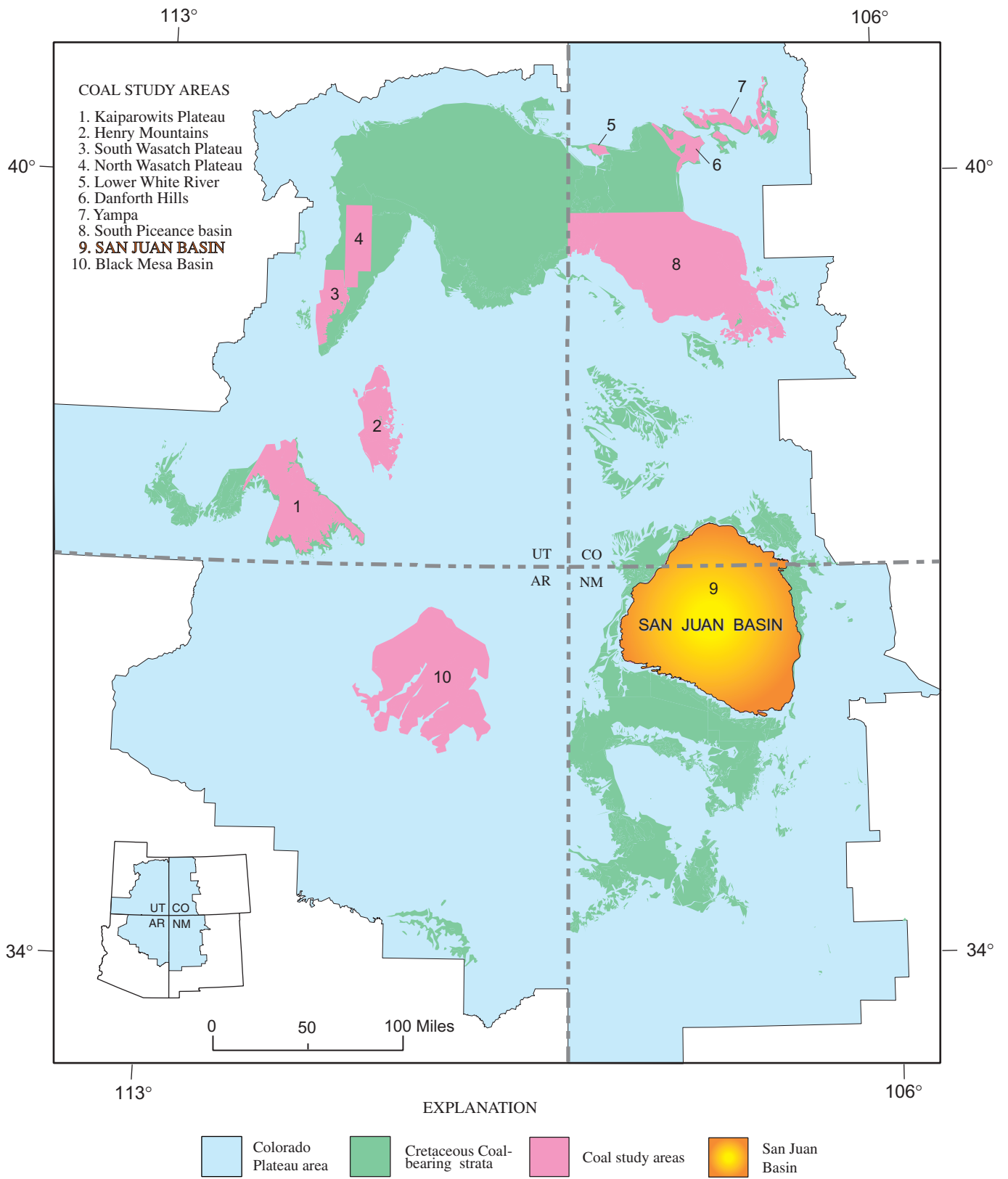


Figure 1. Index map showing the occurrences of Upper Cretaceous coal-bearing rocks and coal study areas in the Colorado Plateau region of the Western United States.

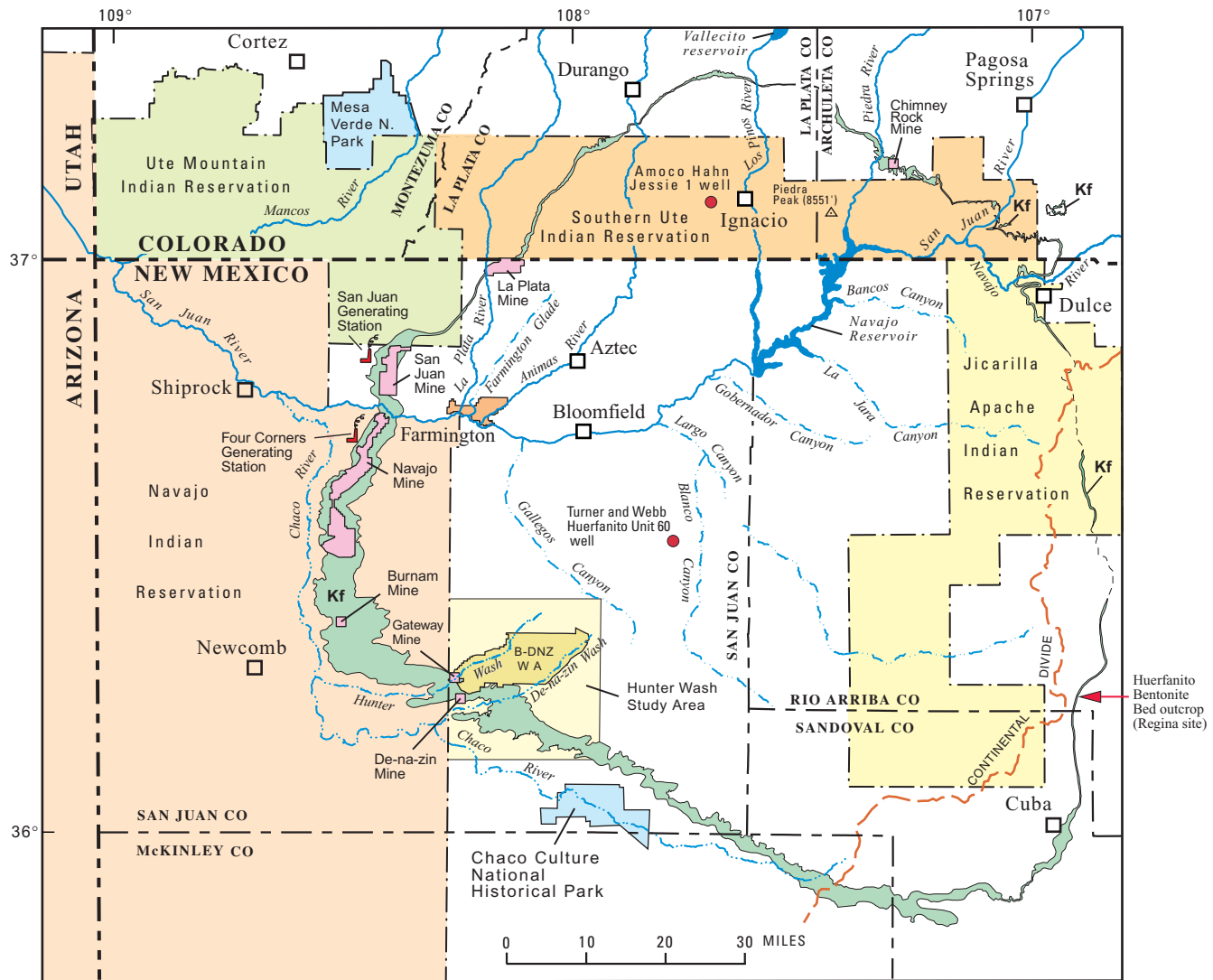


Figure 2. Index map of the San Juan Basin area; the basin is defined in this report as the area inside the outcrop of the Fruitland Formation (Kf). Fruitland outcrop is modified from Fassett and Hinds (1971). Indian Reservation boundaries are from USGS base maps for New Mexico and Colorado. Map does not show scattered tracts of Indian lands outside of reservation boundaries and non-Indian lands within some of the reservation boundaries. The mines shown are all Fruitland coal strip mines. Tonnages of coal produced from these mines are in table 6. B-DNZ WA is Bisti-De-na-zin Wilderness Area.

and others (1980), Kelso and Wicks (1988), Kelso and others (1987), Ayers and Ambrose (1990), and Ayers and others (1994) presented revised estimates of Fruitland coal resources in order to estimate Fruitland coal-bed methane resources in the basin. Papers by Biewick and others (1991) and Boger and Medlin (1991) calculated Fruitland coal resources for the New Mexico part of the basin using different computer-contouring models. Local studies of Fruitland coal were by Shoemaker and Holt (1973), Jentgen and Fassett (1977), Beach and Jentgen (1978), Wilson and Jentgen (1980), Kelso and Rushworth (1982), Sandberg (1986, 1988a, 1988b, 1990), Decker and others (1988), Roberts (1989, 1991), Roberts and Uptegrove (1991), Ambrose and Ayers (1994), Ayers and Zellers (1994), M’Gonigle and Roberts (1997), and Fassett and others

(1997b). Studies of coal quality for strippable Fruitland coals in New Mexico were by Hoffman (1991) and Hoffman and others (1993). Nickelson (1988) published a historical account of coal mining in the New Mexico part of the San Juan Basin that includes all known Fruitland coal mines.

Geography

Drainage

The northeast-trending Continental Divide cuts across the southeast part of the San Juan Basin (fig. 2). Streams west of

the Divide are in the San Juan River drainage, streams east of the Divide are in the Rio Grande drainage. The San Juan River is the master stream in the basin area. Perennial streams flow into the San Juan River from the north and originate in the La Plata or San Juan Mountains in Colorado. These streams are the Animas, La Plata, Mancos, Los Pinos (Pine), Piedra, and Navajo Rivers. The San Juan River flows northwestward into the Colorado River in Utah. The principal intermittent streams draining the basin's arid interior to the south are Chaco River and Largo Canyon. Navajo Reservoir occupies parts of the valleys of the San Juan, Los Pinos, and Piedra Rivers in the northeast quadrant of the basin. Water from Navajo Reservoir is used for irrigation of large tracts of Navajo land south of the towns of Farmington and Bloomfield (Navajo Indian Irrigation Project). Vallecito Reservoir is on the Los Pinos River on the north edge of the basin area.

Landforms

The San Juan Basin is in the Navajo physiographic section of the Colorado Plateau province (U.S. Geological Survey, 1946). The topographic relief in the basin is more than 3,500 ft. Altitudes range from 8,551 ft on Piedra Peak west of the Piedra River in Colorado (fig. 2) to about 5,050 ft on the west side where the San Juan River crosses the basin rim in New Mexico. The most prominent physiographic feature in the area is the relatively steeply dipping monocline (fig. 3), which rims the basin on the northwest, north, and east sides and rises as much as 700 ft above the adjoining terrain on the west side of the basin. The central part of the basin is a dissected plateau, the surface of which slopes gently to the west. The principal streams have cut into the plateau to form deep, steep-walled canyons. On the upland plains between the canyons, stabilized sand dunes are numerous. Along the San Juan, Animas, and La Plata Rivers several stream-terrace levels can be distinguished.

The climate in much of the San Juan Basin is arid to semiarid. Rainfall ranges from as low as 3 or 4 inches a year at lower altitudes to nearly 20 inches a year at higher altitudes, and the annual average is less than 15 inches. Precipitation is generally rare in early and middle summer and is more frequent in late summer and spring. Temperatures range from below 0°F in the winter to above 100°F in the summer. The mean annual temperature at Farmington, N. Mex., is 52.6°F, and the annual range is about 115°F. The daily variation in temperature often exceeds 40°F.

At lower altitudes, short grass, sagebrush, and many varieties of cactus are common. The higher mesas of the basin generally support a growth of pinyon and juniper, scattered sagebrush, and sparse scrub oak. Ponderosa pine grows on the highest areas, mostly around the north and east rims of the basin. Cottonwood trees, tamarisk, and willows grow in the valleys of many of the streams.

Access

Two major U.S. Highways cross the San Juan Basin: U.S. 550, from northwest to southeast, passes through Durango, Colo., and Aztec, Bloomfield, and Cuba, N. Mex.; U.S. 64, from west to east, passes through Shiprock, Farmington, Bloomfield, and Dulce, New Mexico. Several other paved New Mexico highways traverse the basin area and a myriad of unpaved oil-and-gas-well access roads and county roads furnish entry to almost every part of the basin.

General Geology

The San Juan Basin is an asymmetric structural depression that contains Cambrian, Devonian, Mississippian, Pennsylvanian, Permian, Triassic, Jurassic, Upper Cretaceous, Tertiary, and Quaternary rocks. The maximum known thickness of sedimentary rocks in the basin was penetrated by the Amoco Production Company Hahn Jessie 1 well in the SW $\frac{1}{4}$ sec. 15, T. 33 N., R. 8 W., La Plata County, Colorado (fig. 2). This well was drilled to a total depth of 14,503 ft and penetrated Precambrian rocks at 14,288 ft.

The coal-bearing Upper Cretaceous rocks of the basin are shown in a stratigraphic cross section on figure 4. The maximum thickness of Upper Cretaceous rocks in the basin is about 6,000 ft. Upper Cretaceous strata consist of intertonguing marine and nonmarine units that represent four transgressive-regressive episodes: (1) the Dakota Sandstone–Gallup Sandstone cycle, (2) the Borrego Pass Sandstone Lentil–Dalton Sandstone Member subcycle, (3) the Hosta Tongue–upper Point Lookout Sandstone cycle, and (4) the Cliff House Sandstone–Pictured Cliffs Sandstone cycle. The final regression of the sea resulted in deposition of the shoreface Pictured Cliffs Sandstone. All of the regressive shoreface sandstones are overlain by coal-bearing intervals (fig. 4), but the thickest and most continuous coal beds in the basin are in the Fruitland Formation directly overlying the regressive Pictured Cliffs Sandstone.

The Upper Cretaceous rocks preserved in the San Juan Basin were deposited on the western edge of the Western Interior Seaway (fig. 5) more or less continuously over a time span of about 22 m.y., from 95 Ma to 73 Ma. The one significant break in Late Cretaceous deposition occurred at the end of the Turonian when an episode of localized tectonic uplift occurred in the north-central part of the present basin area (fig. 4). This episode of erosion, and (or) nondeposition represents a hiatus of about 1 m.y. and was mostly a sub-sea event (Dyman and others, 1994, fig. 9). Following this late Turonian event, subsidence of the basin area resumed uniformly through most of the rest of Late Cretaceous time.

Tertiary rocks of the basin consist of the Paleocene Ojo Alamo Sandstone (as described by Fassett, 1987, Fassett and Steiner, 1997, and Fassett and others, 2000), part of the Animas

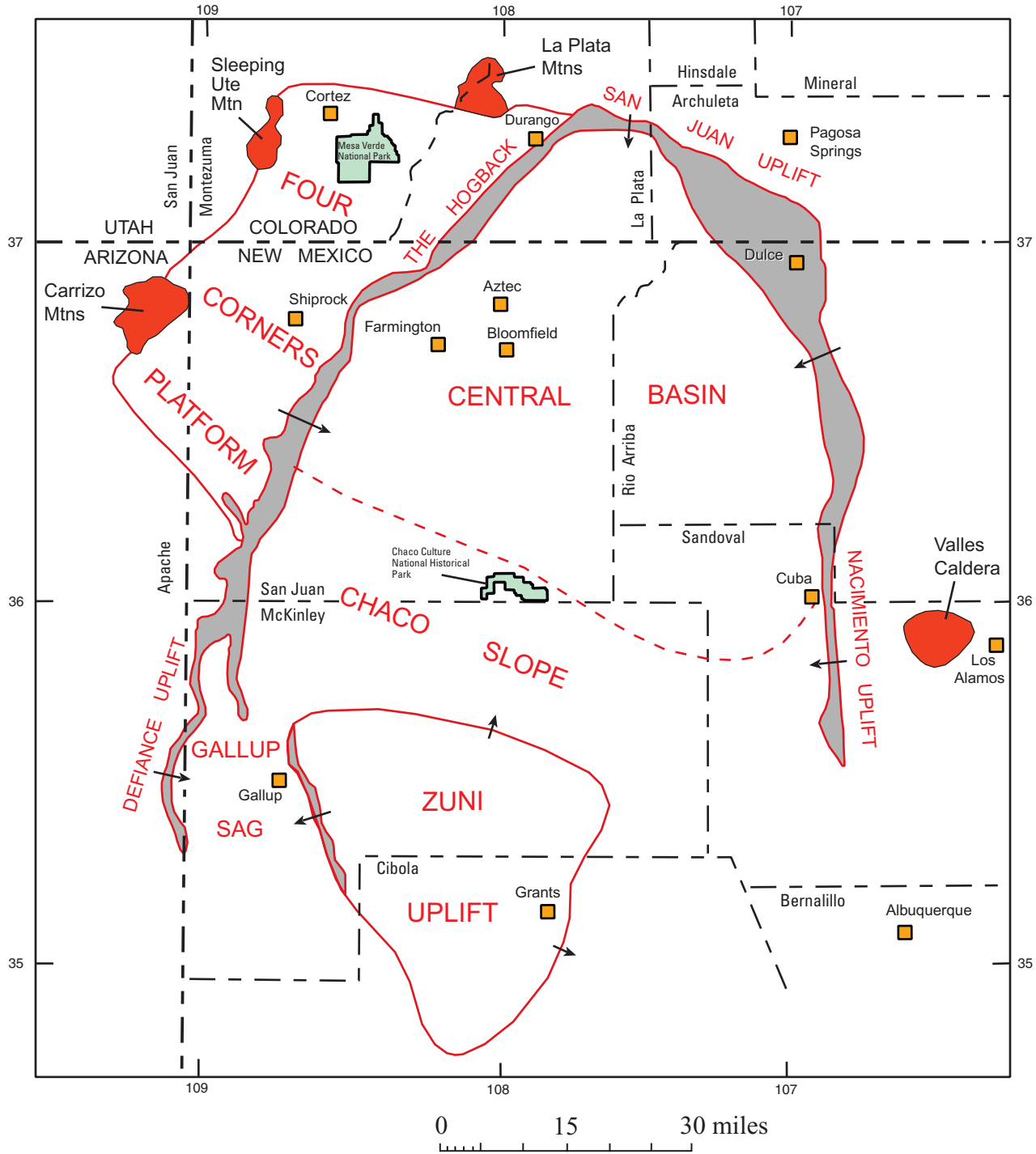


Figure 3. Structural elements of the San Juan Basin. Structural features are generalized from a structure map of the basin area by Thaden and Zech (1984). Areas of steeper dip are shaded; arrows indicate the direction of dip. The dashed line separating the central basin from the Chaco slope is drawn approximately along the outcrop of the base of the Fruitland Formation (top of the Pictured Cliffs Sandstone). Modified from Fassett (1991).

Formation, and the Nacimiento Formation; the Eocene San Jose Formation; and intrusive rocks of possible Oligocene age. Quaternary deposits consist of Pleistocene and Holocene terrace gravels and alluvium. The hiatus at the unconformity between

the Cretaceous Kirtland Formation and Tertiary Ojo Alamo Sandstone in the southern part of the basin represents about 8 m.y. (Fassett and Steiner, 1997). The missing 8 m.y. is from the latest Cretaceous (Maastrichtian Stage) and earliest Paleocene.

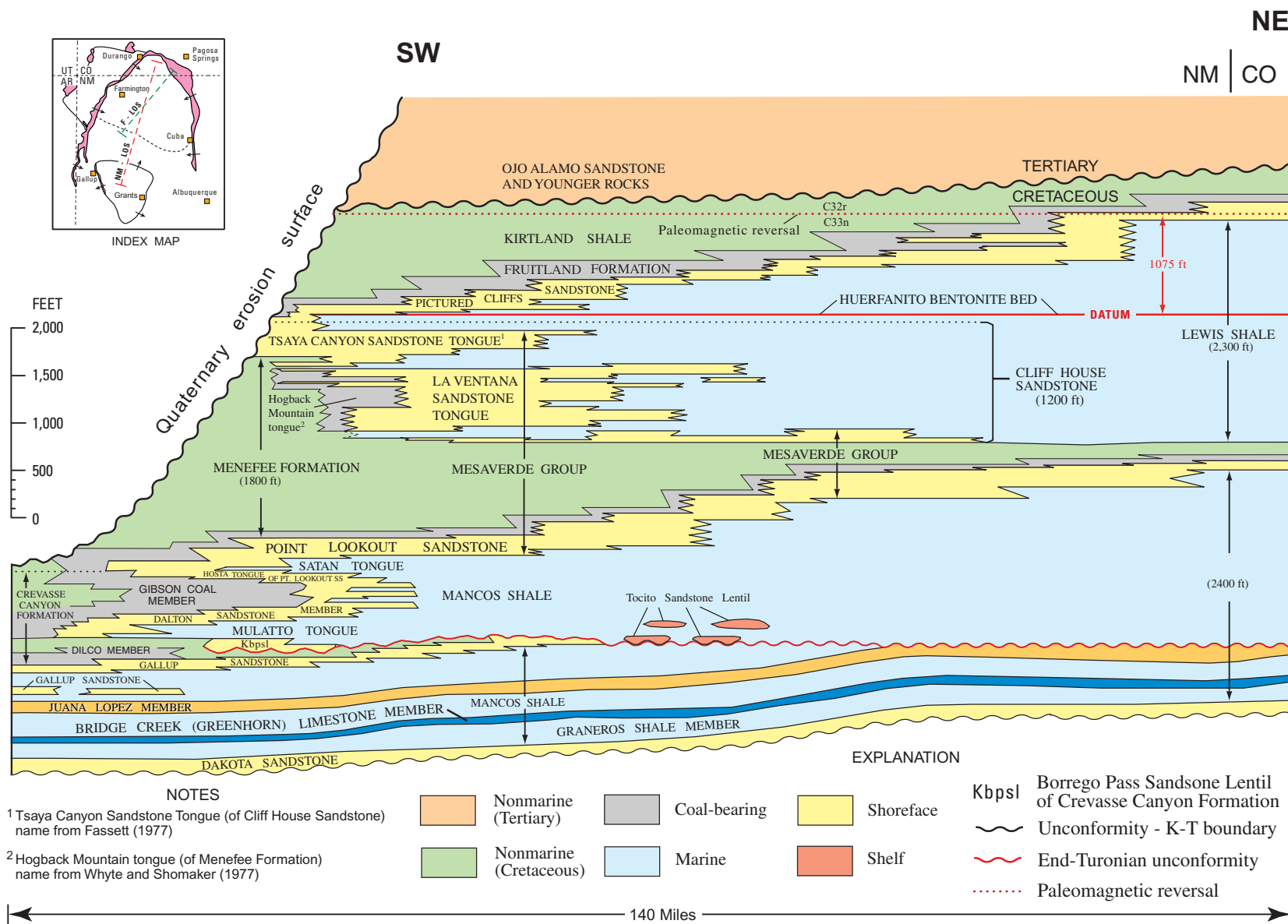


Figure 4. Stratigraphic section showing Upper Cretaceous rocks in the San Juan Basin, New Mexico and Colorado. Tocito Sandstone Lenticil and coal-bearing zones are shown diagrammatically. Stratigraphy of rock units from the Point Lookout Sandstone upward is modified from Fassett (1977), stratigraphy for lower part of section is modified from Nummedal and Molenaar (1995). F - LOS on index map is Fassett (1977) line of cross section; NM - LOS is Nummedal and Molenaar (1995) line of cross section. Position of paleomagnetic reversal from chron C33n to C32r is from Fassett and Steiner (1997). Vertical exaggeration x 55.

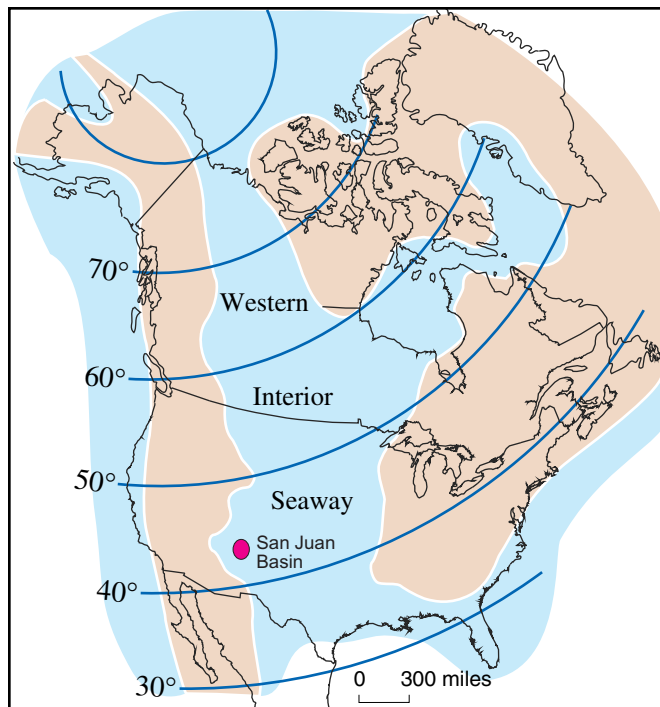


Figure 5. Paleogeographic map of North America in Late Cretaceous (Turonian) time. From Roberts and Kirschbaum (1995, fig. 1) after Williams and Stelk (1975, fig. 5). Approximate location of San Juan Basin is shown.

Regional Structure

The structural elements of the San Juan Basin are portrayed on figure 3. The most prominent feature shown is the horseshoe-shaped, steeply dipping monocline that extends around the west, north, and east sides of the basin. The Zuni uplift to the southwest partially defines the southern limits of the structural basin, but there is no structural feature defining the limit of the basin in the southeast. The Carrizo Mountains, Sleeping Ute Mountain, and La Plata Mountains are laccoliths that punctuate the boundary of the Four Corners platform in the northwest. The central basin structural feature depicted on figure 3 is very nearly the same area shown enclosed by the Fruitland Formation outcrop shown on figure 2. The central basin of figure 3 began to form in early, but not earliest, Paleocene time and continued to downwarp through Eocene time (Fassett, 1985). Precursors of the formation of the basin proper were the intrusions of the Four Corners laccoliths (listed above) which began to form in latest Cretaceous time (Semken and McIntosh, 1997). These authors (p. 77, table 1) presented $^{40}\text{Ar}/^{39}\text{Ar}$ ages ranging from 73.8 Ma to 70.65 Ma for rock samples collected in the Carrizo Mountains.

Energy Minerals

Oil and Gas

The San Juan Basin is the second largest gas-producing basin in the conterminous United States, second in total estimated gas reserves to the Hugoton field of Texas, Oklahoma, and Kansas. The basin has more than 19,000 producing oil and gas wells and through the end of 1997 had produced nearly 20 trillion ft^3 of gas (TCF) and more than 300 million barrels of oil (Oil and gas statistical information for Colorado was provided by Debbie Baldwin of the Colorado Oil and Gas Conservation Commission; for New Mexico by Ernie Busch of the New Mexico Energy Division). Historically, the basin has produced most of its natural gas from fractured sandstone reservoirs in the Dakota Sandstone, Mesaverde Group, and the Pictured Cliffs Sandstone (fig. 4) in the central basin area (fig. 3). Starting in the late 1970's, an increasing amount of gas production has come from Fruitland Formation coal beds, and annual Fruitland coal-gas production (about 1 TCF in 1999) now exceeds gas production from sandstone reservoirs. Most of the oil production in the basin has come from the Tocoito Sandstone Lentil of the Mancos Shale and from fractured Mancos Shale reservoirs (fig. 4). Relatively small amounts of oil and gas have been produced from Paleozoic reservoirs, mostly from structural traps on the Four Corners platform (fig. 3).

Estimates of ultimate gas production from the San Juan Basin prior to the discovery of coal-bed methane in the basin were on the order of 25 TCF. A report by Kelso and Wicks (1988) estimates that Fruitland coal beds in the basin contain nearly 50 TCF of gas in place. If half of this gas is recoverable, the total cumulative production of gas from the San Juan Basin could exceed 50 TCF (25 TCF from sandstone reservoirs and 25 TCF from Fruitland coals). The principal references for the oil and gas fields of the San Juan Basin are Fassett (1978, 1983, 1991).

Upper Cretaceous Coal

All of the coal resources in the San Juan Basin are in Upper Cretaceous rocks, and these coal-bearing strata are shown on figure 4. In the early 1900's, coal from these formations was mined from underground coal mines. Coal from the Crevasse Canyon Formation and the lower part of the Menefee Formation was extensively mined in the vicinity of Gallup, N. Mex.; Hogback Mountain Tongue coals were mined in the La Ventana area a few miles south of Cuba, N. Mex.; and lower Menefee and Fruitland coals were mined in the northwest part of the basin (fig. 4). These old underground coal mines in New Mexico (now all abandoned) are discussed in detail by Nickelson (1988). All of the underground coal mines in the Colorado part of the basin produced from Fruitland or Menefee coals, and only one Menefee mine is still operating.

Beginning in the late 1960's and early 1970's several large strip mines were opened to produce coal for electrical power generation from the Crevasse Canyon, Menefee, and Fruitland Formations. A discussion of the coal production from these large strip mines is in Fassett (1989); production from Fruitland strip mines is in table 6 of this report. The Fruitland Formation contains the bulk of the coal resources in the San Juan Basin, 230 billion short tons, as determined by this study. A detailed tabulation of Fruitland coal resources is in the "Fruitland Coal Resources" section of this report. Coal resources for all of the older Upper Cretaceous coal-bearing units have not yet been compiled. A study of Menefee Formation coals in the southern San Juan Basin by Whyte and Shoemaker (1977) found that the lower Menefee coal zone contained about 1 billion short tons of coal between the depths of 250 and 4,000 ft and the Hogback Mountain Tongue of the Menefee (fig 4) contained about 11.3 billion short tons of coal to depths in excess of 2,000 ft.

Acknowledgments

This report has benefited from the input of numerous colleagues within and outside the USGS. Robert Hettinger of the USGS, Denver, Colo., provided sound, practical advice regarding the intricacies of geophysical-log interpretations of coal-bearing and associated rocks throughout the 5-year life of this project, and I have benefited greatly from conversations with him regarding the basic geologic parameters that control the deposition of coal-bearing rocks throughout the Western Interior of North America. Vito Nuccio critically reviewed the section of this report related to Fruitland coal petrography and thermal maturity and provided decompaction ratios for the rocks discussed in this report using the BasinMod program. Bradford Boyce and Tom Ann Casey, geologic consultants, Durango, Colo., contributed greatly to my knowledge of Fruitland Formation coals as coal-bed methane reservoirs and source rocks. Joe Hewitt in the Farmington, N. Mex., U.S. Bureau of Land Management office supplied me with copies of geophysical well logs and was a constant source of accurate information regarding problems of well locations, elevations, or designations. Gretchen Hoffman with the New Mexico Bureau of Mines and Mineral Resources, Socorro, N. Mex., provided invaluable information regarding Fruitland Formation coal resources and coal-mine production. Laura Biewick, USGS, and Tracy Mercier, contractor to the USGS, Denver, were my tutors in the use of the ArcView software program that was an integral part of the compilation of the database for this study. Laura Roberts, USGS, Denver, prepared all of the initial contour maps for this report using the EarthVision software program and taught me how to do geologic edits of those initial maps in that program. She also prepared all of the coal-tonnage tables for the Fruitland coal resources in the San Juan Basin using EarthVision. William Everham, USGS student aid, helped obtain copies of geophysical logs that were the backbone of the database for this study

and did much of the early drill-hole-location spotting of these holes in the ArcView program. Marvin Millgate, USGS volunteer, provided invaluable assistance in helping to determine the depths of coal beds on bulk-density logs. This report was improved by the careful, detailed reviews of USGS colleagues Steve Condon, Laura Biewick, and Tom Judkins. Most of the chronostratigraphic data in this report were obtained as the result of a U.S. Geological Survey Gilbert Fellowship (awarded in 1988) to study the precise ages of the rocks adjacent to the Cretaceous-Tertiary boundary in the San Juan Basin.

Geology of the Fruitland Formation and Related Rocks

Depositional History

The history of deposition of the Fruitland Formation is closely associated with the depositional history of subjacent stratigraphic units, principally the Pictured Cliffs Sandstone, the Lewis Shale, and the Huerfanito Bentonite Bed of the Lewis Shale (fig. 4).

Lewis Shale

The Lewis Shale is the stratigraphically highest unit of marine shale in the San Juan Basin (fig. 4). It is a light-to dark-gray and black shale that contains interbeds of light-brown sandstone and siltstone, thin-bedded sandy to silty limestone layers, calcareous concretions, and bentonite beds. The Lewis ranges in thickness from 0 ft in the southwestern part of the basin to about 2,400 ft in the northeastern part (fig. 4).

Huerfanito Bentonite Bed of the Lewis Shale

History and Definition

The Huerfanito Bentonite Bed is an altered volcanic ash that was deposited in the Lewis sea at a time shortly after the Cliff House Sandstone shoreline had reached its maximum southwestward transgression and the Pictured Cliffs Sandstone regression had just begun (fig. 4). This bed is in the upper part of the Upper Cretaceous (Campanian) Lewis Shale, and it exhibits unique characteristics on geophysical logs. The Huerfanito was named by Fassett and Hinds (1971, p. 6) for a type well, the Turner and Webb Huerfanito Unit 60-4 well that was completed in November 1960. This well is in the SW $\frac{1}{4}$ SW $\frac{1}{4}$ sec. 4, T. 26 N., R. 9 W., San Juan County, New Mexico (fig. 2). The geophysical log from this well is shown in Fassett and Hinds (1971, fig. 2), and typical logs showing log responses to the Huerfanito are shown in figure 3 of

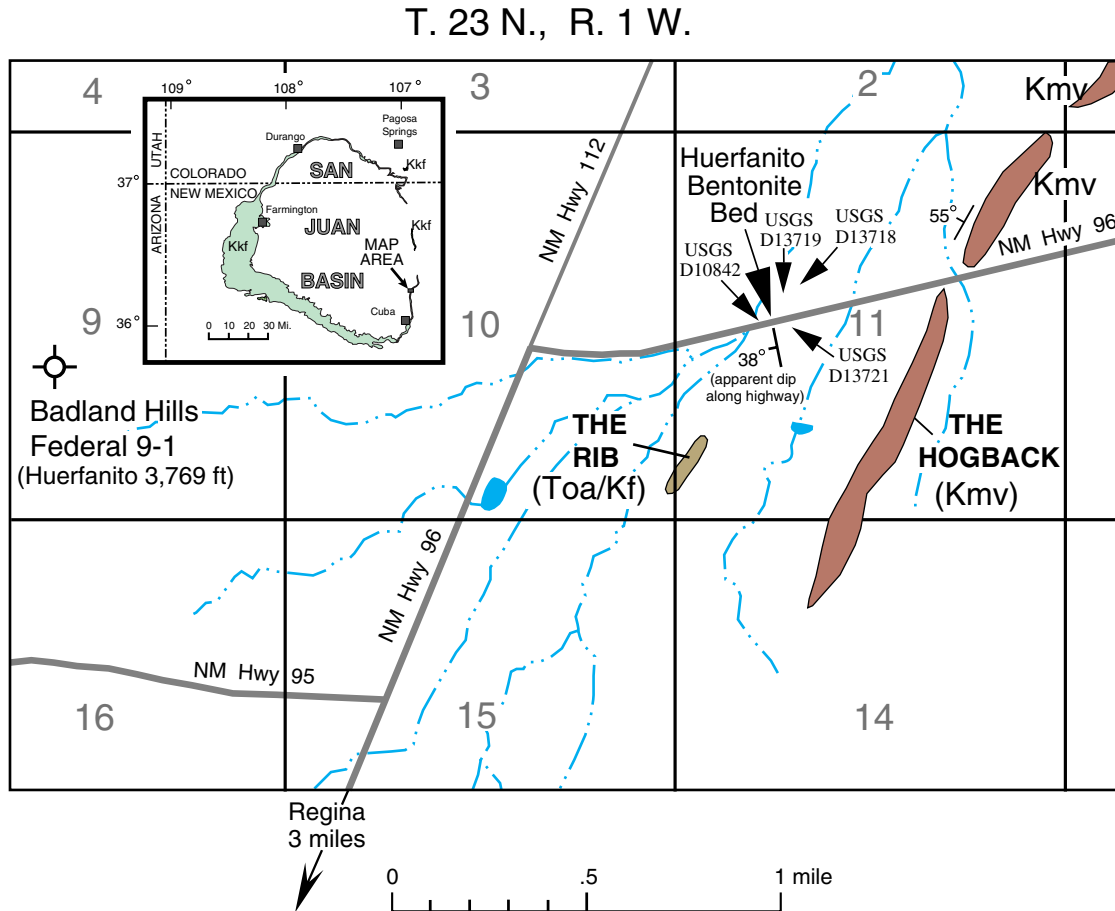


Figure 6. Map showing locations of the Huerfanito Bentonite Bed outcrop, USGS fossil collection sites, and the Federal 9-1 drill hole. The Hogback monocline is held up by Mesaverde Group (Kmv) rocks, the Rib is composed of the Ojo Alamo Sandstone (Toa) and the Fruitland Formation (Kf). There is no Pictured Cliffs Sandstone at this locality; the Fruitland Formation directly overlies the Lewis Shale. A stratigraphic column of Upper Cretaceous and lowermost Tertiary rocks penetrated in the Federal 9-1 well is shown on figure 7. Table 1 contains analytical data for single-crystal, $^{40}\text{Ar}/^{39}\text{Ar}$ age determinations for sanidine crystals from samples of the Huerfanito Bed collected at this locality. Table 2 lists the stratigraphic levels (above and below the Huerfanito) of all collections of *Didymoceras nebrascense* and *Baculites scotti* at this and other fossil-collection sites in the San Juan Basin. This figure is modified from figure 1 of Fassett and others (1997).

that report. Plate 1 of this report is a northeast-trending stratigraphic cross section of the uppermost part of the Upper Cretaceous section in the San Juan Basin from the Huerfanito Bed upward. This cross section uses the Huerfanito as a datum and contains geophysical log traces for 20 wells, evenly spaced across the basin. The Huerfanito 60-4 well is well number 9 on plate 1.

At the time the Huerfanito Bed was defined, it was strictly a subsurface unit, not known to crop out anywhere in the basin, and it had never been cored in any of the thousands of oil and gas wells that had been drilled through it. Consequently, no sample of the bed had ever been obtained to confirm its lithology or to possibly obtain a radiometric age for the bed. Because of its widespread occurrence throughout the subsurface of the San Juan Basin, it was assumed that the bed had originated as a large volcanic ash fall and thus was an isochro-

nous rock unit. This marker bed has subsequently been widely used in numerous publications as a time-stratigraphic datum on geophysical-log cross sections that portray the stratigraphy of Upper Cretaceous rocks in the San Juan Basin.

Subsequent Developments

Fassett and others (1997a) reported the presence of the Huerfanito Bed at a road cut in the Lewis Shale on the southeast edge of the San Juan Basin, about 16 mi north of Cuba, N. Mex. (figs. 2, 6), at a locality named the Regina site. (The Huerfanito had been discovered at this outcrop by USGS geologists, C.M. Molenaar and W.A. Cobban in 1992.) Identification of the Huerfanito Bed at this place was based on its position in the Lewis Shale as projected from the well log of the Badland Hills Federal 9-1 drill hole located 1.9 mi west

of the Regina-site road cut (figs. 6, 7). The Huerfanito was difficult to measure and describe at this outcrop because it is replaced, for the most part, by calcium carbonate in the form of large, lens-shaped limestone concretions that are locally much thicker than the original ash-bed thickness. As best as could be determined, however, the Huerfanito is about 9 inches thick here. This measured thickness is far less than the 12-ft thickness that was estimated by Fassett and Hinds (1971) on geophysical logs. In a discussion of the thickness of the Huerfanito Bed in Fassett and others (1997a, p. 232) the authors concluded that the Fassett and Hinds thickness of 12 ft is not correct and state, "The Huerfanito may well be thicker than 9 in. in the subsurface of the San Juan Basin, but its maximum thickness there is probably no greater than ... 1.5 to 2 ft."

Samples of the Huerfanito Bed were collected at the Regina site, and sanidine crystals separated from it were analyzed by J.D. Obradovich using single-crystal ⁴⁰Ar/³⁹Ar procedures. The analysis yielded a radiometric age of 75.76 ± 0.34 Ma (table 1).

This age is virtually identical to the projected age of the Huerfanito Bentonite Bed (75.83 Ma) estimated by extrapolation from a dated ash bed 95 ft above the Huerfanito Bed in the vicinity of Hunter Wash (figs. 2, 9) in the southwest part of the basin (reported in Fassett and Steiner, 1997, and discussed in more detail in the "Summary of Chronostratigraphy" section of this report. This close match provides independent evidence that the ash bed identified at the Regina site in the southeast part of the San Juan Basin is indeed the Huerfanito Bed.

Subsequent to the discovery of the Huerfanito Bed on the outcrop, ammonite fossils were found at the Regina site above and below the ash bed. This work placed the Huerfanito within a relatively thin biostratigraphic interval very near the boundary between the *Baculites scotti* and the *Didymoceras nebrascense* Western Interior Ammonite Zones (table 2). The best estimate is that the Huerfanito is within and near the top of the *B. scotti* zone (fig. 7 and table 2).

Distribution and Character

Although the Huerfanito Bentonite Bed is present throughout the San Juan Basin, it seems to lose its distinctive character on geophysical logs in some areas. In addition, it has been known for some time that the Huerfanito changes character across the basin area from southwest to northeast (Fassett and Hinds, 1971, p. 7, 8 and fig. 3). One explanation for these changes is that the Huerfanito was diluted by fine-grained clastic material carried across the Lewis sea shelf by sub-sea currents in parts of the basin. It is interesting to note that the Huerfanito is the most pristine and distinctive on conductivity and sonic logs in the southwest part of the basin on what would have been the shallowest part of the shelf (fig. 4 and plate 1), whereas farther offshore, in the northeast part of the basin where water depths were presumably the greatest, the log signature of the Huerfanito is the most blurred on geophysical logs due to dilution by clastic material. This could indicate relatively stronger sub-sea currents moving through

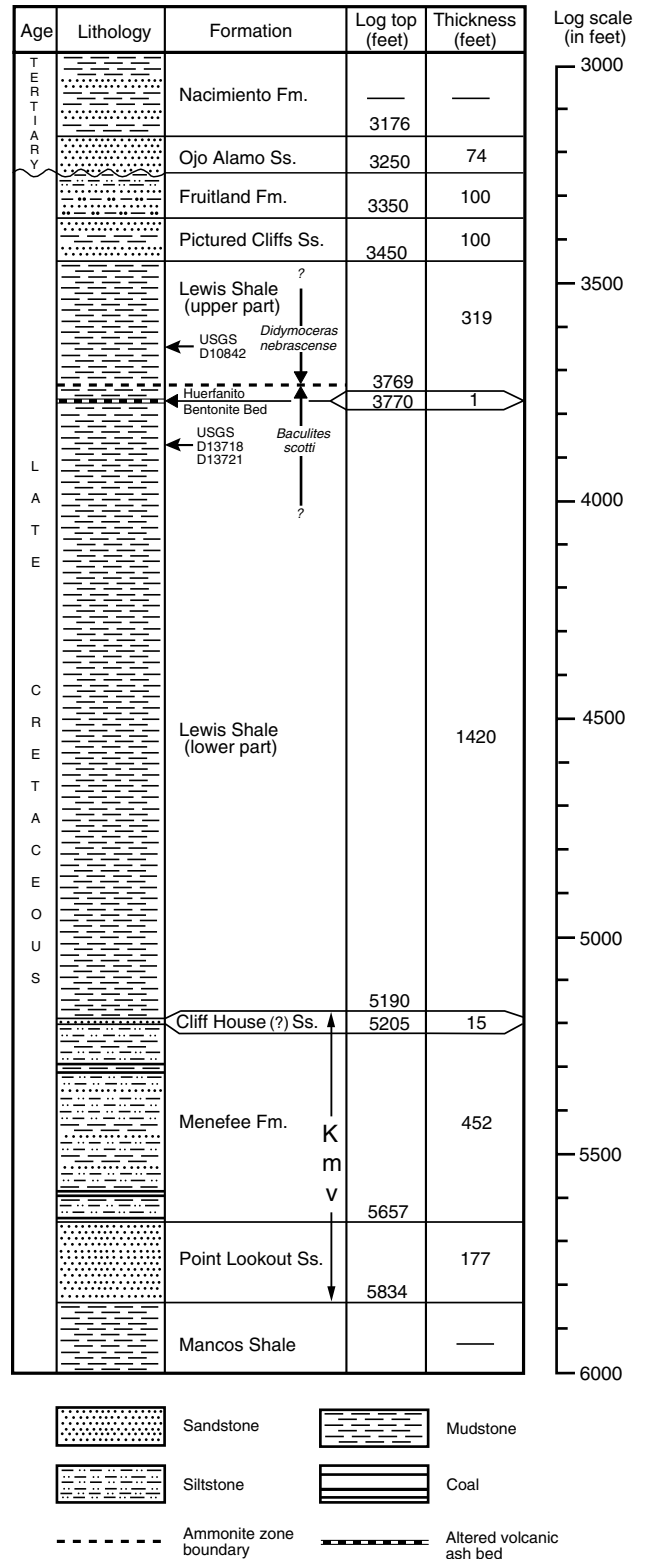


Figure 7. Stratigraphic column showing Upper Cretaceous (Campanian) rocks in the Badland Hills Federal 9-1 drill hole (location on figure 6). Kmv is Mesaverde Group. Projected levels of USGS fossil collections from vicinity of Huerfanito outcrop site (fig. 6) are shown. Huerfanito Bed is in uppermost part of *Baculites scotti* ammonite zone. Figure is modified from figure 2 of Fassett and others (1997).

the deeper part of the shelf area. It is counterintuitive that this ash bed is preserved at all because the evidence for constant, continuous, even distribution of sediment across the entire shelf area during most of Late Cretaceous time is overwhelming, yet the Huerfanito is a distinct and clearly identifiable rock unit on geophysical logs throughout much of the basin—even near the base of the Pictured Cliffs Sandstone in the southwest part of the basin. On well 3 on plate 1 (the Tanner Unit 1), for example, the response of the conductivity curve to the Huerfanito is particularly distinctive where it is only 30 ft below the base of the Pictured Cliffs and thus was probably deposited relatively close to the beach environment. There is no easy explanation of how this ash fall was preserved in what would normally be thought of as a relatively high energy environment where even minor storm activity should have quickly dispersed and destroyed this deposit.

Roberts and McCabe (1992) briefly discussed the Huerfanito and stated “We interpret this ‘bed’ (which is up to 4 m thick), as a condensed interval, which may be a composite of several ash layers...” Observations of the Huerfanito at the Regina outcrop (fig. 6) where it is less than a foot thick do not support this interpretation. The Huerfanito there appears to be single, 9-inch-thick bed of altered volcanic ash deposited by one volcanic eruption. Roberts and McCabe were clearly using the 12-ft thickness for the Huerfanito (“4 m thick”) given in Fassett and Hinds (1971) as part of the basis for their interpretation that the Huerfanito represents a “condensed interval.” Because the Huerfanito had not been observed on the outcrop at the time their report was published, their interpretation could only be based on geophysical-log interpretation, which, in terms of the thickness of the Huerfanito, has proven to be misleading.

Pictured Cliffs Sandstone

General Discussion

The Pictured Cliffs Sandstone is a shoreface sandstone deposited during the final regression of the Western Interior Seaway from the San Juan Basin area (fig. 4 and plate 1). Plate 1 shows that the Pictured Cliffs is at the level of the Huerfanito Bed at well 1 in the southwest part of the basin whereas the top of the Pictured Cliffs is about 1,200 ft above the Huerfanito in well 20 on the northeast edge of the basin. The Pictured Cliffs is time transgressive and is considerably younger in the northeast than in the southwest part of the basin. The stratigraphic rise of the Pictured Cliffs occurs in a series of steps, a pattern typical of nearly all Upper Cretaceous regressive shoreface sandstone beds in the Western Interior of North America. This step-like rise in regressive sandstones was first described and discussed in detail in a paper by Pike (1947) in his classic outcrop study of the Point Lookout Sandstone on the west side of the San Juan Basin.

The geometry of the Point Lookout and the Pictured Cliffs Sandstones, as shown on figure 4, is very similar (except

Table 1. Analytical data for ⁴⁰Ar/³⁹Ar age determinations for sanidine crystals from outcrop samples of the Huerfanito Bentonite Bed collected by C.M. Molenaar in 1992 and recollected by Fassett in 1997 at the Regina site (fig. 6).

[From Fassett and others, 1997a. xtl, crystal; ⁴⁰Ar*, radiogenic argon]

Ash bed name and J value	Irradiation number	Mineral analysis	Run number	⁴⁰ Ar/ ³⁹ Ar	³⁷ Ar/ ³⁹ Ar	³⁶ Ar/ ³⁹ Ar	K/Ca	% ⁴⁰ Ar*	⁴⁰ Ar*/ ³⁹ ArK	Age (Ma)	Error (1 sigma)
Huerfanito Bed	JD021-4	Sanidine	95Z0514	5.94189	0.006248	0.000045	78.42	99.63	5.92029	75.74	0.25
J=0.007243		single xtl	95Z0515	5.95008	0.006189	0.000129	79.17	99.22	5.90369	75.54	0.28
			95Z0516	5.99998	0.006300	0.000216	77.78	98.79	5.92790	75.84	0.32
			96Z0517	5.97914	0.005509	0.000055	88.94	99.58	5.95435	76.17	0.29
			95Z0518	5.93312	0.006025	0.000081	81.33	99.45	5.90085	75.50	0.26
Unweighted mean and error of the mean at the 95 percent confidence level including the error in J											

Ca and K corrections and decay constants:

$$\begin{aligned}
 ({}^{36}\text{Ar}/{}^{37}\text{Ar})_{\text{Ca}} &= 2.69 \pm 0.24 \times 10^{-4} \\
 ({}^{39}\text{Ar}/{}^{37}\text{Ar})_{\text{Ca}} &= 6.79 + 0.051 \times 10^{-4} \\
 ({}^{40}\text{Ar}/{}^{39}\text{Ar})_{\text{K}} &= 9.1 \pm 5.4 \times 10^{-3} \\
 \lambda_{\text{e}} + \lambda_{\text{g}} &= 0.581 \times 10^{-10} \text{ yr}^{-1} \\
 \lambda_{\text{g}} &= 4.962 \times 10^{-10} \text{ yr}^{-1} \\
 {}^{40}\text{K}/\text{K} &= 1.167 \times 10^{-4} \text{ atom/atom}
 \end{aligned}$$

Table 2. Localities and stratigraphic positions, relative to the Huerfanito Bentonite Bed, of known *Didymoceras nebrascense* and *Baculites scotti* fossil collections in the San Juan Basin, New Mexico

[Numbers in bold from the Regina site. Adapted from table 2 of Fassett (1987); from Fassett and others, (1997a)]

Western Interior ammonite zone	U.S. Geological Survey fossil locality number	Distance above (+) or below (-) Huerfanito Bentonite Bed (ft)
<i>Didymoceras nebrascense</i>	D4834 ¹	+400
	D4797 ²	+260
	D10842³	+121
<i>Baculites scotti</i>	D4796 ²	-50
	D13718³	-105
	D13721³	-105

¹ Llaves locality (Cobban and others, 1974; Fassett, 1987).

² Barker Dome locality (Cobban, 1973; Fassett, 1987).

³ **Regina locality (this report).**

for the minor transgressive pulse in the Pictured Cliffs seen at well 11 of plate 1). The stratigraphic rise of the Point Lookout is about 800 ft over the same distance as the Pictured Cliffs regression shown on plate 1, compared to 1,300 ft for the Pictured Cliffs, indicating that the rate of sediment accumulation was greater during the Point Lookout regression. Rates of deposition are discussed in more detail in the "Summary of Chronostratigraphy" section of this report. The apparent differences in the geometry of the Pictured Cliffs as shown on figure 4 and plate 1 are the result of more drill holes being used for plate 1 and because plate 1 has half the vertical exaggeration of figure 4.

The contact of the base of the Pictured Cliffs with the underlying Lewis Shale is drawn as a series of steps with sharp bases on plate 1, but in reality the basal contact of the Pictured Cliffs, and indeed most Western Interior regressive sandstone units, is transitional. These sandstone bodies typically consist of massive sandstone beds at the top grading downward into thinner bedded and finer grained sandstones and siltstones and ultimately into marine shales. Picking the basal contact of a unit such as the Pictured Cliffs is extremely subjective and somewhat arbitrary because of the transitional nature of this contact.

The top of the Pictured Cliffs at its interface with the Fruitland Formation, on the other hand, is almost always a sharp, distinct contact that is easily seen on geophysical logs. This contact is typically between the top of a massive sandstone and the base of an overlying coal bed (plate 1). These lithologies have distinct geophysical-log characteristics. The only difficulty in locating the top of the Pictured Cliffs on geophysical logs is in distinguishing beach sandstones from fluvial-distributary and estuarine deposits in those places where tongues of Pictured Cliffs sandstone extend into the

Fruitland Formation. Because the interpretation of these tongues is quite subjective on logs, plate 1 was constructed in a conservative manner to show them extending a minimum distance into the Fruitland Formation. A tongue of Pictured Cliffs about 150 ft thick is shown extending into the Fruitland at well 16 on plate 1; a thinner Pictured Cliffs tongue is shown in the Fruitland in wells 18 and 19. The geometry of the Pictured Cliffs profile on plate 1 is a product of the dynamics of the interplay between the rate of subsidence and sedimentation accumulation rate (discussed below).

Shoreline Trends

Streams carrying sediment to the Pictured Cliffs Sandstone shoreline were flowing from southwest to northeast (Fassett and Hinds, 1971). The shoreline configuration varied in its detail during the time of this regression but generally maintained a northwesterly trend. Fassett and Hinds (1971) suggested that isopach lines depicting the interval between the Huerfanito Bentonite Bed and the top of the Pictured Cliffs Sandstone should represent a close approximation of Pictured Cliffs shoreline trends (figure 7 of that report). They cautioned, however, that isopach lines would represent shoreline trends only if there had been no significant local tectonism from the time the Huerfanito Bed was laid down until the time the Pictured Cliffs was deposited across the basin area. Figure 8 of this report is an improved isopach map of the interval from the Huerfanito to the top of the Pictured Cliffs, and it is suggested that the isopach lines, except in one area in the northwest part of the basin, probably closely approximate successive shoreline configurations for the Pictured Cliffs during late Campanian time.

The 100-ft isopach line on figure 8 trends northwest

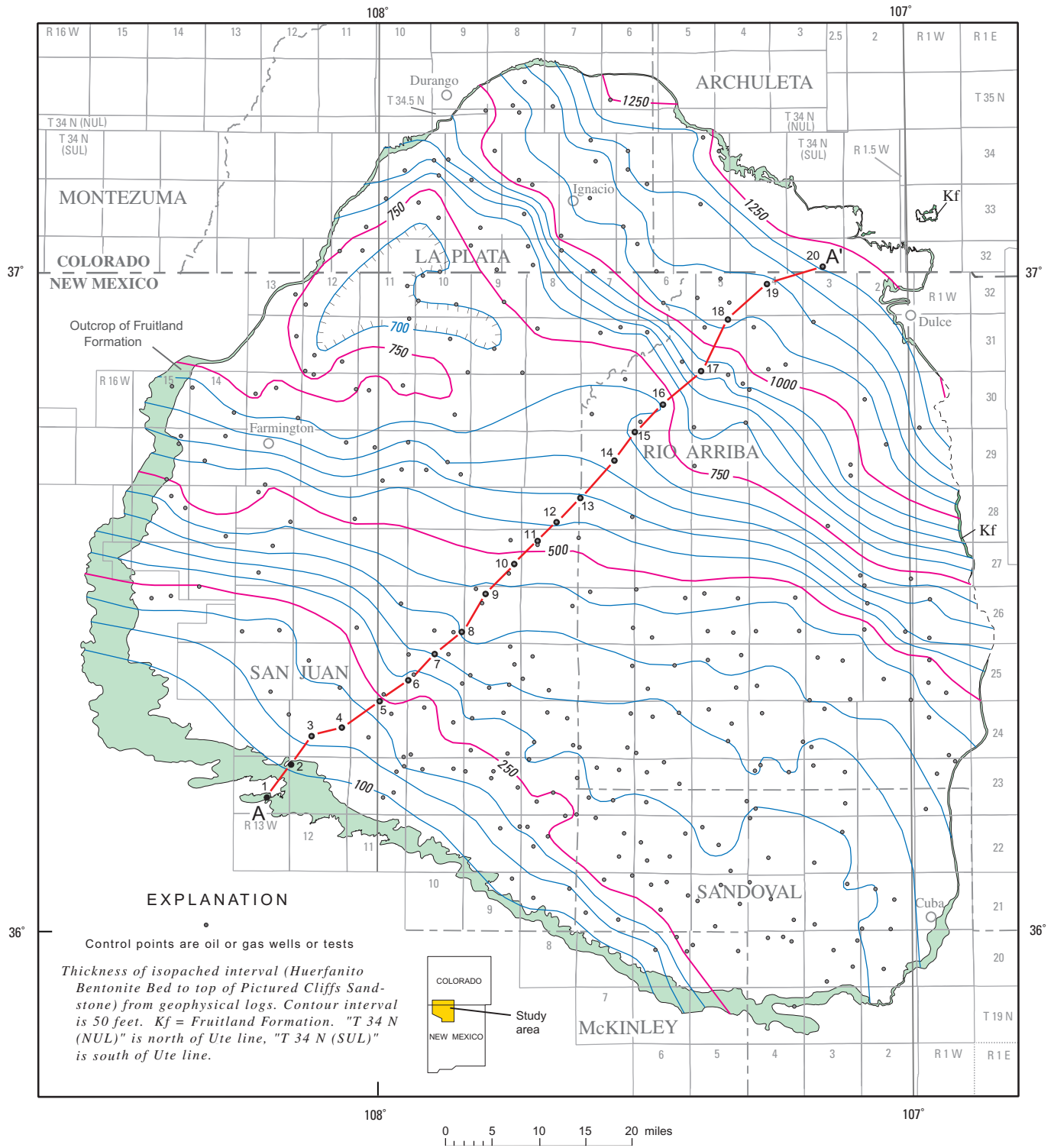


Figure 8. Isopach map of the interval between the Huerfanito Bentonite Bed of the Lewis Shale and the top of the Pictured Cliffs Sandstone. Kf, Fruitland Formation. Cross section A-A' is shown on plate 1.

and is relatively straight and smooth. This indicates a wave-dominated shoreline, where wave action dispersed sediment evenly along the shore. From the time the shoreline was at the 100-ft position to the time it reached the 250-ft position, the shoreline regressed relatively evenly and maintained a north-west trend. Between the 250-ft and the 300-ft line in the southeast part of the basin, however, a relatively rapid regression of the shoreline is indicated over a broad lobe that probably represents a delta complex that was being developed at the mouth of a major river system. The 300-ft line shows that this broad delta lobe, about 30 mi across, had moved the shoreline rapidly northward in the southeast part of the basin, while to the west the shoreline retained its northwesterly linear trend. Figure 8 shows that the increased rate of sediment influx recorded by this delta lobe gradually diminished but continued until the time the shoreline reached the 500-ft position.

From the 500-ft to the 650-ft positions, the shoreline retained a slightly sinuous, relatively linear configuration as it regressed northward across the central part of the basin area. At the 700-ft position a small lobe bulged the shoreline seaward to the northeast in the central part of the basin. At the 750-ft position, it is clear that this isopach line is no longer a good proxy for the shoreline position in the northwest part of the basin. In that area, the interval between the Huerfanito and the top of the Pictured Cliffs thins as shown by the 700-ft depression contour. The only reasonable explanation for this curious configuration is that at a time following deposition of the Huerfanito (75.76 Ma), a relatively small local tectonic event occurred in the area of the 700-ft line, slightly doming the strata on the Lewis seafloor. The doming apparently occurred so slowly that this feature never became a positive high on the seafloor because sedimentation dispersal across this part of the shelf area easily kept up with the slow rate of uplift and the seafloor remained relatively smooth and flat in this area. By the time the Pictured Cliffs shoreline had regressed across this area (around 74.5 Ma, see fig. 17), this minor tectonic event had ended because the Pictured Cliffs and overlying Fruitland coals show no evidence of this event.

The origin of the domed area discussed above is problematic; however, research on the age of the intrusion of the Carrizo Mountains laccolith (fig. 3) by Semken and McIntosh (1997, table 1) showed that the emplacement of the laccolith began at least 73.8 ± 1.0 Ma. The Carrizos are about 40 mi southwest of the paleo-dome expressed between the Huerfanito and Pictured Cliffs in the northwest part of the basin (figs. 3, 8). It is postulated that the low-relief dome that formed on the Lewis seafloor between 75.76 Ma and 74.5 Ma may be underlain by a small magmatic intrusion related to the emplacement of the Carrizo Mountains laccolith, however there is no direct evidence for this hypothesis.

At the position of the 800-ft line, the Pictured Cliffs shoreline has a strong northwest orientation that was retained throughout the rest of the time the Pictured Cliffs shoreline regressed northeastward to its last position in the basin area at the 1,250-ft line.

Rate of Regression

The rate of regression of the Pictured Cliffs shoreline can be inferred from figure 8. The farther apart the contour lines, the more rapid the regression of the shoreline; conversely, the closer together the lines, the slower the rate of regression. This relationship is best seen in cross section on plate 1 where the large stratigraphic rise in the position of the Pictured Cliffs is seen at wells 16, 17, and 18 and on figure 8 where the 750-ft through the 1,050-ft lines are close together. During the time interval from when the shoreline was at the 750-ft position to when it reached the 1,150-ft position, the deposition rate relative to subsidence slowed markedly and the Pictured Cliffs shoreline deposits built up vertically into a thick sandstone complex. The rate of deposition was so slow during this time interval that it fell below the rate of subsidence and the shoreline advanced shoreward 4 or 5 mi, transgressing over a thin tongue of Fruitland Formation backshore swamp deposits, as seen on well 16 of plate 1. The wide spacing between the 1,050- and 1,100-ft lines along the line of section A-A' indicates a rapid regression over that area, as seen between wells 18 and 19 on plate 1. Another period of slower shoreline regression is represented by isopach lines 1,100 to 1,200 (fig. 8) that are closer together, suggesting a slowing in the deposition rate to the extent that another transgressive shift of the shoreline occurred from the position of well 20 back beyond well 18, a distance of about 12 mi. The tongue of Pictured Cliffs in the Fruitland Formation in wells 18 and 19 on plate 1 records that event.

Fruitland Formation

The Fruitland Formation, defined by Bauer (1916, p. 274), is a mixture of mudstones, siltstones, sandstones, carbonaceous shales, and coals deposited in a nearshore swamp environment (Fassett and Hinds, 1971). The basal contact of the Fruitland with the underlying Pictured Cliffs Sandstone is a sharp and clear-cut contact, as discussed above. The upper contact of the Fruitland with the lower shale member of the Kirtland Formation was described by Bauer (1916, p. 274) as follows, "The Fruitland formation is more sandy than the overlying Kirtland Shale into which it merges by a gradational zone containing in many places sandstone lenses that are apparently of fluvial origin." Subsequent workers, frustrated by the ambiguity of this description of the upper contact, and unaware of the time-transgressive nature of the Fruitland, selected different, discontinuous sandstone beds as the top of the Fruitland, but no general consensus was reached on how best to define the Fruitland-Kirtland contact (Fassett and Hinds, 1971, p. 19). Fassett and Hinds suggested that the upper contact should be placed "... at the top of the highest coal bed or carbonaceous shale bed ..." Plate 1 shows the random nature of the occurrence of the highest Fruitland coal bed, from well to well. Because of the difficulty in locating this contact on the outcrop, and

especially in the subsurface on geophysical logs, the lower shale member of the Kirtland Formation and the Fruitland Formation are shown undivided in this report.

In a depositional sense, the Fruitland was the servant to the master Pictured Cliffs Sandstone. The essence of the Fruitland, in terms of its historical definition, is its contained coal beds, and the distribution of Fruitland coals across the basin is intimately related to the rate of regression of the Pictured Cliffs shoreline (plate 1) and to a lesser extent to the positions of northeast-trending distributary channel systems cutting through the Fruitland peat swamps. Fruitland coal distribution in the basin is discussed at greater length in the "Fruitland Coal Resources" section of this report.

Kirtland Formation

The Kirtland Shale was defined by Bauer (1916, p. 274) as predominantly "clayey" but containing white and brown sandstones. He subdivided the Kirtland into a lower shale member, the Farmington Sandstone Member, and an upper shale member. Fassett and Hinds (1971, p. 23) recommended combining the upper shale member of the Kirtland with the Farmington Member, and stated, "In this report a two fold division of the Kirtland Formation is used: the lower shale member of Bauer and the undivided Farmington Sandstone Member and upper shale member of Bauer." The Farmington Sandstone Member and upper shale member of the Kirtland Formation are likewise combined in this report and are referred to as the Farmington Sandstone Member of the Kirtland Formation. Because the Farmington Sandstone Member is such a significant part of the Kirtland, the word "Shale" is not an accurate descriptor for the lithology of the Kirtland and the name is thus changed to Kirtland Formation.

McDermott Member of the Animas Formation

The McDermott Member of the Animas Formation is the youngest rock unit of Late Cretaceous age in the San Juan Basin. The McDermott (Fassett, 1985, p. 319) is a conglomeratic, predominantly volcanoclastic rock unit thought to have been produced by a short-lived, Late Cretaceous episode of volcanism in the vicinity of the present-day La Plata Mountains (fig. 3). The McDermott is present only in the northwest part of the basin where it overlies the Kirtland Formation; thus, it does not appear on the cross sections in this report.

Upper Cretaceous Chronostratigraphy of the San Juan Basin

Earlier Publications

Radiometric ages of the Lewis Shale, Huerfano Bentonite Bed, Pictured Cliffs Sandstone, and Fruitland Formation

were first discussed in detail in a report by Fassett (1987). In that study, the ages of latest Cretaceous Western Interior ammonite zones in the San Juan Basin (based on collections from the upper part of the Lewis Shale) were estimated on the basis of radiometric ages obtained for altered volcanic ash beds associated with some of these ammonite zones in other localities in the Western Interior of North America. The principal reference for those ages was Obradovich and Cobban (1975). The ammonite-zone ages were projected into the Pictured Cliffs Sandstone and Fruitland Formation along time lines to determine the timing of the Pictured Cliffs Sandstone regression across the basin. Subsequent to the Fassett (1987) report, Fassett and Steiner (1997) reported the ages of a series of ash beds in the Fruitland Formation in the southwest part of the San Juan Basin and one ash bed from the upper part of the Lewis Shale in the northeast part of the basin near Chimney Rock in Colorado (near the Chimney Rock mine, fig. 2).

Hunter Wash Study Area

Ash Beds

The localities for five dated ash beds collected in the Hunter Wash study area (reported by Fassett and Steiner, 1997) are shown on figure 9. Three of these beds are in the Fruitland Formation and two are in the Farmington Sandstone Member of the Kirtland Formation. Ash DEP, the stratigraphically lowest, is 7 inches thick and was collected from a thin, high-ash coal bed in the lowermost Fruitland Formation, very close to the top of the Pictured Cliffs Sandstone on the southwest edge of the San Juan Basin. (This coal bed may correlate with the basal coal bed in the USGS AMW 6-1 drill hole on plate 1.) Ash DEP is named for Dog Eye Pond, a stock tank near the collection site that is shown on the Tanner Lake, 1:24,000-scale, USGS topographic quadrangle map. Ash 2 is 8 inches thick and was collected from a coal bed in the lower Fruitland in Hunter Wash (fig. 9). Ash 4 is 13 inches thick and was collected from the top of a thin, high-ash coal bed in Hunter Wash (fig. 9). This is the stratigraphically highest Fruitland coal bed in Hunter Wash. This site marks the beginning of the paleomagnetic traverse of Fassett and Steiner (1997) in Hunter Wash (fig. 9).

Ash H is 11 inches thick and was collected from the Farmington Sandstone Member of the Kirtland Formation in a short, northwest-trending tributary of Hunter Wash (fig. 9). This ash bed is underlain by green-gray mudstone and is overlain by a 4.5-ft-thick chocolate-brown, thin-bedded mudstone. Ash J is 8 inches thick and was collected from the uppermost part of the Farmington Member, only 16 ft below the base of the Paleocene Ojo Alamo Sandstone. It is underlain by a light-gray sandy siltstone bed and is overlain by 2.5 ft of chocolate-brown mudstone. The collection site is in a small rincon that provides a small window into a bedrock exposure of the uppermost Kirtland that is mostly covered by slope-wash material in the rest of this area. The ash-bed-J site is on

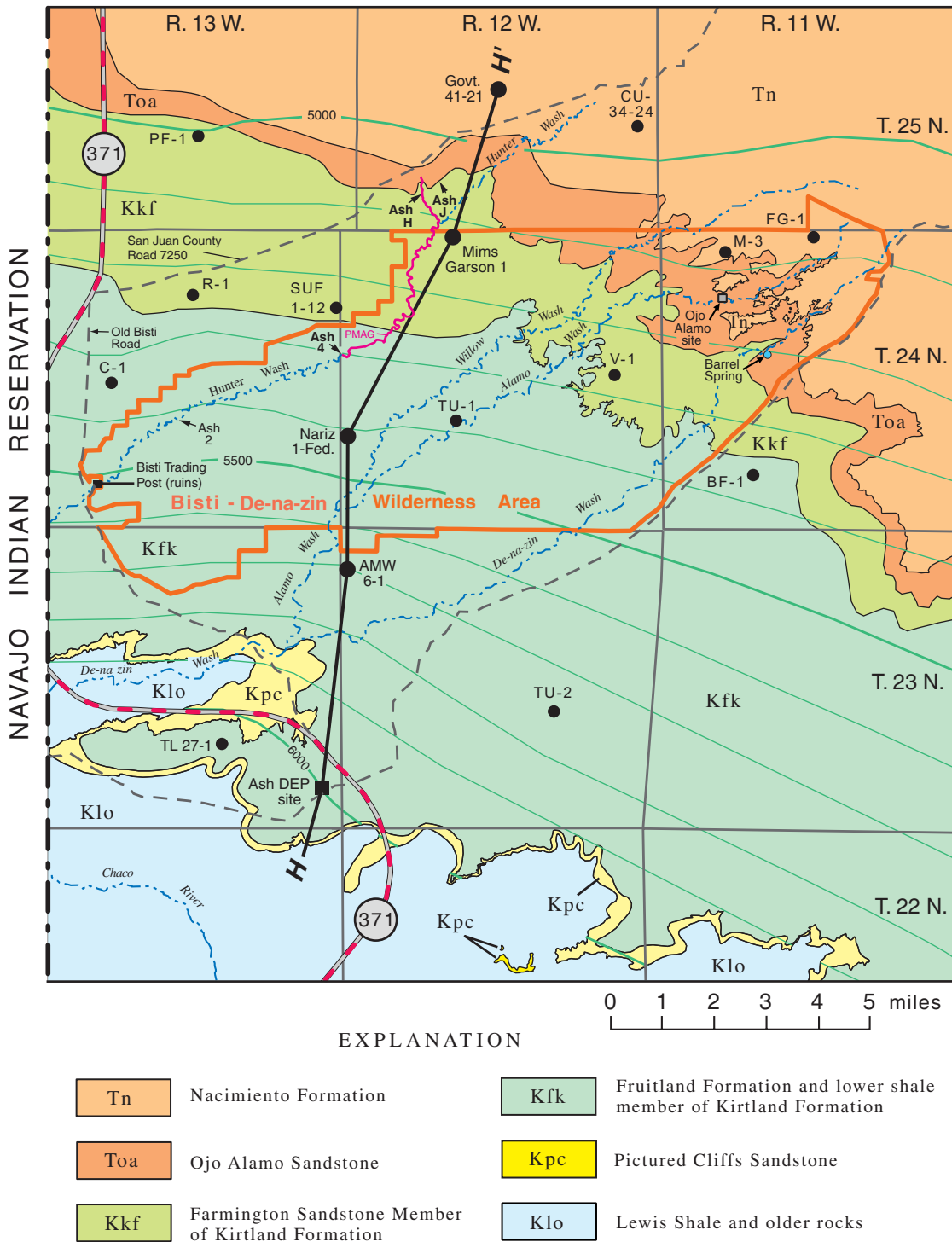
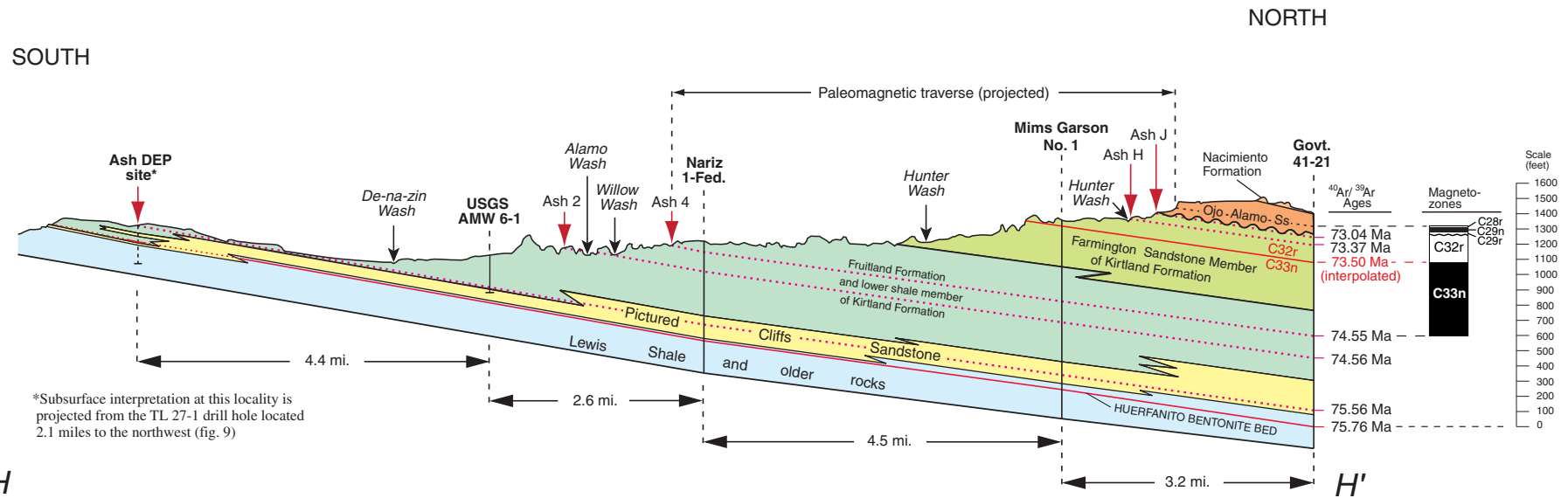


Figure 9. Geologic map of the Hunter Wash study area (fig. 2). Altered volcanic ash bed collection sites are labeled and shown with arrows. Geologic cross section H-H' is shown on figure 10. Structure contour lines (green) are on the Huerfanito Bentonite Bed of the Lewis Shale; contour interval is 100 ft; datum is mean sea level. List of wells used for subsurface control is in table 3. PMAG is line of paleomagnetic traverse along the upper part of Hunter Wash from Fassett and Steiner (1997). Geology compiled and locally modified by the author from USGS MF-Series maps: Brown (1982 a, 1982b), O'Sullivan, Scott, and Heller (1979), O'Sullivan and others (1986), Schneider and others (1979), Scott and others (1979), and Strobell and others (1985).



H

H'

Figure 10. Structural cross section in the Hunter Wash study area. Line of section is on figure 9. Drill holes used for control are shown in table 3. Radiometric ages of ash beds are from Fassett and Steiner (1997) and Fassett and others, (1997). Analytical data for ash bed age determinations are in tables 1 and 4. Paleomagnetic data are from Fassett and Steiner (1997). Topographic profile is from USGS 1:24,000 topographic quadrangle maps. Vertical exaggeration is about 10 x.

Table 3. List of drill holes shown on figure 9—holes on cross section H-H' (fig. 10) in bold type.

Map designation	Company	Drill hole name	T. (N.)	R. (W.)	Sec.	Quarter	Longitude (N.)	Latitude (W.)
PF-1	Magnolia Petroleum	Postelle Federal 1	25	13	28	NE	108.21711	36.37758
Govt. 41-21	Shell Oil	Government 41-21	25	12	21	NE	108.10936	36.39194
CU 34-24	Shell Oil	Carson Unit 34-24	25	12	24	SW	108.06007	36.38118
C-1	Monsanto Chemical	Chaco 1	24	13	20	NW	108.25000	36.30630
R-1	Davis Oil	Riddle 1	24	13	10	NW	108.21880	36.33157
SUF 1-12	R. E. Lauritsen	Southern Union Federal 1-12	24	13	12	SE	108.16810	36.32823
Nariz 1 Fed.	Tesoro Petroleum	Nariz 1-Federal	24	12	30	NW	108.16394	36.29086
Mims Garson 1	Kenneth Murchison	Mims Garson 1	24	12	4	NW	108.12660	36.34864
TU-1	Humble Oil & Refining	Tanner Unit 1	24	12	21	SW	108.12526	36.29547
V-1	H. L. Fanning	Vandersluice 1	24	12	13	SW	108.06836	36.30872
M-3	Tenneco Oil	Monument 3	24	11	5	NW	108.02822	36.34406
BF-1	Magnolia Petroleum	Beamon Fed 1	24	11	29	SE	108.01842	36.27950
FG-1	Davis Oil	Fannin Government 1	24	11	3	NW	107.99730	36.34900
TL 27-1	U.S. Geological Survey	Tanner Lake 27-1	23	13	27	SW	108.20853	36.20172
AMW 6-1	U.S. Geological Survey	Alamo Mesa West 6-1	23	12	6	SW	108.16370	36.25214
TU-2	Humble Oil & Refining	Tanner Unit 2	23	12	23	SW	108.09031	36.21146

the topographic divide between the short tributary where ash H is exposed and Hunter Wash to the east (fig. 9).

Figure 10 is a structural cross section through the Hunter Wash study area (a list of the drill holes used for subsurface control for this cross section and throughout the Hunter Wash area is in table 3). On the south end of the cross section, the Huerfanito Bentonite Bed is shown projected into the basal Fruitland Formation at the outcrop. Because bedrock is masked by alluvium in this area, it is not possible to determine if the Huerfanito is preserved in the Fruitland here. Confirmation of the projected level of the Huerfanito Bed in the basal Fruitland is found in the lithologic descriptions of rocks penetrated in USGS drill hole TL 27-1 (fig. 9) in Jentgen and Fassett (1977, p. 28). At a depth of 106 ft in this well there is the notation "Clay balls (changed bits)." The senior author of this report, Russell W. Jentgen, was on site when this hole was drilled and stated (oral commun., 1977, 1998) that at 106 ft, a bentonitic shale was penetrated that swelled and clogged the drill bit and a new drill bit had to be installed in order to continue drilling. The top of the Pictured Cliffs Sandstone is at a depth of 113 ft in the TL 27-1 drill hole, thus the bentonitic shale was in the lower Fruitland, nearly at the top of the Pictured Cliffs, exactly where a projection of the Huerfanito Bentonite Bed is shown on figure 10.

Ash-Bed Ages

Table 4 provides analytical data for $^{40}\text{Ar}/^{39}\text{Ar}$ age determinations for the Hunter Wash, Chimney Rock, and La Plata mine ash beds. All of the ages were determined by John Obradovich, U.S. Geological Survey, Denver, Colo. Sanidine crystals were separated from the ashes and dated using the $^{40}\text{Ar}/^{39}\text{Ar}$ laser fusion method (methodology described in Obradovich, 1993). Most analyses were of single crystals, but one was of multiple crystals. The ages of the five Hunter Wash ash beds plus the age of the Huerfanito Bentonite Bed (collected at the Regina site (figs. 2 and 6) and discussed in the "Huerfanito Bentonite Bed of the Lewis Shale" section of this report) are shown on the right side of cross section H-H' (fig. 10). The duration of the interval from the oldest to the youngest ash bed at Hunter Wash is 2.72 m.y. (75.76 to 73.04 Ma)

Magnetic Polarity

Figure 11 shows the magnetic polarity column for Upper Cretaceous and lower Tertiary rocks in the Hunter Wash area. The Late Cretaceous polarity reversal from magnetic chron C33n to C32r is 1,076 ft above the Huerfanito Bentonite Bed. The age of the reversal was estimated to be 75.50 ± 0.18 Ma by Fassett and Steiner (1997) on the basis of interpolation between the ages of two ash beds above and three ash beds below the reversal in this area. (The age of this reversal is reviewed in the "Summary of Chronostratigraphy" section of this report.) Fassett and Steiner (1997) reported a short normal-polarity interval in the Paleocene Ojo Alamo Sand-

stone and identified it as chron C29n (fig. 13). Butler and Lindsay (1984) discussed a short normal-polarity interval they had previously reported at several localities in the Ojo Alamo Sandstone in the southern San Juan Basin and had labeled chron C29n. One of their localities was near Alamo Wash, about 5 mi southeast of Hunter Wash (fig. 9). On reexamination of their data, Butler and Lindsay (1984) decided that the normal zone in the Ojo Alamo represented a normal-field overprint and they deleted this normal zone from the Ojo Alamo at all but one of their localities. The Fassett and Steiner report (1997, fig. 2), however, shows that the normal zone in the Ojo Alamo on Hunter Wash represents certain "Cretaceous [or early Paleocene] magnetization of the polarities"—thus an interval of normal polarity (chron C29r of Fassett and Steiner, 1997) is indeed present in the Ojo Alamo in the Hunter Wash section. Because chron C29n is early Paleocene, the Ojo Alamo at Hunter Wash must be Paleocene in age. Chron C29n is underlain by a short reversed-polarity interval identified as C29r in the lowermost part of the Ojo Alamo (fig. 13). The lower part of chron C29r; chrons C30n and C30r, chrons C31n and C31r, chron C32n; and the upper part of chron C32r are missing at the unconformity at the base of the Ojo Alamo.

Paleontology

The Ojo Alamo Sandstone is conformably overlain by and intertongues with the Nacimiento Formation in the Hunter Wash area (Baltz and others, 1966), and Puercan (earliest Paleocene) mammals have been found at several localities in the lower part of the Nacimiento, 26–40 ft above the top of the Ojo Alamo (Williamson and Lucas, 1992, fig. 5). This evidence indicates that the upper part of the Ojo Alamo is earliest Paleocene in age. Palynological data from the Ojo Alamo Sandstone from Hunter Wash and many other localities in the basin universally support an earliest Paleocene age for the entire Ojo Alamo (Fassett and others, 1987, Fassett and others, 2000) and a Late Cretaceous age for the underlying Kirtland Formation.

The Kirtland Formation and the lower part of the Ojo Alamo Sandstone contain a rich and diverse vertebrate fauna in the Hunter Wash area, including dinosaurs, turtles, crocodiles, and mammals (Hunt and Lucas, 1992). The radiometric dating of upper Kirtland ash beds (discussed under "Ash Beds" above) proves that this formation is Cretaceous in age (73.0 Ma) to within a few feet of the basal Ojo Alamo unconformity. The dinosaurs of the Ojo Alamo Sandstone have long been an enigma because other evidence, discussed above, indicates that the Ojo Alamo is Paleocene in age. Vertebrate paleontologists have continued to insist that the lower part of the Ojo Alamo must be Cretaceous because of its contained dinosaurs (Hunt and Lucas, 1992). Two papers, however (Fassett, 1982, and Fassett and others, 1987), suggest that the weight of the evidence indicates that the Ojo Alamo is Paleocene in age and that the dinosaurs within the Ojo Alamo are Paleocene and not Cretaceous in age. The recent discovery of Paleocene pollen beneath a large hadrosaur femur, 50 ft above the base

Table 4. Analytical data for $^{40}\text{Ar}/^{39}\text{Ar}$ age determinations for seven San Juan Basin altered volcanic ash beds from the Hunter Wash and La Plata mine areas in New Mexico and the Chimney Rock area in Colorado—modified from Fassett and Steiner (1997).

[$^{40}\text{Ar}^*$, radiogenic argon]

Ash bed name and J value	Irradiation number	Mineral analysis	Exp. number	$^{40}\text{Ar}/^{39}\text{Ar}$	$^{37}\text{Ar}/^{39}\text{Ar}$	$^{36}\text{Ar}/^{39}\text{Ar}$	K/Ca	% $^{40}\text{Ar}^*$	$^{40}\text{Ar}^*/^{39}\text{Ar}_K$	Age (Ma)	Error (1 sigma)
Ash bed J (Fassett K/T) J=0.006346	JD022	Sanidine single xtl	96Z0082	5.84251	0.009032	0.000174	54.2	98.98	5.78315	<u>74.08</u>	<u>0.30</u>
			96Z0085	5.71103	0.007369	0.000006	66.5	99.82	5.70112	73.05	0.26
			96Z0086	5.72075	0.009275	0.000009	52.8	99.81	5.71022	73.16	0.32
			96Z0087	5.72830	0.008386	0.000086	58.4	99.41	5.69492	72.97	0.41
			96Z0088	5.91112	0.013007	0.000050	37.7	99.61	5.88880	<u>75.40</u>	<u>0.26</u>
			96Z0089	5.73928	0.009932	0.000181	49.3	98.93	5.67799	72.75	0.29
			96Z0090	5.73461	0.009117	0.000024	53.7	99.73	5.71939	73.27	0.28
Unweighted mean and standard deviation w/o errors in J										73.04	0.20
Weighted mean and weighted standard deviation w/o errors in J										73.05	0.20
Unweighted mean and error of the mean at the 95% confidence level including the error										73.04	0.25
Ash bed H(1) (Hunter Wash 6) J=0.006965	JD06	Sanidine single xtl	91Z1277	5.98932	0.003994	0.000074	122.7	99.49	5.95875	73.36	0.26
			91Z1278	6.08627	0.003978	0.000412	123.2	97.85	5.95573	73.32	0.28
			91Z1280	5.99126	0.005336	0.000101	91.8	99.36	5.95270	73.29	0.26
			91Z1281	5.95985	0.003085	0.000006	158.9	99.82	5.94926	73.24	0.25
			91Z1282	5.97041	0.004894	0.000016	100.1	99.77	5.95695	73.34	0.30
Unweighted mean and standard deviation w/o errors in J										73.31	0.05
Weighted mean and weighted standard deviation w/o errors in J										73.31	0.05
Unweighted mean and error of the mean at the 95% confidence level including the error										73.31	0.21
Ash bed H(2) (Hunter Wash 10) J=0.006997	JD06	Sanidine single xtl	91Z1283	5.97047	0.004577	0.000052	107.1	99.60	5.94633	73.54	0.24
			91Z1284	5.97268	0.003751	0.000093	130.6	99.39	5.93637	73.42	0.27
			91Z1285	5.95048	0.004290	0.000056	114.2	99.57	5.92504	73.28	0.54
			91Z1286	5.95753	0.004314	0.000014	113.6	99.78	5.94464	73.52	0.34
			91Z1287	5.96512	0.010414	0.000054	47.1	99.72	5.96512	73.77	0.40
Unweighted mean and standard deviation w/o errors in J										73.51	0.18
Weighted mean and weighted standard deviation w/o errors in J										73.51	0.14
Unweighted mean and error of the mean at the 95% confidence level including the error										73.51	0.34
Mean age and uncertainty for two samples sets, H(1) and H(2) (standard error of mean)										73.37	0.08
Mean age and uncertainty for two samples sets, H(1) and H(2) (95% confidence level)										73.37	0.18

Table 4. Analytical data for $^{40}\text{Ar}/^{39}\text{Ar}$ age determinations for seven San Juan Basin altered volcanic ash beds from the Hunter Wash and La Plata mine areas in New Mexico and the Chimney Rock area in Colorado—modified from Fassett and Steiner (1997)—*Continued*.

Ash bed name and J value	Irradiation number	Mineral analysis	Exp. number	$^{40}\text{Ar}/^{39}\text{Ar}$	$^{37}\text{Ar}/^{39}\text{Ar}$	$^{36}\text{Ar}/^{39}\text{Ar}$	K/Ca	% $^{40}\text{Ar}^*$	$^{40}\text{Ar}^*/^{39}\text{Ar}_K$	Age (Ma)	Error (1 sigma)
Ash bed 4 (Kirtland 86-0-07) J=0.007239	JD029	Sanidine	99Z0566	5.87492	0.009246	0.000118	53.0	99.26	5.83201	74.60	0.29
			99Z0567	5.83590	0.008767	0.000075	55.9	99.48	5.80576	74.27	0.26
			99Z0568	5.84367	0.008589	0.000002	57.1	99.84	5.83492	74.63	0.35
			99Z0569	5.86337	0.008552	0.000040	57.3	99.65	5.84343	74.74	0.34
			99Z0571	5.89673	0.009239	0.000214	53.0	98.79	5.82556	74.52	0.33
Unweighted mean and standard deviation w/o errors in J										74.48	0.23
Weighted mean and weighted standard deviation w/o errors in J										74.51	0.14
Unweighted mean and error of the mean at the 95% confidence level including the error										74.55	0.29
Ash bed 2(1) (Kirtland 86-0-05) J=0.008114	JD010	Sanidine multiple xtl	93Z0355	5.21431	0.016830	0.000068	29.1	99.47	5.18647	74.36	0.26
			93Z0356	5.20874	0.022911	0.000029	21.4	99.70	5.19303	74.46	0.25
			93Z0357	5.20897	0.032658	0.000096	15.0	99.33	5.17419	74.19	0.27
			93Z0358	5.22023	0.020443	0.000010	24.0	99.80	5.20991	74.69	0.31
			93Z0359	5.21996	0.012477	0.000100	39.3	99.28	5.18231	74.31	0.30
Unweighted mean and standard deviation w/o errors in J										74.40	0.19
Weighted mean and weighted standard deviation w/o errors in J										74.39	0.18
Unweighted mean and error of the mean at the 95% confidence level including the error										74.40	0.54
Ash bed 2(2) (Kirtland 86-0-05) J=0.007235	JD021	Sanidine single xtl	95Z0555	5.89423	0.007657	0.000175	64.0	98.98	5.83445	74.59	0.32
			95Z0556	5.86859	0.007135	0.000071	68.7	99.50	5.83945	74.65	0.23
			95Z0557	6.09035	0.007425	0.000863	66.0	95.68	5.82725	74.50	0.34
			95Z0558	5.95920	0.007210	0.000349	68.0	98.13	5.84797	74.76	0.33
			95Z0559	5.89310	0.006899	0.000121	71.0	99.25	5.84918	74.77	0.31
95Z0560	5.86243	0.005295	0.000020	92.5	99.75	5.84805	74.76	0.25			
Unweighted mean and standard deviation w/o errors in J										74.67	0.11
Weighted mean and weighted standard deviation w/o errors in J										74.68	0.10
Unweighted mean and error of the mean at the 95% confidence level including the error										74.67	0.35

Table 4. Analytical data for $^{40}\text{Ar}/^{39}\text{Ar}$ age determinations for seven San Juan Basin altered volcanic ash beds from the Hunter Wash and La Plata mine areas in New Mexico and the Chimney Rock area in Colorado—modified from Fassett and Steiner (1997)—*Continued.*

Ash bed name and J value	Irradiation number	Mineral analysis	Exp. number	$^{40}\text{Ar}/^{39}\text{Ar}$	$^{37}\text{Ar}/^{39}\text{Ar}$	$^{36}\text{Ar}/^{39}\text{Ar}$	K/Ca	% $^{40}\text{Ar}^*$	$^{40}\text{Ar}^*/^{39}\text{Ar}_K$	Age (Ma)	Error (1 sigma)
Ash bed 2(3) (Kirtland 86-0-05) J=0.007248	JD022	Sanidine single xtl	96Z0091	5.88379	0.007845	0.000176	62.5	98.97	5.82352	74.58	0.30
			96Z0092	5.87229	0.007859	0.000158	62.3	99.06	5.81731	74.50	0.30
			96Z0093	5.87863	0.006452	0.000143	75.9	99.13	5.82790	74.64	0.32
			96Z0094	5.88236	0.007517	0.000135	65.2	99.18	5.83437	74.72	0.28
			96Z0095	5.89134	0.007593	0.000218	64.5	98.76	5.81875	74.52	0.27
			96Z0096	5.83790	0.007549	0.000093	64.9	99.38	5.80227	74.31	0.25
Unweighted mean and standard deviation w/o errors in J										74.55	0.14
Weighted mean and weighted standard deviation w/o errors in J										74.53	0.15
Unweighted mean and error of the mean at the 95% confidence level including the error										74.55	0.16
Mean age and uncertainty for three samples sets, 2(1), 2(2), and 2(3) (standard error of mean)										74.56	0.06
Mean age and uncertainty for three samples sets, 2(1), 2(2), and 2(3) (95% confidence level)										74.56	0.13
Ash DEP (Lower Fruitland) J=0.008068	JD010	Sanidine multiple xtl	93Z0365	5.31701	0.009886	0.000057	49.6	99.53	5.29182	75.42	0.27
			93Z0366	5.31513	0.006601	0.000002	74.2	99.83	5.30607	75.62	0.21
			93Z0367	5.3147	0.022029	0.000002	22.2	99.85	5.30671	75.63	0.23
			93Z0368	5.32145	0.001855	0.000014	264.2	99.75	5.30832	75.65	0.30
			93Z0369	5.30936	0.009924	0.000016	49.4	99.75	5.29637	75.49	0.28
Unweighted mean and standard deviation w/o errors in J										75.56	0.10
Weighted mean and weighted standard deviation w/o errors in J										75.57	0.10
Unweighted mean and error of the mean at the 95% confidence level including the error										75.56	0.41
Ash CR(1) (Chimney Rock 9/6/89) J=0.006346	JD018	Sanidine single xtl	94Z0628	6.66639	0.012451	0.000058	39.4	99.62	6.64129	74.47	0.36
			94Z0629	6.64388	0.012715	0.000002	38.5	99.87	6.63523	74.41	0.21
			94Z0630	6.67716	0.011271	0.000132	43.5	99.29	6.63008	74.35	0.25
			94Z0631	6.72427	0.012361	0.000228	39.6	98.88	6.64877	74.55	0.29
			94Z0632	7.73688	0.011889	0.003877	41.2	85.09	6.58302	73.83	0.34
			94Z0633	6.63383	0.011463	0.000002	42.8	99.87	6.62515	74.29	0.21
94Z0634	6.67627	0.010826	0.000088	45.3	99.49	6.64201	74.48	0.25			
Unweighted mean and standard deviation w/o errors in J										74.34	0.24
Weighted mean and weighted standard deviation w/o errors in J										74.36	0.19
Unweighted mean and error of the mean at the 95% confidence level including the error										74.34	0.34

Table 4. Analytical data for $^{40}\text{Ar}/^{39}\text{Ar}$ age determinations for seven San Juan Basin altered volcanic ash beds from the Hunter Wash and La Plata mine areas in New Mexico and the Chimney Rock area in Colorado—modified from Fassett and Steiner (1997)—*Continued.*

Ash bed name and J value	Irradiation number	Mineral analysis	Exp. number	$^{40}\text{Ar}/^{39}\text{Ar}$	$^{37}\text{Ar}/^{39}\text{Ar}$	$^{36}\text{Ar}/^{39}\text{Ar}$	K/Ca	% $^{40}\text{Ar}^*$	$^{40}\text{Ar}^*/^{39}\text{Ar}_K$	Age (Ma)	Error (1 sigma)
Ash CR(2) (Chimney Rock 260) J=0.006346	JD018	Sanidine single xtl	94Z0581	6.65022	0.011035	0.000052	44.4	99.64	6.62666	74.31	0.26
			94Z0582	6.66070	0.011591	0.000148	42.3	99.22	6.60876	74.11	0.24
			94Z0583	6.69819	0.011409	0.000249	43.0	98.78	6.61636	74.20	0.27
			94Z0584	6.67044	0.011849	0.000155	41.4	99.19	6.61667	74.20	0.24
			94Z0586	6.66142	0.010789	0.000075	45.4	99.54	6.63092	74.36	0.28
			94Z0587	6.73294	0.012570	0.000374	39.0	98.24	6.61444	74.18	0.26
			94Z0588	6.65070	0.011966	0.000124	41.0	99.33	6.60592	74.08	0.25
			94Z0589	6.67283	0.011058	0.000100	44.3	99.44	6.63525	74.41	0.27
Unweighted mean and standard deviation w/o errors in J										74.23	0.12
Weighted mean and weighted standard deviation w/o errors in J										74.22	0.12
Unweighted mean and error of the mean at the 95% confidence level including the error										74.23	0.19
Mean age and uncertainty for two samples sets, CR(1) and CR(2) (standard error of mean)										74.25	0.06
Mean age and uncertainty for two samples sets, CR(1) and CR(2) (95% confidence level)										74.25	0.13
Ash LP (La Plata Mine) J=008075	JD010	Sanidine single xtl	93Z0360	5.22181	0.018976	0.000053	25.8	99.56	5.19871	74.19	0.32
			93Z0361	5.22126	0.028708	0.000045	17.1	99.61	5.20122	74.22	0.26
			93Z0362	5.22103	0.025860	0.000047	19.0	99.60	5.20024	74.21	0.25
			93Z0363	5.23686	0.025109	0.000045	19.5	99.61	5.21652	74.43	0.25
			93Z0364	5.22582	0.010336	0.000001	17.4	99.83	5.21717	74.44	0.23
Unweighted mean and standard deviation w/o errors in J										74.30	0.13
Weighted mean and weighted standard deviation w/o errors in J										74.31	0.12
Unweighted mean and error of the mean at the 95% confidence level including the error										74.30	0.38

Ca and K corrections and decay constants:

$$(^{36}\text{Ar}/^{37}\text{Ar})_{\text{Ca}} = 2.69 \pm 0.24 \times 10^{-4}$$

$$(^{39}\text{Ar}/^{37}\text{Ar})_{\text{Ca}} = 6.79 \pm 0.051 \times 10^{-4}$$

$$(^{40}\text{Ar}/^{39}\text{Ar})_{\text{K}} = 9.1 \pm 5.4 \times 10^{-3}$$

$$\lambda_{\epsilon} + \lambda_{\epsilon'} = 0.581 \times 10^{-10} \text{ yr}^{-1}$$

$$\lambda_{\beta} = 4.962 \times 10^{-10} \text{ yr}^{-1}$$

$$^{40}\text{K}/\text{K} = 1.167 \times 10^{-4} \text{ atom/atom}$$

Notes: For ash beds H, 2, and CR, weighted-mean age determinations were made for multiple sample sets: for ash bed H, the two samples sets shown produced a mean age and uncertainty of 73.37 ± 0.08 (standard error of mean) and 73.37 ± 0.18 Ma (95% confidence level); for ash bed 2, the three samples sets shown produced a mean age and uncertainty of 74.56 ± 0.06 (standard error of mean) and 74.56 ± 0.13 Ma (95% confidence level); for ash bed CR, the two samples sets shown produced a mean age and uncertainty of 74.25 ± 0.06 (standard error of mean) and 74.25 ± 0.13 Ma (95% confidence level). These mean ages and uncertainties are used for these ash beds in this report. The underlined numbers for ash J in the “Age (Ma)” and “1 sigma” columns were excluded from the weighted-mean age determination for this ash bed.

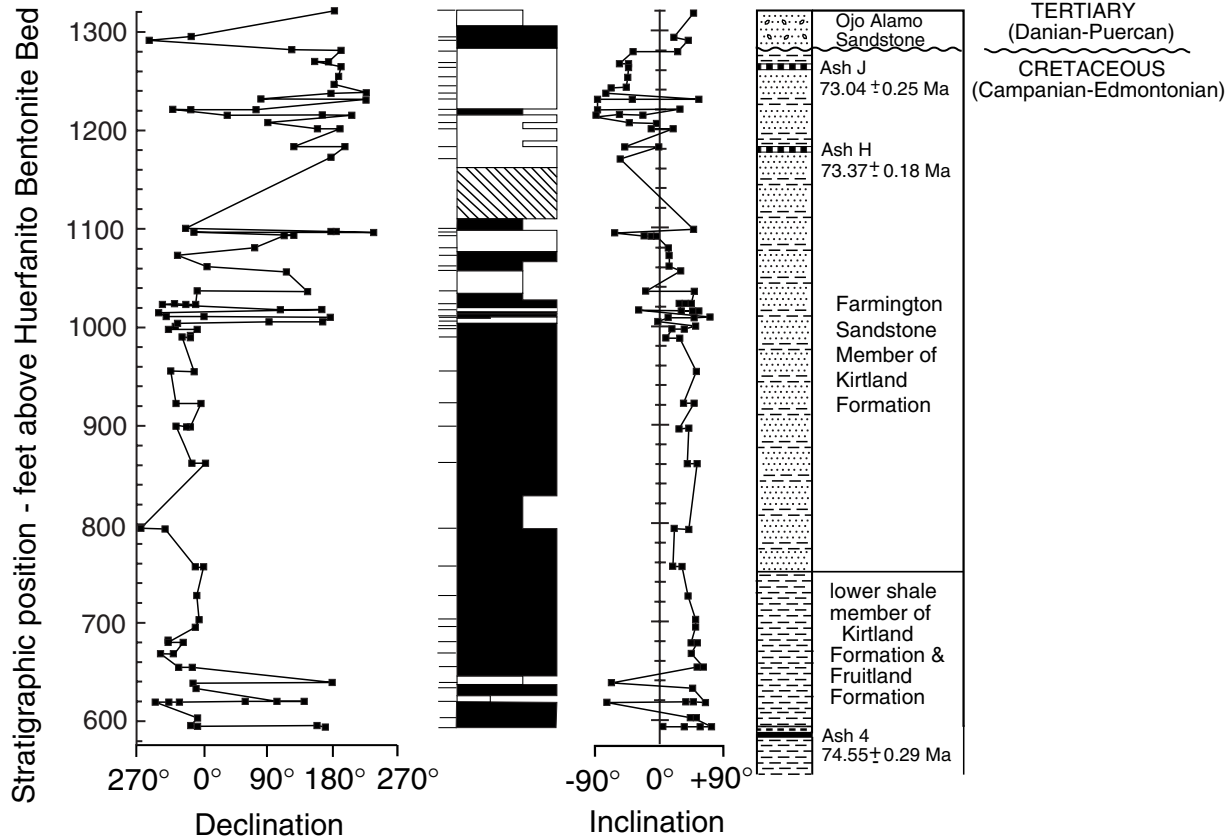


Figure 11. Hunter Wash magnetostratigraphic data. Black is normal, white is reversed polarity, and hachures indicate an unsampled interval. The magnetic-polarity column width indicates the degree of certainty of the polarity interpretations; full column width indicates Cretaceous or early Paleocene (CP) magnetization of the polarities, two-thirds column width indicates probable CP magnetization, and one-third column width means some indication of CP polarity but with high uncertainty. Sample positions are shown by tick marks on the left side of the polarity column. The unconformity at the base of the Tertiary Ojo Alamo Sandstone is 1,276 ft above the Huerfanito Bentonite Bed. Paleomagnetic traverse in Hunter Wash is shown on figure 9. From Fassett and Steiner (1997).

of the Ojo Alamo Sandstone in the west-central part of the San Juan Basin (Fassett and others, 2000; Fassett and Lucas, 2000), strongly supports the argument that the Ojo Alamo and its contained dinosaurs are Paleocene in age. A recent estimate for the age of the Cretaceous-Tertiary boundary is 65.5 ± 0.1 Ma (Obradovich, 1999); therefore, the Ojo Alamo in the San Juan Basin must have an age slightly less than 65.5 Ma. The unconformity at Hunter Wash between the Kirtland Shale and the Ojo Alamo Sandstone thus represents about 8 m.y. of missing time (73–65Ma).

Chimney Rock Study Area

Ash Beds

The Chimney Rock study area is on the northeast edge of the San Juan Basin near the Chimney Rock mine (fig. 2). The geology of the upper part of the Lewis Shale, the Pictured

Cliffs Sandstone, and the lower part of the Fruitland Formation was studied in detail in this area by Fassett and Steiner (1997) as part of a broader study of the paleomagnetism of uppermost Cretaceous rocks at several localities in the San Juan Basin. In the process of conducting paleomagnetic sampling through the upper part of the Lewis Shale at Chimney Rock, several very thin bentonite beds were discovered. Most of these altered volcanic ash beds are less than 1 inch thick, with the thickest being about 3 inches. Ash beds in this exposure are commonly replaced by calcium carbonate and sometimes grade into thicker zones of calcite concretions. Samples of several ash beds were collected at this site, but only one, the CR bed, contained sanidine crystals suitable for $^{40}\text{Ar}/^{39}\text{Ar}$ age determination.

The CR ash bed (named for Chimney Rock) is located about 180 ft below the base of the Pictured Cliffs Sandstone at a stratigraphic level 909 ft above the level of the Huerfanito Bentonite Bed (figs. 12, 13). This ash ranges from 1 inch to less than 1/8 inch thick and is in places replaced by calcium

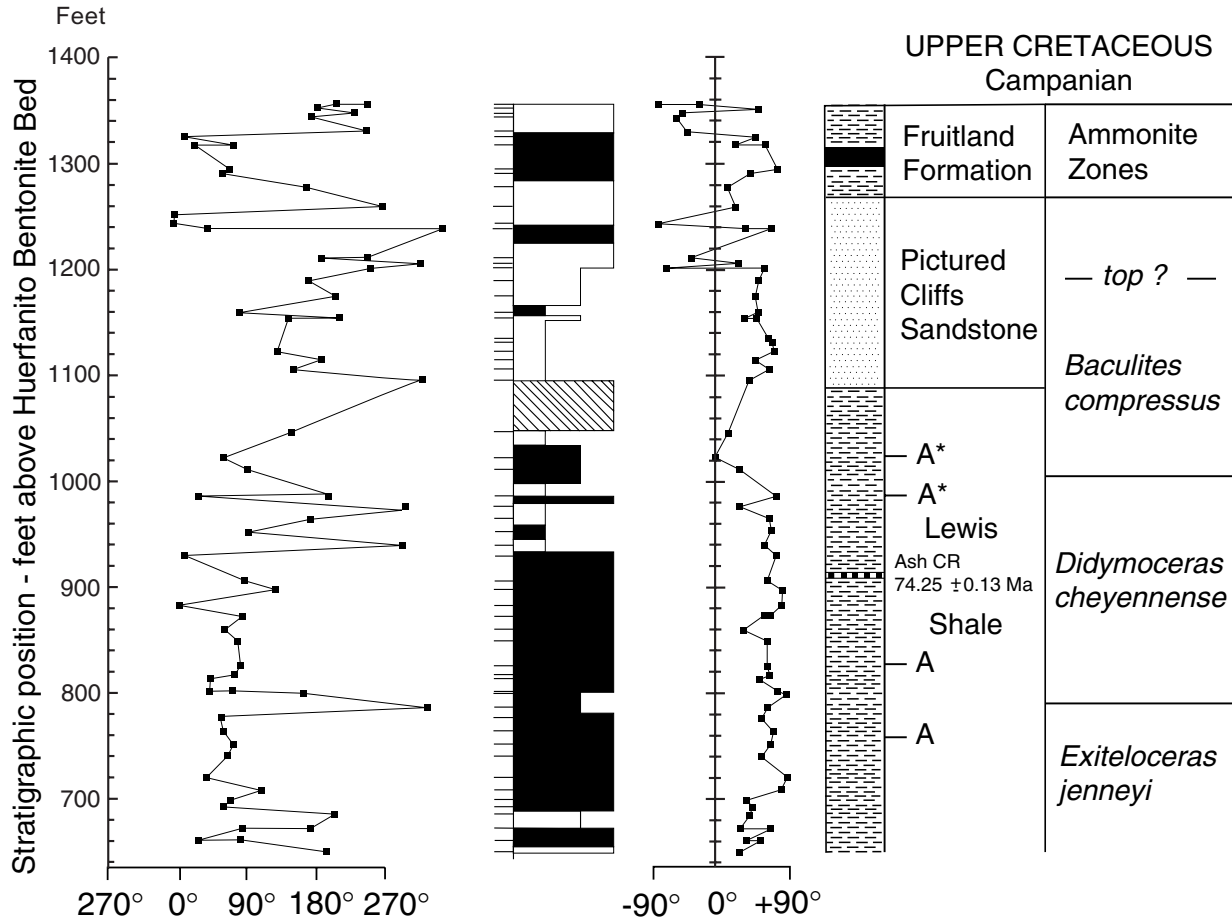


Figure 12. Chimney rock magnetostratigraphic data. Black is normal, white is reversed polarity, and hachures indicate an unsampled interval. The magnetic-polarity column width indicates the degree of certainty of the polarity interpretations; full column width indicates Cretaceous magnetization of the polarities, two-thirds column width indicates probable Cretaceous magnetization, and one-third column width means some indication of Cretaceous polarity but with high uncertainty. Sample positions are shown by tick marks on the left side of the polarity column. Level of volcanic ash bed CR and its age are shown. A's to the right of the lithologic column in the Lewis Shale designate levels of ammonite collections made for this study; A's with asterisks indicate ammonite collections from Cobban and others (1974). Interval colored black in the lithologic column is a Fruitland coal bed. From Fassett and Steiner (1997).

carbonate. In spite of its thinness, it was possible to collect two samples of this bed: the first from the lower, purer clay part and the second from the upper part that appeared to be contaminated by reworked Lewis Shale. These samples, CR(1) and CR(2) in table 4, have coarser and finer sandine-crystal fractions and the lowermost sample, CR(1), contains the coarser fraction, as would be expected for an air-fall deposit.

Age of Ash Bed CR

Two single-crystal ⁴⁰Ar/³⁹Ar ages were obtained for samples CR(1) and CR(2) from the Chimney Rock site. Table 4 shows the weighted mean age for the two samples with a resultant mean age for the CR ash bed of 74.23±0.13 Ma.

La Plata Mine Ash Bed

An altered volcanic ash bed about 14 inches thick was collected near the top of a thick coal bed in the lower part of the Fruitland Formation at the La Plata coal mine (fig. 2). This ash bed, labeled LP (for La Plata mine), is estimated to be 980 ft above the Huerfanito Bentonite Bed. Table 4 shows the analytical data for this ash bed and its resultant mean age of 74.30±0.35 Ma.

Ammonite Zonation of Lewis Shale at Chimney Rock Site

Ammonite collections from the Chimney Rock area were reported by Cobban and others (1974) and Fassett (1987).

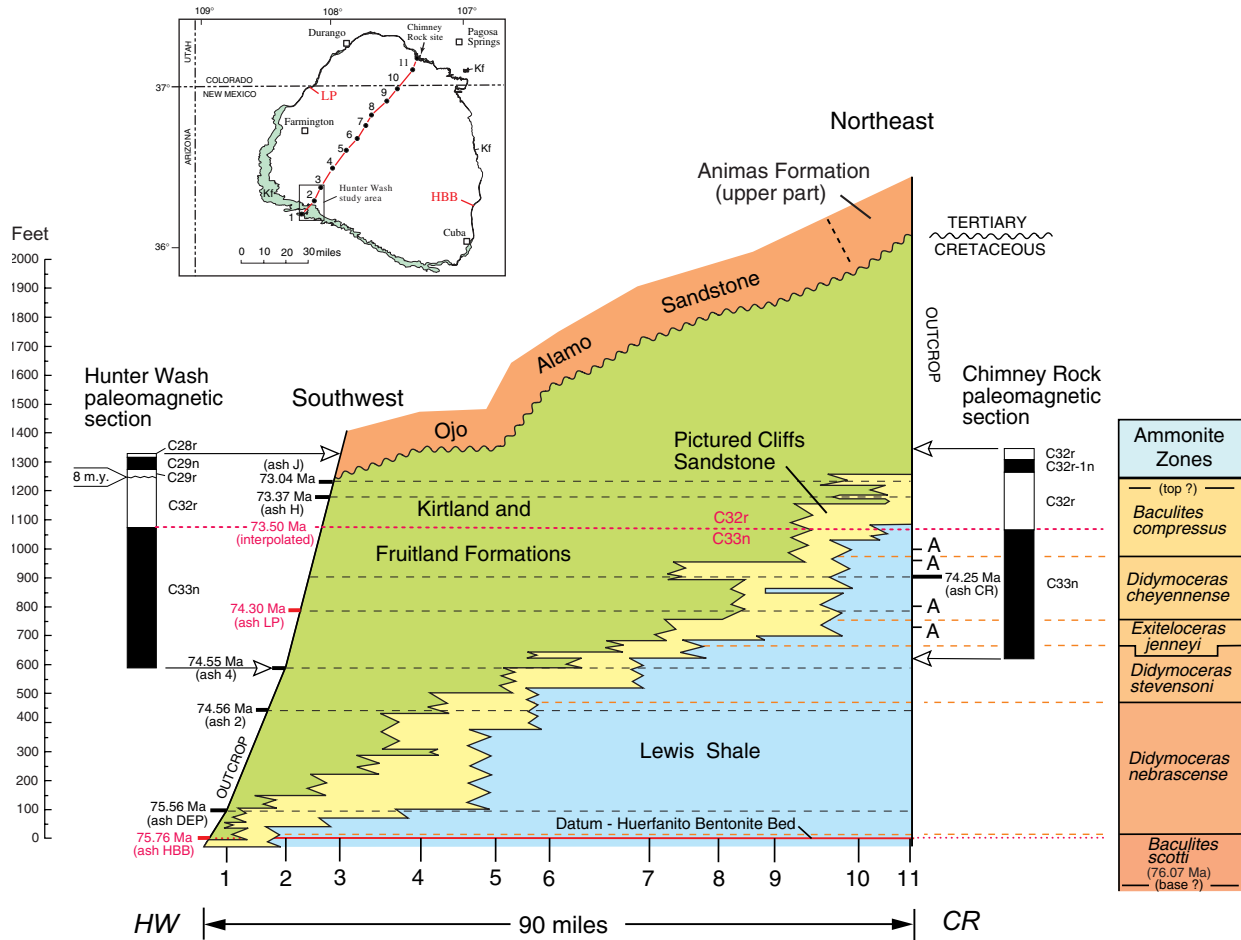


Figure 13. Stratigraphic cross section from Hunter Wash to Chimney Rock (modified from Fassett and Steiner, 1997, fig. 4). Ash-bed sample localities are shown on index map. Ash-bed ages are from tables 1 and 4. Ash-bed ages shown in red are projected into the Hunter Wash section. Letters A at the Chimney Rock section show levels of ammonite collection sites. Lower ammonite-zone boundaries are modified from Fassett (1987). On magnetic chron sections, black is normal polarity, white is reversed polarity. Vertical exaggeration is 200 x. Age of magnetic-polarity reversal of 73.50 Ma is the mean of six interpolated reversal ages based on the five dated ash beds from the Hunter Wash locality (fig. 16).

More recent ammonite collections near Chimney Rock by Fassett and Cobban were reported in Fassett and Steiner (1997). Figures 12 and 13 show the stratigraphic levels of these ammonites collections and show the boundaries of the *Exiteloceras jenneyi*–*Didymoceras cheyennense* and *D. cheyennense*–*Baculites compressus* ammonite zones at this locality.

Magnetic Polarity

The same magnetic-polarity reversal, from normal to reversed polarity (chron C33n to C32r), that was found at the Hunter Wash area in the continental Farmington Sandstone Member of the Kirtland Formation was found in the uppermost marine Lewis Shale in the Chimney Rock area. (A more detailed discussion of the paleomagnetic polarity at the Chimney Rock site is in Fassett and Steiner, 1997.) Figure 12 shows the paleomagnetic data obtained at the Chimney Rock site.

The magnetic-polarity reversal from chron C33n to C32r is estimated to be 1,066 ft above the Huerfanito Bentonite Bed at the Chimney Rock site, virtually at the same stratigraphic level above the Huerfanito Bed as at the Hunter Wash site.

Summary of Chronostratigraphy

Ammonite Zones in Upper Lewis Shale

Figure 13 shows a northeast-trending stratigraphic cross section from Hunter Wash to the Chimney Rock area. All of the chronostratigraphic data discussed herein are summarized on this illustration. On the right side of this figure, the Western Interior ammonite zones are shown for the time represented by regression of the Pictured Cliffs Sandstone shorelines across the San Juan Basin. These ammonite-zone boundaries, first

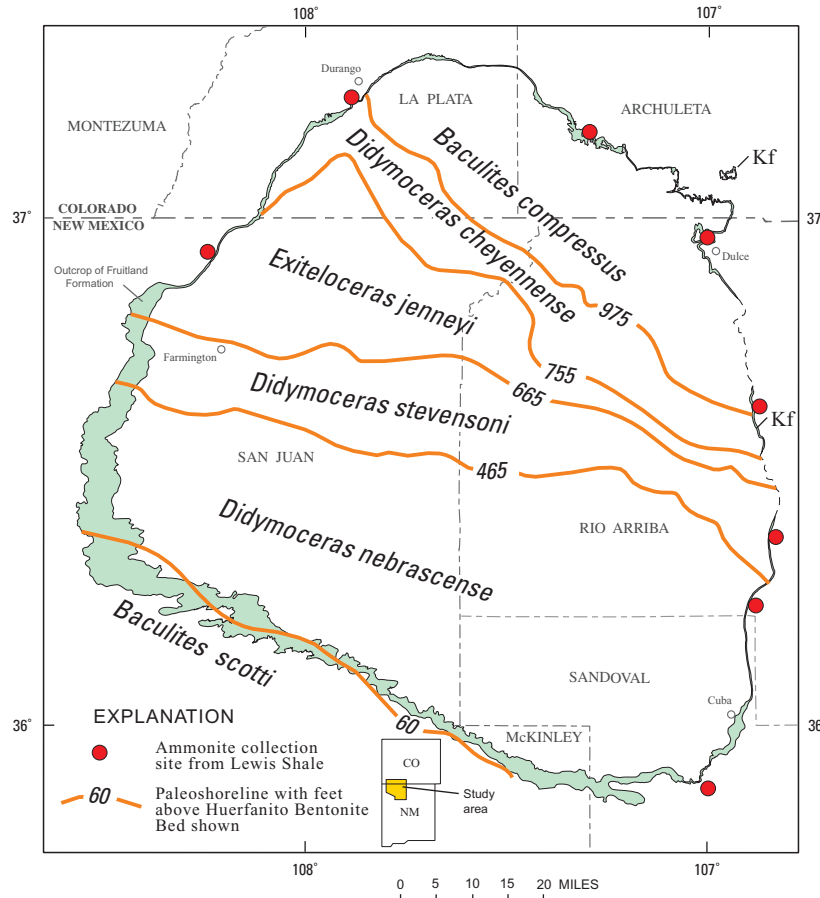


Figure 14. Bio-isochrone map showing positions of Pictured-Cliffs-seaway shorelines at times of first and last appearances of Western Interior ammonites in the upper Lewis Shale in late Campanian time. Paleo-shoreline positions are estimated based on positions of isopach lines of figure 8. Kf, Fruitland Formation This map is a modification of figure 5 of Fassett (1987).

shown in Fassett (1987), have been modified in this report on the basis of additional ammonite collections from the Chimney Rock and Regina sites (figs. 2 and 6). The distances of the five ammonite zone boundaries above the Huerfanito Bed (fig. 13) are plotted on the bio-isochrone map shown on figure 14. This map shows the positions of successive Pictured Cliffs Sandstone shorelines at times when the various Western Interior ammonites shown appeared or disappeared in the San Juan Basin. For example, at the time the shoreline was at the 60-ft contour line position, the Western Interior ammonite zone fossil *Baculites scotti* had become extinct and *Didymoceras nebrascense* first appeared. This bio-isochrone map provides a useful tool for visualizing the regression of the Pictured Cliffs Sandstone shoreline across the San Juan Basin relative to the evolution of late Campanian ammonites.

Ash-Bed Ages

Figure 15 is a chart showing the uncertainty ranges for the $^{40}\text{Ar}/^{39}\text{Ar}$ ash-bed ages discussed above. Uncertainties range

from ± 0.13 m.y. for ash beds 2 and CR to ± 0.41 m.y. for ash DEP. The greatest uncertainty is ± 0.41 m.y. for ash DEP; the age of this ash was determined using the multiple-crystal method.

Age of Magnetic Polarity Reversal from C33n to C32r

Fassett and Steiner (1997) estimated the age for the magnetic-polarity reversal (C33n to C32r) to be 73.50 ± 0.18 Ma on the basis of interpolation between five dated ash beds collected in the Hunter Wash area that bracketed the reversal (fig. 13). Subsequent to that study, ash bed 4, which had been first dated using multicrystal methodology was redated using single-crystal procedures, and its age has changed from 74.11 ± 0.64 Ma to 74.55 ± 0.29 Ma (table 4 and fig. 15). In addition, the age of ash bed LP (La Plata mine ash bed) is used in this report to calculate the age of the C33n-C32r reversal. Figure 16 is a chart showing the eight known $^{40}\text{Ar}/^{39}\text{Ar}$ dated ash beds in the Fruitland and Kirtland Formations of the San Juan Basin projected into the magnetic polarity column at

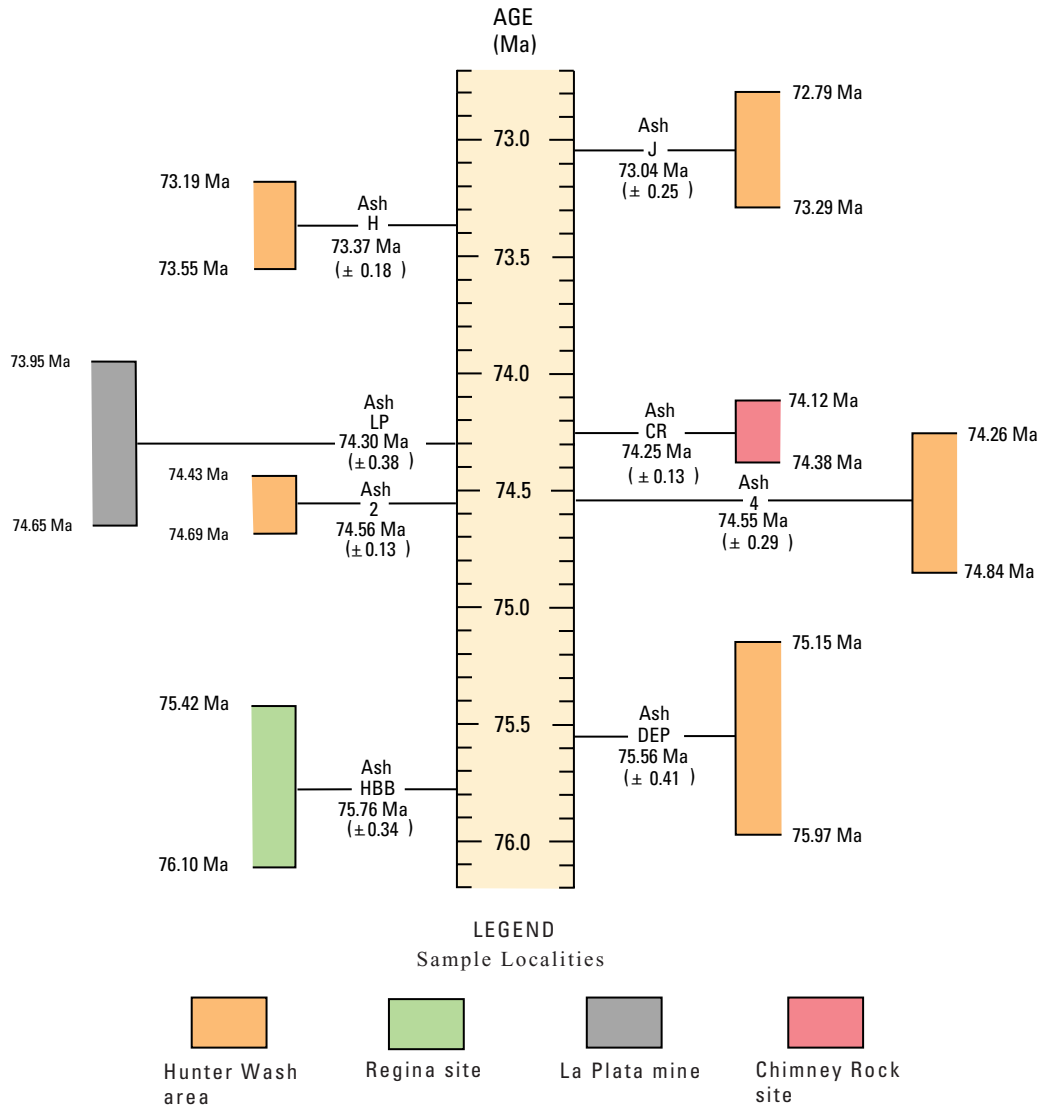


Figure 15. Chart showing uncertainty ranges for dated ash beds in the San Juan Basin. Ash-bed ages are from tables 1 and 4; all ages (except for ash DEP) are based on single-crystal ⁴⁰Ar/³⁹Ar analyses of sanidine crystals from altered volcanic ash beds. Age for ash DEP is based on a multiple-crystal age determination. Sample localities are shown on figures 2, 9, and 13.

Hunter Wash. Five of the ash beds, J, H, 4, 2, and DEP are located in an area of continuous exposure of the Fruitland and Kirtland about 12 mi long in the Hunter Wash study area (figs. 9, 10). Figure 16 shows the interpolated age of the C33n-C32r reversal using two dated ash beds above the reversal (J and H) and six dated ash beds below the reversal (CR, LP, 4, 2, DEP, and HBB). As figure 16 shows, 12 age interpolations for the reversal are possible based on these dated ash beds. The results range from 73.39 Ma for bracketing ashes J and 2, to 73.71 Ma for ashes H and CR for a very tight spread of only 0.32 m.y. The mean age for all 12 interpolations is 73.54±0.17 Ma

If only the ages of the five ash beds in the Hunter Wash area are considered, six interpolated ages for the magnetic-polarity reversal result (fig. 16). The range of these six ages is

from 73.39 to 73.61 for a spread of 0.22 m.y. The mean age for the six interpolated Hunter Wash reversal ages is 73.50±0.19 Ma, the same age reported by Fassett and Steiner (1997).

At the Chimney Rock site, the C33n-C32r magnetic polarity reversal and dated ash CR are present in the same measured section (fig. 13). The reversal cannot be dated by extrapolation at Chimney Rock because the rate of sediment accumulation for the interval between the reversal and ash bed CR is not known. The rock-accumulation rate for the interval between ashes CR and HBB at Chimney Rock is 602 ft/m.y. (fig. 17B), however, calculations based on data from the Hunter Wash site clearly indicate that the rock rate for this interval is extremely variable ranging from 475 to 1,285 ft/m.y. (fig. 17A). Thus, the rate of 602 ft/m.y. is only an

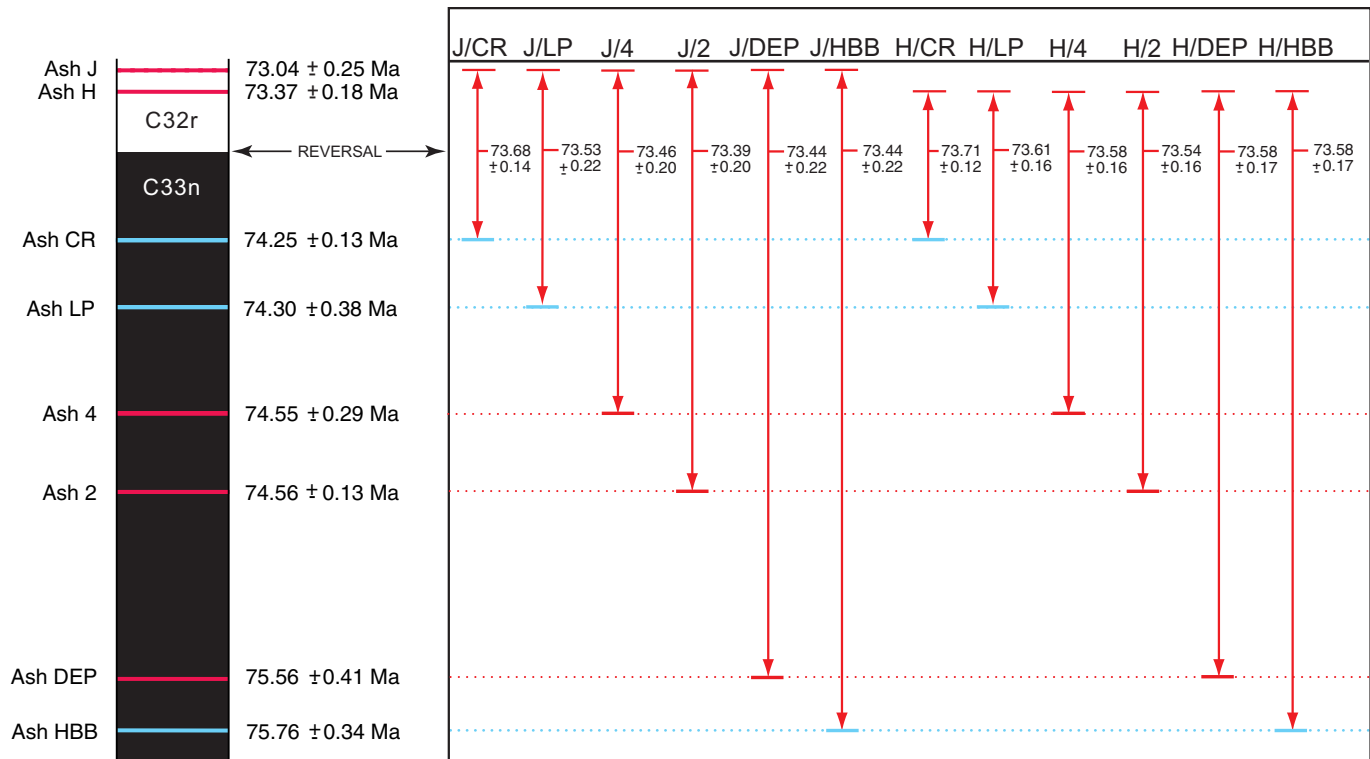


Figure 16. Interpolated ages and uncertainties (in millions of years) for magnetic polarity reversal C33n-C32r in the Hunter Wash area. Black is normal polarity, white is reversed polarity. Mean interpolated age of the reversal using all ash beds is 73.54 ± 0.17 Ma; mean age for the five Hunter Wash ash beds is 73.50 ± 0.19 Ma. Ash beds shown in blue are projected into the Hunter Wash section. Ash-bed ages are from tables 1 and 4. Ash-bed localities are shown on figure 13.

average and has no value for extrapolating the rock rate above ash CR.

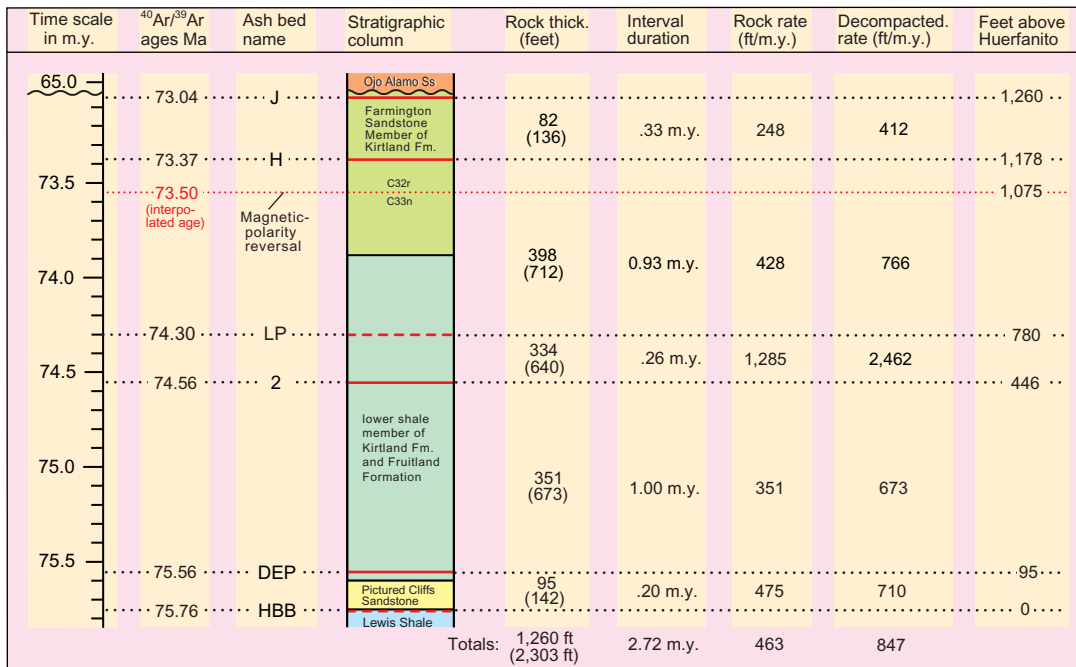
The age of the reversal at Chimney Rock can be estimated by projecting the two ashes stratigraphically higher than the CR ash bed in the Hunter Wash area to the Chimney Rock area (fig. 13) and interpolating between these projected ages. Figure 16 shows the results of these interpolations to be 73.68 ± 0.14 Ma for ashes J/CR and 73.71 ± 0.12 Ma for ashes H/CR, within 0.18–0.21 m.y. of the reversal age of 73.50 Ma calculated at Hunter Wash. Because the C33n-C32r paleomagnetic reversal was a geologically instantaneous event, it must be the same age at Chimney Rock as at Hunter Wash: 73.50 ± 0.19 Ma. On the basis of this age, the rock-accumulation rate for the interval between ash bed CR and the reversal is 209 ft/m.y. and the sediment-accumulation rate is 375 ft/m.y. at the Chimney Rock locality (fig. 17B).

The range for all calculated ages for the polarity reversal C33n-C32r at Hunter Wash and Chimney Rock (73.39 Ma to 73.71 Ma, fig. 16) is only 0.32 m.y. This extremely tight grouping provides confidence in the accuracy of the age-determination process. It must be emphasized, however, that all of the calculations described above are based on an assumption of a linear rate of sediment accumulation between dated ash beds, and, as figure 17 illustrates, this is probably not the case. Fortunately, with eight dated ash beds distributed over a rock interval of 1,260 ft, potential errors due to changes in sediment-accumulation rates within intervals between the

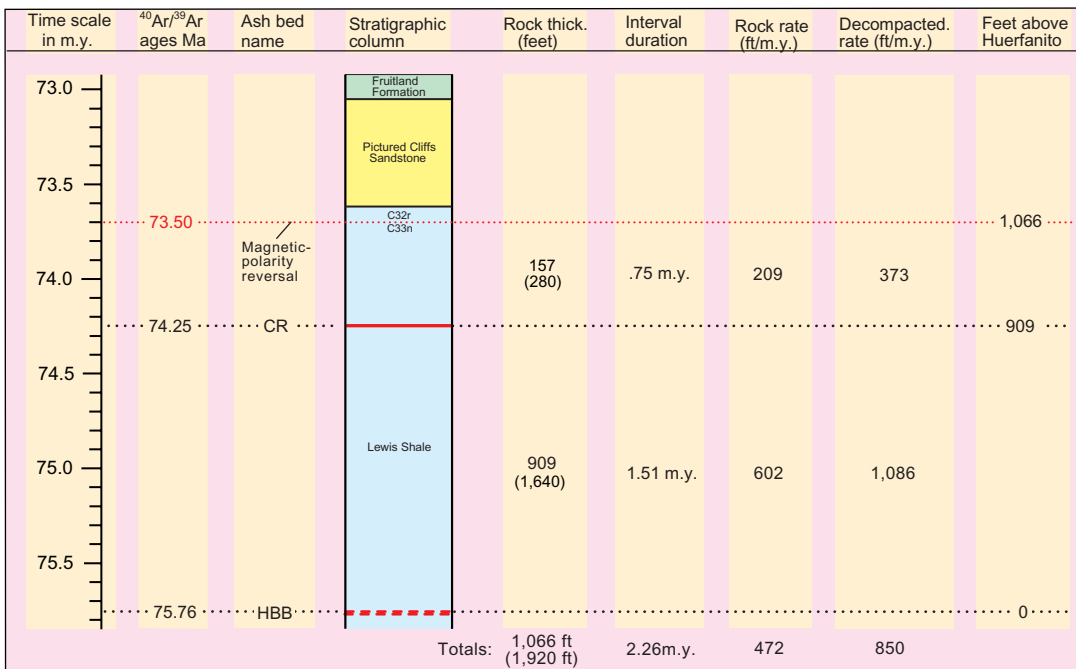
ash beds are minimized. Also, the geometry of the Pictured Cliffs Sandstone, as portrayed in map view (fig. 8) and cross section (fig. 13 and plate 1), provides an independent check on changes in sediment-accumulation rates. The age of the magnetic-polarity reversal from chron C33n to C32r in the San Juan Basin as determined in this report of 73.50 ± 0.19 Ma. confirms the age determination of Steiner and Fassett (1997) of 73.50 ± 0.18 Ma. The biochronologic age of the C33n-C32r reversal in terms of Western Interior ammonite zones is *B. compressus* (fig. 13).

Rates of Sediment Accumulation and Pictured Cliffs Shoreline Regression

Figures 17A and 17B are chronostratigraphic charts for the Hunter Wash and Chimney Rock areas, respectively. Rates of sediment accumulation (decompacted rates) for the Hunter Wash area (fig. 17A) vary from a low of 412 ft per million years for the interval between ashes H and J to a rate of 2,462 ft per million years for the interval between ashes LP and 2. The sediment-accumulation rate for the Chimney Rock area (fig. 17B) between beds HBB and CR is 1,086 ft/m.y., and between CR and the C33n-C32r reversal it is 373 ft/m.y. (fig. 17B). The overall average rate of sediment accumulation for the time of Pictured Cliffs Sandstone regression across the present basin area is 847 ft/m.y. at Hunter Wash and 850 ft/m.y. at Chimney Rock (fig. 17).



A - Hunter Wash area



B - Chimney Rock area

Figure 17. Chronostratigraphic charts for *A*, Hunter Wash area, and *B*, Chimney Rock area. Ages of ash beds, thicknesses of intervals between dated ash beds, and distances above the Huerfanito Bentonite Bed for dated ash beds are shown. Ash bed 4 is not shown because it has the same age as ash 2 and the age for ash 2 is more precise. Rock rates (duration in m.y./thickness of rock interval) and rates of sediment accumulation (duration in m.y./decompacted rock thickness) are also shown. Decompacted rock thicknesses are shown in parentheses in "Rock thick." column; these thicknesses were estimated from data generated by the BasinMod software program. Ash beds shown with dashed line are projected into the sections. Ash-bed collection localities are shown on figure 13.

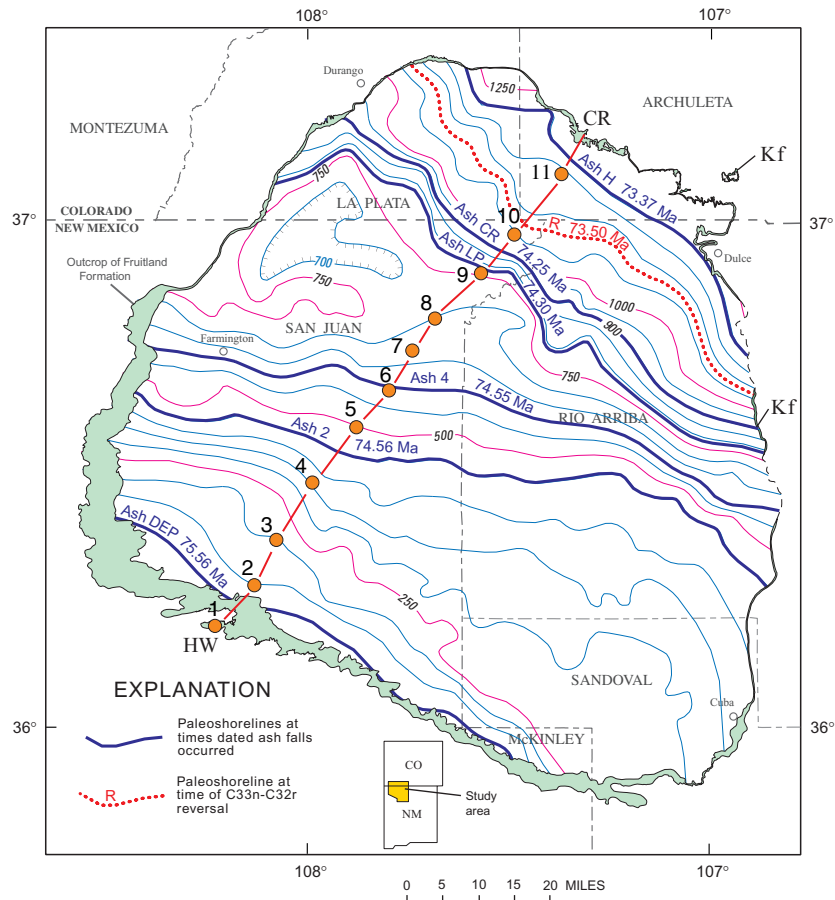


Figure 18. Map showing positions of Pictured Cliffs Sandstone shorelines at times when dated San Juan Basin ash beds were deposited and when paleomagnetic reversal C33n-C32r occurred. Ages of ash beds from table 4. Kf, Fruitland Formation; HW, Hunter Wash; CR, Chimney Rock. Cross section HW-CR is on figure 13. Huerfanito-Pictured Cliffs isopach lines from figure 8.

The large volcanic eruptions that produced the Hunter Wash, Chimney Rock, and La Plata mine ash beds were random events. Not all ash falls that occurred in Campanian time are preserved in the rock record, and not all ash falls that are preserved contain sanidine crystals that can be radiometrically dated. Rates of sediment accumulation between dated ash falls, therefore, are averages for random intervals, and the ash beds themselves in no way mark boundaries where changes in rates of sediment accumulation took place as figure 17 might appear to indicate.

Figure 18 shows the approximate positions of Pictured Cliffs shorelines at the times ash beds DEP, 2, 4, LP, CR, and H were deposited. (The shoreline position for ash bed J is at the 1,260-ft level above the Huerfanito Bed and is thus at or just beyond the outcrop of the Fruitland Formation in the northeast part of the basin.) Shoreline positions corresponding to dated volcanic ash beds (ash falls) are projected on the Huerfanito-Pictured Cliffs Sandstone isopach map (fig. 18) based on their distances above the Huerfanito Bentonite Bed (fig. 17). The distance between the Pictured Cliffs shoreline

position at the time ash DEP was deposited and its position when ash 2 was deposited is about 25 mi, measured along the line of cross section HW-CR (fig. 18). The time difference between these ash beds is 1 m.y.; thus the average rate of shoreline regression for this interval was 25 mi/m.y. (Ash beds 2 and 4 have essentially the same ages, thus, the time interval between them cannot be used to determine rates of shoreline regression. Similarly, ash beds LP and CR have virtually the same age and so cannot be used to measure rates of shoreline regression.) The distance between shorelines 2 and CR is 37 mi with a time difference of 0.31 m.y. for a regression rate of 119 mi/m.y. The distance between shorelines CR and H is 16 mi with a time difference of 0.88 m.y., yielding a regression rate of about 18 mi/m.y. The distance across the basin from shoreline DEP to shoreline H is 78 mi; the time difference between these two ash beds is 2.19 m.y. for an average shoreline regression rate of 36 mi/m.y.

In human terms, the average rate of Pictured Cliffs shoreline retreat from Hunter Wash to Chimney Rock was 0.04 mi, or 211 ft per thousand years, 2.11 ft per 100 years, or .02 ft or

0.2 inch per year. The average rate of sediment accumulation during this same time period was 925 ft per million years, 0.93 ft or about 11 inches per thousand years, 0.9 inch per 100 years, or 0.009 inch per year. (This thickness is equal to about the lower end of the diameter of a fine-grained particle (¼ mm) on the Wentworth scale. Thus to move the shoreline back 0.2 inch in a year required a sediment delivery rate to the shoreline equivalent to a thickness of 0.009 inch or a layer of very fine to fine-grained sandstone one grain thick.)

Comparing the shoreline-position map of figure 18 with the cross section HW-CR on figure 13, the period of relatively slow deposition (673 ft/m.y., fig. 17) and slow regression (25 mi/m.y.) between ash beds DEP and 2 corresponds to the large vertical buildup and thickening of the Pictured Cliffs Sandstone between wells 1 and 4 on figure 13. Between shoreline positions 2 and CR (fig. 18) the rate of sediment accumulation was high (2,700 ft/m.y.) and the rate of shoreline regression was fast (119 mi/m.y.). In cross section (fig. 13), the Pictured Cliffs is relatively thin from about well 4 to between wells 8 and 9, reflecting this episode of rapid sediment accumulation and rapid shoreline regression. Between shoreline positions CR and H, the sediment-accumulation rate decreased (550 ft/m.y.) and the rate of shoreline regression slowed to 18 mi/m.y. Figure 13 again reflects these changes with a large vertical rise in the stratigraphic level of the Pictured Cliffs Sandstone between wells 9 and 11. These changes in the rates of sediment accumulation and shoreline regression had a profound affect on the accumulation and distribution of coal in the Fruitland Formation, as will be discussed in detail in the "Fruitland Coal Resources" section of this report.

Rate of Subsidence of San Juan Basin Area During Pictured Cliffs Time

Figure 19 shows the location of the San Juan Basin area on the western edge of the Western Interior Seaway during the time the Pictured Cliffs Sandstone shoreline regressed across the basin area. Sediment accumulation and shoreline movements in the San Juan Basin area were controlled by two principal variables: the rate of creation of accommodation space and the rate of sediment delivery to the shoreline by rivers. The creation of accommodation space has two basic components—tectonic subsidence and eustatic sea-level change. Jervy (1988) observed, in his general discussion of the concept of accommodation space, that if the rate of subsidence greatly exceeded the rate of sea-level rise or fall, then no apparent change in the rate of creation of accommodation space would result from changes in sea level. In his words (p. 47, 48), "At points in the basin where extremely rapid subsidence prevails, no decrease in accommodation is experienced, even though sea level is falling." Because the rates of subsidence in the San Juan Basin (and, indeed, in much of the Western Interior Seaway) were extremely rapid throughout much of Late Cretaceous time, changes in eustatic sea level that may have occurred would have had no perceptible affect on the creation of accommodation space. Thus, accommodation-

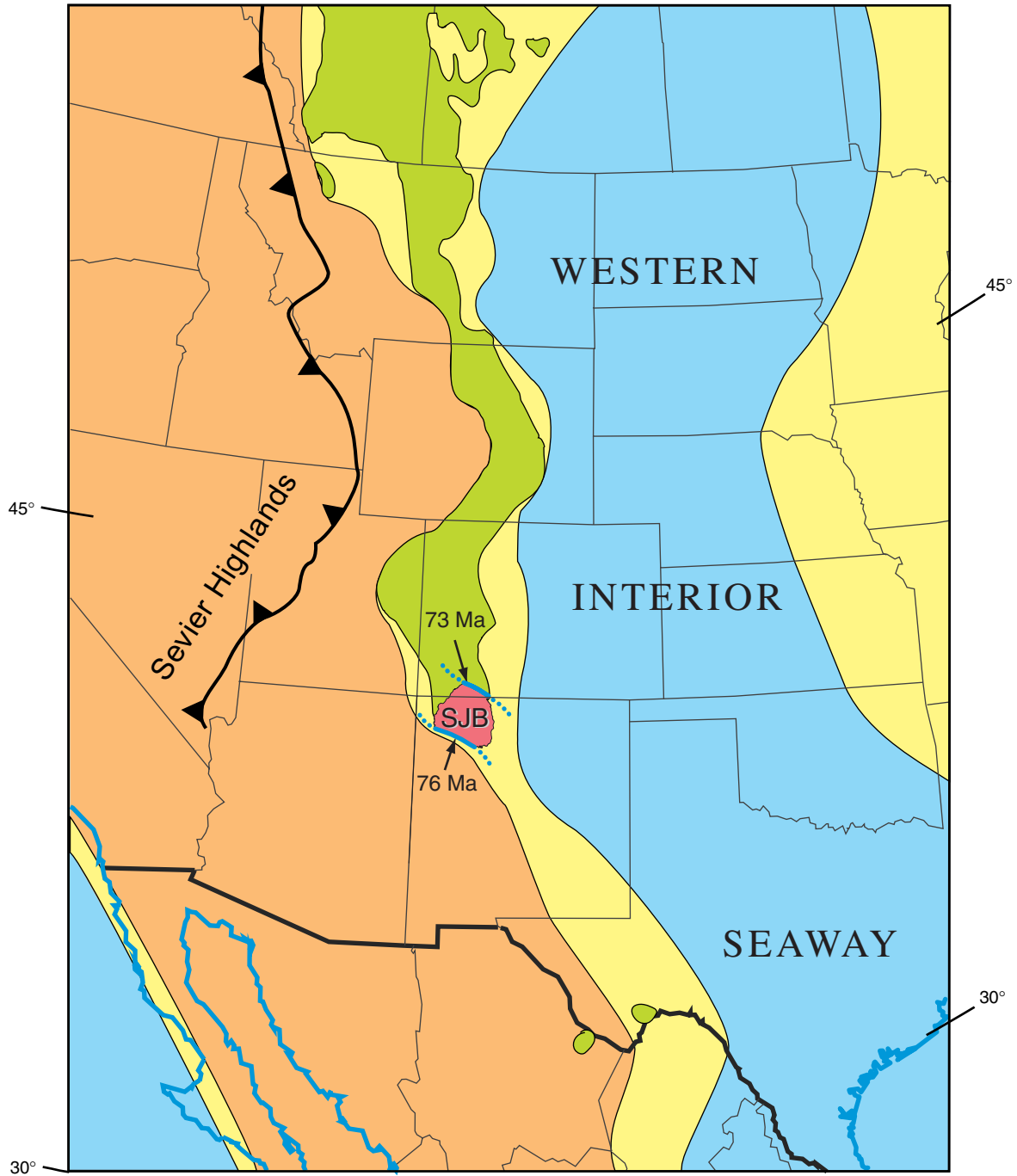
space creation in the San Juan Basin during the time that the Pictured Cliffs Sandstone was being deposited was essentially controlled by the rate of subsidence.

The average rate of sediment accumulation during Pictured Cliffs regression was 850 ft/m.y. (fig. 17) and the rate of shoreline movement averaged 36 mi/m.y. Because the shoreline regressed 78 mi across the basin area (fig. 18) between about 76 Ma and 73 Ma (fig. 19), the rate of sediment influx during this time period must have exceeded the rate of basin subsidence. To try and separate the rate of basin subsidence from the sediment-supply rate, it is necessary to focus on segments of the rock record that record times when shoreline regression ceased and shoreline transgression occurred because, at those times, sediment-accumulation rates must have been lower than subsidence rates.

Plate 1 shows that there are two places in the basin where the Pictured Cliffs Sandstone is significantly thicker and intertongues with the overlying Fruitland Formation: between holes 15 and 17 and between holes 17 and 20. The tongues of Pictured Cliffs Sandstone in the Fruitland at hole 16 and at holes 18 and 19 (plate 1) represent times when the rate of sediment accumulation must have been less than the rate of basin subsidence, causing the Pictured Cliffs shoreline to halt its regression and briefly transgress over the backshore swamp deposits of the Fruitland. Figure 13 shows the stratigraphic positions of the dated ash beds discussed in this report. Fortunately, the intervals between ash bed CR and the C33n-C32r reversal (between holes 7 and 10) and ash beds H and J (in holes 10 and 11) on figure 13 include tongues of Pictured Cliffs Sandstone that represent transgressions of the shoreline.

The interval between ash bed CR and the C33n-C32r reversal (between holes 7 and 10, fig. 13) contains, in its lower part, a large Pictured Cliffs Sandstone tongue in the Fruitland that represents a significant southwestward transgression of the Pictured Cliffs shoreline nearly to hole 7. The top of this tongue represents an extremely rapid regression of the shoreline to a position northeast of hole 9 and then a stabilization of the location of the shoreline to well above the level of the C33n-C32r reversal. Stratigraphically, this interval can be divided into successive episodes of (1) shoreline transgression, (2) rapid regression, and (3) shoreline stabilization. Because 373 ft/m.y. is an average sedimentation rate for this interval (fig. 17B), the time of transgression of the Pictured Cliffs tongue in the lower part of this interval must represent a period of sediment accumulation less than the average of 373 ft/m.y., possibly 350 ft/m.y. Therefore, the basin-area subsidence rate must have been approximately 350–375 ft/m.y. during this time interval.

The interval between ash beds H and J (in holes 10 and 11, fig. 13) contains two transgressive tongues of Pictured Cliffs separated by vertical upbuilding of the Pictured Cliffs representing times of (1) a brief transgression of the shoreline, (2) rapid regression, and (3) a longer episode of shoreline transgression and stabilization. Because the average sedimentation rate for this interval is 412 ft/m.y., the times of transgression of the Pictured Cliffs tongues in this interval must



EXPLANATION








- | | | | | | | | |
|-------------------------------------------------------------------------------------|------------------------------|-------------------------------------------------------------------------------------|---------------------|-------------------------------------------------------------------------------------|-----------------------|---------------------------------------------------------------------------------------|---------------------------------|
|  | Alluvial plain and highlands |  | Coal-forming Swamps | | 30° Paleolatitude | | USA-Mexico border |
|  | Shoreface |  | Shallow marine |  | Thrust fault |  | Paleoshorelines, San Juan Basin |
| | | | |  | Present-day shoreline | | |

Figure 19. Paleogeographic map of western North America in latest Campanian time: 79 to 72 Ma (Late Cretaceous). Position of San Juan Basin (SJB) is shown in red. Paleoshoreline positions and ages for the Pictured Cliffs Sandstone in vicinity of San Juan Basin are shown. Map is modified from figure 19 of Roberts and Kirschbaum (1995).

represent times of sediment accumulation less than the average of 412 ft/m.y., possibly 350 ft/m.y. Therefore, the basin-area subsidence rate must have been approximately 350–412 ft/m.y. during this time interval. The rate of subsidence of the San Juan Basin area during the regression of the Pictured Cliffs Sandstone shoreline is thus estimated to have been about 375 ft/m.y. When the rate of sediment supply exceeded 375 ft/m.y., regression occurred; when it fell below this threshold, transgression of the Pictured Cliffs shoreline took place.

Depositional Model for Lewis/Pictured Cliffs/Fruitland System

This Report

As discussed above, two principal interactive processes control rates of shoreline regression: the rate of creation of accommodation space and the rate of sediment influx. Figure 20 is a diagrammatic portrayal, in cross section, of the dynamics of the deposition of the Pictured Cliffs Sandstone and associated rocks during the time that the Pictured Cliffs shoreline regressed across the basin area. This figure is greatly simplified in order to focus on the basic elements of this depositional model. In the three panels, the downward-pointing arrows are meant to indicate a constant and even subsidence rate for the basin area throughout the time represented. At time A, the shoreline is at the extreme left side of the diagram and the volcanic ash fall that will ultimately become the Huerfanito Bentonite Bed has just been deposited on the seafloor. From time A to time B, sediment influx has exceeded the rate of subsidence and the shoreline has migrated to the right to about the middle of the diagram. Between times A and B, sediment has been more or less uniformly distributed across the entire area. At time B, continental sediments are accumulating on the left, marine shoreface sediments in the center, and offshore marine rocks are accumulating to the right. Note that the subaerial surface of deposition is essentially continuous with the shoreface and submarine surfaces of deposition and the combined surfaces have the same slope. (The beach environment is shown as being slightly elevated above the backshore area; the magnitude of this elevation is greatly exaggerated on this diagram.)

As the shoreline regressed, sediment was being deposited simultaneously in the continental, shoreface, and marine environments. Sediment size graded from the beach environment where relatively well sorted, fine- to medium-grained sandstones were being deposited out into the marine realm where clay-sized material was being distributed evenly across the shelf. The continuous continental-shoreface-marine surface of deposition was, of course, always a time line in cross section and a time plane in three dimensions. Note that in the panel representing time B, this surface of deposition is parallel to the Huerfanito Bentonite Bed. Another hypothetical time line is shown in the time B panel to emphasize the parallelism of

depositional surfaces in this model.

At time C (fig. 20) the shoreline had regressed all the way to the right side of the diagram. During this period of regression, sediment influx continued to exceed the rate of subsidence and sediment was evenly dispersed across the continental-shoreface-marine surface of deposition. From time B to time C, the surface of deposition maintained a consistent slope, resulting in time lines and planes continuing to be parallel surfaces so that the surface of deposition at time C was still parallel to the Huerfanito Bentonite Bed. A comparison of the stratigraphic cross section on figure 13 drawn with the Huerfanito as a datum shows the same basic relations of the continental, shoreface, and marine rocks as shown on the time-C panel of figure 20. The validity of this model of deposition for the Lewis/Pictured Cliffs/Fruitland is confirmed by the two isochrons shown on figure 13: the Huerfanito Bentonite Bed and the magnetic polarity reversal from chron C33n to C32r are essentially parallel as the depositional model depicted on figure 20 predicts.

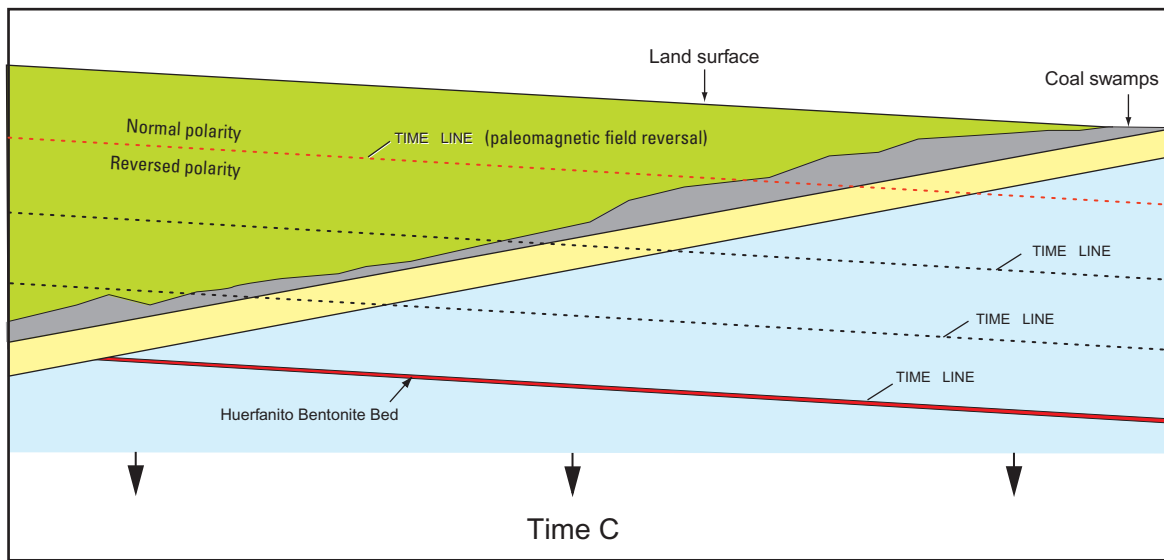
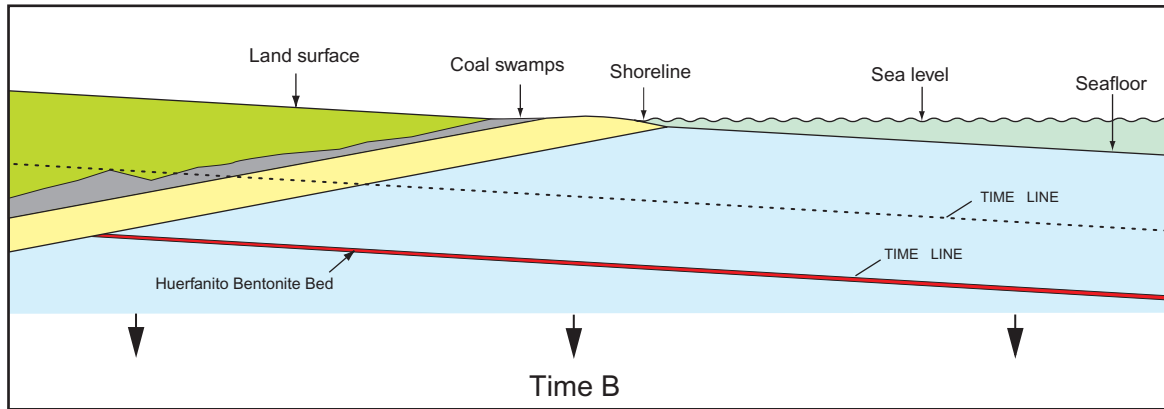
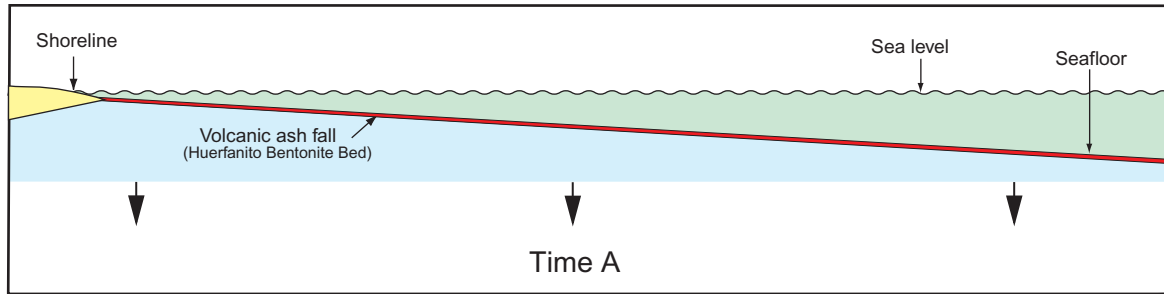
Ayers Model

A new and substantially different model for deposition of the Fruitland Formation, its coal beds, and associated rocks was presented by Ayers and Ambrose (1990) and Ayers and others (1994). This model (herein called the Ayers model) suggested that differential tectonism within the San Juan Basin had controlled the regression of the Pictured Cliffs Sandstone shoreline and accumulation of Fruitland coal beds. The Ayers model was offered as an alternative to the model for deposition of the Fruitland Formation and associated rocks presented in Fassett and Hinds (1971). (The Fassett and Hinds model is essentially the same as the model of this report.)

Whitehead (1993, figs. SJ 1.7, SJ 1.10) presented the Ayers model as a valid alternative to the model of Fassett and Hinds (1971). In a discussion of the origin of Fruitland Formation coal beds in the San Juan Basin, Whitehead stated (p. 119),

These coal deposits are interpreted (Ayers et al., 1991) [*sic*—the date for this citation is actually 1990] as coastal swamps that accumulated landward of the wave-dominated Pictured Cliffs shoreline. Increased subsidence northeast of an inferred hingeline created accommodation space allowing thick, strike-elongate Pictured Cliffs sandstones and Fruitland peats to form (Ayers and Zellers, 1988; fig. SJ-1.10a). In this model, coal beds are extensive and may override Pictured Cliffs barrier sandstones. Alternatively, uniform aggradation of the area has been proposed (fig. SJ-1.10b) using the Huerfanito Bentonite as a datum (Fassett and Hinds, 1971; Fassett, 1987). In this model, coal seams terminate against the Pictured Cliffs sandstone tongues, and thus the coal beds are much less extensive.

Because two conflicting models have been offered for deposition of the Pictured Cliffs Sandstone, the Fruitland Formation and its contained coal beds, and associated rocks, it is necessary to evaluate and compare these models to determine which one best fits the available data.



EXPLANATION

	Continental		Shoreface
	Coal-bearing		Marine

Figure 20. Diagrammatic time-sequence diagrams showing in cross section the deposition of a regressive shoreface sand and associated marine and continental sediments at three points in time. The arrows at the bottom of each sequence are meant to indicate continuous, even subsidence of the basin area as these rocks were being deposited. After Fassett (1987).

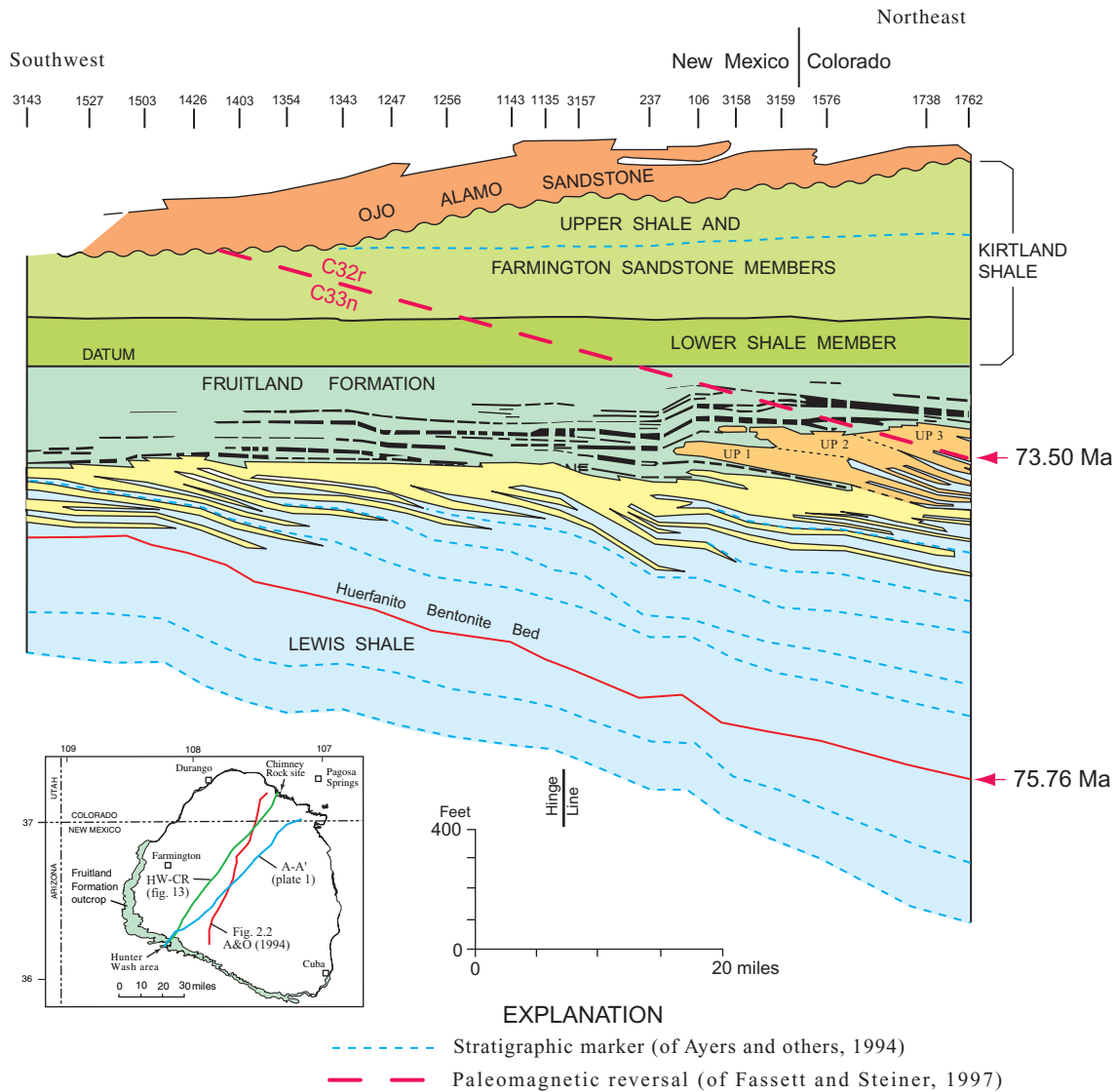


Figure 21. Stratigraphic cross section redrawn from Ayers and others (1994, fig. 2.2); vertical exaggeration is 132 x. Line of this section is labeled “Fig. 2.2 A&O (1994)” on index map. Vertical breaks in coal beds indicate fractures in continuous coal beds, according to Ayers and others. Paleomagnetic reversal from normal polarity (C33n) to reversed polarity (C32r) has been drawn on this cross section to show the true attitude of a time line in this rock sequence. Magnetic polarity data and radiometric ages are from Fassett and Steiner (1997). “HW-CR (fig. 13)” on index map is line of section for stratigraphic cross section on figure 13 of this report. “A-A’ (plate 1)” on index map is line of section for cross section A-A’ on plate 1 of this report.

Figure 21 shows a northeast-trending stratigraphic cross section across the San Juan Basin taken from Ayers and Ambrose (1990) and Ayers and others (1994). This cross section (figure 2.2 of Ambrose and Ayers, 1994) is described and discussed in detail in Ayers and Zellers (1994). The cross section is constructed using the contact between the Fruitland Formation and the lower shale member of the Kirtland Shale as a datum. The stratigraphic cross sections on plate 1 and figure 13 that illustrate the depositional model of this report have the same northeast orientation and are close to the line of section of figure 21 of the Ayers reports; traces of the three sections are shown on the index map on figure 21.

Ayers and Zellers (1994) discuss the depositional setting for the Pictured Cliffs Sandstone and the Fruitland Formation and state (p. 73), “Principal aspects of these relations are summarized ... in the depositional model (Ayers and others, this volume, fig. 2.20).” They discuss the geologic history of the Pictured Cliffs Sandstone regression as follows (p. 83):

The Pictured Cliffs shoreline prograded rapidly basinward across the southern half of the basin. After the shoreline crossed the structural hingeline, sporadic structural activity began and the northern part of the basin subsided more rapidly to accommodate greater thickness of sediment. The changing balance between sediment input and pulsatory subsidence

north of the hingeline resulted in oscillation and aggradation of the shoreline, accounting for the most significant stratigraphic rise of the Picture Cliffs in the basin Further testing is needed to verify the existence of the structural hingeline; seismic studies would be especially useful.

The Ayers depositional model (fig. 21) is the first model to suggest that tectonic events caused the accumulation of thick, vertical buildups of the Pictured Cliffs Sandstone and thick Fruitland coals in the north-central San Juan Basin. Figure 21 shows the top of the Pictured Cliffs Sandstone as a relatively flat surface across the southwest half of the basin. In the north-central part of the basin, the top of the Pictured Cliffs is shown as gently curving downward. In the northeast part of the basin, three tongues of sandstone labeled upper Pictured Cliffs 1, 2, and 3 are shown stacked on top of the Pictured Cliffs proper. The Huerfanito Bentonite Bed is shown dipping into the Lewis Shale parallel to several other Lewis Shale "stratigraphic marker" beds. These beds are time lines, according to Ayers and others (1994), that represent deposits on successive, Lewis Shale clinoform surfaces. The datum for this cross section is the base of the lower shale member of the Kirtland Shale, a horizontal time line in continental deposits. Another "stratigraphic marker" and time line is shown in the Farmington Sandstone Member of the Kirtland Shale parallel to the lower shale member contact. Fruitland Formation coal beds are shown to be continuous across most of the length of this cross section and exhibit a stratigraphic rise over the sandstone unit labeled Pictured Cliffs 1, 2, and 3 in the northeast (correlations of Fruitland coal beds are discussed in detail in the "Fruitland Coal-Bed Correlations" sections of this report). Ayers and others attribute the geometry of the rock units shown on figure 21 to a tectonic bending of the basin area over a "hingeline" at the time these rocks were being deposited. (The location of the "hingeline" is shown at the bottom of their cross section (fig. 21); this "hingeline" is further discussed in the "Basin Structure" section of this report).

The depositional model illustrated by figure 21 can be criticized for many of its details but the basic nature of the model does not survive the simple test of superimposing the magnetic polarity reversal between magnetic chrons C33n and C32r on this illustration. As discussed in the "Upper Cretaceous Chronostratigraphy of the San Juan Basin" section of this report, the C33n-C32r magnetic-polarity reversal represents a virtually instantaneous geologic event and is thus a time plane in three dimensions. When this time line is drawn on figure 21 at its proper orientation at a level 1,076 ft above the Huerfanito Bed, it is clear that the portrayal of time lines on figure 21 by Ayers and others, especially in the continental Fruitland and Kirtland, is incorrect. If the Ayers and others model were correct, the C33n-C32r reversal would be within the Farmington Sandstone Member across the basin and would be parallel to the base of the lower shale member of the Kirtland Formation and the "stratigraphic marker" shown in the upper part of the Farmington Sandstone Member, which it clearly is not. The entire weight of the evidence compiled to date for the chronostratigraphy of the Lewis/Pictured Cliffs/

Fruitland depositional system supports the depositional model portrayed on figure 13.

Roberts and McCabe (1992, p. 119) also challenged the interpretation of Ayers and others and wrote:

Ayers and Zellers (1991) use the base of the Ojo Alamo Sandstone as a datum to show that Fruitland Formation coal beds migrated over Pictured Cliffs shoreline sandstones. However, the base of the Ojo Alamo Sandstone is an erosional surface that truncates underlying formations from northwest to southeast across the basin (Fassett and Hinds, 1971). In addition, the base of the Ojo Alamo is Tertiary in age whereas the Huerfanito Bentonite is much closer in age (Campanian) to the Fruitland and may be genetically related, as discussed above. We do not agree with Ayers and Zellers' (1991) premise that individual coal beds can be parallel to the Huerfanito Bentonite Bed only if the stratigraphic rise of the Fruitland Formation is due entirely to eustasy or to uniform basin subsidence: Fassett (1987) has clearly shown that the base of the Fruitland is diachronous.

Basin Structure

Huerfanito Bentonite Bed Structure

Figure 22 is a structure map of the San Juan Basin contoured on the Huerfanito Bentonite Bed of the Lewis Shale. Geophysical logs from 350 drill holes were used as control points for this map. The Huerfanito Bed is most easily distinguished in the southern two-thirds of the basin on conductivity logs. The Huerfanito 60-4 well (hole 9, plate 1), the type log for the Huerfanito Bentonite Bed (Fassett and Hinds, 1971, fig. 2, p. 6), shows the distinctive log signature of the Huerfanito Bed on the conductivity log. In the northern part of the basin, the gamma-ray log is a better tool to distinguish the Huerfanito on geophysical logs. (A more detailed discussion of the character of the Huerfanito Bentonite Bed on geophysical logs is in Fassett and Hinds, 1971, p. 6, 8, and fig. 3.) As discussed above, in some parts of the basin, primarily in the north-central part, there is no recognizable response to the Huerfanito on any geophysical logs, and it is thought that in those areas the ash fall was dispersed and destroyed by currents moving along the seafloor. Although Huerfanito control points are somewhat sparse in the northern part of the basin (fig. 22), there are still sufficient points to delineate the basin structure there. Because 100-ft contours do not add significant detail outside the 3,000-ft contour line, only 500-ft contour lines are shown on figure 22 in those areas.

The structural axis of the San Juan Basin is in the north-central part (fig. 22) where the basin floor is irregular. The deepest part of the basin is outlined by the 2,100-ft contour line in a relatively small northwest-trending area. The 2,200- and 2,300-ft contour lines show a northwest trend but bend around a southeast-trending structural nose (figs. 22, 23). Some smaller structural wrinkles are indicated by the 2,700- and 2,800-ft lines in the northwest part of the basin.

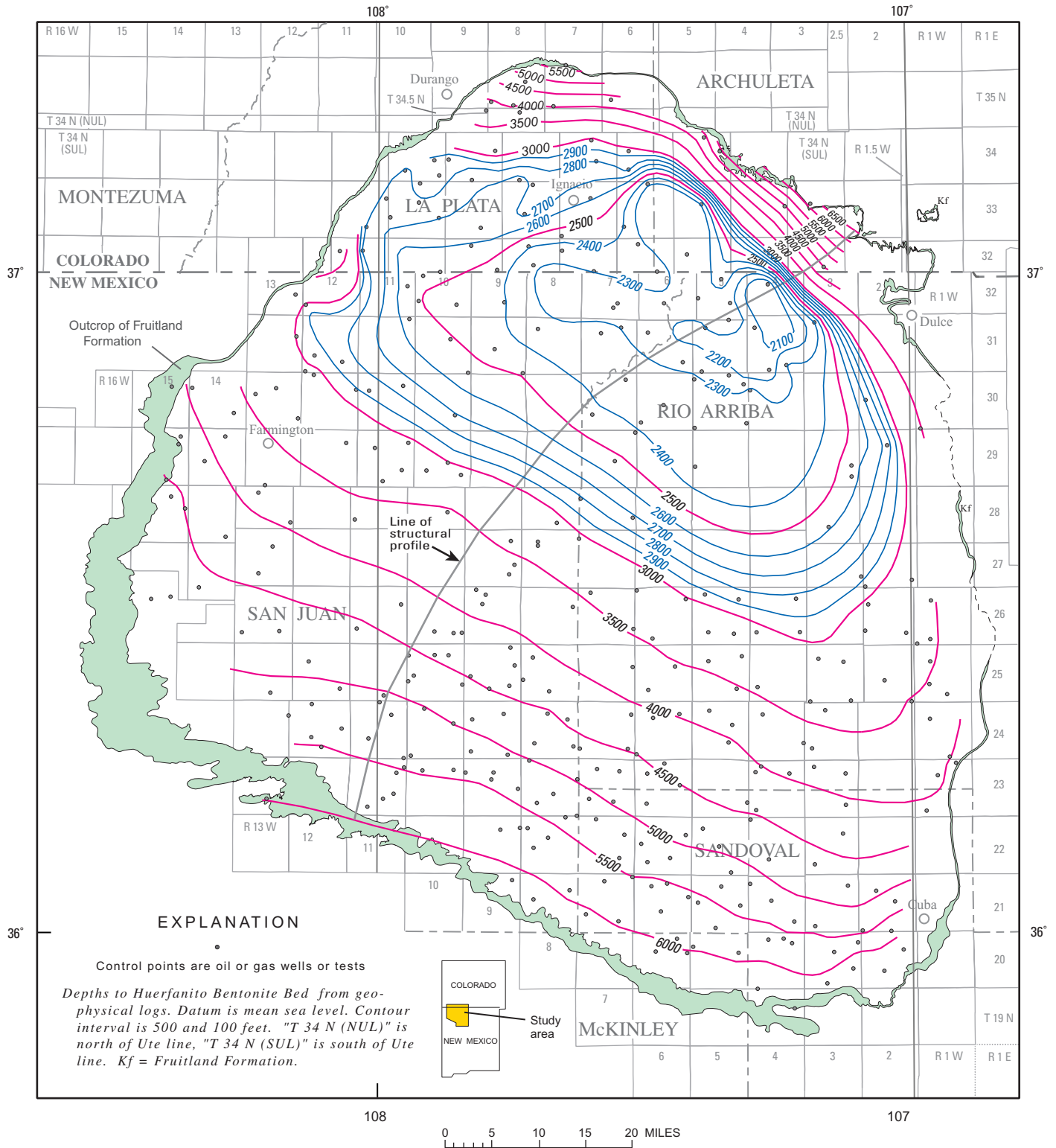


Figure 22. Contour map of the Huerfanito Bentonite Bed of the Lewis Shale. Structural profile is on figure 23.

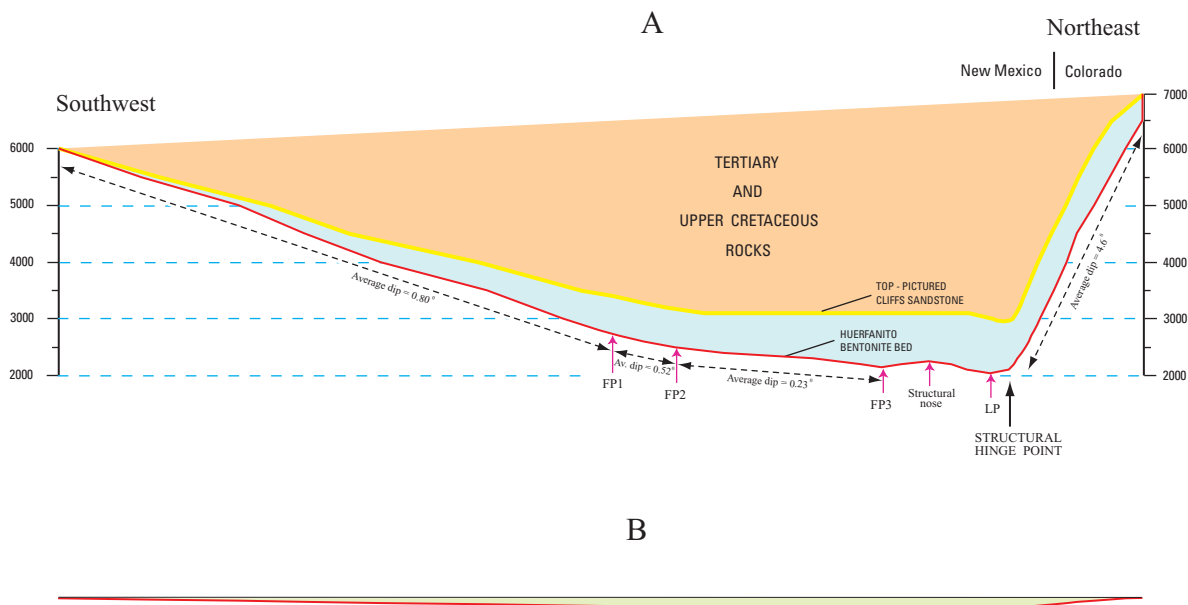


Figure 23. Structural profiles for Huerfanito Bentonite Bed and top of Pictured Cliffs Sandstone (base of Fruitland Formation) across San Juan Basin. Lines of profile are slightly different in the structurally deepest part of the basin. Profile lines are shown on figures 22 and 24. Vertical exaggeration for view A is $\times 24$; view B has no vertical exaggeration. FP1, FP2, and FP3 are flex points where the structural dip changes in the Huerfanito Bed. LP is lowest structural point on the Huerfanito Bed in the basin.

Figure 23 shows a northeast-trending structural profile of the Huerfanito Bed across the basin. This line of profile is curved to maintain a right-angle orientation to the Huerfanito structure lines and to pass through the structurally deepest part of the basin (fig. 22). The Huerfanito profile is at the 6,000-ft level in the southwest, dips gently to a structural deep slightly below the 2,100-ft level nearly 75 mi to the northeast, and rises steeply over the last 12 mi to the 6,500-ft level on the northeast edge of the basin. A prominent structural hinge point is present in the northeast in the deepest part of the basin (fig. 23).

The regional dip of the Huerfanito Bed averages 0.80° from the southwest part of the basin to a structural flexure shown with an arrow labeled FP1 (fig. 23). This flexure is at an elevation of about 2,750 ft. Between the southwest edge of the basin and FP1, three minor flex points occur and dips between these points range from 0.56° to 0.97° . Between FP1 and FP2, at the next flexure point (elevation of about 2,500 ft), the dip of the Huerfanito decreases to 0.52° . And between FP2 and FP3, (elevation of about 2,200 ft), the dip flattens to 0.23° . Between FP3 and LP, the lowest point on the Huerfanito structural profile on figure 23, the dip of the Huerfanito reverses over a structural nose. And, finally, between the structural hinge point and the northeast end of the line of profile, the Huerfanito rises evenly toward the surface with an average dip of 4.6° .

Ayers and others (1994) attached great significance to the area of structural flexure between points FP1 and FP2 on figure 23. On their Huerfanito structure map (their figure 2.5)

they show a linear feature that, for the most part, follows the 2,600-ft Huerfanito structure-contour line. They labeled this line “structural hingeline” and in their discussion of the feature stated (p. 18):

An inferred structural hingeline coincides with the 2,600-ft contour at the southwestern margin of the basin floor and projects to crop out at the La Plata mine (fig. 2.5)... This structural hingeline is interpreted to be a zone of complex, northwest-trending, en echelon normal faults, with net downdrop to the north; width of the zone is 6 to 10 mi. Its presence is inferred from the coincidence of geologic anomalies that are apparent in regional maps and cross sections.

Ayers and others (1994, p. 18) list nine “geologic anomalies” that occur at the “hingeline” including “marked thickening of the interval from the Huerfanito Bentonite to the top of the uppermost Pictured Cliffs sandstone”, changes in marker beds in the Lewis Shale, changes in thermal maturity patterns, and changes in coal-bed methane composition. Elsewhere in their report they stated (p. 37, 38):

... we conclude that syndepositional tectonic activity controlled the depositional system [Pictured Cliffs Sandstone and Fruitland Formation] and, indirectly, the occurrence of thick Fruitland coal. Pulsatory differential subsidence across the hingeline at the southwestern margin of the basin floor caused a relative sea-level rise, which resulted in stillstands of the Pictured Cliffs shoreline.

It is clear from this statement that these authors thought that the “inferred structural hingeline” had been a significant tectonic element in the San Juan Basin at the time that the Pictured Cliffs Sandstone and the Fruitland Formation were being deposited.

On figure 23, the “hingeline” of Ayers and others would lie between flex points FP1 and FP2 at an elevation between 2,500 and 2,750 ft (in good agreement with their placement of the “hingeline” at an elevation of 2,600 ft). Figure 23 shows that the regional dip between the south edge of the basin and FP1 is 0.80° , the dip between FP1 and FP2 is 0.52° , and north of FP2 the dip flattens to 0.23° . The change in dip at FP1 is 0.28° (from 0.8° to 0.52°), and the change in dip at FP2 is 0.29° (from 0.52° to 0.23°). It is puzzling that Ayers and others selected this area of very gentle flexure as the site of a Late Cretaceous “hingeline” having a profound influence on deposition of the Pictured Cliffs Sandstone and overlying Fruitland Formation coal beds. A more significant tectonic flexure is present near the north edge of the basin where the Huerfanito bends sharply upward (labeled “structural hinge point” on fig. 23) yet Ayers and others attribute no significance to this feature.

The present basin structure began to form in Paleocene time following deposition of the Ojo Alamo Sandstone and continued into late Eocene time when the basin reached its final form around 35 Ma (Fassett, 1985). The “hingeline” referred to by Ayers and others is therefore a mid-Paleocene to late-Eocene feature. The inference by Ayers and others that the “hingeline” was an active tectonic feature in Campanian time (around 74 Ma) is an interesting conjecture that does not appear to be supported by any data.

Pictured Cliffs Sandstone Structure

Geophysical logs from 710 drill holes were used to construct a structure contour map on top of the Pictured Cliffs Sandstone (fig. 24). This map was prepared primarily to determine the maximum thickness of overburden on Fruitland coal beds (fig. 39). The Pictured Cliffs structure map does not portray the true basin structure because of the 1,200 ft of stratigraphic rise of the top of the Pictured Cliffs northeastward across the basin (plate 1, fig. 13). A comparison of the Huerfanito and Pictured Cliffs structure maps shows a similar structural pattern, but only the Huerfanito shows the true structure of the basin. For example, the structural nose seen in the deepest part of the basin on the Huerfanito structure map (fig. 22) and on the structure profile of the Huerfanito (fig. 23) is not seen on the Pictured Cliffs structure map (fig. 24) or profile (fig. 23) because this part of the basin is an area of abrupt stratigraphic rise in the top of the Pictured Cliffs that masks this structural feature. The structure profile for the top of the Pictured Cliffs (fig. 23) is horizontal from just northeast of point FP2 to beyond the area of the structural nose shown on the Huerfanito structure profile because the structural deepening of the basin in this area of about 500 ft (fig. 22) is exactly

offset by the 500 ft of stratigraphic rise in the top of the Pictured Cliffs across this same area (plate 1, fig. 13).

The Pictured Cliffs structure map (fig. 24) is included in this report because it is a useful tool in visualizing the depth distribution of Fruitland coals throughout the basin. In addition, if the surface elevation of a point on this map is known, the depth to the base of the Fruitland at that point can be quickly estimated.

Assessment of Fruitland Formation Coal Resources

Methodology

Base Map Preparation

The base map used for all of the San Juan Basin maps in this report was assembled using ARC/INFO and ArcView GIS (Geographic Information System) software. The land grid, consisting of township and section polygons, was provided by the Bureau of Land Management in digital form for the States of New Mexico and Colorado. County lines are from USGS digital files, and other cultural features are from numerous sources including digital files of USGS base maps for New Mexico and Colorado. The Fruitland Formation outcrop was added to the base map as follows: (1) the geologic map of the San Juan Basin from Fassett and Hinds (1971, plate 1) was scanned, (2) the outcrop lines for the top and bottom of the Fruitland Formation were digitized on the computer screen using the scanned image of the geology of the basin as a template in ArcView, (3) the resultant file was fitted to the land-grid file in ARC/INFO, and (4) in some areas the outcrop pattern was modified by the author to correct the outcrop placement based on newer, larger scale mapping, matching of outcrop position to topographic expression using USGS 1:24,000 topographic quadrangle maps, and field-checking. The various contour maps for this report were prepared using EarthVision; those files were fitted to the base-map file using ArcView. Final drafting of the maps was done in Adobe Illustrator after importing the ArcView shape files via the Map-Publisher extension. The ArcView files for this report are in Appendix 1.

The Fruitland Formation outcrop shown on the maps in this report is the most accurate presentation for the entire basin prepared to date. For the New Mexico part of the basin, a report by Beaumont (1998) shows the base of the Fruitland outcrop on two maps at a scale of 1:250,000. Beaumont’s maps were prepared using all published large-scale geologic maps available and included his unpublished geologic mapping; thus, they show the base of the Fruitland outcrop in more detail in places than the Fruitland outcrop map in this report. However, the maps in the Beaumont report were not

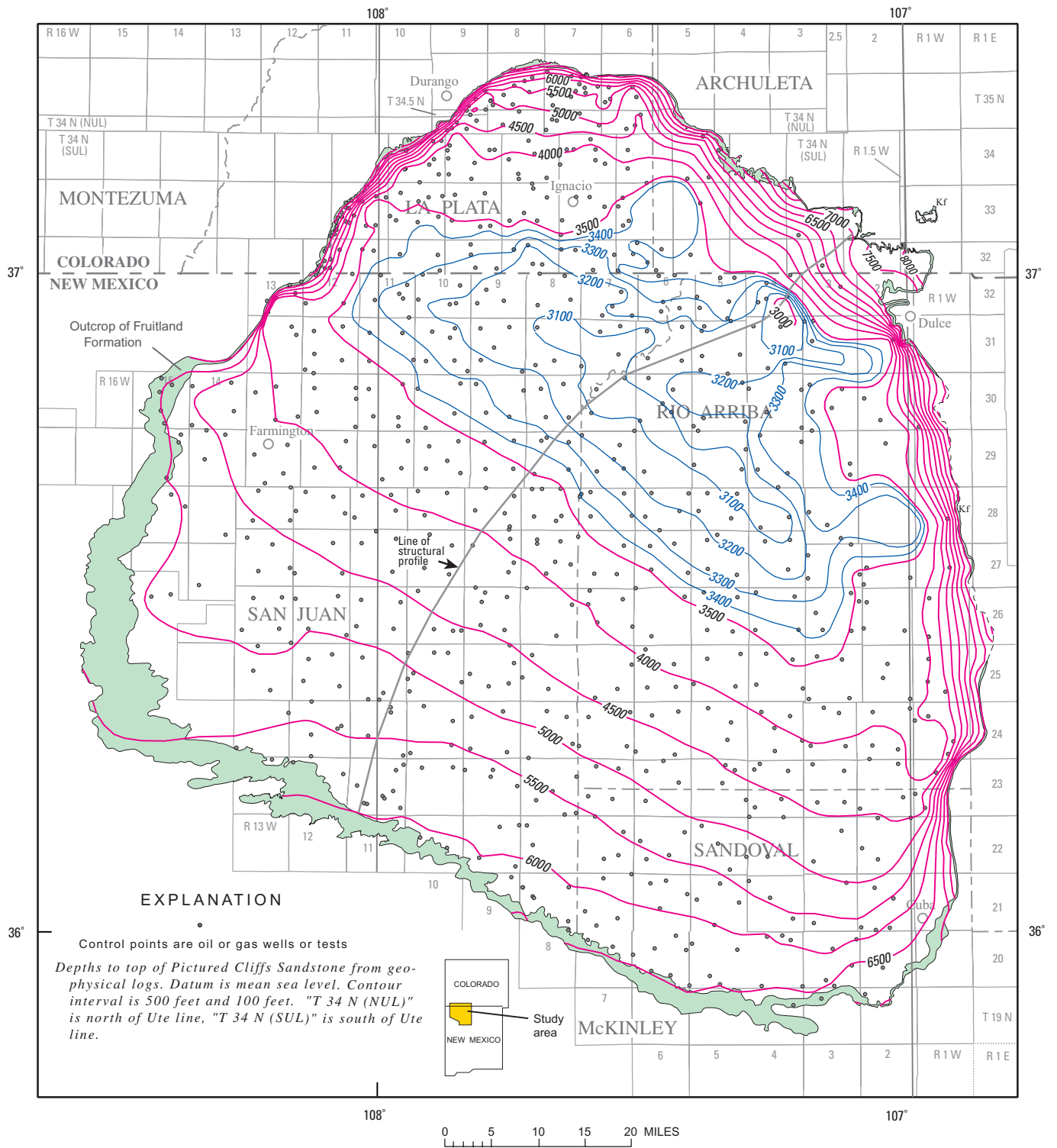


Figure 24. Contour map on the top of the Pictured Cliffs Sandstone—base of the Fruitland Formation. Structural profile is on figure 23. Note: Because of the stratigraphic rise of the top of the Pictured Cliffs Sandstone northeastward across the basin, this map is not a true representation of the structure of the basin. The true structure is shown on the Huerfano structure map (fig. 22).

fitted to the land grid using modern GIS procedures. The large-scale geologic map of the Hunter Wash area (fig. 9) compiled from published 1:24,000 geologic maps and extensively field-checked by the author is the most accurate geologic map available for that area.

The outcrop is labeled “Fruitland Formation outcrop” around the entire periphery of the basin on the maps in this report, but on the east side of the basin, the Kirtland and Fruitland have been mapped together, undivided. The Fruitland is missing in two areas on the east side of the basin (for example, fig. 8). In those areas, the unconformable contact between the Ojo Alamo Sandstone and the Lewis Shale is shown as a dashed line. The Fruitland is present in a 10-mi-long outcrop in T. 27, 28 N., R. 1 W. on the east side of the basin. (See figure A2-3 for more detail on the outcrop distribution of the Kirtland and Fruitland Formations and the Ojo Alamo Sandstone.)

Geophysical Logs

More than 20,000 publicly available geophysical logs from oil or gas wells or tests exist in the San Juan Basin. This vast database allowed for careful selectivity in choosing only the highest quality geophysical logs for geologic interpretations and coal-thickness determinations for this study. In addition, because of the large numbers of logs available, the spacing of data points could be optimized to maximize the accuracy of the assessment in a reasonable time frame.

The quality and types of geophysical logs available in the San Juan Basin is extremely variable. The earliest coal assessment study for the basin (Fassett and Hinds, 1971) used mostly resistivity logs in conjunction with gamma ray–neutron and sonic logs to measure coal thicknesses because those were the best logs available at that time. In the 1970’s, with the discovery of large quantities of coal-bed methane in Fruitland Formation coal beds, an intense coal-bed-methane drilling boom began that resulted in thousands of new wells being drilled through the Fruitland Formation. It quickly became standard procedure to run bulk-density logs in these wells to identify the coal-bed reservoirs, precisely determine their depths and thicknesses, and evaluate the coal beds in terms of their ash content. Those high-definition logs were used exclusively in this study for measuring Fruitland coal beds and determining the density of coal beds.

The quality of bulk-density logs varies, but the tops and bottoms of coal beds and thicknesses of layers of non-coal material within coal beds (partings) can usually be selected on these logs to within 1 ft. Figure 25 is an example of a good-quality bulk-density log; such logs are almost always configured with a caliper and gamma-ray log trace, as shown here. The log on figure 25 is representative of the majority of the logs used to determine coal-bed thicknesses in this report. Typically, bulk-density logs through Fruitland coals in coal-bed methane wells have a depth scale in 2-ft increments as shown on figure 25.

The bulk-density curve on figure 25 has two density scales at the top of the log. The upper scale goes from a density of 2.0 on the left to 3.0 on the right; units of measurement are in grams per cubic centimeter (g/cm^3). The primary log curve is on the left side of the log track (here shown in brown) and measures the densities of most sedimentary rocks. The lower bulk-density scale goes from 1.0 to 2.0 g/cm^3 and measures the rock densities tracked by the backup bulk-density curve on the right side of the log track (shown in blue). In the Fruitland Formation, the only rocks that have a density less than 2.0 g/cm^3 are carbonaceous shales and coal beds. To distinguish coal beds from carbonaceous shale beds on bulk-density logs, a density value of 1.75 g/cm^3 is used as the maximum density for coal because it is at about this density value that coals contain 50 percent ash; rock with a higher density is not considered to be coal. (The American Society for Testing and Materials (1995) has defined coal as “A readily combustible rock containing more than 50 % by weight and more than 70 % by volume of carbonaceous material including inherent moisture”)

In this study, the tops and bottoms of coal beds were selected on bulk-density logs at the point where the backup bulk-density curve crosses the vertical line with a value of 1.75 g/cm^3 on the log scale. On figure 25, the portion of the bulk-density log to the left of the 1.75- g/cm^3 line is shaded to emphasize the presence of coal beds. The lowest density reading in a coal bed on this log (1.3 g/cm^3) is at 1,056 ft. Coal of this density is pure coal and contains no ash.

The only significant pitfall in the use of bulk-density logs for coal-bed-thickness determinations occurs in badly caved drill holes. The walls of the drill hole logged on figure 25 are relatively smooth, as shown by the caliper-log trace; only two, thin, caved intervals at depths of 1,105 ft and 1,132 ft are recorded. Both of these caved intervals are in coal beds and the cavings are only about 1 inch deep. Such small cavings have little affect on the bulk-density log reading. In some wells, however, cavings can be quite deep—sometimes exceeding the original width of the drill hole. In those holes, the bulk-density log will read an average density of the rock deep within the caving and the fluid that is filling the caving (usually water or drilling mud). Thus, the bulk density measured in a deeply caved drill bore will be substantially less than the true density of the rock penetrated by the drill hole. Every effort was made not to use density logs from badly caved drill holes for this study, but in rare instances where such holes had to be used (in areas of limited availability of density logs) the tops and bottoms of coal beds in caved intervals were selected on the gamma-ray curve because this curve is much less affected by caving. It is good practice in drill holes that contain deeply caved intervals to compare the resistivity log to the bulk-density log to determine whether coal beds are present within the caved interval. A bulk-density log in a badly caved drill hole through the Fruitland is shown on figure 30 and is discussed in the “Comparison with Earlier Studies” part of the “Geographic Distribution of Fruitland Formation Coal” section of this report.

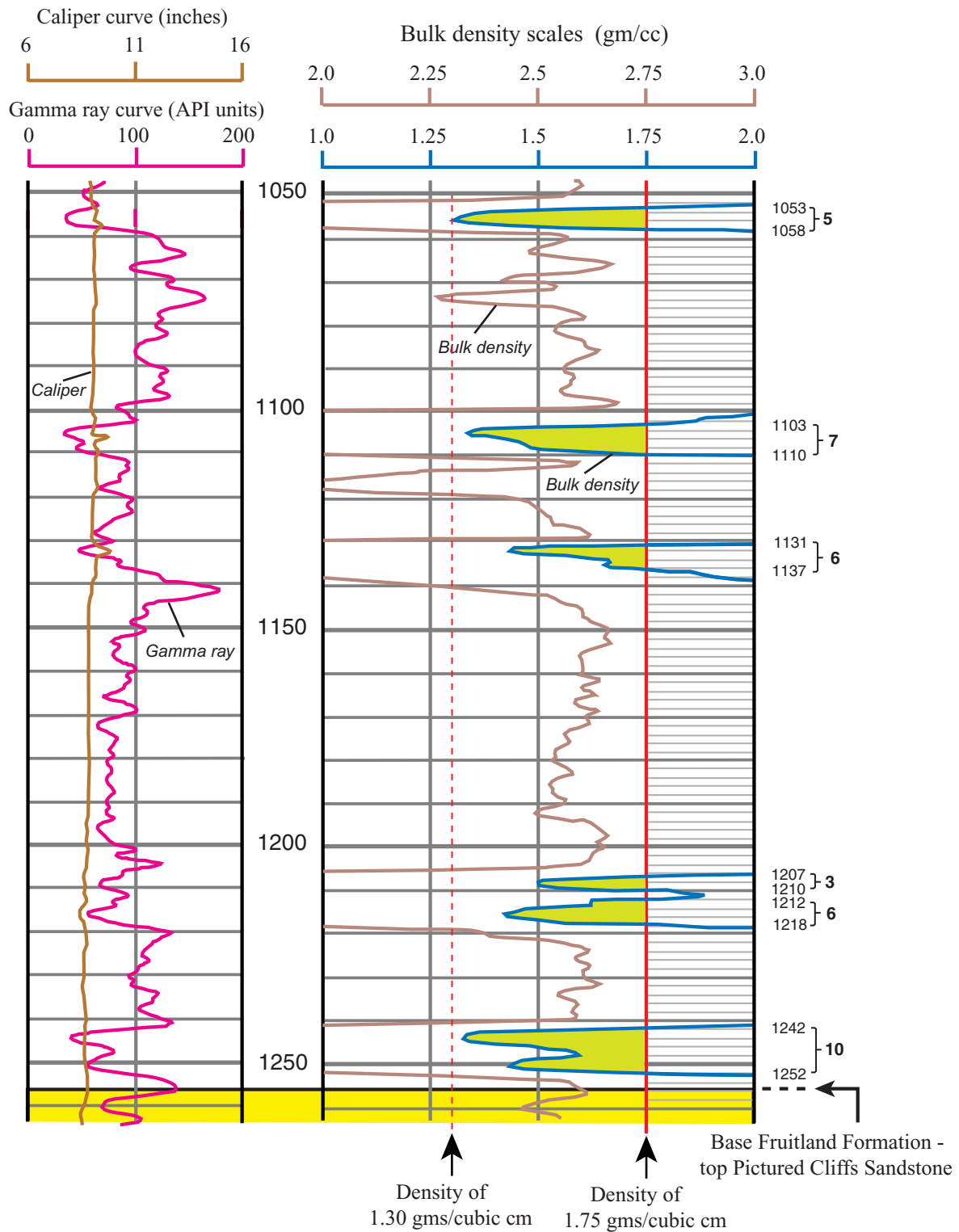


Figure 25. Good-quality density log showing the bulk-density, gamma ray, and caliper log traces for Fruitland Formation coal beds. Log is from the Amoco Production Company State of Colorado Ax No. 1 well located in NE¼NE¼ sec. 16, T. 35 N., R. 7 W., La Plata County, Colorado. Coal is defined in this report as having a density of less than 1.75 grams per cubic centimeter (shown in green). Depths to top and base of coal beds and coal-bed thicknesses are shown in feet on right side of column. Total coal thickness in this well is 37 ft.

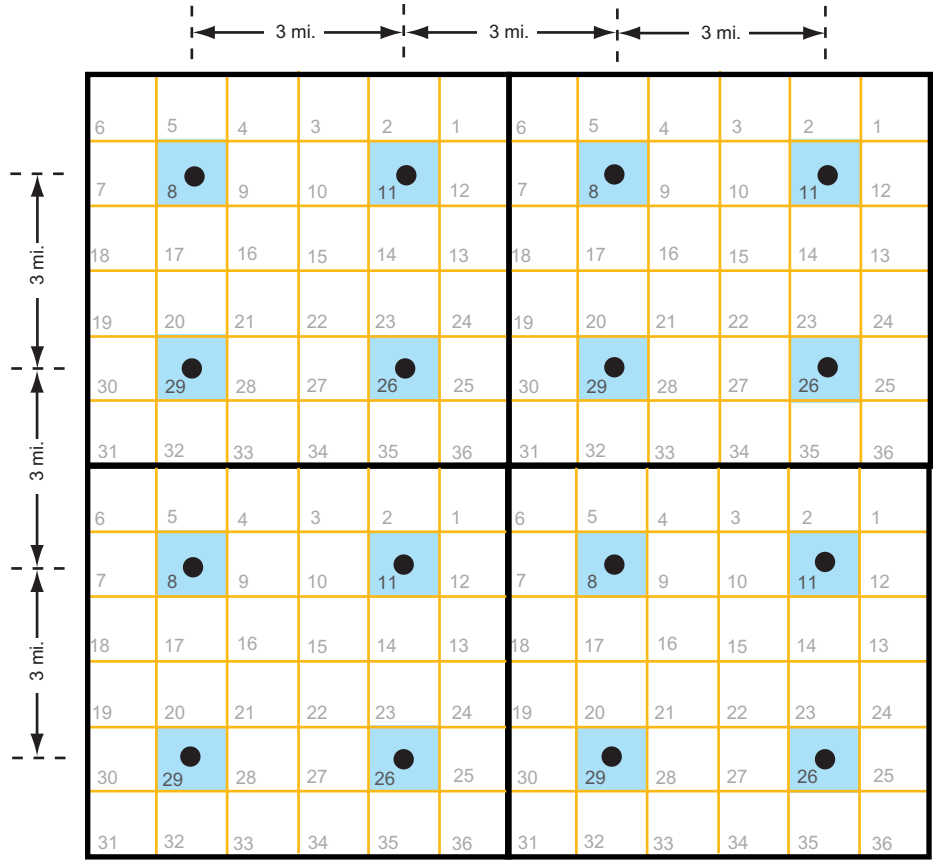


Figure 26. Diagram showing the ideal spacing for drill holes for coal assessment in the San Juan Basin.

Distribution of Data Points

U.S. Geological Survey standards for coal classification (Wood and others, 1983, fig. 4) describe four reliability categories for making coal assessments based on distances from control points at which coal thicknesses are measured. These categories are measured, 0 to 0.25 mi; indicated, 0.25 to 0.75 mi; inferred, 0.75 to 3.0 mi; and hypothetical, beyond 3.0 mi. Identified coal is the sum of the measured, indicated, and inferred coal and includes all the coal that is within 3.0 mi of a control point. In this report, coal quantities are reported for the identified and hypothetical categories.

One of the primary goals for this assessment was to have most of the assessed coal be in the identified category (control points less than 3 mi apart). The ideal placement of control points to meet this spacing requirement is in sections 8, 11, 29, and 26 in each township in the basin (fig. 26). An additional criterion for coal-thickness control points was that they be exclusively bulk-density logs, as discussed above.

Figure 27 shows the distribution of the 734 control points in which more than 1.2 ft of coal was measured for this coal assessment. (The total database for this coal assessment

contains 752 drill holes; 18 of these holes, along the east side of the basin, contained coal beds less than 1.2 ft thick or no coal and are not shown on figure 27.) Figure 27 was constructed in EarthVision by striking 3-mi-radius arcs around each control point; the areas shown in blue are within 3 mi of a control point and thus are areas of identified coal resources in the basin. Areas shown in brown are areas of hypothetical coal (more than 3 mi from a control point). This map shows that most of the Fruitland coal assessed in this report (88 percent) is in the identified category.

The two largest areas of hypothetical coal are along the east and west sides of the basin (fig. 27). The four areas of hypothetical coal on the west side, south of Farmington, N. Mex., are on the Navajo Indian Reservation (fig. 2). Although this area has been densely drilled in various coal exploration projects, the Navajo Tribe prefers to keep this data proprietary. Coal thicknesses in these areas, however, do not appear to be greatly variable, and coal thicknesses can be projected into these areas with a good degree of confidence. (Coal thicknesses are discussed in more detail in the “Geographic Distribution of Fruitland Formation Coal” section of this report.) The areas of hypothetical coal in the southeast—near Cuba, N.

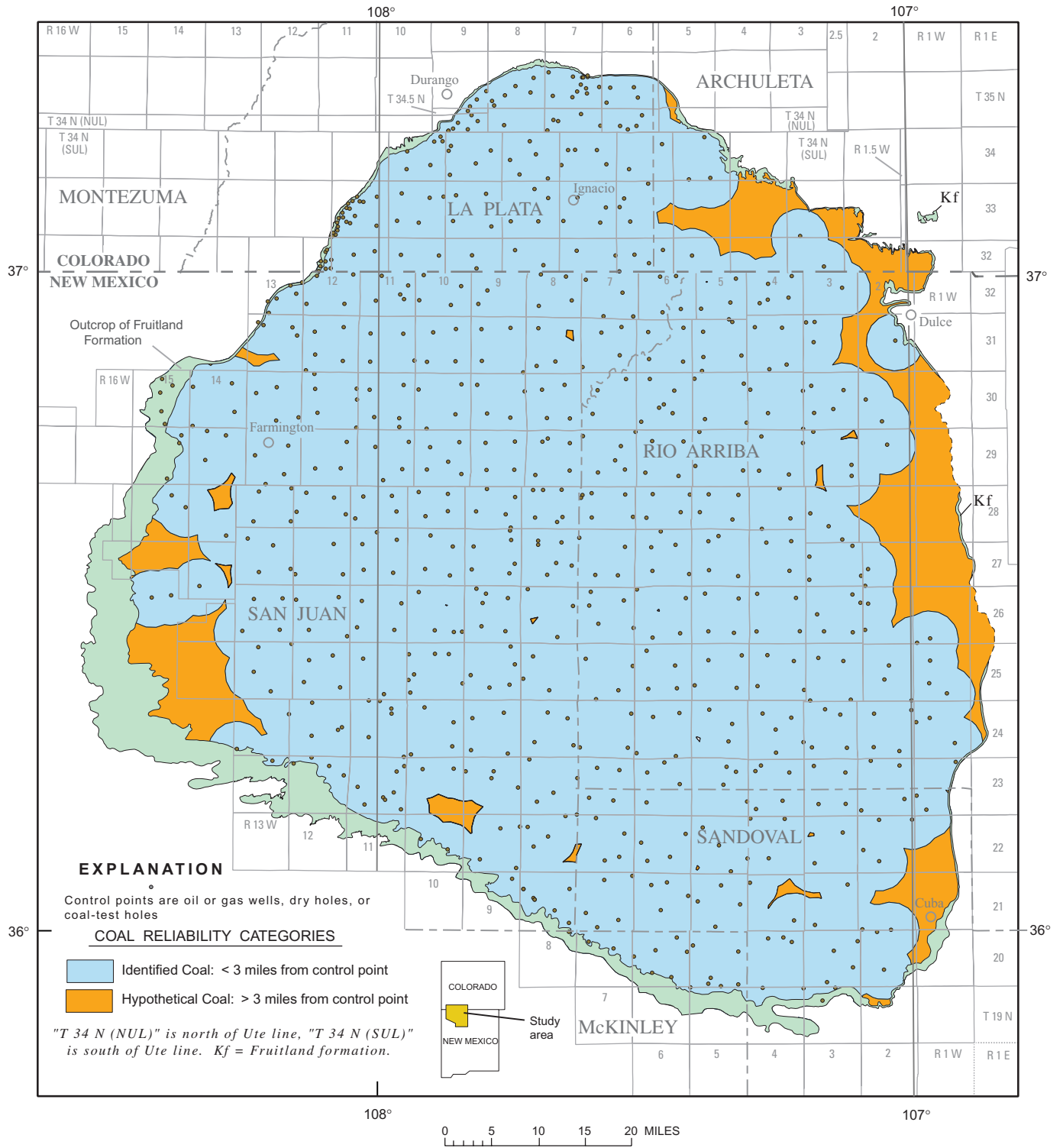


Figure 27. Map of San Juan Basin showing coal-reliability categories as defined by Wood and others (1983). The 752 drill holes used for control for the San Juan Basin Fruitland Formation coal assessment are shown. Kf, Fruitland Formation.

Mex. (fig. 27), and along the east-central and northeast edges of the basin—contain few drill holes but there is little Fruitland coal in those areas; in fact, the only areas of zero Fruitland coal in the basin are on the east side within these hypothetical coal areas (fig. 28). The large block of hypothetical coal in Ts. 32, 33 N., Rs. 4, 5 W. is on the east side of the Southern Ute Indian Reservation (fig. 2) and has never been drilled. Fruitland coals appear to be thin in that area based on nearby outcrop data and projections of coal-thickness isopach lines (fig. 28). The other scattered small areas of hypothetical coal in the basin are artifacts of being just beyond the 3-mi limit from several control points and do not represent significant data gaps in those areas.

Three clusters of data points are present on figure 27 in the northwest part of the basin near the Fruitland outcrop. The cluster of data points in T. 35 N., R. 7 W. and the one south of Durango, Colo., are from detailed, large-scale studies of coal-bed methane gas seeps (Fassett and others, 1997b). The cluster of data points on the west edge of the basin just north of the Colorado State line is from a cooperative USGS–Southern Ute Indian Tribe core-drilling project (Roberts, 1989). Data from these reports are discussed in detail in the “Fruitland Coal-Bed Correlations—Earlier Studies” section of this report.

Core Data

Core data were used for control for the coal assessment in four areas (fig. 28). The cluster of core data points north of the State line near the Fruitland outcrop was discussed above. The four core data points near the Fruitland outcrop on the northwest edge of the basin, just south of the State line, the four core data points on the Fruitland outcrop west of Farmington, and the row of core holes parallel to the Fruitland outcrop along the southern edge of the basin (fig. 28) are from a core-drilling project conducted by the New Mexico Bureau of Mines and Mineral Resources (Hoffman, 1991; Hoffman and others, 1993). Three USGS core-drilling projects were conducted to evaluate Fruitland coal in New Mexico; the data from those projects are reported in Jentgen and Fassett (1977), Wilson and Jentgen (1978), and Beach and Jentgen (1980). These projects generally had a drilling density of four coal test holes per section and thus represent very dense data sets compared to the basin-wide density of four holes per township used for this assessment. These core-hole data were not used for the assessment because the drill holes were too close together to be shown and contoured at the scale of the maps used in this report, and average coal thicknesses for these dense data sets were similar to thicknesses of the more widely spaced data points used for this coal assessment in the areas of the core drilling. Many other private coal-coring projects were conducted on coal leases and Preference-Right Lease Application areas along the Fruitland outcrop in the southwest and south parts of the basin. That information is in the files of the U.S. Bureau of Land Management offices in Farmington and Albuquerque, N. Mex. No attempt was made to integrate

those data into this study because coal thicknesses were relatively well known in those core-drilling areas and the data sets were too dense to be easily shown at the scale of this project. Hundreds of Fruitland coal core holes have been drilled on the Navajo Reservation (fig. 2) on the west side of the basin, but, as mentioned above, data from those holes have not been released by the Navajo Indian Tribe.

Coal Outcrop Measurements

No measurements of outcropping Fruitland coal beds are used as control points for this assessment. Outcrop coal measurements were rejected because they seldom represent the total Fruitland coal thickness at any outcrop locality because of partial cover by alluvium and (or) burning or weathering of the coal. Large numbers of Fruitland coal outcrop measurements have been published over the years in USGS map and book publications, and many of those measurements are shown on the net-coal isopach map (fig. 28). Outcrop measurements of coal are useful to provide a minimum total-coal-thickness value at various points around the Fruitland outcrop, especially in areas where well-log or core data are sparse.

Database

Data Point Locations

Locations for the data points used for construction of the contour maps in this report were determined in decimal degrees of latitude and longitude in the ArcView GIS software program using a custom tool designed to measure locations of the data points in feet from section lines. The map was scaled in meters, distance units were in feet, projection was Lambert Conformal Conic, and the central meridian was at long 107.75°W. Locations for oil and gas wells or tests (given in feet from the nearest section lines) were from geophysical log headers. Some core-hole and other data-point locations were determined by measuring footages of data points from section lines on USGS 1:24,000 topographic quadrangle maps and then placing these points on the ArcView map using the custom measuring tool. After the data points had been entered into the ArcView file, the projection of the file was changed to geographic decimal degrees, converting the data-point locations to decimal degrees of latitude and longitude. Latitude and longitude coordinates for all of the data points shown on the various maps in this report were determined using this procedure.

Geophysical Log Data

Coal-bed depths measured from bulk-density logs (see example, fig. 25) were entered into the StratiFact database

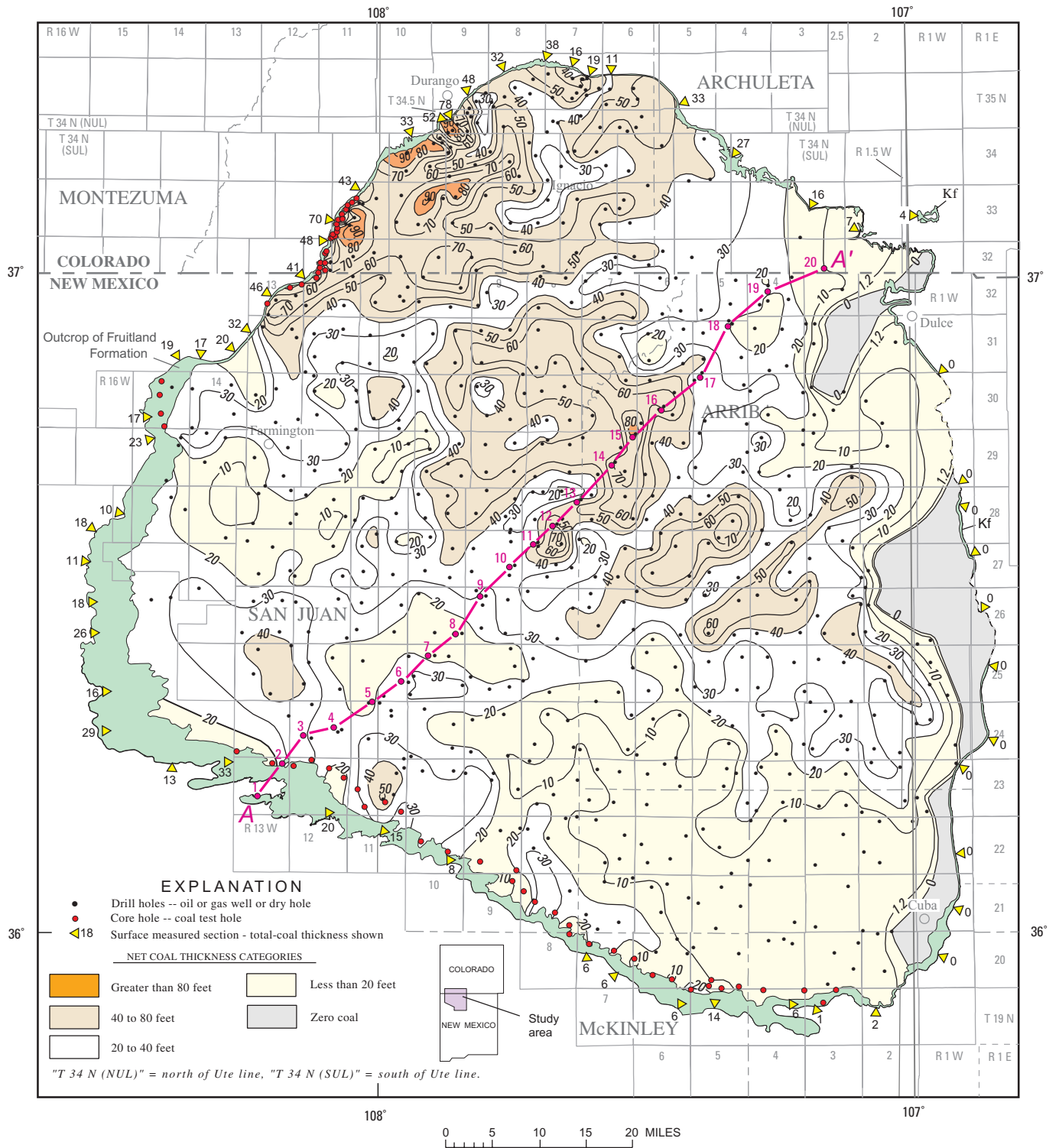


Figure 28. Net-coal isopach map for Fruitland Formation coal beds. Outcrop coal measurements from Fassett and Hinds (1971). Coal thicknesses at control points are net coal in beds 1.2 ft thick or greater. Coal measurements are from density logs or drill core. A maximum density of 1.75 g/cm³ was used as a cutoff for coal measurements on density logs (fig. 25). Contour interval is 10 ft. Cross section A-A' is on plate 1. Kf, Fruitland Formation.

management system along with a unique point ID, the latitude and longitude coordinates, drill-hole elevation and total depth, selected geologic formation tops, and other relevant information for each data point. (An edited version of the StratiFact database is in table A2-1.) After data clean-up (discussed below under “Data Screening for Errors”) x , y , z (data point) files were created from the StratiFact data files and exported as Excel spread sheets containing x , y locations in longitude and latitude and the total coal thickness or other geologic parameters as the z value. USGS classification standards (Wood and others, 1983) do not allow the inclusion of bituminous coal beds less than 14 inches thick in the resource base; thus, the coal thickness data set was run through another program that deleted all coal beds less than 14 inches thick, deleting the 1-ft-thick coal beds from the database. (The impact of deleting these thin coal beds was minimal because there were few 1-ft-thick coal beds in the original database.)

Contour Map Preparation

Data files for the geologic and coal-thickness parameters were imported into the EarthVision software program for gridding and contouring. After the first contour map was generated for each data set, the maps were modified in EarthVision by the author to incorporate his geologic knowledge of the area. The final contour maps were imported into Adobe Illustrator using the MapPublisher extension for final drafting. All of the other illustrations in this report were also prepared in Adobe Illustrator. Various contour intervals were tested for each map in this report; the final selection was based on the contour interval that best presented the data legibly on a page-size illustration without loss of geologically significant data. Contour intervals range from 10 ft for the net-coal isopach map (fig. 28) to 500 ft for the Huerfanito and Pictured Cliffs structure maps (figs. 22, 24). Control points used to construct each contour map are shown along with the township-and-range land grid to enable users to easily locate contour lines and data points geographically.

Data Screening for Errors

The data used to create the contour maps in this report were checked for accuracy in two ways: (1) generating a preliminary contour map in StratiFact and reexamining data sources for anomalous values at single points (sometimes called “bull’s-eyes”), and (2) having a second person review the basic data source (usually geophysical logs) to confirm the original data selection points. All of the contour maps were checked with the preliminary-map method. This method is highly efficient because the most common errors of incorrect well site elevations, incorrect well locations, mistakes in the selection of geologic formation tops, and typographical errors in data entry are obvious as bull’s-eyes. The preliminary-map method works well in identifying errors that are about the

same magnitude or larger than the contour interval selected for the contour map. For example, a 100-ft error in the elevation of a drill hole would be obvious on a structure map contoured at 100 ft, whereas an error in elevation of 50 ft might not be so apparent. The preliminary-map procedure was used for all of the contour maps in this report to eliminate apparent errors in data values.

The isopach map of total coal thickness (fig. 28) was more difficult to check using the preliminary-map method because coal-thickness values are more random and what may at first appear to be an anomaly may in actuality be an abrupt change in coal thickness and not a data error. About 20 percent of the bulk-density logs were reexamined in the process of checking apparent anomalies on the StratiFact preliminary maps. Approximately 50 percent of the bulk-density logs were examined by a second person to confirm coal depth and thickness data. The author was the final reviewer for all of the data in this report.

A few data points that appeared to be anomalous after careful checking of the basic data were found to have deviated (inclined) well bores. Lists of deviated wells in the basin were obtained from the New Mexico and Colorado Oil and Gas authorities and all deviated holes were purged from the database.

Geographic Distribution of Fruitland Formation Coal

Net-Coal Isopach Map

Figure 28 is the net-coal isopach map for Fruitland coal in the San Juan Basin. (“Coal” or “coal thickness” refer to net-coal thickness in this discussion.) The distribution of control points averages about four per township throughout most of the basin, or one control point every 3 mi. The principal areas of sparser data are in the northeast, east-central, and west-central parts of the basin (see “Distribution of Data Points” section for more detail on these areas). Outcrop coal-thickness measurements (including zero-coal data points) were not used to construct the net-coal isopach map (fig. 28), but they represent minimum coal-thickness values that are useful for estimating coal thicknesses in areas where subsurface data are sparse. Zero-coal areas on the east side of the basin are discussed in more detail below.

Fruitland Coal Distribution

Map View

Areas underlain by more than 40 ft of net coal are colored brown on figure 28. In the northern part of the basin, five such areas collectively form a northwest-trending wedge that is widest in the northwest and tapers to the southeast. In the

southwest part of the basin, two small areas are underlain by more than 40 ft of coal. Five small areas are underlain by coal more than 80 ft thick in the northwest part of the basin (colored orange, fig. 28); four of these areas are close together near the northwest edge of the basin. The fifth area is defined by one control point near well 15 on line of cross section A-A'. Several areas underlain by coal less than 20 ft thick (shown in yellow) are present in the southern part of the basin; these areas collectively form a broad, northwest-trending band of thinner coal. Another band of coal less than 20 ft thick is parallel to the east edge of the basin; this band is narrow to the south and broadens to the north.

A large area of coal less than 10 ft thick is present in the southeast part of the basin. This area corresponds remarkably well to the area between the 250-ft and 300-ft contour lines of figure 8. In the "Shoreline Trends" section of this report, it was suggested that the shoreline had regressed rapidly to the north in this area because a large delta was building out into the Pictured Cliffs sea at that time. The area of coal less than 10 ft thick (fig. 28) thus records a time when a major distributary channel complex was rapidly depositing a broad wedge of mostly sand-size material in the southeast part of the basin area, preventing the formation of significant peat swamps there.

In addition to the northwest-trending areas of thin and thick coal that parallel Pictured Cliffs Sandstone paleoshoreline orientations (figs. 8, 14, 18), a northeast-trending pattern of thick and thin coal is also visible on the net-coal isopach map (fig. 28). For example, three ribbons of thin coal (less than 40 ft thick) trending northeast cut through the wedge of thicker net coal discussed above. These features are normal to paleoshoreline trends and probably represent the positions of paleo-river channels that apparently maintained their geographic positions during the Pictured Cliffs shoreline retreat across those areas. The most prominent of these thin coal bands trends slightly north of east in the north-central part of the basin, crossing the New Mexico–Colorado State line in T. 32 N., R. 6 W. (fig. 28). Within this relatively narrow, linear band, the total coal thickness is less than 40 ft thick to less than 30 ft thick. Two other bands of thin coal trending northeast are in the east central part of the basin southeast and parallel to the line of cross section A-A'. These bands of thinner coal abut two linear bands of thicker coal also with a northeast trend. Other, less well defined linear bands of northeast-trending thick and thin coal are present in other parts of the map area.

Two areas of zero coal are present on the east side of the basin. A northeast-trending lobe of zero coal is present in the northeast part of the basin, mostly south of the New Mexico State line (fig. 28). Another band of zero coal parallels the southeast edge of the basin; this band is narrow to the south and thickens to nearly 10 mi wide to the north. As noted above, the Fruitland is missing in two areas on the east side of the basin (fig. 28). In Tps. 29, 30 N., R. 1 W. the area of missing Fruitland is shown by a dashed line. Because there is no Fruitland coal in this area, there should be a narrow band of zero Fruitland coal paralleling and west of the dashed

contact line; however, the computer contouring program had insufficient drill-hole data to generate a zero coal line in this area.

Fruitland coal beds thin abruptly eastward near the east side of the basin. For example, in the east-central part, (Tps. 25–28 N., Rs. 2, 3 W.) net-coal thicknesses of more than 40 ft decrease to 0 ft of coal over a very short distance. Fassett and Hinds (1971, p. 53, 54) suggested that this thinning of Fruitland coals along the east edge of the basin was the result of slight uplift along a linear, northerly trend in that area that occurred as the Pictured Cliffs shoreline was regressing across the basin. That uplift could not have been very great or it would have created a clastic wedge of sediment in the Fruitland with an eastern source and no such clastic wedge is present. An alternative explanation is that thicker Fruitland coals were deposited across this area but tectonic uplift along the east side of the basin, prior to deposition of the Tertiary Ojo Alamo Sandstone, resulted in their removal by erosion. (See appendix figures A3-1 through A3-5 for more detail on the geometry of the Fruitland Formation and associated rocks in the San Juan Basin.) The true answer regarding why Fruitland coals thin abruptly on the east side of the San Juan Basin is probably a complex combination of these two possible causes.

Coal-Bed Geometry

The line of section A-A' is shown on the net-coal isopach map to facilitate comparison of Fruitland coal distribution in map view with its distribution as seen in cross section. Plate 1 is a northeast-oriented stratigraphic cross section across the San Juan Basin constructed with the Huerfano Bentonite Bed as a datum. The rock units shown are the Upper Cretaceous Lewis Shale, Pictured Cliffs Sandstone, Fruitland Formation and lower shale member of the Kirtland Formation (undivided) and the Farmington Sandstone Member of the Kirtland Formation. The Tertiary Ojo Alamo Sandstone unconformably overlies the Cretaceous rocks. The general distribution of Fruitland coal beds (plate 1) shows an area of thicker coal in the southwest (drill holes 1–6), a zone of relatively thin coals (holes 7–10), a zone of increasing coal thickness (holes 11–17), and a zone of relatively thin coal in the northeast part of the basin (holes 18–20). The magnetic-polarity reversal from chron C33n to C32r (73.50-Ma isochron) is shown as a red dashed line in the upper part of the Farmington Sandstone Member in the southwest and in the Pictured Cliffs Sandstone in the northeast.

As discussed previously, the Pictured Cliffs Sandstone rises stratigraphically across the basin more than 1,200 ft and is nearly 2.5 m.y. younger in the northeast than in the southwest; thus, the coal beds in drill hole 1 on plate 1 are nearly 2.5 million years older than the coals in drill hole 20. It is helpful to keep this relationship in mind when comparing the coal distribution shown on the map on figure 28 and in cross section on plate 1. The three-dimensional distribution of Fruitland coals in time and space in the San Juan Basin is termed the geometry of the coal.

Map–Cross Section Comparison

The geophysical drill-hole logs shown on cross section A-A' (plate 1) are nearly all resistivity logs; these logs were used because they are the most definitive for selecting formation boundaries. Resistivity logs are not, however, the best logs on which to measure coal beds. Consequently, the coal beds illustrated on this cross section are not as precisely measured as the coal beds measured on bulk-density logs that were used to construct the net-coal isopach map of figure 28. (Net-coal thicknesses for the drill holes shown on cross section A-A' were not used as control points for the net-coal isopach map (fig. 28); these two illustrations were prepared independently.) In the northern part of the basin, the identification of coal beds on resistivity logs is difficult (see discussion in Fassett and Hinds, 1971, p. 50–52). A good example is drill hole 14 where a high-resistivity bed is present just below 3,300 ft. This bed appears to be a coal bed on the resistivity log, but the bulk-density logs from nearby drill holes show that in reality it is a sandstone bed. In this part of the basin, bulk-density logs were examined from drill holes as near as possible to the drill holes on this cross section to confirm all of the coal picks shown.

Cross section A-A' (plate 1) shows that coal beds have very little lateral continuity and are at an increasingly higher stratigraphic level from southwest to northeast. The net-coal thicknesses for the drill holes shown on this cross section include a different set of coal beds at every control point. For example, drill hole 2 on the cross section contains 7 thin Fruitland coal beds with a net-coal thickness of nearly 30 ft. Drill hole 3 contains one thick and two thin coal beds with a net thickness of a little over 30 ft. The net coal thickness in holes 2 and 3 is nearly identical, but a close examination of the coal beds in these two holes shows that the thick coal bed in hole 3 splits into two thinner coal beds in hole 2. The next lower thin coal bed in hole 3 correlates perfectly with a thin coal in hole 2, and the lowest thin coal bed in hole 3 pinches out to the southwest and is not present in hole 2. The lowermost 4 coal beds in hole 2 pinch out to the northeast, and none are present in hole 3. Generally, coal beds correlate across only two holes and many coal beds are present in only one of the drill holes shown on section A-A'. This lack of continuity of coal beds between drill holes is true as well for most of the drill-hole control points shown on the net-coal isopach map (fig. 28). (Correlation of Fruitland coal beds is discussed in more detail in another section of this report.)

Cross section A-A' (plate 1) crosses the northwest-trending thick net-coal band (fig. 28) between holes 11 and 17. Net-coal thicknesses across this band range from 40 ft to more than 80 ft near hole 15. On the net-coal isopach map (fig. 28), this band of thick coal appears to be somewhat variable in thickness but relatively continuous. Cross section A-A', however, portrays the geometry of the individual coal beds. The 60 ft of net coal at hole 12 includes 10 coal beds, whereas the 60 ft of net coal at hole 16 includes 6 totally different coal beds. Moreover, the coal beds in hole 16 are tens to hundreds of thousands of years younger than the coal beds in hole 12.

The cross section, between holes 18 and 20, clearly shows the details of the thinning coal seen on the net-coal isopach map in the northeast part of the basin.

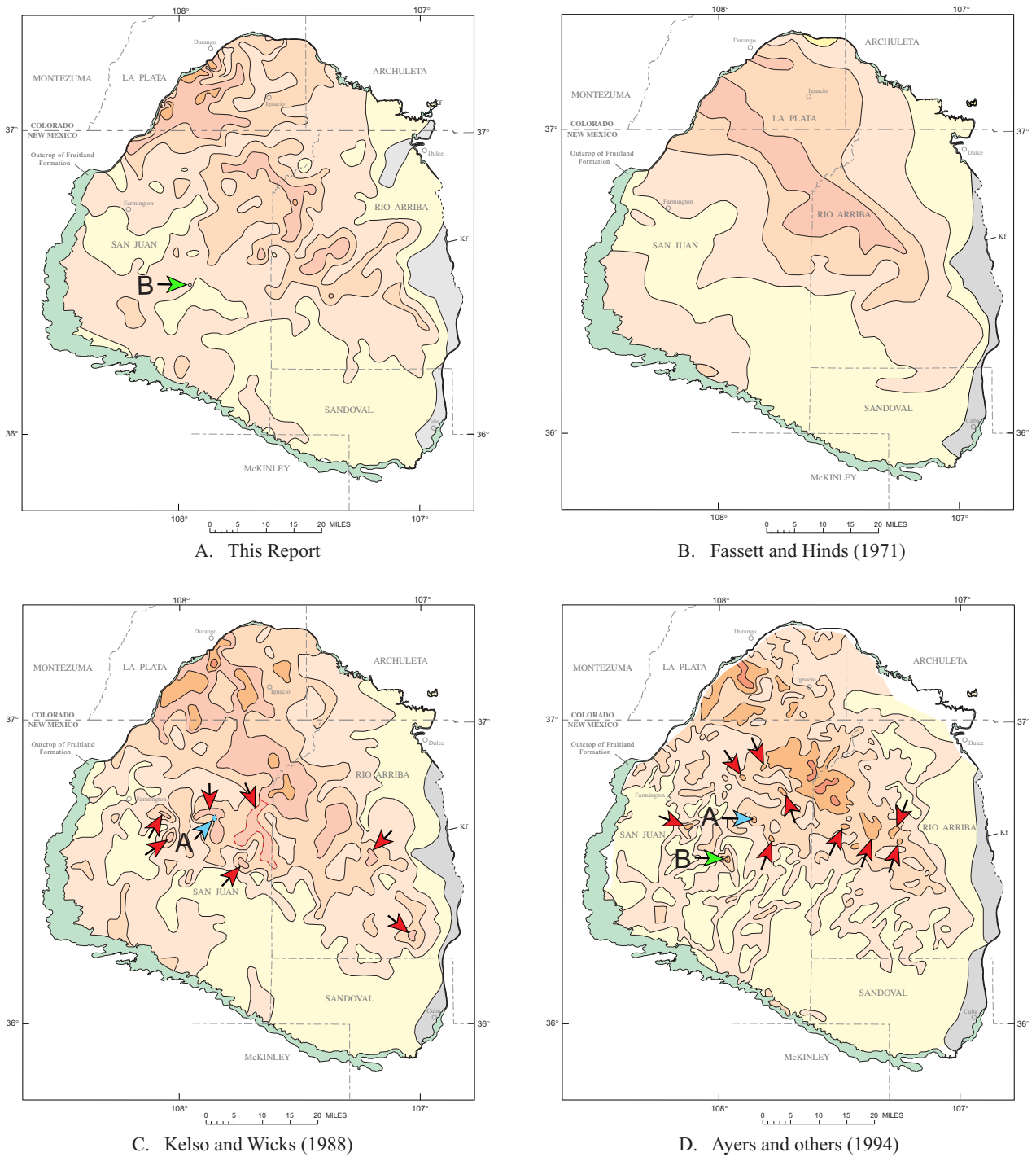
Comparison with Earlier Studies

Basin-Wide Studies.—Three earlier reports portrayed the distribution of Fruitland Formation coal beds throughout the San Juan Basin: Fassett and Hinds (1971), Kelso and Wicks (1988), and Ayers and others (1994). A comparison of the net-coal isopach maps from those reports with the net-coal map of this report is on figure 29. The procedures and methods used to determine Fruitland coal thicknesses for each of these maps were somewhat different.

Fassett and Hinds (1971).—This report was the first attempt to quantify coal resources in the subsurface of a Western Interior coal basin using geophysical logs of oil and gas wells to measure coal thicknesses. (The use of geophysical logs for coal resource assessment was pioneered by the Illinois State Geological Survey in the 1950's; one of the first publications to provide a detailed discussion of the methodology of using resistivity logs to measure coal thicknesses in the subsurface was Hopkins (1968).) As discussed in the "Geophysical Logs" section of this report, Fassett and Hinds (1971) relied primarily on resistivity logs (supported by radioactivity logs, sonic logs, and drilling-rate records) on which to measure coal-bed thicknesses. In the late 1960's when the database for that report was compiled, the geophysical log file for the San Juan Basin primarily consisted of resistivity logs. The authors used geophysical logs from 270 drill holes and 54 coal measurements made on the outcrop as control points to construct the total-coal isopach map shown on panel B of figure 29. Coal beds less than 16 inches thick were generally ignored and non-coal partings more than 1 ft thick were excluded from the total coal thicknesses determined from geophysical logs (Fassett and Hinds, 1971, p. 52).

Kelso and others (1987) and Kelso and Wicks (1988).—These reports contained identical net-coal isopach maps (panel C of fig. 29) for Fruitland coal beds in the San Juan Basin. These authors recalculated Fruitland coal resources to establish a more detailed database for coal-bed-methane resource estimates for the basin. The 1987 report contains more detail regarding the methodology used to measure coal thicknesses and states (p. 121), "A net coal isopach map was constructed using data from gamma-density, density-porosity, and a limited number of gamma ray-neutron geophysical logs Net coal values do not include coals thinner than 2 ft with efforts made to exclude partings and shaley units within individual coals." (Parting thicknesses excluded were not given.) Kelso and Wicks (1988, p. 71) state that 549 well logs were used to characterize Fruitland coals but only 471 wells are present on their net-coal isopach map (their fig. 5).

Ayers and Ambrose (1990) and Ayers and others (1994).—This study was conducted to estimate the amount of coal-bed methane in Fruitland coal beds in the San Juan Basin. Even though the 1990 and 1994 reports are similar, the net-



EXPLANATION
Net Coal Thickness Categories







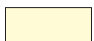
	Greater than 100 feet		60 to 80 feet		20 to 40 feet (30 to 50 feet on D)		Zero coal ("Fruitland Fm. truncated" on D)
	80 to 100 feet (70 to 100 feet on D)		40 to 60 feet (50 to 70 feet on D)		Less than 20 feet (less than 30 feet on D)		

Figure 29. Comparison of three, published, Fruitland Formation net-coal isopach maps with the net-coal isopach map of this report. Kf, Fruitland Formation. Arrows on panels A, C, and D indicate small areas or bull's-eyes of thick coal discussed in text. Area of coal 60–80 ft thick on panel C outlined by dashed line is also discussed in the text.

coal isopach map from the 1994 report is a modified version of the map in the 1990 report and is the isopach map shown on panel D of figure 29. Ayers and others stated (p. 38, 39) that logs from 1,731 wells were used “to evaluate and map Fruitland coal beds.” Wells used as control points for the net-coal isopach map in the 1994 report are not shown, but the 1990 net-coal isopach map shows 1,350 wells used as control points. It is not clear what kinds of geophysical logs were used to measure Fruitland coal-bed thicknesses, but the implication is that a variety of log types was used including density logs, gamma ray–neutron, sonic logs, and resistivity logs. The methodology used to measure coal beds on logs is summarized in Ayers and others (1994, p. 26), “On geophysical logs, the thickness of a bed is commonly measured halfway between the shale baseline and the peak corresponding to that bed. On the bulk-density log ... coal-seam thickness was measured at a density of approximately 1.80 g/cm^3 , which is a slightly conservative measurement. We recorded the thickness of coal seams thicker than 2 ft ($>0.6 \text{ m}$); partings thinner than 2 ft (0.6 m) in thick coal seams were included as coal because of the limits of resolution of the geophysical logs.” The Ayers and others net-coal isopach excluded Fruitland coal beds shallower than 400 ft.

The original versions of the net-coal isopach maps shown on panels A and B (fig. 29) had a contour interval of 10 ft; those maps were redrawn to show only the 20-ft contour lines to more directly compare the thick and thin coal patterns of those maps with the net-coal isopach maps on panels C and D. The map on panel C was published with a 20-ft contour interval and is shown here as it was published. The map on panel D is also shown as published with contours of 30 ft, 50 ft, 70 ft, and 100 ft.

The northwest-trending distribution pattern for areas of thicker and thinner net coal in the San Juan Basin is seen on all of the net-coal isopach maps on figure 29. The northeast-trending pattern is not seen on panel B, but is evident on the other three isopach maps. (Figure 28 of this report has a 10-ft contour interval and thus shows the northeast trend in greater detail.)

The net-coal isopach maps of panels C and D generally show thicker coal than the panel A map of this report. The C and D maps also contain several bull’s-eyes of thick coal (60–80 ft thick on panel C and greater than 70 ft thick on panel D) southwest of the main thick coal trend. These bull’s-eyes are shown by arrows on figure 29 on panels C and D. The bull’s-eye areas are in different places on maps C and D except for the one shown with a blue arrow (labeled A) on both maps. This small, thick-coal area of map D is shown superimposed on the larger area of thick coal on map C.

Examination of the bulk-density logs in the areas shown by arrows on maps C and D indicates that, in those areas, cavings in the bore holes were measured as coal beds on bulk-density logs thus inflating the net-coal thicknesses in those holes. None of the thick coal areas shown with arrows on maps C and D actually exist including the relatively large area of coal 60–80 ft thick outlined by a dashed line on map C.

Figure 30 shows the density log for the drill hole that defines the bull’s-eye of thick coal (more than 70 ft thick) shown with a green arrow and labeled B on panel D of figure 29. On panel A, this same well (shown with a green arrow labeled B) is in the 20 to 40 ft interval of net-coal thickness, near the 20-ft line. Figure 30 shows how these greatly differing net-coal thicknesses were obtained from the log of the same well. This figure shows the bulk-density, gamma ray, and caliper logs for this drill hole. Intervals with a density less than 1.75 g/cm^3 to the left of the 1.75 g/cm^3 line, are shaded, for emphasis, on the bulk-density curve. Intervals with a hole diameter greater than 11 inches are shaded on the caliper log trace; normal drill hole diameter is $7 \frac{7}{8}$ inches and cavings in the hole to a diameter greater than 11 inches have a definite impact on the bulk-density log trace, causing it to mimic coal beds. Tops and bottoms of “coal beds” using the criteria of Ayers and others (1994) are listed under column A on figure 30. True tops and bottoms of coal beds as measured for this study are listed under column B on figure 30. Intervals where the caved drill hole caused the bulk-density log to give a false coal signature are shown with a rectangle with an X in it in the shaded portion of the bulk-density log trace. The 1.8 g/cm^3 density is shown with a dashed line on figure 30 to indicate at what point Ayers and others picked the tops and bottoms of coal beds for their study.

Figure 30 shows that Ayers and others (1994) obtained a net coal thickness of 72 ft for this hole—nearly three times greater than its true thickness of 26 ft—for two reasons: (1) they used a coal-density cut-off of 1.8 g/cm^3 rather than 1.75 g/cm^3 to measure coal thicknesses on the bulk-density log, and (2) they were apparently unaware that caved zones in bore holes can mimic the low-density coal response on a bulk-density log. In general, net-coal isopach maps C and D show thicker coal throughout the basin than net-coal isopach map A (fig. 29).

Other Studies

Biewick and others (1991).—This study of Fruitland coal resources was limited to the New Mexico part of the San Juan Basin and used data in the U.S. Geological Survey’s National Coal Resources Data System (NCRDS) to construct a net-coal isopach map and for resource calculations. The net-coal isopach map (their fig. B2) used 630 data-point locations. Because most of the data points in the NCRDS database came directly from the Fassett and Hinds (1971) report, the Biewick and others isopach map was very similar to the net-coal isopach of that report (panel B, fig. 29). Their isopach map is also similar to the net-coal isopach map of this report (fig. 28), except that it does not show the northeasterly pattern of thick and thin coals that are present in the northwest-trending thick coal area.

Boger and Medlin (1991).—This study also calculated Fruitland coal resources using the database generated by Biewick and others (1991) from the NCRDS database but used an experimental kriging methodology to contour the data points. The resulting net-coal isopach (fig. C3) for the New Mexico

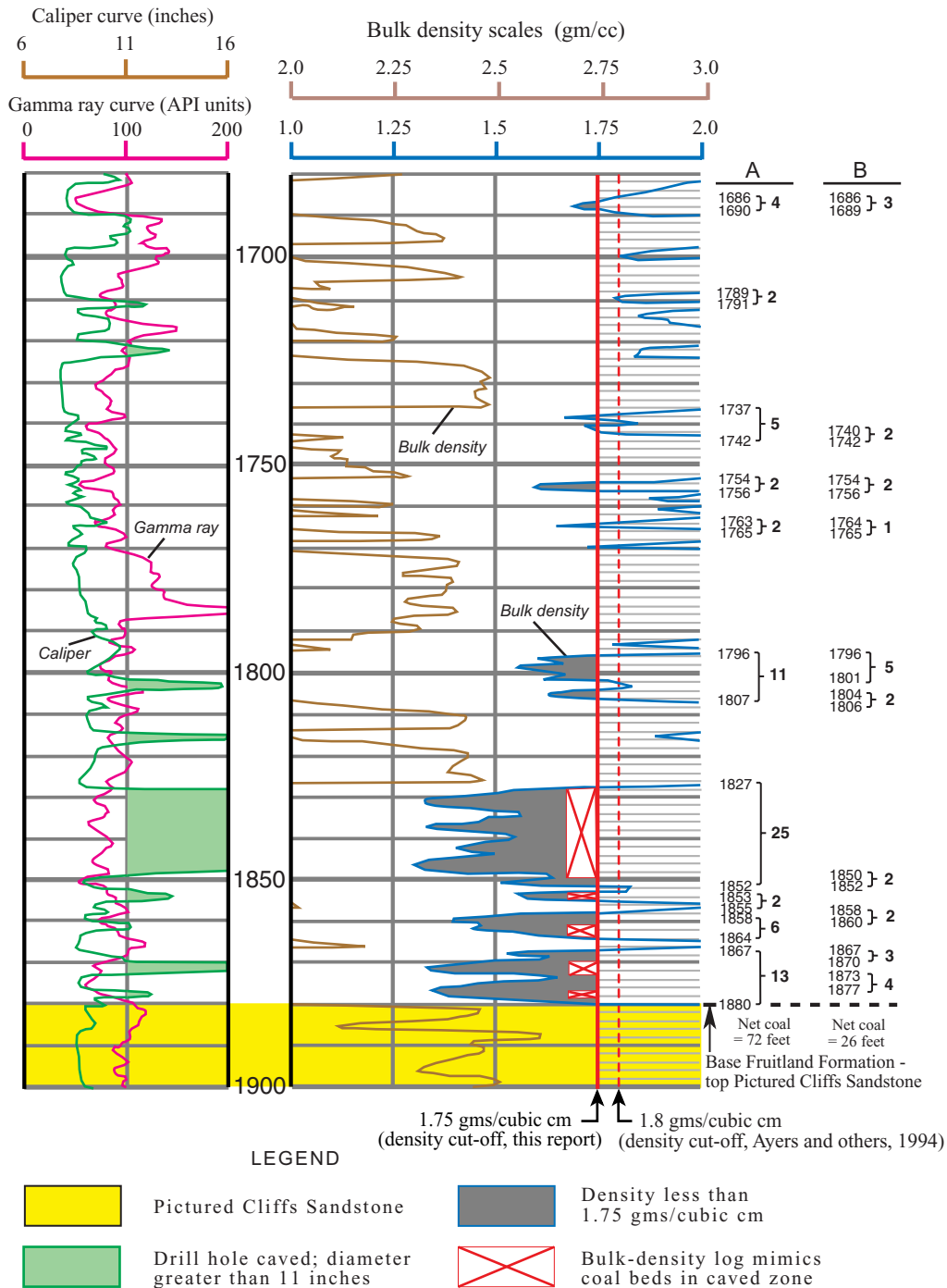
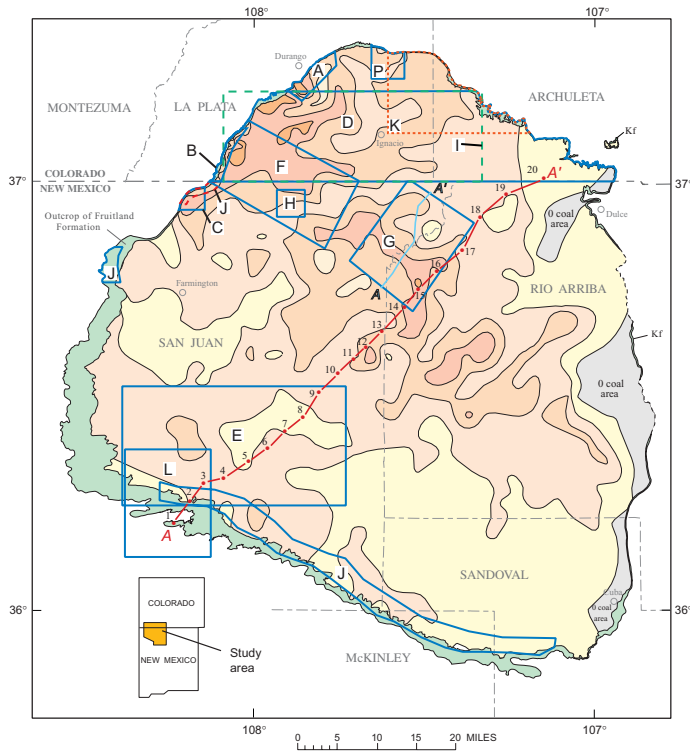


Figure 30. Density log from the Southland Royalty Company Federal 12-14 well in SE¼SW¼ sec. 12, T. 26 N., R. 11 W., San Juan County, New Mexico. Well location is shown with green arrow labeled B on panels A and D of figure 29. Column A contains all intervals of density less than 1.8 g/cm³; column B lists true coal thicknesses in this well with a density less than 1.75 g/cm³ and excluding low-density intervals resulting from cavings in drill hole. This figure illustrates how incorrect (thicker than true values) net-coal determinations were made for the bull's-eye areas shown by arrows on panels C and D of figure 29.

part of the San Juan Basin is quite similar in its portrayal of Fruitland coal distribution throughout the New Mexico part of the basin to the Biewick and others net-coal isopach and the Fassett and Hinds (1971) net-coal isopach.

Several other local studies of Fruitland coal resources were conducted by Shoemaker and Holt (1973), Kelso and others (1980), Sandberg (1988a, 1988b, 1990), Roberts (1991), Ayers and Zellers (1994), Ambrose and Ayers (1994), and



References For Areas Shown on Map

- A/P - Fassett and others, 1997b
- B - - - Roberts, 1989 and Roberts and Uptegrove, 1991
- C - - - Roberts, 1991
- D - - - Sandberg, 1988a, 1988b, 1990
- C/D - Shomaker and Holt, 1973
- E - - - Sandberg, 1986
- F - - - Ambrose and Ayers, 1994
- G - - - Ayers and Zellers, 1994
- H - - - Decker and others, 1988
- I - - - Kelso and others, 1980 and Kelso and Rushworth, 1982
- J - - - Hoffman, 1991 and Hoffman and others, 1993
- K - - - M'Gonigle and Roberts, 1997
- L - - - Hoffman and Jones, 1998

Figure 31. Map showing areas of published detailed subsurface studies of Fruitland coal beds. Base map is Fruitland net-coal isopach map from panel A, figure 29; darker colors indicate thicker coal. Basin-wide cross section A-A' is on plate 1. Short cross section A-A' in area G is on figure 32. Kf, Fruitland Formation.

M'Gonigle and Roberts (1997). All of these reports contained net-coal isopach maps showing Fruitland coal distribution in their study areas. A more detailed discussion of each of these reports is presented in the following section of this report.

Subsurface Studies

Local Studies

**Fruitland Coal-Bed Correlations—
Earlier Studies**

Surface Mapping

Mapping of Fruitland Formation coal beds by the U.S. Geological Survey began in the early 1900's, and, by the late 1950's, maps of the entire coal-bearing outcrop of the Fruitland had been published at a variety of scales. Those map publications are listed and discussed in Fassett and Hinds (1971, p. 54–57). All of the early mappers reporting on Fruitland coal beds on the outcrop stated that the beds were lensing and discontinuous and could rarely be correlated for more than a few miles. More recent mapping of outcropping Fruitland coal beds has been conducted by Roberts (1991), Roberts and Uptegrove (1991), and Fassett and others (1997b) in the northwest part of the basin. These reports also note the lensing nature of Fruitland coal beds and state that, even though zones of coal appear to be relatively continuous, individual coal beds usually cannot be correlated for more than a few miles at the most.

The locations of local subsurface study areas for Fruitland coal in the San Juan Basin are shown on figure 31, and an abbreviated citation for each study is also provided. Full citations for these reports are in the "References Cited" section of this report. Some of the study areas overlap, especially in the Colorado part of the basin. Each of the studies is briefly summarized below in chronological order. The letter designating the area on figure 31 and the author(s) and year of the report are listed at the beginning of each summary.

C/D—Shoemaker and Holt (1973).—This was the first local study that characterized subsurface Fruitland coal in detail using the geophysical-log methodology developed by Fassett and Hinds (1971). This study focused on the coal resources underlying the Ute Mountain Ute and Southern Ute Indian Reservations (fig. 2). On the Ute Mountain Ute Reservation, geophysical logs from 11 oil and gas tests and 13 coal test holes were used to estimate the coal resources underlying the reservation area. Coal thicknesses for each hole were given, but no attempt was made to correlate the coal beds. For the Southern Ute Reservation, 228 oil and gas tests and 90 coal test holes were used to evaluate Fruitland coal beds in the subsurface. To the extent possible, the authors of this

report selected one oil and gas drill hole per section to measure Fruitland coal beds. No cross sections were constructed, and only the most general observations were made regarding the continuity of Fruitland coal beds in this area. This report has been largely superseded by the Sandberg (1990, area D), Roberts (1991, area C), and in part by the Ambrose and Ayers (1994, area F) reports.

I—Kelso and others (1980).—This study included the western two-thirds of the Southern Ute Indian Reservation. The primary focus of the study was to determine Fruitland Formation coal tonnage in order to estimate the amount of coal-bed methane that might be present in the coal beds. Geophysical logs from 231 oil and gas test holes were used to measure coal-bed thicknesses throughout the area. Most of these holes are located in T. 32 N., Rs. 6–11 W., T. 33 N., Rs. 7–11 W., and T. 34 N., Rs. 9, 10 W. Some of these townships contain as many as 26 holes used for coal-thickness measurements. The average number of holes for the townships listed is 18. The report states that gamma ray–neutron logs were used exclusively to measure Fruitland coal beds. The warning is given, however, that (p. 14) “The response of gas bearing sandstones and coals can be confused on gamma ray–neutron logs. Since this type of log was used for picking coals in this study, it should be noted that the total coal thickness may be exaggerated by the inclusion of gas-bearing sandstones.”

Three stratigraphic cross sections across the study area were included in the report. These sections utilized a mixture of gamma ray–neutron logs and resistivity logs, but coal beds were not shown on the logs and no attempts were made to correlate Fruitland coal beds or zones on these cross sections. All of the cross sections used the top of the Pictured Cliffs Sandstone as a datum. The Kelso and Rushworth (1982) report describes Fruitland coals in two holes about a half-mile apart just northwest of Ignacio, Colo. (within area I—the Kelso and others, 1980, study area). Correlation of coal beds between these holes is not discussed.

E—Sandberg (1986).—This report focused on correlating Fruitland coal beds in the subsurface in a rectangular area in the southwest part of the San Juan Basin. Five stratigraphic resistivity-log cross sections on which all Fruitland coal beds are correlated are included in the report. All of these cross sections use the Huerfanito Bentonite Bed as a datum. The average spacing of drill holes on the cross sections is about 2 mi. Sandberg identified and named six coal beds in this report and showed the distribution of these beds on a map of the area. In the four northeast-trending cross sections, the top of the Pictured Cliffs Sandstone is shown to be rising stratigraphically and Sandberg states, “Where the Pictured Cliffs Sandstone–Fruitland Formation contact rises stratigraphically, progressively younger coal beds appear at the base of the Fruitland [Lower coal beds] end abruptly northeastward, and stratigraphically higher ones take their place.” Most of the beds shown consist of two or more benches separated by non-coal partings, and these benches are usually quite variable in their thickness and continuity.

Sandberg’s Navajo bed is the most continuous coal bed

in the area. It is about 10 ft thick and is correlated for 11 mi on northwest-trending cross section E-E’ and for 12 mi on northeast-trending cross section B-B’. Sandberg states that “The Navajo bed underlies much of the southern two-thirds of the area but disappears against the Pictured Cliffs Sandstone northeast of the Bisti oil field.” Drill holes 41 and 42 on Sandberg’s cross section D-D’ are the same holes as holes 3 and 4, respectively on stratigraphic cross section A-A’ (plate 1) of this report. Plate 1 shows the Huerfanito at a depth of 665 ft in the Tanner Unit 1 hole, whereas Sandberg shows the Huerfanito at a depth of 680 ft in this same drill hole. A relatively minor difference, but moving the Tanner Unit 1 log up 15 ft makes the thick coal bed in that hole correlate better with the thick coal bed in drill hole 4 on plate 1, which in the author’s opinion is not the case. This “coal bed” is named the Bisti bed in Sandberg’s report.

D—Sandberg (1988a, 1988b, 1990).—These three reports describe the results of a study of the Fruitland coal resources of the Southern Ute Indian Reservation. The 1990 report is the preferred reference because the illustrations are at a larger scale and it is more readily available. The 1988a report, however, contains a northeast-trending stratigraphic cross section of the Pictured Cliffs–Fruitland interval that is not present in the 1990 report. This section is on a line between Farmington, N. Mex., and Ignacio, Colo., and shows the Fruitland coal beds at each control point, identifies coal zones, but does not correlate individual coal beds. Geophysical logs from about 500 oil and gas drill holes and 24 coal test holes were used as a database for this study. Three east-trending and two north-trending stratigraphic cross sections are included in the report, and all use the Huerfanito Bentonite Bed as a datum. Fruitland coal beds are shown at each control point, but coal beds are not correlated. Three coal zones are correlated across the study area. Geophysical logs of five of the drill holes included in the cross sections are shown to demonstrate the log characteristics of Fruitland coal beds. The cross sections show that Fruitland coal beds are lensing and are generally not continuous for more than a few miles.

H—Decker and others (1988).—This report is a study of the Cedar Hill gas field, the first coal-bed methane field discovery in the San Juan Basin. The report focuses on gas production and reservoir characteristics but includes an arcuate cross section across the field showing the occurrence and continuity of Fruitland coal beds. The basal Fruitland coal is shown to be continuous over about a 1-mi² area on this cross section but the authors state that this bed (p. 222) “... is commonly split into several individual coal benches by shale partings ...” and varies in thickness from 4 to 26 ft. An upper zone of Fruitland coals is also shown on the cross section and consists of from one to four thin beds.

B—Roberts (1989).—This study consisted of a detailed exploratory core drilling project in the Fruitland Formation near the west side of the San Juan Basin in Colorado on the Southern Ute Indian Reservation. The report describes the results of the 23-hole core drilling project in which the Fruitland was cored along a 9-mi corridor east of and parallel

to the Fruitland outcrop. The average spacing for these holes was less than half a mile. Roberts (p. 5) observed "Individual coal beds present in the drill holes are lenticular and cannot be correlated between drill holes; however the zones in which coal beds occur can be correlated." The distribution and correlation of Fruitland coal zones was shown on a northeast-trending cross section using 22 of the core holes as control points; the top of the Pictured Cliffs Sandstone is the datum. This section shows that the lowermost A coal zone is continuous across the entire area and the D coal zone is continuous across about half the area, splitting into an Upper D and Lower D coal to the north. Stratigraphically higher "local" coal beds were discontinuous in this area. The Roberts and Uptegrove (1991) study mapped Fruitland coal beds on the outcrop adjacent to the area where the core hole drilling project was conducted. A correlation diagram was constructed showing the variability of Fruitland coal beds in the area. No attempt was made to correlate the outcropping coal beds with the coal beds in the core holes.

C—Roberts (1991).—In a study of subsurface Fruitland coal on the Ute Mountain Ute Indian Reservation Roberts examined geophysical logs from 50 drill holes. Density, gamma ray–neutron, and resistivity logs were used for coal identification and correlation. Subsurface coals were correlated with nearby outcropping Fruitland coal beds. Roberts used 34 of the 50 drill holes plus three measured surface sections as control points to construct three cross sections showing correlation and distribution of Fruitland coal beds in this area. Average spacing of control points was about 1 mi. Roberts reported that two informally named coal beds, the Main coal bed and the Ute Canyon coal bed, were present throughout the study area for a distance of about 10 mi on section B. The Upper Main coal bed, lower Ute Canyon coal bed, and other "local" coal beds were discontinuous in the area.

J—Hoffman and others (1993).—This study involved the drilling of Fruitland coal test holes in three areas in New Mexico—two in the northwest and one paralleling the Fruitland outcrop along the southern edge of the basin. The principal focus of the study was to obtain samples of Fruitland coal for physical and chemical analyses. Four stratigraphic cross sections show the distribution of Fruitland coal beds in the cored areas; all use the Pictured Cliffs Sandstone as a datum. Fruitland coal beds are correlated between drill holes. The cross section in the northwest contains nine drill holes and trends northeast, extending across the two areas labeled J on figure 31. Four holes are present in the southern of these two areas, and five holes are in the northern area with a gap of about 10 mi separating the two areas. The three cross sections in the south contain 38 drill holes and trend southeast, parallel to the Fruitland outcrop over a distance of about 75 mi. Fruitland coals are most continuous in the southwest part of the study area (Bisti area) with some beds being continuous for as much as 15 mi even though they thicken, thin, and split over this distance.

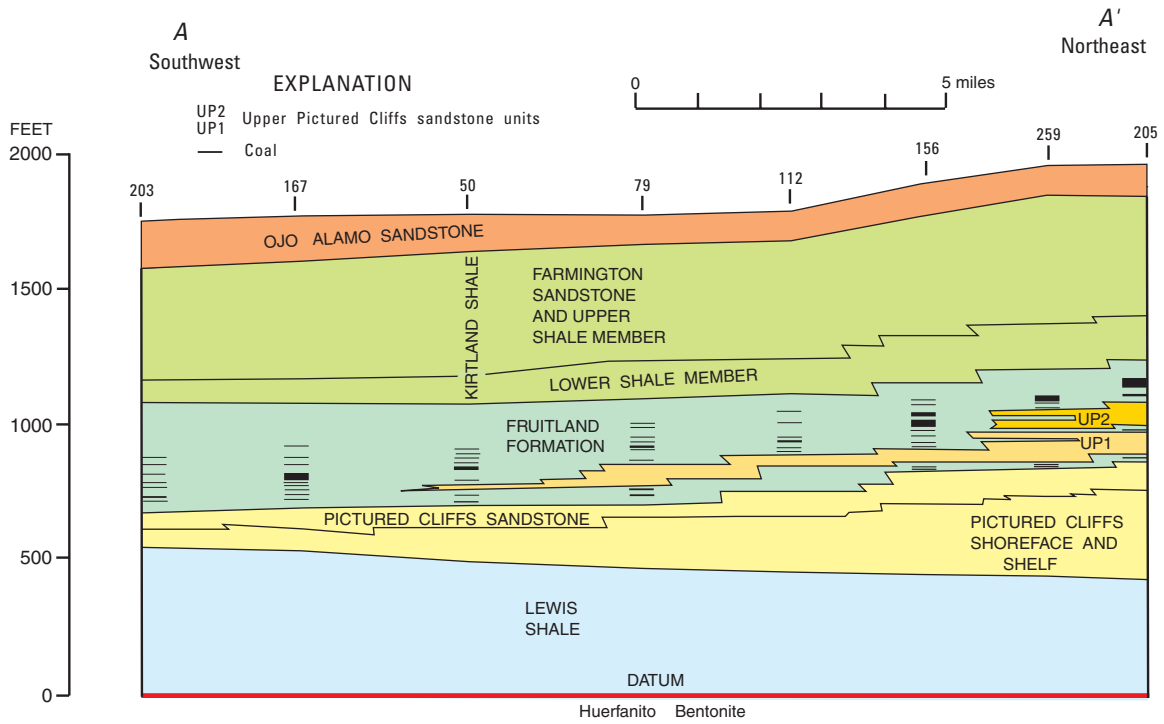
F—Ambrose and Ayers (1994).—This study was essentially focused on coal-bed-methane-producing wells in the

Cedar Hill gas field area but also included studies of Fruitland coal beds in adjacent areas including the core-hole data from the Roberts (1991) report discussed above. The report includes a northwest-trending, two-hole, stratigraphic cross section showing the distribution of Fruitland coal beds over this 4.5-mi area. The traces of the resistivity logs of the two holes are shown on the section; the datum is the top of the Pictured Cliffs Sandstone. The distribution of coal beds is quite different in these two wells, and no apparent correlations of coal beds are visible. The authors, however, put the coals into lower, middle, and upper coal groups. A 12-hole, northeast-trending structural cross section correlates Fruitland coal beds along a 14-mi-long area. This section shows great discontinuity of coal beds with beds thickening, thinning, pinching out, and splitting over relatively short distances. Lower Fruitland coal beds are shown pinching out against the stratigraphically higher tongues of the Pictured Cliffs Sandstone; stratigraphically higher coal beds appear to the northeast.

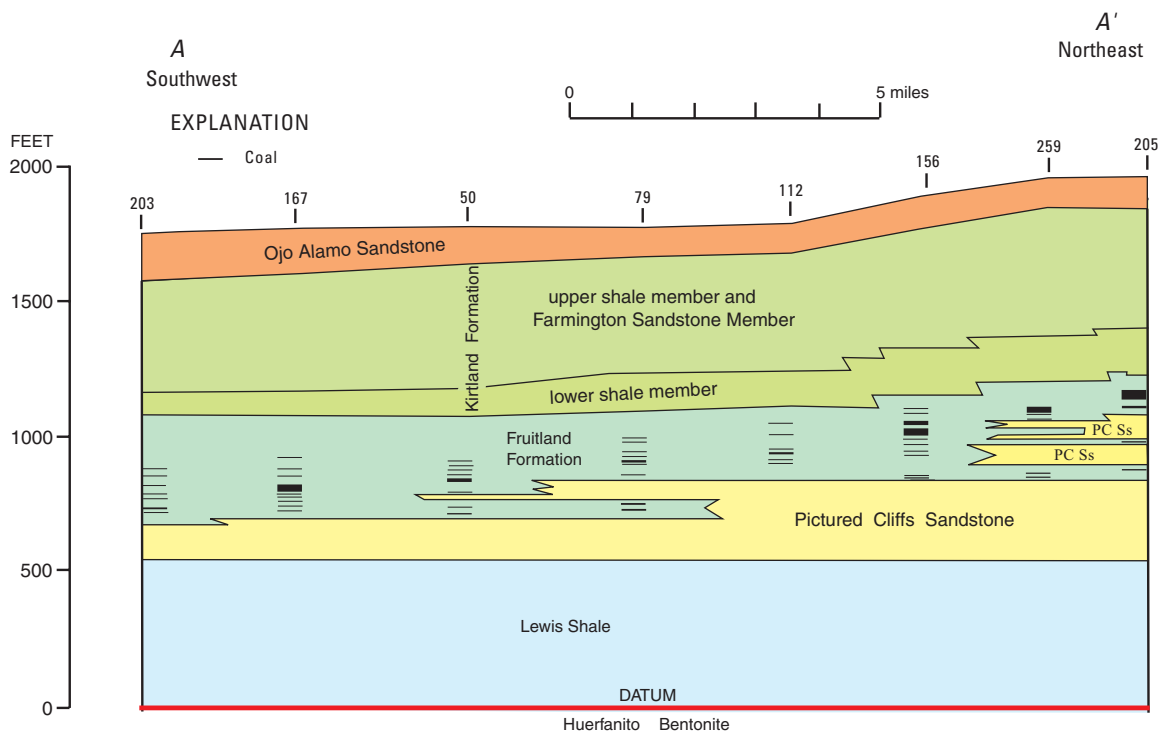
Figure 3.12 of Ambrose and Ayers is a stratigraphic cross section using the core holes for the northern part of the Roberts (1991) core-hole study area and using the top of the lowest coal bed as a datum. These authors offer a slightly different correlation of the Fruitland coal beds in this area than the one presented in the Roberts report.

G—Ayers and Zellers (1994).—This report focused on the coal-bed-methane resources of a 220-mi² area in the north-central part of the basin. The study involved the use of 400 drill-hole logs, mostly from producing Fruitland coal-bed methane wells. The Ayers and Zellers study is significant because it suggested an interpretation of the geometry and depositional history of the Pictured Cliffs Sandstone and the correlation of Fruitland coal beds that was greatly different from previous studies of the Pictured Cliffs and Fruitland in the San Juan Basin. Ayers and Zellers suggested that Pictured Cliffs–Fruitland deposition was controlled in the north-central part of the basin by tectonic subsidence along what they termed a "hingeline" that trended northwest across the basin. They wrote, "We suggest that structural activity caused a higher rate of subsidence in the northern part of the basin northeast of the structural hingeline This greater subsidence created more accommodation space, causing a stillstand of the Pictured Cliffs shoreline and allowing the accumulation of thick Fruitland peats." Ayers and Zellers offered no data to support this interpretation but provided illustrations in their report to show the results of their proposed geologic history. Three of their illustrations are herein reproduced and discussed in order to evaluate their interpretations.

Figure 32 contains two panels showing A, a reproduction of figure 4.1 of the Ayers and Zellers report, and B, a more conventional interpretation of this cross section. The line of this cross section is A-A' in area G of figure 31. Panel B uses the same coal-bed and formation-boundary intercepts as on panel A (except for the top of the Pictured Cliffs in well 112); no attempt was made to reinterpret the original well logs to redraw this figure. The relationship of the Pictured Cliffs Sandstone to tongue UP1 of the Pictured Cliffs as depicted



A. Figure 4.1 from Ayers and Zellers (1994)



B. Reinterpretation of figure 4.1 of Ayers and Zellers (1994)

Figure 32. Two interpretations of Pictured Cliffs Sandstone–Fruitland Formation stratigraphy in the north-central San Juan Basin. Panel A is cross section A-A' from Ayers and Zellers (1994, fig. 4.1). Panel B is a more conventional portrayal of these rocks. Line of cross section is shown in area G of figure 31.

on panel A is geologically not possible. Ayers and Zellers state in their report that the main body of the Pictured Cliffs represents a regression of the Pictured Cliffs shoreline to the northeast and that the Pictured Cliffs rises stratigraphically to the northeast, as shown on panel A, northeast of well 79. They state that tongue UP1 represents a transgression of the Pictured Cliffs shoreline to the southwest. Yet on panel A, UP1 is shown *descending* stratigraphically to the southwest. This interpretation could not be correct because by the time the Pictured Cliffs shoreline had reached well 205 on panel A, Fruitland sediments would have accumulated to at least the level of the top of the main body of the Pictured Cliffs at well 205 and probably slightly higher to allow for some regional slope of the land surface from the position of well 50 to the position of well 205. A transgressive pulse of the Pictured Cliffs shoreline from the position of well 205 would thus have resulted in, at the most, a relatively flat base to tongue UP1 or even a slight stratigraphic rise in a landward direction to the southwest.

A more realistic portrayal of the data presented in panel A is shown on panel B, where the Pictured Cliffs tongue at well 50 connects to the main body of the Pictured Cliffs between wells 79 and 112. The geologic history resulting in this geometry was (1) regression of the Pictured Cliffs shoreline to about the position of well 112, (2) transgression of the shoreline to a position southwest of well 50, and finally, (3) regression of the Pictured Cliffs shoreline to the northeast edge of the area at well 205. This scenario calls for no lowering in the stratigraphic level of the Pictured Cliffs tongues to the southwest. The two Pictured Cliffs Sandstone tongues present in wells 259 and 205 represent two additional pulses of Pictured Cliffs shoreline transgression and regression following the regression of the Pictured Cliffs shoreline northeast of well 205.

Figure 4.16 of Ayers and Zellers shows coal-bed correlations on their structural cross section C-C' over a distance of 5 mi along the same line of section as their cross section 4.1 (A-A' of area G, fig. 31), discussed above. Wells 50 and 167 are common to both cross sections (note that the numbers of coal beds, their thicknesses, and their positions are quite different for wells 50 and 167 on figures 4.1 and 4.16). Ayers and Zellers' structural cross section C-C' is shown on panel A of figure 33. Because coal-bed correlation is more difficult on a structural cross section, the panel A cross section was changed to a stratigraphic cross section on panel B of figure 33 using the top of the Pictured Cliffs as a datum but maintaining the original coal-bed correlations shown on panel A. The resultant correlations of panel B, however, appear unrealistic in terms of the upper two coal beds being time-transgressive and climbing over the tongue of Pictured Cliffs between wells 12 and 403. Panel C is a modification of the panel B correlation diagram showing a more probable correlation of these coal beds. This diagram shows that, even over a distance as short as 5 mi, Fruitland coal beds are lensing and discontinuous.

Panel A of figure 34 shows cross section B-B' from the Ayers and Zellers report (their figure 4.18). The line of section

for B-B' is almost identical to the northern two-thirds of their cross section A-A' (figure 4.1) shown in area G on figure 31. Well 205 is common to both cross sections (note again that coal-bed numbers, thicknesses, and positions are different in well 205 of figures 4.18 and 4.1). On figure 4.18, Ayers and Zellers presented two interpretations of the geometry of the Fruitland and associated rocks; the first interpretation (a) uses the Huerfanito Bentonite Bed as a datum; the second, interpretation (b) uses the base of the Ojo Alamo Sandstone as a datum. There are problems with both of these depictions. On the section using the Huerfanito as a datum (interpretation a), the geometry of the stratigraphically rising main body of the Pictured Cliffs appears to be appropriate, but again, as in their cross section A-A' (fig. 32 of this report), the authors show the transgressing tongue of Pictured Cliffs, UP1, becoming stratigraphically lower to the southwest. It is suggested that the lowermost part of UP1 connects with the main body of the Pictured Cliffs near well 213 as drawn on panel B of figure 32 and discussed above. In addition, Ayers and Zellers show the Ojo Alamo Sandstone rising stratigraphically between wells 70 and 213 and intertonguing with the Farmington Sandstone Member. This depiction is incorrect because there is a substantial unconformity (7–8 m.y.) separating the Tertiary Ojo Alamo from the Upper Cretaceous Farmington Sandstone Member. This contact should be drawn as a straight line between wells 70 and 213 and depicted as an unconformable contact.

Ayers and Zellers justified the use of the base of the Ojo Alamo as a datum on cross section 4.18b (fig. 34) as follows (p. 80–81):

Using a datum above the Fruitland Formation (fig. 4.18b) gives a different perspective of basin-filling processes and suggests structural control of the Pictured Cliffs shoreline and, indirectly, the distribution of thick Fruitland coal seams Therefore, the base of the Ojo Alamo Sandstone was used as a local datum. From fig. 4.18b we surmise that differential subsidence north of a structural hingeline ... controlled movement of the Pictured Cliffs shoreline by creating more accommodation space in the northern part of the basin. In fig. 4.18b, it is apparent that (1) if the increased thickness of Lewis Shale between wells 70 and 213 is due to differential subsidence, then thick coals in well 70 may override UP1 and UP2 in well 213 rather than terminate against them as suggested in fig. 4.18a, and (2) if less rapid aggradation is required at well 70 to keep pace with aggradation in well 213, then more time is available for uninterrupted peat accumulation at well 70, and hence the greater thickness of peat southwest of UP1. Because Upper Cretaceous strata thicken basinward, in part because of increased basin subsidence, coal seams are not parallel to the Huerfanito Bentonite.

It is clear from this quotation that Ayers and Zellers considered their depiction of the Fruitland Formation and associated rocks on figure 4.18b to be a linchpin for their arguments that “differential subsidence” north of a “structural hingeline” was the explanation for thick coals overriding tongues of Pictured Cliffs Sandstone. The flaw in this argument is that the base of the Ojo Alamo Sandstone is an unconformity representing about 7–8 m.y. of missing time (fig. 13, plate 1).

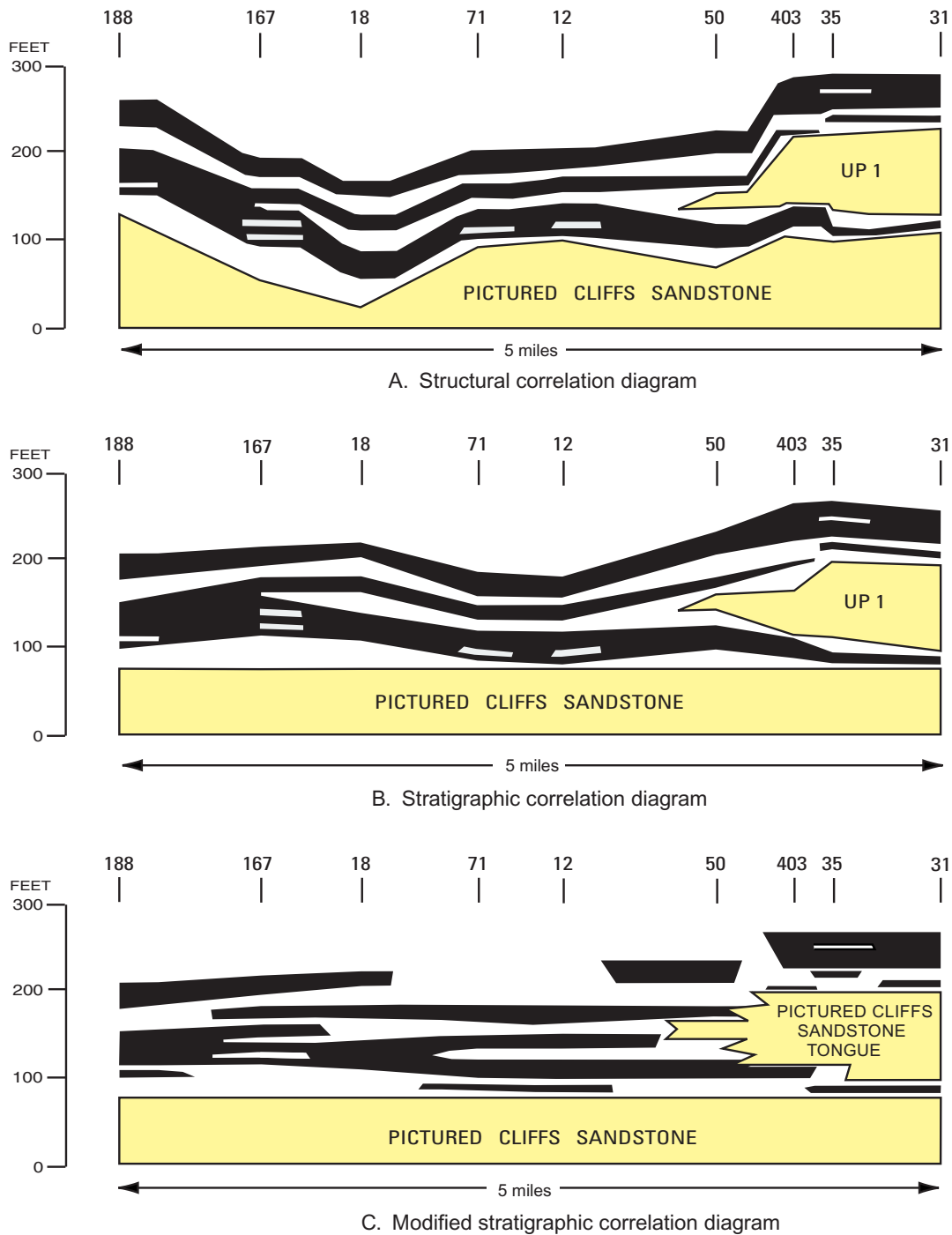
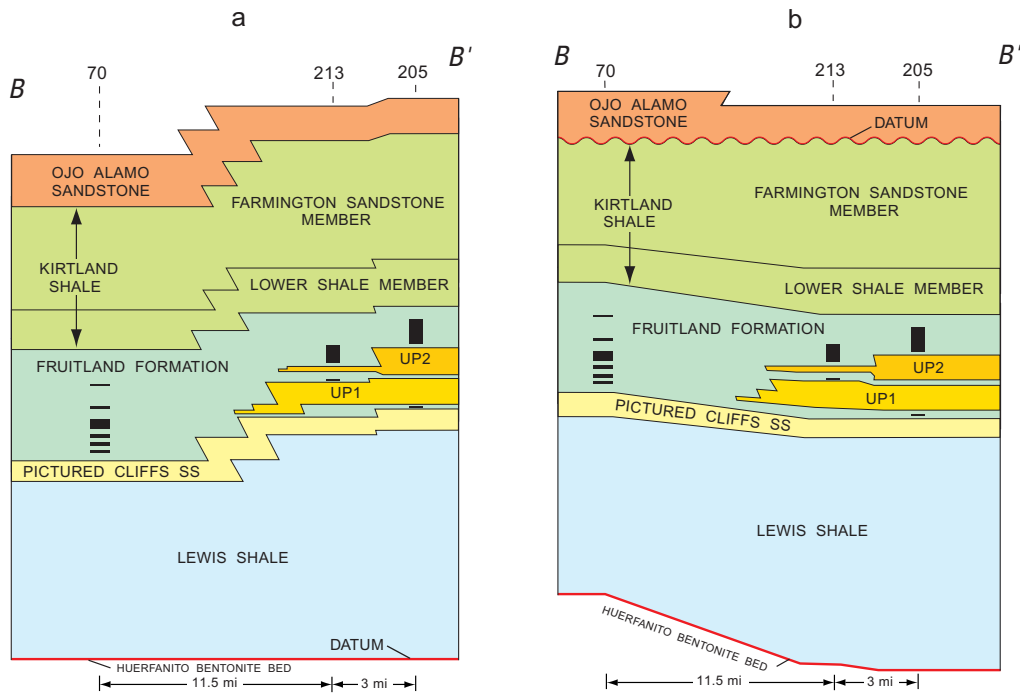
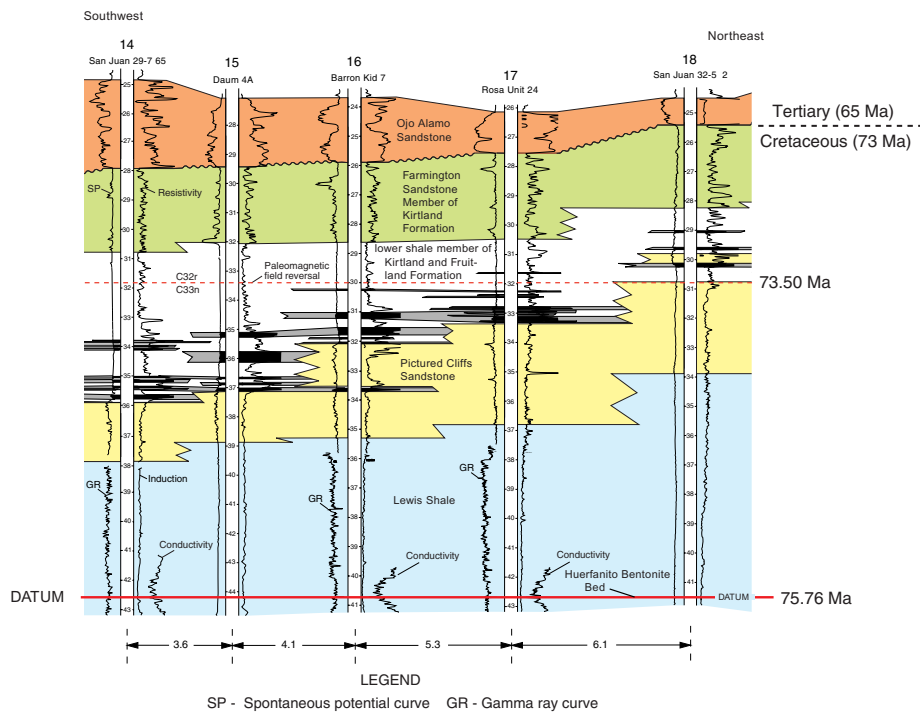


Figure 33. Alternative interpretations of coal-bed correlation diagram C-C' from Ayers and Zellers (1994, fig. 4.16). Panel A shows original figure which is a structural cross section; panel B is modification of A showing coal-bed correlations unchanged but with a stratigraphic datum—the top of the Pictured Cliffs Sandstone; panel C is a modified stratigraphic cross section portraying a more likely correlation of these coal beds. Line of cross section is nearly the same as the south end of section A-A' of Ayers and Zellers (1994, fig. 4.1). Line of section A-A' is in area G of figure 31, section A-A' is on figure 32; control points 50 and 167 are common to A-A' and this cross section.



A. Figure 4.18 from Ayers and Zellers (1994)



B. Segment of cross section A-A' (plate 1 of this report)

Figure 34. Comparison of stratigraphic interpretations of Fruitland Formation and associated rocks as presented by Ayers and Zellers (1994) and this report. Panel A shows two interpretations of stratigraphy for section B-B' by Ayers and Zellers with different datums. Line of section B-B' is nearly the same as section A-A' shown in area G of figure 31; control point 205 is common to both sections. Panel B shows part of cross section A-A' (plate 1) of this report; this section is parallel to and about 6 miles southeast of the Ayers and Zellers cross sections (fig. 31).

During that 7- to 8-m.y. time span, subsidence of the basin area ceased; Upper Cretaceous rocks were uplifted, especially in the southeast part of the basin; and erosion subsequently removed as much as 1,200 ft of strata on the east side of the basin (figs. A3-2 through A3-5). Next, uplift, north or northwest of the present basin area, created a highland that became the source of high-energy, braided-stream deposits that are now the conglomeratic Ojo Alamo Sandstone. (See Fassett, 1985, p. 318–322, for a detailed description of these geologic events.) These events effectively decoupled the erosion surface on which the Ojo Alamo Sandstone was deposited from any events that may have controlled the deposition of the Pictured Cliffs Sandstone and overlying Fruitland coal beds more than 10 m.y. earlier. The use of an overlying unconformity as a datum to interpret the depositional history of underlying rocks is geologically invalid, and the use of that interpretation to justify a radically new structural interpretation for deposition of the Pictured Cliffs and Fruitland cannot be defended.

Cross section A-A' (plate 1) of this report is parallel to and about 6 mi southeast of the Ayers and Zellers cross sections discussed above and shown in area G of figure 31. Panel B of figure 34 shows the segment of the A-A' cross section that corresponds to the cross sections of Ayers and Zellers. The radiometric ages of the Huerfano Bentonite Bed and the reversal in the Earth's magnetic field from magnetic chron C33n to C32r are shown on this cross section to emphasize the temporal evolution of the Lewis Shale, Pictured Cliffs Sandstone, and Fruitland Formation and to emphasize the parallelism of time lines within these rock units. Correlation of Fruitland coal beds and other rock units on panel B are more realistic and accurate than either of the two depictions shown on panel A.

A/P—Fassett and others (1997b).—This report was a study of two separate areas near the outcrop of the Fruitland Formation in the northern part of the San Juan Basin. The study was conducted to try to determine the source of methane seeping from Fruitland Formation coal beds at several gas seeps on the northern rim of the basin. An integral part of this study was to conduct the most precise correlation of Fruitland coal beds possible, especially from the outcrop into the subsurface, to determine if these coals could be conduits for gas moving updip from producing gas wells. The study included large-scale surface mapping of Fruitland coal beds adjacent to the seep areas.

In the Pine River gas-seep study area (area P on figure 31), four closely spaced test holes were drilled downdip from gas seeps to try to determine the source of the gas seeps. These holes are less than 0.2 mi apart, and three of them were cored through the Fruitland coals to provide a closely spaced subsurface data set with which to correlate Fruitland coal beds. (Coal thickness measurements from drill core from these three holes confirmed the accuracy of determinations of coal thicknesses and coal quality based on the density logs of these holes.)

Stratigraphic cross section A-A' on figure 35 is a copy of figure 1-3a from the Fassett and others study (1997b) showing

detailed correlations of Fruitland coal beds in the Pine River area over a distance of 4.4 mi using five wells and drill holes for control. This east-trending cross section is parallel to the Fruitland Formation outcrop. The basal coal lying directly on top of the Pictured Cliffs is continuous across the area but splits and thins to the east. The thick middle coal bed also extends across the area but splits both to the east and west. Other coal beds on this cross section are discontinuous along the line of section.

Cross section B-B' on figure 35 is figure 1-4a from the Fassett and others study (1997b), showing detailed correlations of Fruitland coal beds over a distance of 3 mi using seven wells and drill holes for control. The three northernmost drill holes are cored. This north-trending cross section is at right angles to the Fruitland outcrop, and the base of the Fruitland ranges from a depth of 221 ft in the Killian Deep hole in the north to 1,968 ft in the Streeter GU 1 gas well to the south. All of the coal beds shown are clearly discontinuous and lensing, and the lowermost thicker coal beds on the southwest end of the cross section either pinch out or split, thin, and grade into carbonaceous shales on the north end of the cross section near the Fruitland outcrop. The stratigraphically higher and thinner coal beds on the north end of the section are all discontinuous and none are present in the deeper, coal-bed-methane-producing wells to the south. Two additional larger scale and more detailed cross sections in the vicinity of the Pine River gas seeps are in the Fassett and others report (fig. 1-6).

Figure 36 is a stratigraphic coal-correlation diagram from the Fassett and others study (fig. 1-8) in the Durango, Colo., area (area A, fig. 31). This cross section is 6.8 mi long and uses 8 coal-bed methane gas wells for control. More than 50 separate coal beds are present on this section, all of which, to a greater or lesser degree, are discontinuous, lensing, or splitting. None of the coal beds extend across the entire line of section. The most continuous coal bed is the one directly overlying the Pictured Cliffs Sandstone in the northeast part of the section, but this bed pinches out to the southwest between the University 9-2 and the Wheeler 8-1 wells. The very thick tongue of Pictured Cliffs Sandstone in the Federal 4-1 well (but not present in the University 9-2 well less than a mile to the southwest) is the most striking feature on this cross section. All of the thick lower Fruitland coal beds southwest of this Pictured Cliffs tongue pinch out against it to the northeast or wedge out into it as seen in the Federal 4-1 well. This thick Pictured Cliffs tongue was mapped on the outcrop less than a mile northwest of this well. From the Federal 4-1 well to the northeast, a different, stratigraphically higher sequence of thick lower Fruitland coals appear, but these coal beds are discontinuous and none are present in the Day-V-Ranch 35-1 well. Three additional coal-correlation diagrams oriented at right angles to the section on figure 36 are in the Fassett and others report. Those sections appear to show somewhat more continuity of the coal beds along the line of depositional strike of the Fruitland (southeasterly), but they are relatively short cross sections (about 1.5 mi long) and only use two or three wells each for correlation purposes.

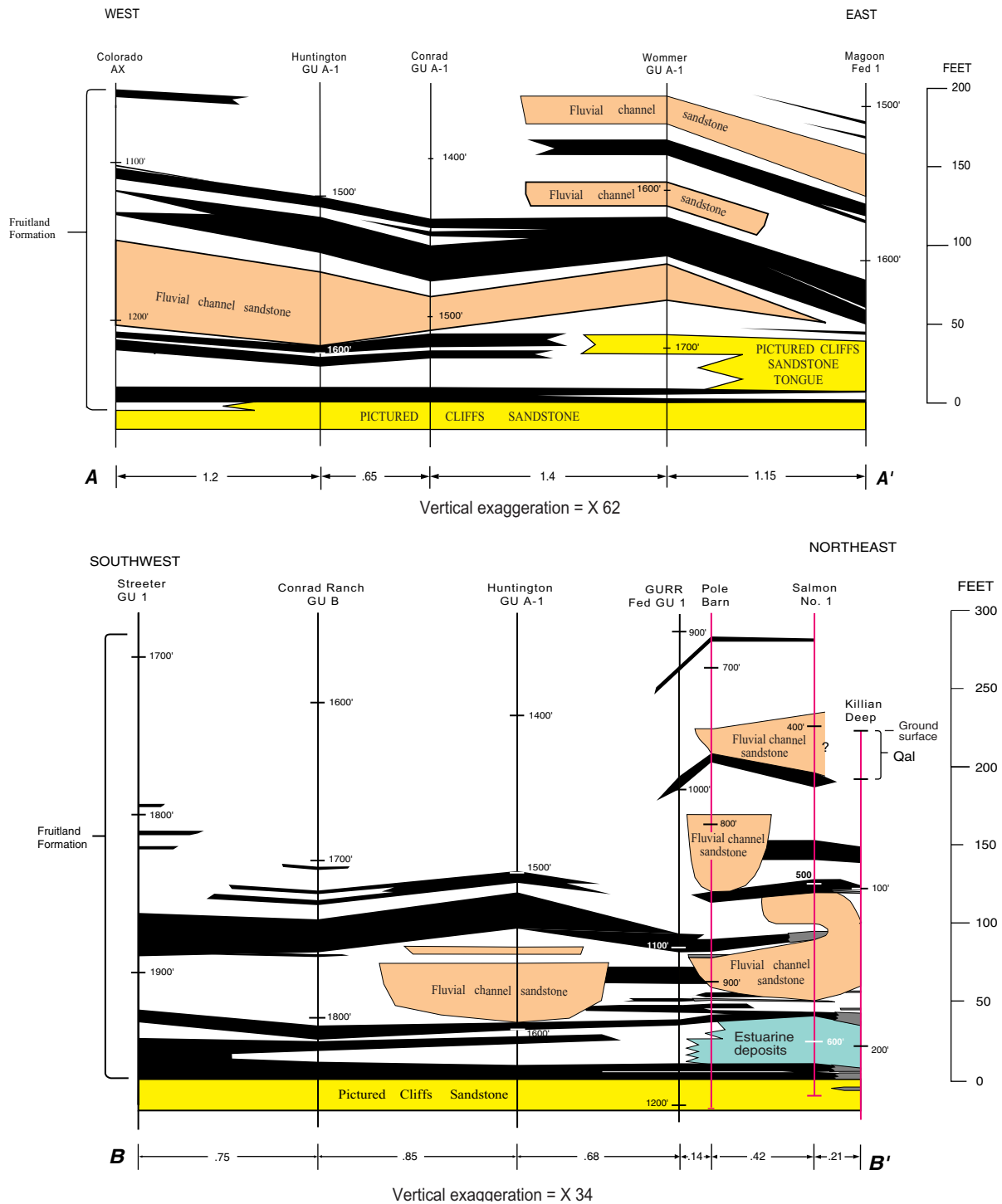


Figure 35. Fruitland Formation coal-bed correlation diagrams from the Pine River gas-seep study (Fassett and others, 1997). These cross sections are in area P on figure 31. Cross section A-A' is parallel to and about 1.5 mi south of the Fruitland Formation outcrop; section B-B' is at right angles to section A-A'. The Huntington GU A-1 well is common to both sections. The datum for both cross sections is the top of the Pictured Cliffs Sandstone. Cross sections are from figures 1-3a (A-A') and 1-4a (B-B') of Fassett and others (1997). Drill holes shown in red were cored.

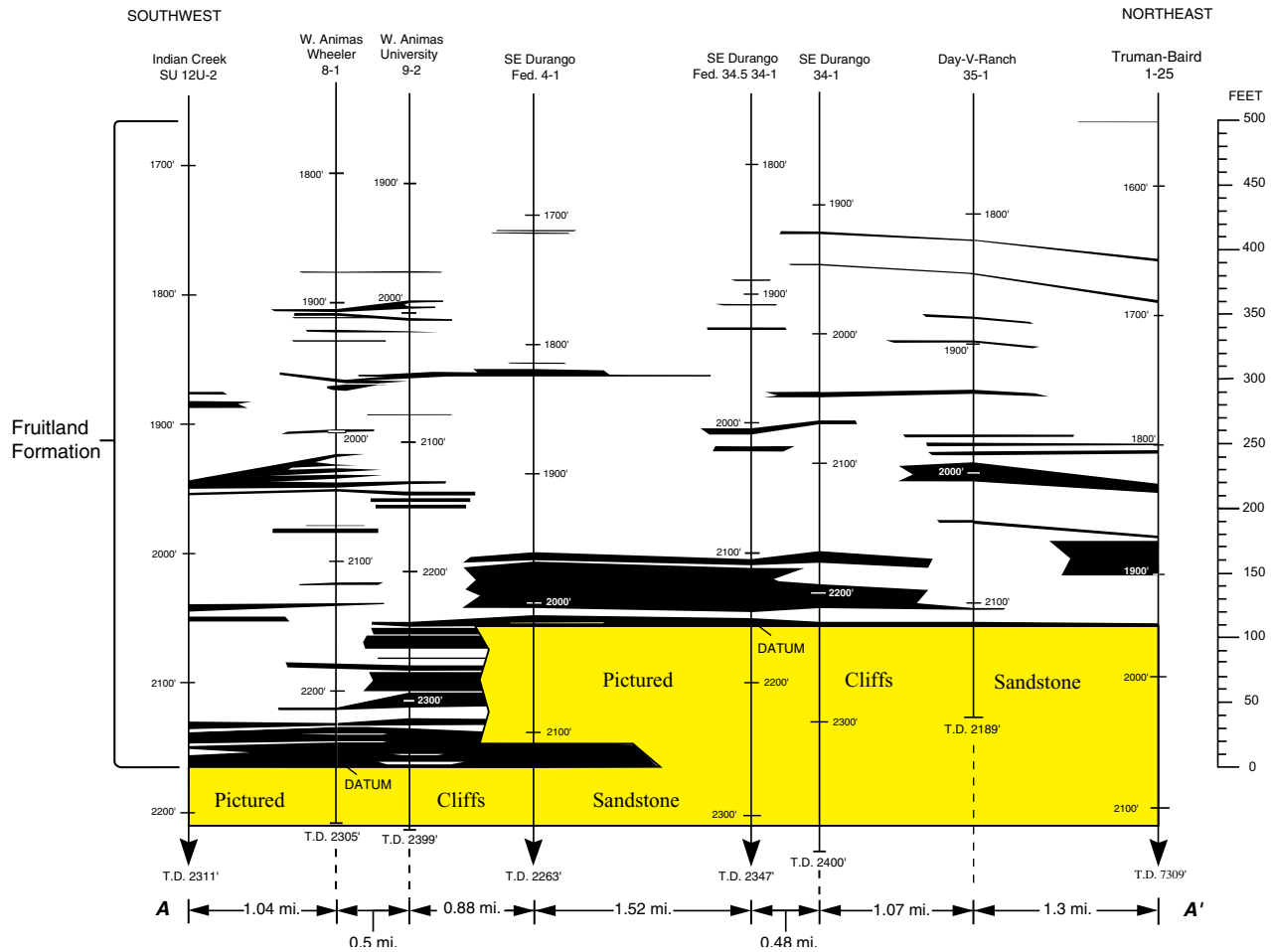


Figure 36. Fruitland Formation coal-bed correlation diagram from the Durango gas-seeps study area. This cross section is in the area labeled A on figure 31. Cross section is parallel to and about 1 mi south of the Fruitland Formation outcrop. Cross section is figure 1-8 of Fassett and others (1997). Vertical exaggeration is x 48.

K—M’Gonigle and Roberts (1997).—This study focused on determining the Fruitland coal resources in the part of the San Juan National Forest that overlies the northwest part of the San Juan Basin. Geophysical logs from 82 drill holes were used to measure the thicknesses of Fruitland coal beds in the study area. The report does not indicate what kind of geophysical logs were used but L.N.R. Roberts (oral commun., 1999) states that a mixture of density, gamma ray–neutron, and resistivity logs were used to measure the coal for that study. The report states, “The lenticular nature of Fruitland Formation coal beds precludes consistent correlation of individual beds between wells; therefore, it was not practical to calculate resources for individual beds.” This report did not include a Fruitland coal-bed correlation diagram.

K—Hoffman and Jones (1998).—This study was sponsored by the USGS to determine the availability of Fruitland coal in a block of four 7½-minute quadrangles: Bisti Trading Post, Alamo Mesa West, Tanner Lake, and The Pillar 3 NE, in the southwest part of the San Juan Basin (figs. 31, A6-1). (This report is also part of Rohrbacher and others. chap. F, this

CD-ROM.) Fruitland coals were shown to be present in four zones in the study area named, from bottom up, the red, green, blue, and yellow coal zones.

Three structural cross sections in this report show correlations of the four coal zones. Cross section A-A’ is about 12 mi long and parallels the outcrop of the Fruitland Formation; 25 drill holes were used for control for this section. Coal depths on this section range from about 30 ft to 200 ft. The red coal zone is continuous across the entire line of section, although individual coal beds within the zone are quite variable in number and thickness and do not correlate well. The green zone is present only in the northwest part of the study area, and the blue and yellow zones are present across most of the study area with some gaps in their continuity. Individual coal beds within these zones are not readily correlateable.

Two cross sections at right angles to the outcrop, B-B’ and C-C’, also show coal-zone correlations in the study area. Each of these sections uses 12 drill holes for control. Depths of coal beds range from 30 ft to 460 ft on these two sections. As in cross section A-A’, the basal red coal zone is the most

continuous, and the overlying green, blue, and yellow zones are less continuous. The numbers and thicknesses of coal beds within each coal zone appear to be quite variable, and individual coal beds do not appear to correlate well.

Basin-Wide Studies

Fassett and Hinds (1971).—In this study of the Fruitland and its contained coal beds throughout the subsurface of the San Juan Basin, the authors (p. 54–57) discussed the difficulty in correlating Fruitland coal beds in the subsurface and stated that Fruitland coals are extremely lenticular and can only rarely be correlated for even a few miles. They wrote (p. 57), “Dependable correlation of the coal beds requires control spacing of not more than 1 or 2 mi and even less spacing in areas of very abrupt facies change. Because of the spacing of control points used in this study, individual coal beds have not been correlated.” These authors did, however, graphically portray the distribution of coal beds at each of the 324 control points used for their Fruitland coal study on plate 3 of their report and identified, by name and location, all of the drill holes used for control.

Kelso and others (1987), Kelso and Wicks (1988).—Kelso and others (p. 121) stated that “The spacing between control points averages 5 mi and correlation of individual beds was not possible at this scale. No grouping or zone determinations was established due to the lack of traceable markers.” Kelso and Wicks referred to two cross sections that were constructed to help determine the distribution of Fruitland coal beds across the San Juan Basin, but these cross sections were not included in these two reports and, as far as is known, have never been published.

Ayers and others (1994).—This report did not directly address the correlation of individual Fruitland coal beds in their basin-wide study of Fruitland coal. The authors did state, however, in a section of their report headed “Number of Coal Seams” (p. 30) that “Fruitland coal occurs in as many as 16 seams in the San Juan Basin (fig. 2.18); these coal seams are most abundant in a 40-mi-wide, northwest-trending belt of six or more coal seams that bisects the basin; seams are most numerous in the northwestern half of this trend.” On a northeast-trending stratigraphic cross section (fig. 2.2, reproduced herein on figure 21), these authors present a basin-wide correlation of Fruitland coal beds. On this cross section these authors have correlated two Fruitland coal beds in the upper part of the Fruitland in the northern part of the basin for nearly 60 mi to the southwest. In the southwest part of the basin they correlate the basal Fruitland coal bed for more than 50 mi to the northeast. These correlations show these coal beds parallel to the Fruitland Formation–Kirtland Formation contact (the datum for the cross section) except in the northern part where several coal beds are shown overriding Pictured Cliffs Sandstone tongues.

The correlations of Fruitland coal beds shown on the figure 2.2 of the Ayers and others report are not correct. These long-distance correlations of Fruitland coals are based

on showing these continuous coal beds as being parallel to the Fruitland–Kirtland contact and on the assumption that this contact is a time line. It has been demonstrated in earlier discussions that the Fruitland and overlying Kirtland are time-transgressive across the basin by as much as 2 m.y. (figs. 4, 13, and plate 1); thus, the basic assumption that coal beds can be correlated parallel to the Fruitland–Kirtland contact is seriously in error and cannot be defended. The statement by Ayers and others (p. 30) that there are no more than 16 Fruitland coal beds in the basin is also in error. There are hundreds of Fruitland coal beds in the basin; specific numbers of coal beds are discussed in detail below.

Fruitland Coal-Bed Correlations—This Report

Cross Section A-A'

Stratigraphic cross section A-A' (plate 1) portrays the correlations of Fruitland Formation coal beds in 20 drill holes across the basin from southwest to northeast. Where there was a question regarding the presence or thickness of coal beds on the resistivity logs on this cross section, bulk-density logs from nearby wells were examined to confirm the existence and thicknesses of the coals. As the net-coal isopach map shows (fig. 28), there is a bulk-density log within a mile of almost all of the drill holes shown on cross section A-A'.

There are hundreds of individual Fruitland coal beds in the San Juan Basin. Cross section A-A' has more than 60 coal beds on it. The short cross section (less than 7 mi long) shown on figure 36 contains more than 50 coal beds. The distribution of Fruitland coals is intimately related to the regression and stratigraphic rise of the Pictured Cliffs Sandstone from southwest to northeast. Coal beds are commonly in the lowermost 200 ft of the Fruitland—within 200 ft stratigraphically of the top of the Pictured Cliffs Sandstone. Thus, as the Pictured Cliffs rises across the basin, so do the overlying Fruitland coal beds. Many of the coal beds shown on cross section A-A', especially in the upper part of the Fruitland, are only present in one drill hole. The number of coal beds in a drill hole ranges from two in holes 4, 8, 19, and 20 to 10 in holes 12, 14, and 17. Two of the drill holes on the cross section on figure 36, the West Animas Wheeler 8-1 and the West Animas University 9-2 wells, each have 21 coal beds.

Correlation of coal beds on cross section A-A' (plate 1) was based on using the Huerfanito Bentonite Bed as the datum. The basic assumption was that coal beds are generally not time-transgressive and thus they will generally correlate along time planes parallel to the Huerfanito Bed. A further assumption was that no differential tectonism had occurred between the time the Huerfanito was deposited and the time when Fruitland peats were being deposited. These assumptions are validated by the presence of a second time line, the magnetic-chron reversal from C33n to C32r, well above the level of most of the Fruitland coals that is essentially parallel

to the Huerfanito Bentonite Bed. If a coal bed occurs at the same stratigraphic level in adjacent drill holes, it is assumed to be the same bed. In reality this may not be true because coal beds at the same level in adjacent holes may pinch out between those holes, and undoubtedly that probably occurs for some of the beds that are shown to correlate on this cross section. Thus the correlations shown on cross section A-A' should be considered to be probable, but by no means certain.

It is the exception for a Fruitland coal bed to correlate across more than two of the drill holes shown on section A-A'. There are only four instances where this occurs: The thin basal coal in drill hole 4 correlates to holes 3 and 2 to the southwest but pinches out against the stratigraphically rising Pictured Cliffs to the northeast. A thin coal bed splits from the top of a thicker coal bed in hole 12 and can be correlated in holes 11, 10, 9, and 8 to the southwest, a distance of about 19 mi. (This is by far the longest distance a Fruitland coal bed is correlated on this cross section.) From drill hole 14, the lowest Fruitland coal bed correlates to hole 13 and splits into two coal beds in hole 12. And the coal bed that pinches out between massive tongues of the Pictured Cliffs northeast of hole 16 can be correlated to the southwest to holes 15 and 14 where it splits and pinches out to the southwest.

Computer Correlations

Earlier studies of Fruitland coal beds in the basin, principally Fassett and Hinds (1971), indicated that, even though Fruitland coals were discontinuous in a northeasterly direction, at right angles to Pictured Cliffs shoreline trends, Fruitland coal beds would probably correlate better in a southeasterly direction along depositional strike of the Pictured Cliffs. This paradigm was tested using the StratiFact PC software program. The graphics part of the StratiFact program allows for quick and easy construction of cross sections by selecting a series of drill holes in map view and viewing a cross section of those drill holes. The display shows all of the coal beds in each drill hole and a variety of correlation lines can be quickly drawn between coal beds to try and find the best correlations possible. A dozen cross sections can easily be constructed in an hour in this way using any combination of drill holes in the database.

After the database for the 752 drill holes selected for this study had been entered into the StratiFact program, hundreds of different cross sections were generated to test whether Fruitland coal beds could be correlated in any preferred orientation of cross section lines. The results of those correlation experiments were essentially negative. It was found that Fruitland coals were just as lensing and discontinuous parallel to Pictured Cliffs shoreline trends as they were at right angles to those trends. Other experimental cross sections were drawn in areas of thick coal shown on the net-coal isopach map (fig. 28) to test whether better correlations would be found parallel to those trends. The results of these attempted correlations were

again essentially negative—even though thicker Fruitland net coal occurs in a specific area along a trend, the individual coal beds in the drill holes within that trend were found to be quite discontinuous and lensing. Because no areas of the basin appear to contain extensively correlateable coal beds, no additional coal-correlation diagrams were prepared for this report. (The StratiFact digital database for this study has been added to the USGS NCRDS (National Coal Resources Data System) and is in Appendix 2 of this report and is thus available for interested users to conduct their own coal-correlation studies.)

Altered Volcanic Ash Beds as Markers

Fruitland coal beds contain altered volcanic ash beds in many parts of the San Juan Basin. Rarely, these ash beds occur in non-coal strata of the Fruitland. In the process of measuring coal beds on bulk-density logs, every effort was made to identify possible ash beds, and these beds were included in the database as possible aids for coal-bed correlation. Altered ash beds do not produce a unique response on geophysical logs. On some logs, they produce an off-scale kick on the gamma ray log trace, and they can also produce a high-level resistivity response on conductivity logs. These log characteristics, however, appear to be somewhat variable. Ash beds are seen mostly in coal beds because they are best preserved in a sequestered peat-swamp environment as opposed to higher energy environments outside the swamps where they normally would be quickly dispersed and diluted by mixing with other clastic material following rainfall and runoff. The StratiFact cross-section program was used to try to correlate all of the ash beds in the database, but with little success. In only one or two very limited areas could an altered ash be correlated between adjacent drill holes.

In the area of the Roberts (1989) report (area B on fig. 31), altered ash beds were reported in coal beds in drill core, on geophysical logs, and in coal beds on the nearby outcrop. Roberts and McCabe (1992) found that Fruitland coal beds in this area contained distinctive ash beds that could be used as coal-bed correlation tools both on the outcrop and in the subsurface. They stated (p. 125), "One tonstein within the D coal zone can be traced in the subsurface for over 5 km."

In the southwest part of the basin, the DEP ash bed (discussed in the "Hunter Wash Study Area" section of this report and shown on figs. 9 and 10) and the thin dirty coal bed in which it occurs were found to be present on the outcrop about 3 mi west of the DEP ash-bed collection site. This coal bed is poorly exposed and cannot be continuously traced between the two localities. The presence of the ash bed in the same position within this coal bed, however, makes the correlation of this coal bed certain. In summary, altered ash beds have not been found to be a useful aid for coal-bed correlation except in limited areas in the San Juan Basin.

Fruitland Coal Character

Coal Quality

Early USGS reports and maps contained proximate analyses of coal samples collected from small active or abandoned Fruitland coal mines around the northern rim of the San Juan Basin. The locations of 30 of these mines are shown in Fassett and Hinds (1971, fig. 19), and the relevant data for these mines is in table 8 of that report. Figure A3-6 is modified from figure 19 of Fassett and Hinds (1971); table A3-1 is a modification of table 8 from that report. Many of the measured sections in the northwest and north parts of the basin shown on figure 28 were measured at or near these old Fruitland coal mines. No composite report summarizing these coal analyses has been published. Fassett and Hinds (1971, table 4) presented results from proximate analyses of Fruitland coal samples from 65 locations throughout the basin. (At two locations, two coal beds were sampled; thus, table 4 contains analyses of 67 coal samples.) Four coal samples were from outcropping coal beds, three were from core holes, and the remaining 58 were cuttings samples collected from drilling oil or gas wells in the interior part of the basin. On the basis of these data, Fassett and Hinds (1971) constructed a series of maps showing the distribution of coal-quality values throughout the basin. The Fassett and Hinds report has been out of print for many years and thus is no longer readily available and because no newer Fruitland coal quality data have been published for the deep basin, the coal-quality table and coal-quality figures from Fassett and Hinds (1971) are discussed briefly herein and are reproduced in Appendix 3 of this report for easy reference.

The 58 coal cuttings samples discussed above were processed in an unorthodox manner. The cuttings samples were collected from drilling oil or gas wells and consisted of a mixture of fragments of coal and other rock types coated with drilling mud. It was thus necessary to process these samples to remove extraneous, non-coal material prior to submitting the coal samples for analyses. This processing involved thoroughly washing the coal cuttings with water to remove drilling mud, air-drying the samples at ambient temperatures, and then immersing the cuttings in carbon tetrachloride (specific gravity 1.59) to remove non-coal fragments with a density greater than 1.59. The resulting samples submitted for analyses thus consisted of a mixture of coal fragments ranging from nearly pure coal to coal containing no more than 40 percent ash.

Table A3-2 (table 4 of Fassett and Hinds) presents these high-graded coal analyses. The as-received values certainly do not fully represent coal beds in the ground. The drilled coal beds would have contained thin interbeds of non-coal rock and high-ash coal (typical of most Fruitland coal beds on the outcrop) and fragments of these non-coal layers would have been eliminated from the samples in the flotation process described above. The as-received heating values are higher and ash values are lower in table A3-2 than these values would be for an in-the-ground complete-coal-bed sample. The calculated

analyses values, however, such as the moisture- and ash-free heating values and fixed carbon and sulfur percentage values (table A3-2) are more representative of the coal in place from which the cuttings samples came. (Subsequent analyses of Fruitland coal core samples from the few drill holes for which such data have been published have confirmed the accuracy of these calculated values.)

Figure A3-7 (fig. 23 of Fassett and Hinds, 1971) shows the sample locations and as-received heating values in Btu's (British thermal units) for coal samples from those locations. Figure A3-8 (fig. 25 of Fassett and Hinds) is a contour map of moisture- and ash-free Btu values in the basin showing that these values range from 13,460 Btu in the southwest to 15,720 in the north-central part of the basin. Figure A3-9 (fig. 26 of Fassett and Hinds) is a contour map of fixed carbon percentages (moisture and ash free). This map shows that fixed carbon ranges from 54.8 percent in the southwest to 72.4 percent in the north-central part of the basin. The moisture- and ash-free Btu map and the fixed-carbon percentage map both show increasing thermal maturity of Fruitland coals toward the present basin axis and reflect greater depth of burial in that area. (The thermal maturity of Fruitland coals is discussed in more detail below in the "Vitrinite Reflectance" section of this report.)

Sulfur percentages (as-received) range from 0.5 to 2.2 percent; only six of the 67 samples analyzed had a sulfur percentage in excess of 1.0 percent (table A3-2, fig. A3-10). The average sulfur content for all samples was 0.75 percent. Figure A3-10 (not from Fassett and Hinds, 1971) shows the distribution of as-received sulfur values listed in table A3-2 and plotted on a map of the San Juan Basin. This map shows remarkable uniformity of sulfur content throughout the basin, and there are no discernible trends in these values. The five sulfur values in excess of 1.0 percent on figure A3-10 (localities 10, 12, 13, 54, 58) appear to be anomalous, and, if these values are excluded, the average sulfur value for the other 60 localities is 0.67 percent.

Moisture content for Fruitland coals is generally higher in samples from the outcrop or from shallower drill holes (< 112 ft deep) near the outcrop and ranges from 2.5 to 12.0 percent in those areas. Coal samples from drill holes in the deeper parts of the basin have moisture contents ranging from 0.8 to 9.5 percent; only three deep samples had moisture contents exceeding 5 percent. Average moisture content for deep coals is 2.5 percent. (Ash-content percentages are discussed below in the "Coal Density" section of this report.)

Hoffman and others (1993) published a detailed study of Fruitland coal quality based on coal core samples from relatively shallow holes in the northwest and southern parts of the basin. Core-hole depths were less than 400 ft except for one hole that was nearly 800 ft deep. Coal test holes were drilled at 49 sites; nine in the northwest and 40 in the southern part of the basin. At each site a pilot hole was drilled to determine depths to coal beds and a twin hole was drilled nearby in which all coal beds 2.5 ft thick or greater were cored. Partings in the coal less than 0.8 ft thick were included

in the coal samples that were analyzed; thicker partings were excluded. A total of 252 coal samples from 45 core holes were analyzed; 90 samples from nine core holes in the northwest areas and 162 samples from 36 core holes in the southern part of the basin. The Hoffman and others study areas are shown on figure 31 of this report; the core hole locations are shown on figure 28.

Analyses results for the northwest area (named the Fruitland area by Hoffman and others, 1993) are summarized in table 6 of their report. The weighted average, moist mineral-matter-free (mmmf) heating value was 10,732 Btu. Other values were presented as the mean for coal samples analyzed on a dry basis as follows: ash 21.17 percent, sulfur 0.88 percent, and fixed carbon 42.29 percent. Moisture was 7.61 percent equilibrium moisture and 6.70 on the as-received basis. Coal rank for this area was reported to be high-volatile B to C bituminous. Hoffman and others subdivided the southern area into the Bisti and Star Lake coal fields. The Bisti area (northwest) contained 16 core holes and the Star Lake area (southeast) contained 20 core holes. Analyses results for the Bisti area were: weighted average, mmmf heating value 10,308 Btu; mean dry-basis ash value, 21.32 percent; sulfur 0.59 percent; and fixed carbon 41.71 percent. Moisture, as-received, was 13.81 percent; equilibrium moisture was 14.88 percent. Star Lake analyses were: weighted average, mmmf heating value 11,253 Btu; mean dry-basis ash value, 25.62 percent; sulfur 0.63 percent; and fixed carbon 38.45 percent. Moisture, as-received, was 11.34 percent, and equilibrium moisture was 14.11 percent. Coal rank for the Star Lake area was reported to be subbituminous A extending into high-volatile C bituminous. For the Bisti area, coal rank was reported to be subbituminous A.

Two test holes were drilled by the Southern Ute Indian Tribe and the U.S. Department of Energy about 3 mi north of Ignacio, Colo. (fig. 37), in sec. 25, T. 34 N., R. 8 W., La Plata County, Colorado, to determine the coal-bed methane potential of Fruitland coal beds in that area (Kelso and Rushworth, 1982). Samples of coal and non-coal material, each less than 1 ft thick from core samples from these test holes were analyzed. The results of the analyses of just the coal samples from each drill hole were averaged, as follows: Oxford No. 1 (NE $\frac{1}{4}$ SE $\frac{1}{4}$ sec. 25)—four samples—moist mineral-matter-free (mmmf) heating value 15,474 Btu, fixed carbon 78.9 percent. As received basis: moisture 1.6 percent, ash 35.5 percent, sulfur, 1.17 percent. Oxford No. 2 (SE $\frac{1}{4}$ SW $\frac{1}{4}$ sec. 25)—four samples—moist mineral-matter-free (mmmf) heating value 15,959 Btu, fixed carbon 81.3 percent. As-received basis: moisture 1.0 percent, ash 32.8 percent, sulfur 0.51 percent. The rank of the coal from these drill holes, low-volatile bituminous, is the highest reported in the basin.

Roberts (1989) presented coal analyses for 155 samples of coal from core in the northwest part of the basin in Colorado (see fig. 31 for location of the Roberts study area). Non-coal partings exceeding 3/8 inch thick were excluded from the sampled coal. An additional 71 samples of the thicker partings, roof, and floor rock were also analyzed, but composite

weighted-average analyses for coal and partings was not done. On the basis of the analyses of the 155 coal samples, coal rank appears to range from high-volatile C bituminous to high-volatile A bituminous in the Roberts study area. Ash, moisture, and sulfur percentages appear to be similar to those of Fruitland coals from other parts of the basin. Roberts and McCabe (1992) discuss the ash content of Fruitland coals in the Roberts' (1989) study area in great detail but do not discuss the other components of these coals there.

In summary, Fruitland coal is low sulfur (average less than 1 percent) and high ash (probably averaging about 30 percent). Moisture content is variable, ranging from 5 to 10 percent at shallow depths near the outcrop to less than 3 percent in the deeper parts of the basin. Heating values range from 10,300 Btu (mmmf) along the southwest margin of the basin to nearly 16,000 Btu in the north-central part. Fixed-carbon percentages (mmmf) range from around 40 percent in the southwest to more than 80 percent in the north-central area. Coal rank ranges from subbituminous A in the south to low-volatile bituminous in the north-central part of the basin. Coal rank generally increases from the southwest edge of the basin to north of the present basin axis and then diminishes somewhat to the north to the northern edge of the basin. (See "Vitrinite Reflectance" section, below, for a more detailed discussion of the thermal maturity of Fruitland coals.) Fruitland coal is almost all non-agglomerating with the exception of one small area at the Chimney Rock mine (fig. 2) on the northeast edge of the basin.

Maceral Content

There are no published, basin-wide studies of the petrography of Fruitland coals in the San Juan Basin; however, Hoffman and others (1993) and Hoffman (1991) presented maceral content for Fruitland coals from 33 core samples from drill holes in two areas near the Fruitland outcrop—from four drill holes in the northwest and 13 drill holes in the southern part of the basin (areas J and L on fig. 31). The results of that study showed that the average Fruitland coal maceral content for both areas is about 70 percent vitrinite, 16 percent inertinite, and 14 percent liptinite. Mavor and Nelson (1997, table 4-2) presented Fruitland coal maceral data for three wells in the northern part of the basin and showed that the average maceral content for these wells was 84.5 percent vitrinite, 12.8 percent inertinite, and 2.7 percent exinite (a liptinite maceral). The higher percentage of vitrinite and lower percentage of exinite in the northern San Juan Basin data set could indicate a change in the kinds of organic material accumulating in Fruitland coal swamps at that time or could be an artifact of liptinite macerals becoming more reflective with greater depth of burial and heating. Levine (1993, p. 56) states that "The reflectivity of the liptinite macerals is initially lower than vitrinite ... but changes very rapidly at around 1 % reflectance to match that of vitrinite. Above around 1.2 % R_o , the liptinite macerals are essentially indistinguishable from vitrinite." Thus the decrease

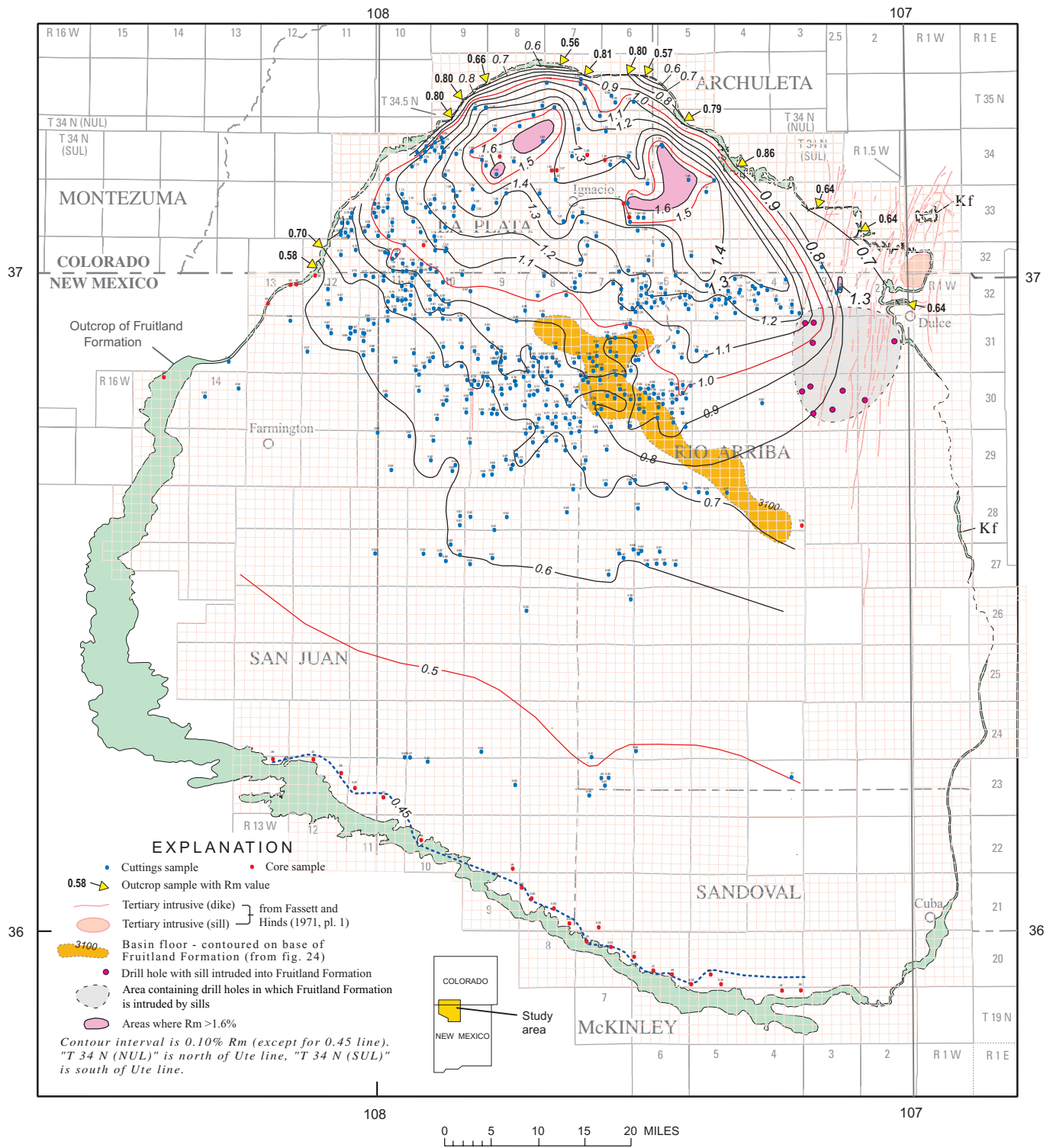


Figure 37. Thermal-maturity map of Fruitland Formation coal samples from 568 locations. Mean vitrinite reflectance values in percent (R_m) are contoured.

in the liptinite-maceral (exinite) percentage in the northern part of the basin may only be apparent. Available data are too limited to demonstrate any significant basin-wide trends in maceral percentages for Fruitland Formation coals.

Vitrinite Reflectance

The first published vitrinite reflectance maps of the San Juan Basin were in Rice (1983, figs. 12, 13). The map in that report showing R_m values for Fruitland coal samples (fig. 12) contained only 19 data points and only two contour lines with values of 0.6 and 1.0. Rice (1983, p. 1207) noted that the highest R_m -value data point had a value of 1.45 and was located at the north end of the basin, north of the present-day structural axis. He further noted that the “maximum depth of burial combined with typical or present-day geothermal gradients cannot account for temperatures necessary for high-rank coal formation.” Rice suggested that batholiths, emplaced in Oligocene time in the nearby San Juan Mountains “provided an added heat source required for the advanced levels of thermal maturation.”

Bond (1984) discussed the thermal maturity of Upper Cretaceous rocks in the northern part of the San Juan Basin and stated that maximum heat flow and greatest depth of burial coincided with intrusive and extrusive activity in the San Juan volcanic field in late Oligocene time. He stated that at that time (30–25 Ma) an apron of volcanoclastic material from the San Juan volcanic center to the northeast was deposited in the northern part of the basin area. His estimate for maximum burial of basal Fruitland coal beds at that time was 8,750 ft. Bond (1984) did not call upon exotic heat sources to account for the thermal maturity of Upper Cretaceous rocks in the San Juan Basin. Subsequently, other workers discussed heat flow in the basin (see Clarkson and Reiter, 1988) and suggested that an external heat source must have contributed to the high thermal maturity of Fruitland coals in the northern San Juan Basin and proposed that the heat-transfer mechanism was heat advection by ground-water flow from the nearby San Juan volcanic field to the north.

Law (1992, fig. 4) constructed a thermal maturity map of the basin based on 98 data points with a contour interval of 0.1 R_m and contour lines having values ranging from 0.5 to 1.5 R_m . This map shows a northerly increase in thermal maturity values toward the northeast part of the basin from 0.5 to 1.3 R_m over a distance of more than 70 mi. A relatively narrow, linear, northwest-trending area of thermal maturity 1.3 R_m or higher is shown in the northeast part of the basin; this area is nearly 35 mi long. Northward from this axis of highest thermal maturity, contour lines are closely spaced and decrease in value from 1.3 R_m to about 0.7 R_m at the Fruitland outcrop (a distance of less than 15 mi). Law (1992, p. 206) suggested that because present-day heat flow is insufficient to account for the elevated levels of thermal maturity for Fruitland coals in the northern part of the basin “a convective heat-transfer event 40–20 m.y. ago” resulting from “the circulation of relatively

hot fluids into the basin from a heat source located north of the San Juan Basin, in the vicinity of the San Juan Mountains” was the most likely cause of the elevated levels of thermal maturity in Fruitland coals in the northern San Juan Basin.

Scott and others (1994, fig. 9.3) constructed a thermal maturity map of the basin based on “more than 140 measured and 72 calculated vitrinite reflectance values.” Calculated values were based on the mathematical conversion to vitrinite-reflectance values of published volatile percentages for Fruitland coals (mostly from Fassett and Hinds, 1971). The pattern of vitrinite-reflectance contour lines on this map is similar to the map produced by Law (1992, fig. 4) discussed above, except for the position of the 0.5- R_m line. This line is shown to be much farther south on the Law map than on the Scott and others map. Scott and others point out that there is “a general correlation between the structural configuration of the San Juan Basin ... and Fruitland coal rank” but point out that “in the northern third of the basin, low-volatile bituminous coals are structurally higher than lower rank coals located to the south along the structural axis of the basin.” Scott and others (1994, p. 167) briefly discuss the various heat-flow studies in the northern part of the basin (discussed above) and offer the opinion that “The correlation between vitrinite reflectance and structure in the San Juan Basin suggests that burial depth and structural evolution of the basin were probably the major factors controlling the thermal maturity of Fruitland coals” obviously rejecting the “introduction of additional heat” theories espoused by earlier researchers.

Mean vitrinite reflectance values in percent (R_m) for Fruitland Formation coal-bed samples presented in this report are from the following published sources: Fassett and Nuccio (1990), Pawlewicz and others (1991), Law (1990, 1992), Hoffman (1991), Hoffman and others (1993), and Kelso and Rushworth (1982). Unpublished data were provided by Amoco Production Company, EnerVest San Juan Operating LLC, and Emerald San Juan Co. Coal samples were mostly from drill holes, but 14 coal samples were from Fruitland coal mines or from outcropping Fruitland coal beds. Most drill-hole samples were cuttings; however, 36 coal samples were from drill core.

At some data points, vitrinite-reflectance values were determined from coal samples at different stratigraphic levels within the Fruitland. In this report, only one R_m value per data point is shown on the thermal maturity map for the basin (fig. 37). In the southern part of the basin where R_m values are low (less than 0.5 percent), values from multiple coal samples in the same drill hole were averaged. In the northern part of the basin where R_m values are much higher, the highest R_m value, usually from the deepest sample in the drill hole, is used.

R_m values for Fruitland coals from 350 drill holes (Fassett and Nuccio, 1990, and Pawlewicz and others, 1991)—were determined by the USGS in a cooperative program with the Aztec, N. Mex., District Office of the New Mexico Oil Conservation Division. Beginning in 1988, the New Mexico Oil Conservation Division required all oil and gas operators to send drill cuttings from coal beds in the Fruitland and Menefee Formations to the USGS in Denver. The samples were

cleaned, crushed, and mounted in epoxy on a microscope slide and then planed and polished. Mean random vitrinite reflectance was measured from randomly oriented vitrinite grains in immersion oil using a non-rotating stage on a Zeiss Universal research microscope. Plane-polarized incident white light and a 546-nm monochromatic filter were used (for a complete explanation of this procedure see Stach and others, 1982). The number of readings per sample varied depending on the amount of clean vitrinite in the sample. In most of the samples, vitrinite was abundant, the number of readings per sample was between 30 and 50, and the resulting histograms were unimodal. If the number of readings was greater than 30 and the standard deviation was small, then the mean vitrinite reflectance value was statistically valid. Depths of coal cuttings were provided by the companies drilling the wells and no attempt was made to correct or adjust these depths precisely to specific coal beds on geophysical logs. R_m values published in the Law (1990) report were also determined in the USGS Denver laboratory using the procedures described above.

Vitrinite-reflectance values for Fruitland coal samples from the Amoco and EnerVest drill holes were determined using procedures similar to those of the USGS. Slightly different analytical procedures used in the other published reports listed above are described in those publications. Because each data set used to construct the vitrinite-reflectance contour map (fig. 37) overlapped with at least one other data set, it was possible to compare values from adjacent drill holes, (or the same drill hole in a few instances) from the different data sets. These comparisons showed that vitrinite-reflectance values from overlapping data sets were virtually identical.

The vitrinite-reflectance database for Fruitland coals presented in this report (table A4-1) consists of mean R_m values from 620 selected locations. This selected database was compiled by deleting data points from the source databases (listed above) that were judged to be anomalous, that is those with R_m values more than 0.3 percent lower than nearby data points. The assumption was that these anomalously low values could have come from cavings from higher coal beds. Anomalously high values were not deleted from the database in this initial screening process.

Figure 37 is a thermal maturity map for the San Juan Basin contoured on vitrinite-reflectance values. To create this map, first, a preliminary contour map was created by the Golden Software program, Surfer, using the 620 data points in table A4-1. This preliminary contour map was examined and 53 data points having anomalous R_m values were deleted. The final Surfur-drawn map was then created using the remaining 567 data points and that map was imported into Adobe Illustrator where the contour lines were edited to produce the final thermal maturity map (fig. 37).

This map shows that R_m values for Fruitland coals range from less than 0.45 to more than 1.6 and are highest in the northern part of the basin. Along the southern edge of the basin, the 0.45 contour line is near, and parallel to, the Fruitland Formation outcrop. (Control for the 0.45 contour line is from the Hoffman, 1991, and Hoffman and others, 1993,

database.) The thermal-maturity contours in the southern part of the basin, in the area between the 0.45 and the 0.9 contour lines, show a pattern of decreasing distances between successively higher value contours: The distance between the 0.45 and the 0.5 lines is about 15 mi; between the 0.5 and 0.6 lines, it is about 15 mi; between the 0.6 and 0.7 lines, it is about 8 mi; between the 0.7 and 0.8 lines, it is about 4 mi; and between the 0.8 and 0.9 lines, the distance is about 2 mi. These distances are somewhat variable, but the general pattern is apparent.

This pattern of decreasing spacing between R_m contour lines is a good example of the observation by Levine (1993, p. 58) that "Vitrification increases exponentially with rank, increasing only very slowly at low rank and more rapidly at high rank." At higher R_m values than 0.9, however, the pattern of decreasing spacing of the thermal maturity contour lines ends and from the 0.9 contour line to the 1.6 line, the contour lines are more or less evenly spaced. The reason for this apparent contradiction beyond the 0.9 contour line is that the structural deepening of the basin decreases in this area. Figures 22–24 show this decrease for the present-day structure of the basin in the vicinity of the 0.9 contour line. Thus, the *decreasing rate* of increase in depth of burial in the area between the 0.9 and the 1.5 R_m contour lines has offset the exponential increase in thermal maturity with depth of burial in this area.

Scott and others (1994, p. 167) stated that "The rather abrupt increase in vitrinite reflectance values greater than 0.70 % in the northern basin coincides with a structural "hingeline." Because of their more limited vitrinite-reflectance database, the thermal maturity map of these authors (fig. 9.3) did not clearly portray the regularly decreasing distances between contours that are shown on figure 37 of this report. As a result, these authors saw an apparent "abrupt" change in spacing of thermal maturity contours at the 0.7 R_m line, whereas, in reality, the increase of vitrinite-reflectance values north of the 0.7 R_m line is an artifact of the pattern of decreasing distances between contours northward in accord with Levine's (1993) observation that "vitrification increases exponentially with rank."

In the northern part of the basin, thermal maturity of Fruitland coals decreases over a distance of about 10 mi, from 1.6 R_m at the basin's thermal-maturity axis, to 0.56 R_m at the Fruitland outcrop (fig. 37). The spacing pattern of the thermal-maturity contours reflecting the exponential relationship discussed above is masked by the steeper dip of the rocks in the northern part of the basin (see figs. 23, 24).

Several localized perturbations occur in the vitrinite-reflectance contour lines in the central part of the basin, especially for the 0.6- to 0.9- R_m lines. The data points causing these perturbations generally have vitrinite-reflectance values of 0.05 R_m higher or lower than the prevailing values in these areas. In these areas, where clusters of two or more apparently anomalous data points occur, the data points are retained and honored by the vitrinite-reflectance contour lines. These anomalies all occur in an elliptical area that trends northeast, suggesting that there may have been some related local causes

for these features. Even though vitrinite-reflectance values are primarily a recorder of maximum heat, they are to some extent affected by coal maceral composition (Levine, 1993, p. 58). Thus, the origin of these relatively small, local variations in vitrinite values may be the result of local variations in heat flow at the time of maximum burial of the coal beds or reflect physical and (or) chemical changes in the peat-bog environments at the time the material was deposited.

In the northeast part of the basin, a large number of dikes and sills are present. These intrusives, discussed in Fassett and Hinds (1971, p. 34), are shown on figure 37. It is notable that this intrusive complex has had no apparent effect on the regional pattern of thermal maturity in this area of the basin as indicated by the surface outcrop samples along the northeast edge of the basin; however, subsurface data points in this area are sparse. In T. 32 N., R. 3 W., New Mexico, a single vitrinite-reflectance data point has an elevated R_m value of 1.3. This anomalous value is almost certainly the result of the sampled coal bed having been heated by a nearby dike or sill.

Ten of the drill holes used for determining Fruitland coal thicknesses in this study were found to contain what appear to be igneous sills on geophysical logs. (Undoubtedly, the Fruitland has been intruded by sills in other wells in this area, but examining the logs of all of the wells in this area for Fruitland sills was beyond the scope of this project.) The locations of these 10 holes are shown on figure 37 and the depths to the sills in each hole are in table A2-1. The numbers of sills in these holes range from 1 to 5 and the sills are mostly concentrated in the lower, coal-bearing part of the Fruitland. The Fruitland sills occur at depths ranging from 3,461 ft to 3,776 ft in this area. No samples of coal from these drill holes were available for vitrinite-reflectance determinations. The sills range in thickness from 1 ft to 10 ft and average about 4 ft thick. It appears on the geophysical logs that the sills have selectively intruded into coal beds and have, at least in part, digested the coal beds in the process.

In 1989, the Ojo Alamo Sandstone was found to contain gas in this area in four wells (Hoppe, 1992). Hoppe stated (p. 371), "Except for the presence of H_2S , gas composition of the Ojo Alamo, Fruitland coal and Pictured Cliffs is similar." In his paper, Hoppe discussed the presence of igneous sills in the Fruitland in this area and suggested that "igneous solutions intruded the area, heated and forced gas from the coal seams, which then migrated to the structural highs and porous zones of an overlying reservoir—the Ojo Alamo." He further stated that alternatively, the gas could have migrated from deeper source rocks.

In 1997, the East Blanco gas field, was developed in the Ojo Alamo Sandstone in T. 30 N., R. 3 W. (Oil and Gas Journal, 1998) within the area shown on figure 37 where the Fruitland is intruded by sills. In 1999, about 50 gas wells were producing methane from the Ojo Alamo Sandstone in that area. As Hoppe (1992) pointed out, the Ojo Alamo does not normally produce natural gas in the San Juan Basin, and he suggested that the most probable source of the Ojo Alamo gas was the underlying Fruitland Formation coal beds. The

discovery of numerous igneous sills intruding the coal-bearing part of the Fruitland in 10 of the wells used for Fruitland coal measurements in this area (fig. 37) supports the suggestion that the presence of these sills contributed to the liberation of gas from Fruitland coal beds. Rather than "hot solutions" associated with the sills heating the coal beds and driving off the gas, however, it seems apparent that the hot magma itself intruded into the Fruitland coals, partly or completely digesting them, resulting in the release and generation of large volumes of coal-bed methane in this area. This process would have resulted in extreme overpressuring of the Fruitland Formation causing the gas to migrate upward into the next-highest available reservoir, the overlying Ojo Alamo Sandstone, where it was trapped. The intrusion and digestion of the Fruitland coals by magma is probably also responsible for the high levels of H_2S in the Ojo Alamo gas because H_2S is never present in methane generated from coal beds under normal conditions.

The Ojo Alamo, throughout the basin, consists of a series of overlapping, disconnected, channel-sandstone lenses interbedded with mudstones (Fassett and Hinds, 1971, p. 28), thus each sandstone lens is an isolated sandstone reservoir and trap. The intrusion of large numbers of dikes and sills in an area of structural tension may have created fracture pathways facilitating the migration of Fruitland gas upward into the Ojo Alamo sandstone lenses.

As discussed above, the high thermal maturity of Fruitland coal beds in the northern part of the San Juan Basin has been attributed to conductive heating from a nearby buried batholith, heat transfer by hot fluids, and simply depth of burial. Figure A5-1 is an isostatic residual gravity anomaly map of the San Juan Basin reprinted from Heywood (1992) on which the thermal maturity contour lines of figure 37 are superimposed. This figure clearly illustrates that the areas of highest thermal maturity of Fruitland coals in the northern part of the basin are not underlain by high-density, shallow, intrusive bodies; thus, conductive heating of Fruitland coals by an anomalous underlying heat source can be ruled out. Of interest on this figure is the presence of the high-gravity anomaly located just east of the dikes and sills discussed above. The area of this anomaly is overlain by Upper Cretaceous rocks and there is no surface expression of this feature in this area. This higher density rock body is a logical source for the intrusives in the northeast part of the San Juan Basin.

The transfer of heat into the northern San Juan Basin by hot fluids that originated in the San Juan volcanic area to the north does not seem to be supported by available data. Certainly these hot fluids did not move through the Fruitland Formation or older Cretaceous rocks from the north because, if they had, thermal-maturity values for these rocks would increase northward. Figure 37 clearly shows vitrinite-reflectance values for Fruitland coals decreasing from the basin's thermal axis to its northern edge. Turner and Fishman (1991) discuss the thermal history of the basin as it affected the Brushy Basin Member of the Morrison Formation and state (p. 553) that a coal sample from the Dakota Sandstone between

the San Juan Basin and the San Juan volcanic field “has the lowest reflectance value thus far obtained from the study area ($R_{\text{mean}} = 0.53 \pm 0.07\%$).” They conclude, “Thus, heat associated with the San Juan volcanic field was apparently conducted vertically rather than laterally away from the volcanic center or associated batholith.”

Law (1992, p. 206) suggested that hot fluids “heated by the deeply buried batholith [in the San Juan volcanic area]” moved laterally southward “along faults and fractures into the north end of the San Juan Basin. As the heated fluids ascended through Cretaceous and Tertiary rocks, the high-temperature fluids would have raised subsurface temperatures and altered the organic matter to higher levels of thermal maturity.” The even spacing of the vitrinite-reflectance contours from the 0.9 to the 1.6 lines would seem to argue against an elevation of the thermal gradient by hot fluids moving up from depth along a northwest-trending fracture zone in the areas of highest thermal maturity shown on figure 37. Such a process would presumably have created a relatively narrow zone or series of zones of high thermal maturity values and thermal-maturity values abruptly diminishing on both sides of that zone, rather than the even pattern shown on figure 37 in the northern part of the basin.

Because the spacing pattern of thermal-maturity contours (fig. 37) mimics the structural form of the basin, it seems most likely that the pattern of thermal maturity of Fruitland coal beds is reflecting depth of burial of these rocks, as suggested by Bond (1984) and Scott and others (1994) rather than an exotic heat source that pumped heat into the basin center from the San Juan volcanic center to the north. The present structural basin floor for Fruitland coals—depicted on the Pictured Cliffs structure map (fig. 24) and superimposed on the thermal maturity map (fig. 37)—is about 20 mi southeast of the thermal-maturity axis in the basin. It is suggested that the structural axis of the basin was once located northwest of its present position (in the position of the thermal-maturity axis shown on figure 37) but as the structural evolution of the basin proceeded, the structural axis shifted through time to its present location.

Fruitland Coal Resources

Coal Density

Coal tonnage determinations are the product of three parameters: coal thickness, the area underlain by coal, and coal density. Coal thickness and area are determined by direct measurements, and the product of these values is conventionally reported in acre-ft. Coal density determinations are more difficult because coal beds are complex mixtures of organic matter, inorganic matter, and water (moisture). The primary factor affecting Fruitland coal density in the San Juan Basin is ash content. Ash in coals is present in two forms: as dispersed inorganic mineral grains in a coal matrix and as discrete

layers of inorganic material (partings) within coal beds. Partings range from carbonaceous shales (more than 50 percent ash) to relatively pure layers of inorganic rock material.

The ash content of Fruitland coal samples determined by proximate analyses of floated Fruitland coal samples collected as drill cuttings (table A3-2) ranges from 10.5 to 35.7 percent and averages about 19 percent. Because processing of these cuttings samples essentially removed all fragments of coal partings that contained more than 40 percent ash, the ash-content values for this sample set must represent mostly dispersed inorganic mineral grains in the coal matrix. Figure A3-11 is a contour map of these ash-content values (from Fassett and Hinds, 1971, fig. 24) showing a pattern of higher ash coal (> 20 percent) in the eastern part of the basin and an area of lower ash coal (< 15 percent) in the west-central part of the basin.

Bulk-density logs can be used to accurately determine the density of coal beds in the ground. Figure 38 shows the

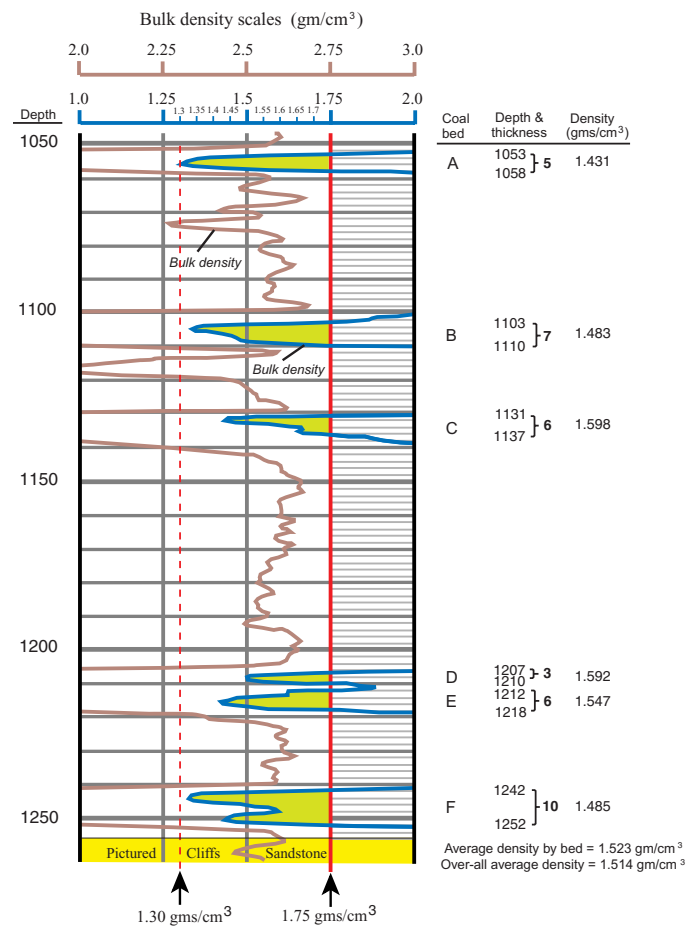


Figure 38. Type bulk-density log (fig. 25) showing the density of each of the Fruitland Formation coal beds in this drill hole. Log is from the Amoco Production Company State of Colorado Ax No. 1 well located in NE¼NE¼ sec. 16, T. 35 N., R. 7 W., La Plata County, Colorado. Density was determined by averaging densities in 1-ft increments for each coal bed.

bulk-density curves from the type bulk-density log of figure 25. This log was used to measure the average density of each coal bed using the procedure described in Mavor and Nelson (1997, example 5-2). The average density for each coal bed was measured on the bulk-density log in 1-ft increments, and these densities were averaged to determine the density of each coal bed. The average density for all coal is an average of the densities for all of the 1-ft increments. The average coal density for the drill hole on figure 38 is 1.514 g/cm^3 . The ash content for coal of this density is about 30 percent for a typical Fruitland coal (Mavor and Nelson, fig. 7-7). To convert coal density to short tons of coal per acre-ft, the density is multiplied by 1,360, the weight of an acre-ft of water. For the drill hole on figure 38, this computation yields a value of 2,059 short tons of coal per acre-ft.

Coal densities for the Amoco Ax 1 well (fig. 38) range from 1.431 g/cm^3 for bed A (about 8 percent ash) to 1.598 g/cm^3 for bed C (about 40 percent ash). Converting these densities to short tons per acre-ft, as above, yields a range of 1,946 to 2,173 short tons per acre-ft for beds A and C, respectively. Because the precise distribution of ash percentages or coal-bed densities are not known for the entire basin, an average density of 1.47 (about 28 percent ash) is assumed for Fruitland coals. The resultant density value of 2,000 short tons of coal per acre-ft was used for coal-tonnage determinations in this report. This number may be slightly low, but it provides a conservative estimate of Fruitland coal tonnage in the basin.

Traditionally, coal densities used for resource calculations in USGS reports are those of Wood and others (1983, p. 21, 22, and table 2). These authors state:

The specific gravity of coal varies considerably with rank and with differences in ash content. The values shown in table 2 are close to the average specific gravities of unbroken or unmined coal in the ground (in situ) for the four major rank categories and are to be used in preparing U.S. Geological Survey estimates of coal resources and reserves.

Table 2 of Wood and others (1983) gives the specific gravity and short tons per acre-ft for the four coal ranks as follows: lignite, 1.29 g/cm^3 , 1,750 short tons/acre-ft; subbituminous, 1.30 g/cm^3 , 1,770 short tons/acre-ft; bituminous, 1.32 g/cm^3 , 1,800 short tons/acre-ft; and anthracite, 1.47 g/cm^3 , 2,000 short tons/acre-ft. Comparing Wood and other's density of 1.32 g/cm^3 for "average" bituminous coal with the density value of 1.3 derived for pure (0 percent ash) Fruitland bituminous coals of the San Juan Basin (Mavor and Nelson, 1997) indicates that "average specific gravities of unbroken or unmined coal in the ground" (Wood and others, 1983), refers to extremely low ash coal (less than 5 percent). Because the densities for the high-ash Fruitland coals can be conservatively estimated to be on the order of 1.47 g/cm^3 (about 28 percent ash), it is clear that to use 1,800 short tons per acre-ft as prescribed in Wood and others (1983) would seriously underestimate Fruitland coal resources.

Procedures, Categories, and Maps Used

Fruitland coal tonnages for the San Juan Basin were calculated using the EarthVision software program. The net-coal isopach map (fig. 28) was the source for coal thicknesses and 2,000 short tons of coal per acre-ft was used for all tonnage calculations. The bounding polygon for the basin for coal resource calculations was the top of the Pictured Cliffs Sandstone (base of the Fruitland Formation). Coal tonnages were determined in five overburden categories: 0–500 ft, 500–1,000 ft, 1,000–2,000 ft, 2,000–3,000 ft, and more than 3,000 ft. Coal tonnages were calculated for (1) the States of Colorado and New Mexico, (2) counties, (3) $7\frac{1}{2}$ -minute quadrangles, (4) townships, (5) areas of Federal and non-Federal surface ownership, and (6) areas of Federal and non-Federal coal ownership. In addition, for the two States and six counties, coal tonnages were calculated by reliability categories of identified and hypothetical coal and by standard USGS thickness categories of 1.2–2.3 ft, 2.3–3.5 ft, 3.5–7.0 ft, 7.0–14.0 ft, and greater than 14 ft. All coal tonnages are in tables A6-1–A6-5.

State, county, and township boundary lines are shown on most of the basin maps in this report (fig. 28, for example). Maps showing other areas for which coal tonnages were determined are in Appendix 6, as follows: Figure A6-1, shows $7\frac{1}{2}$ -minute quadrangles within the basin, figure A6-2 shows Federal and non-Federal surface ownership, and figure A6-3 shows Federal and non-Federal coal ownership. Figure A6-4 shows the distribution of net Fruitland coal in the standard USGS coal-thickness categories listed above.

Figure 39 shows overburden thicknesses for the Fruitland throughout the basin. This overburden map primarily reflects the basin structure on the base of the Fruitland Formation as portrayed on figure 24, but topography also plays a role, especially in the Colorado part of the basin where the land surface is considerably higher than it is in most of the New Mexico part of the basin. The San Juan River canyon is clearly evident in the north-central part of the basin. This overburden map was the source of data for the overburden categories in tables in Appendix 6.

Coal Tonnage

Table 5 is a summary table showing short tons of coal resources by State and county and by five overburden categories. The table shows that the total Fruitland coal resource for the San Juan Basin is 230 billion short tons; 180 billion short tons in New Mexico and 50 billion short tons in Colorado. (Detailed tables of Fruitland coal tonnage are in Appendix 6.) By overburden categories, 39 percent of the coal is deeper than 3,000 ft, 29 percent is between 2,000 and 3,000 ft deep, 17 percent is between 1,000 and 2,000 ft deep, 7 percent is between 500 and 1,000 ft deep, and 8 percent is less than 500 ft deep. The 4,000-ft depth-of-overburden line is shown on the overburden map (fig. 39), but coal resources were not calculated for this category.

The first basin-wide coal-tonnage estimate for Fruitland

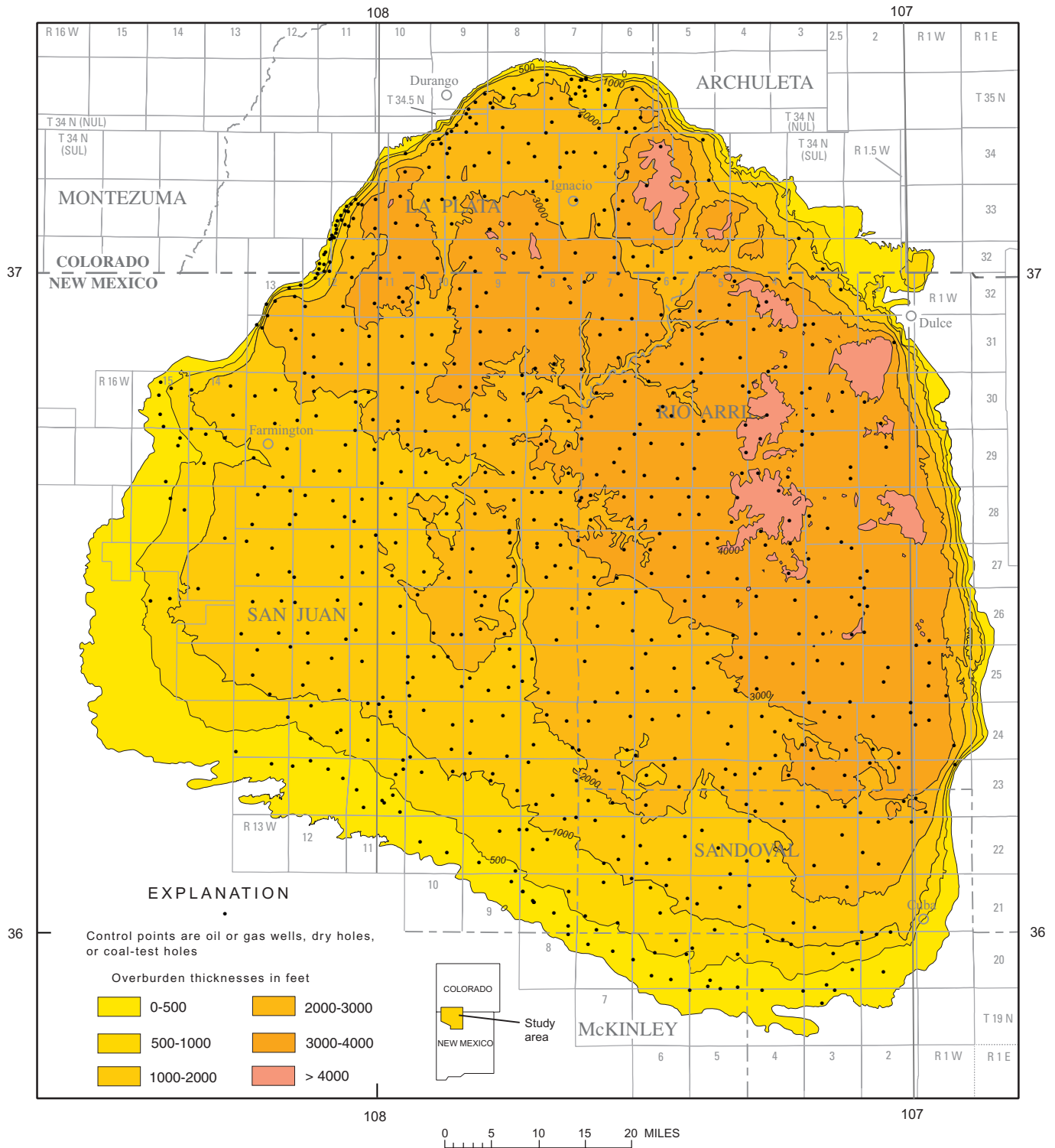


Figure 39. Overburden on top of the Pictured Cliffs Sandstone (base of the Fruitland Formation) in the San Juan Basin.

Table 5. Estimated coal resources (in millions of short tons) in beds 1.2 ft thick or greater, Fruitland Formation, San Juan Basin, Colorado and New Mexico.

[Values rounded to two significant figures. Totals may not add due to independent rounding]

State	County	Overburden categories (ft)					Grand Total
		0-500	500-1,000	1,000-2,000	2,000-3,000	>3,000	
Colorado	Archuleta	970	690	1,400	3,100	3,600	9,800
	La Plata	1,600	1,000	3,900	19,000	14,000	40,000
Colorado Totals		2,600	1,700	5,400	22,000	18,000	50,000
New Mexico	McKinley	1,700	300	0	0	0	2,000
	Rio Arriba	140	85	380	13,000	53,000	66,000
	San Juan	14,000	12,000	32,000	29,000	17,000	100,000
	Sandoval	490	1,400	2,300	1,700	250	6,200
New Mexico Totals		16,000	14,000	34,000	44,000	70,000	180,000
Grand Total		19,000	16,000	40,000	66,000	88,000	230,000

coals in the San Juan Basin by Fassett and Hinds (1971, table 7) was 201 billion short tons. That study used a figure of 1,770 short tons of coal per acre-ft to calculate the basin's coal resources. If 2,000 short tons of coal per acre-ft is substituted for the calculation, the total coal tonnage becomes 227 billion short tons; virtually the same tonnage number in this report when rounded to two significant figures. Kelso and Wicks (1988, p. 75) estimated the coal resources for the San Juan Basin to be 219 billion short tons. They used a coal-tonnage value between 1,800 and 1,900 short tons per acre-ft on a township-by-township basis according to the rank of the coal in each township, thus it is difficult to recreate a tonnage for their report had they used 2,000 short tons per acre-ft. However, if an average of 1,850 short tons per acre-ft is assumed for their original calculation and their tonnage is adjusted using a value of 2,000 short tons per acre-ft, their tonnage would have been 237 billion short tons of coal; 240 billion short tons rounded to two significant figures. In the "Comparison with Earlier Studies" section under the "Geographic Distribution of Fruitland Formation Coal" section of this report, it was concluded that Kelso and Wicks had inflated coal thicknesses due to inclusion of caved portions of some drill holes as coal; thus, their tonnage figure of 240 billion short tons is probably too large.

Ayers and others (1994, p. 38) estimated the total Fruitland coal resource in the basin to be 245 billion short tons. These authors provided no indication of the number of short tons of coal per acre-ft that they used to calculate this number; thus, it is impossible to compare their total coal tonnage number with that from other reports in a meaningful way. There is no question, however, that Ayers and others overestimated coal thicknesses in several parts of the basin as the result of including cavings in drill holes as measured coal (see fig. 30 and related discussion above). It is suggested, therefore, that the 245-billion-short-ton resource number for Fruitland coals in the basin is too high.

Two other reports calculated Fruitland coal tonnage for the New Mexico part of the San Juan Basin. Biewick and

others (1991, p. 25) estimated total Fruitland coal tonnage for the New Mexico part of the basin as 168 billion short tons using a coal tonnage of 1,770 short tons per acre-ft. Substituting 2,000 short tons per acre-ft yields 190 billion short tons of coal compared to 180 billion short tons for this report (table 5). Boger and Medlin (1991, p. 42) calculated total Fruitland coal tonnage for New Mexico as 160 billion short tons, again using 1,770 short tons of coal per acre-ft for the coal density. Substituting 2,000 short tons per acre-ft yields an adjusted tonnage of 181 billion short tons of coal; virtually the same number calculated in this report.

Strippable Coal Resources

Shoemaker and others (1971, table 13) considered coal to a depth of 250 ft to be strippable and estimated that these reserves in New Mexico total about 5.041 billion short tons; of this total, 2.441 billion short tons are less than 150 ft deep. These authors did not include coal beds less than 3 ft thick at depths less than 150 ft and beds 5 ft thick between depths of 150–250 ft. Layers of non-coal material more than 0.7 ft thick were excluded from their coal measurements. Hoffman (1996) calculated the demonstrated reserve base for strippable Fruitland coal in New Mexico for depths of overburden between 20 and 200 ft, assuming that coal with less than 20 ft of overburden would be too badly weathered to be mined. That study only included coal within 1 mi of a point of measurement, and coal beds thinner than about 2.5 ft were not included. Mined Fruitland coal was subtracted from the total. Hoffman's strip-coal tonnage was 3.674 billion short tons. Beaumont (1998) discussed near-surface coal deposits in the San Juan Basin (less than 200 ft of overburden). He showed a 200-ft depth line for Fruitland coals, but did not offer an estimate of the tonnage of remaining strippable Fruitland coal.

Table 5 of this report shows 19 billion short tons of coal in the 0–500 ft of overburden category for the Fruitland, basin wide, and 16 billion short tons at 0–500 ft in the New Mexico

Table 6. Coal production in short tons by year from Fruitland Formation strip-coal mines in the San Juan Basin.

[Data for New Mexico through 1997 from Beaumont (1998); data for 1998 from the New Mexico Energy, Minerals, and Natural Resources Department. Colorado coal production data from Colorado Geological Survey]

Year	New Mexico						Colorado		Basin yearly totals
	Navajo	San Juan	La Plata	Gateway	De-Na-Zin	Burnham	Chimney Rock	Martinez Strip	
1963	1,190,763								1,190,763
1964	2,116,069								2,116,069
1965	2,397,982								2,397,982
1966	2,032,447								2,032,447
1967	2,435,318								2,435,318
1968	2,332,652								2,332,652
1969	3,337,419						342		3,337,761
1970	6,020,950								6,020,950
1971	6,652,049								6,652,049
1972	6,898,262								6,898,262
1973	7,389,321	350,724							7,740,045
1974	6,955,000	956,688							7,911,688
1975	6,073,000	1,245,449							7,318,449
1976	7,010,000	1,223,670							8,233,670
1977	7,420,066	1,843,076						4,366	9,267,508
1978	6,100,000	2,613,038						38,676	8,751,714
1979	5,203,000	4,000,534				3,370			9,206,904
1980	7,733,000	4,538,000			13,177	38,340		8,425	12,330,942
1981	6,845,000	4,119,000			211,145	50,581	255,013		11,480,739
1982	7,144,802	4,906,034			229,585	89,459	259,477		12,629,357
1983	8,958,056	4,975,770		202,229	23,000	363,338	252,500		14,774,893
1984	8,403,000	5,151,579		213,846	9,697	31,221	267,809		14,077,152
1985	6,978,000	5,110,790		202,733	34,077		193,885		12,519,485
1986	6,841,000	5,215,966	594,643	188,168	31,378				12,871,155
1987	7,343,000	3,128,220	1,628,034	172,324	51,185				12,322,763
1988	9,087,000	2,847,000	1,538,133	116,485	106,113				13,694,731
1989	8,874,000	4,737,379	1,467,309						15,078,688
1990	8,670,000	4,572,231	1,908,093						15,150,324
1991	7,385,000	2,920,611	1,054,097						11,359,708
1992	9,087,000	3,062,200	1,327,408						13,476,608
1993	9,082,000	3,871,052	1,651,149						14,604,201
1994	7,781,000	4,430,304	1,686,899						13,898,203
1995	8,412,000	4,164,909	1,851,295						14,428,204
1996	7,031,000	4,381,946	2,418,800						13,831,746
1997	7,505,000	3,055,151	3,413,694						13,973,845
1998	8,420,000	2,880,000	3,880,000						15,180,000
Totals	233,144,156	90,301,321	24,419,554	1,095,785	709,357	576,309	1,229,026	51,467	351,526,975

part of the basin. The Fruitland outcrop dips steeply in the Colorado part of the basin, probably precluding large-scale strip mining of Fruitland coals in that area for the foreseeable future. An approximation of the original strippable coal tonnage for the Fruitland in New Mexico can be made by taking a fraction of the 16 billion short tons determined to be present in the 0- to 500-ft overburden category. At a maximum stripping depth of 200 ft, the tonnage is 6.4 billion short tons. This total includes all coal beds greater than 1.2 ft thick. If this 6.4 billion short tons of coal is reduced by 10 percent for weathered coal with less than 20 ft of overburden (640 million short tons) and by the total Fruitland coal mined through the end of 1998 (350 million short tons, table 6), the remaining tonnage is about 5.3 billion short tons of coal.

Hoffman's (1996) number of 3.7 billion short tons of Fruitland coal between 20 and 200 ft of overburden in the New Mexico demonstrated reserve base is a minimum number because she did not include areas that were more than a mile from a point of measurement. The actual remaining reserve base for Fruitland coal in the New Mexico part of the San Juan Basin (through 1998) is thus greater than 3.7 but probably not more than 5.3 billion short tons of coal. These numbers do not represent recoverable coal because environmental, societal, technologic, and economic conditions that are involved in any coal-mining operation will determine how much of the reserve base can be recovered.

Fruitland Coal Mining

Fassett and Hinds (1971, p. 70) stated that "Approximately 30 known mines and prospect drifts have been excavated in Fruitland coal beds; the majority of these were small truck mines, which were operated briefly for local markets." That study showed the locations of these small operations (fig. A3-6) and presented production data for them (table A3-1) where it was known. Nickelson (1988) discussed all of the known Fruitland coal mines in the New Mexico part of the San Juan Basin.

A new generation of large Fruitland strip-coal mines began with the opening of the Navajo coal mine in 1963, the San Juan mine in 1973, and the La Plata mine in 1986 (fig. 2). Four smaller strip mines were opened in the 1970's and 1980's, but the last of these was shut down in 1988. Nearly all of the coal produced from these mines has been used to produce electricity at the Four Corners Generating Station and the San Juan Generating Station (fig. 2). An overview of these power plants and coal mines is in Fassett (1989). Table 6 shows reported coal production from Fruitland strip mines by year; total Fruitland coal production from these mines through 1998 was 352 million short tons. A detailed discussion of Fruitland coal mining is beyond the scope of this report but the reports by Shoemaker and others (1971), Nickelson (1988), Hoffman (1996), and Beaumont (1998) provide excellent overviews of the strippable Fruitland coal resources and mining in the New Mexico part of the San Juan Basin.

References Cited

- Ambrose, W.A., and Ayers, W.B., 1994, Geologic controls on coalbed methane occurrence and production in the Fruitland Formation, Cedar Hill field and the COAL site, *in* Ayers, W.B., Jr., and Kaiser, W.R., eds., Coalbed Methane in the Upper Cretaceous Fruitland Formation, San Juan Basin, New Mexico and Colorado: New Mexico Bureau of Mines and Mineral Resources Bulletin 146, p. 41–61.
- American Society for Testing and Materials [ASTM], 1995, Standard classification of coals by rank [ASTM designation F388-395]: 1995 Annual book of ASTM Standards, v. 05.05, p. 169–171.
- Ayers, W.B., Jr., and Ambrose, W.A., 1990, Geologic controls on the occurrence of coalbed methane, Fruitland Formation, San Juan Basin, *in* Ayers, W.B., Jr., Kaiser, W.R., Ambrose, W.A., Swartz, T.E., Laubach, S.E., Tremain, C.M., and Whitehead, N.H., III, eds., Annual Report Prepared for the Gas Research Institute: The University of Texas at Austin, Bureau of Economic Geology, GRI-90-0014.1, p. 9–72.
- Ayers, W.B., Jr., Ambrose, W.A., and Yeh, J.S., 1994, Coalbed methane in the Fruitland Formation, San Juan Basin—Depositional and structural controls on occurrence and resources, *in* Ayers, W.B., Jr., and Kaiser, W.R., eds., Coalbed Methane in the Upper Cretaceous Fruitland Formation, San Juan Basin, New Mexico and Colorado: New Mexico Bureau of Mines and Mineral Resources Bulletin 146, p. 13–40.
- Ayers, W.B., and Zellers, S.D., 1991, Geologic controls on Fruitland coal occurrence, thickness, and continuity, Navajo Lake area, San Juan Basin, *in* Geologic Controls on Occurrence and Producibility of Coalbed Methane, Fruitland Formation: Chicago, Ill., Gas Research Institute, Report GRI 91/0072, p. 9–46.
- Ayers, W.B., and Zellers, S.D., 1994, Coalbed methane in the Fruitland Formation, Navajo Lake area: Geologic controls on occurrence and producibility, *in* Ayers, W.B., Jr., and Kaiser, W.R., eds., Coalbed Methane in the Upper Cretaceous Fruitland Formation, San Juan Basin, New Mexico and Colorado: New Mexico Bureau of Mines and Mineral Resources Bulletin 146, p. 63–85.
- Baltz, E.H., Ash, S.R., and Anderson, R.Y., 1966, History of nomenclature and stratigraphy of rocks adjacent to the Cretaceous-Tertiary boundary, western San Juan Basin, New Mexico: U.S. Geological Survey Professional Paper 524-D, 23 p.
- Bauer, C.M., 1916, Stratigraphy of a part of the Chaco River valley: U.S. Geological Survey Professional Paper 98-P, p. 271–278 [1917].
- Beach, L.J., and Jentgen, R.W., 1978, Coal test drilling for the San Juan mine extension, San Juan County, New Mexico: U.S. Geological Survey Open-File Report 80-1289, (unpaginated).
- Beaumont, E.C., 1998, Distribution of near-surface coal deposits in San Juan Basin, New Mexico: New Mexico Bureau of Mines and Mineral Resources Resource Map 19, 2 sheets, scale 1:250,000.
- Biewick, L.R.H., Medlin, A.L., Hunter, J.F., and Kohn, K.K., 1991, Coal resources of the San Juan Basin, *in* Molnia, C.L., Jobin, D.A., O'Connor, J.T., and Kottlowski, F.E., eds., Coalfields of New Mexico: Geology and Resources: U.S. Geological Survey Bulletin 1972, p. 15–33.
- Boger, L.W., and Medlin, A.L., 1991, Coal resource estimation in the

- San Juan Basin using geostatistical methods, *in* Molnia, C.L., Jobin, D.A., O'Connor, J.T., and Kottlowski, F.E., eds., *Coalfields of New Mexico: Geology and Resources: U.S. Geological Survey Bulletin 1972*, p. 35–43.
- Bond, W.A., 1984, Application of Lopatin's method to determine burial history, evolution of the geothermal gradient, and timing of hydrocarbon generation in Cretaceous source rocks in the San Juan Basin, northwestern New Mexico and southwestern Colorado, *in* Woodward, J., Meissner, F.F., and Clayton, J.L., eds., *Hydrocarbon Source Rocks of the Greater Rocky Mountain Region: Rocky Mountain Association of Geologists Guidebook*, p. 433–447.
- Butler, R.F., 1985, Mineralogy of magnetic minerals and revised magnetic polarity stratigraphy of continental sediments, San Juan Basin, New Mexico: *Journal of Geology*, p. 535–554.
- Brown, J.L., 1982a, Geologic map of the Alamo Mesa East quadrangle: U.S. Geological Survey Miscellaneous Field Studies Map MF-1497, scale 1:24,000.
- Brown, J.L., 1982b, Geologic map of the Huerfano Trading Post SW quadrangle: U.S. Geological Survey Miscellaneous Field Studies Map MF-1498, scale 1:24,000.
- Clarkson, G., and Reiter, M., 1988, An overview of geothermal studies in the San Juan Basin, New Mexico and Colorado, *in* Fassett, J.E., ed., *Geology and Coal-Bed Methane Resources of the Northern San Juan Basin, Colorado and New Mexico: Rocky Mountain Association of Geologists Guidebook*, p. 285–291.
- Cobban, W.A., 1973, Significant ammonite finds in uppermost Mancos Shale and overlying formations between Barker dome, New Mexico, and Grand Junction, Colorado, *in* Fassett, J.E., ed., *Cretaceous and Tertiary Rocks of the Southern Colorado Plateau: Four Corners Geological Society Memoir*, p. 148–153.
- Cobban, W.A., Landis, E.R., and Dane, C.H., 1974, Age relations of upper part of Lewis Shale on east side of San Juan Basin, New Mexico, *in* Siemers, C.T., ed., *Ghost Ranch Central-Northern New Mexico: New Mexico Geological Society Guidebook 25*, p. 279–282.
- Decker, D., Jeu, S.J., Cooper, J.D., and Wicks, D.E., 1988, Geology, geochemistry, reservoir engineering, and completion methods at the Cedar Hill field, San Juan County, New Mexico: A field study of classic coal degasification behavior, *in* Fassett, J.E., ed., *Geology and Coal-Bed Methane Resources of the Northern San Juan Basin, Colorado and New Mexico: Rocky Mountain Association of Geologists Guidebook*, p. 221–235.
- Dyman, T.S., Merewether, E.A., Molenaar, C.M., Cobban, W.A., Obradovich, J.D., Weimer, R.J., and Bryant, W.A., 1994, Stratigraphic transects for Cretaceous rocks, Rocky Mountains and Great Plains regions, *in* Caputo, M.V., Peterson, J.A., and Franczyk, K.J., eds., *Mesozoic Systems of the Rocky Mountain Region, USA: Denver, Colo., Rocky Mountain Section of the Society for Sedimentary Geology*, p. 365–391.
- Fassett, J.E., 1977, Geology of the Point Lookout, Cliff House, and Pictured Cliffs Sandstones of the San Juan Basin, New Mexico and Colorado, *in* Fassett, J.E., ed., *San Juan Basin III: New Mexico Geological Society Guidebook 28*, p. 193–197.
- Fassett, J.E., ed., 1978, Oil and gas fields of the Four Corners area: Four Corners Geological Society, v. I and II, 728 p.
- Fassett, J.E., ed., 1983, Oil and gas fields of the Four Corners area: Four Corners Geological Society, v. III, p. 729–1143.
- Fassett, J.E., 1985, Early Tertiary paleogeography and paleotectonics of the San Juan Basin area, New Mexico and Colorado, *in* Flores, R.M., and Kaplan, S.S., eds., *Cenozoic Paleogeography of the West-Central United States (Rocky Mountain paleogeography symposium 3): Denver, Colo., Rocky Mountain Section, Society of Economic Paleontologists and Mineralogists*, p. 317–334.
- Fassett, J.E., 1987, The ages of the continental Upper Cretaceous Fruitland Formation and Kirtland Shale based on a projection of ammonite zones from the Lewis Shale, San Juan Basin, New Mexico and Colorado, *in* *The Cretaceous-Tertiary Boundary in the San Juan and Raton Basins, New Mexico and Colorado: Geological Society of America Special Paper 209*, p. 5–16.
- Fassett, J.E., 1989, Coal resources of the San Juan Basin, *in* Anderson, O.J., Lucas, S.G., Love, D.W., and Cather, S.M., eds., *Southeastern Colorado Plateau: New Mexico Geological Society 40th Annual Field-Trip Guidebook*, p. 303–307.
- Fassett, J.E., 1991, Oil and gas resources of the San Juan Basin, New Mexico and Colorado, *in* Gluskoter, H.J., Rice, D.D., and Taylor, R.B., eds., *Economic Geology, Geological Society of America, The Geology of North America Series, v. P-2*, p. 357–372.
- Fassett, J.E., Cobban, W.A., and Obradovich, J.D., 1997a, Biostratigraphic and isotopic age of the Huerfanito Bentonite Bed of the Upper Cretaceous Lewis Shale at an outcrop near Regina, New Mexico, *in* Anderson, O.J., Kues, B.S., and Lucas, S.G., eds., *Mesozoic Geology and Paleontology of the Four Corners Region: New Mexico Geological Society 48th Annual Field-Conference Guidebook*, p. 229–232.
- Fassett, J.E., Condon, S.M., Huffman, A.C., and Taylor, D.J., 1997b, Geology and structure of the Pine River, Florida River, Carbon Junction, and Basin Creek gas seeps, La Plata County, Colorado: U.S. Geological Survey Open-File Report, OF-97-59, 125 p.
- Fassett, J.E., and Hinds, J.S., 1971, Geology and fuel resources of the Fruitland Formation and Kirtland Shale of the San Juan Basin, New Mexico and Colorado: U.S. Geological Survey Professional Paper 676, 76 p.
- Fassett, J.E., and Lucas, S.G., 2000, Evidence for Paleocene dinosaurs in the Ojo Alamo Sandstone, San Juan Basin, New Mexico, *in* Lucas, S.G., and Heckert, A.B., eds., *Dinosaurs of New Mexico: New Mexico Museum of natural History and Science Bulletin No. 17*.
- Fassett, J.E., Lucas, S.G., Zielinski, R.A., and Budahn, J.R., 2000, Compelling new evidence for Paleocene dinosaurs in the Ojo Alamo Sandstone, San Juan Basin, New Mexico and Colorado, USA, *in* *Catastrophic Events and Mass Extinctions: Impacts and Beyond: Houston, Tex., LPI Contribution no. 1053, Lunar and Planetary Institute*, p. 45–46.
- Fassett, J.E., and Nuccio, V.F., 1990, Vitrinite reflectance values of coal from drill-hole cuttings from the Fruitland and Menefee Formations, San Juan Basin, New Mexico: U.S. Geological Survey Open-File Report 90-290, 21 p.
- Fassett, J.E., and Steiner, M.B., 1997, Precise age of C33n-C32r magnetic polarity reversal, San Juan Basin, New Mexico and Colorado, *in* Anderson, O.J. and others, eds., *Mesozoic Geology and Paleon-*

- tology of the Four Corners Region: New Mexico Geological Society Guidebook 48, p. 239–247.
- Heywood, C.E., 1992, Isostatic residual gravity anomalies of New Mexico: U.S. Geological Survey Water-Resources Investigations Report 91-4065, 27 p.
- Hoffman, G.K., 1991, Quality assessment of strippable coals in north-west New Mexico: drilling data, chemical, and petrographic analyses for the Fruitland, Menefee, Crevasse Canyon, and Moreno Hill Formation[s]: New Mexico Bureau of Mines and Mineral Resources Open-File Report 377, (unpaginated).
- Hoffman, G.K., 1996, Demonstrated reserve base for coal in New Mexico, modified from final report for cooperative agreement DOE-FC0193E123974: New Mexico Bureau of Mines and Mineral Resources Open-File Report 428, 89 p., 2 appendixes.
- Hoffman, G.K., Campbell, F.W., and Beaumont, E.C., 1993, Quality assessment of strippable coals in northwest New Mexico: Fruitland, Menefee, and Crevasse Canyon Formation coals in San Juan Basin, and Moreno Hill Formation coals in Salt Lake field: New Mexico Bureau of Mines and Mineral Resources Bulletin 111, 84 p.
- Hoffman, G.K., and Jones, G.E., 1998, Availability of coal resources in the Fruitland Formation, San Juan Basin, northwest New Mexico: New Mexico Bureau of Mines and Mineral Resources Open-File Report 438, 15 p.
- Hoppe, W.F., 1992, Hydrocarbon potential and stratigraphy of the Pictured Cliffs, Fruitland, and Ojo Alamo Formations in the northeastern San Juan Basin, New Mexico, *in* Lucas, S.G., Kues, B.S., Williamson, T.E., and Hunt, A.P., eds., San Juan Basin IV: New Mexico Geological Society Guidebook 43, p. 359–371.
- Hopkins, M.E., 1968, Harrisburg (No. 5) coal reserves of southeastern Illinois: Illinois State Geological Survey Circular 431, 25 p.
- Hunt, A.P., and Lucas, S.G., 1992, Stratigraphy, paleontology and age of the Fruitland and Kirtland Formations (Upper Cretaceous), San Juan Basin, New Mexico, *in* Lucas, S.G., Kues, B.S., Williamson, T.E., and Hunt, A.P., eds., San Juan Basin IV: New Mexico Geological Society Guidebook 43, p. 217–239.
- Jentgen, R.W., and Fassett, J.E., 1977, Sundance-Bisti-Star Lake 1976 drilling in McKinley and San Juan Counties, northwestern New Mexico: U.S. Geological Survey Open-File Report 77-369, 80 p.
- Jervey, M.T., 1988, Quantitative geological modeling of siliciclastic rock sequences and their seismic expression, *in* Wilgus and others, eds., Sea Level Changes: An Integrated Approach: Society of Economic Paleontologists and Mineralogists Special Publication No. 42, p. 47–69.
- Kelso, B.S., Decker, A.D., Wicks, D.E., and Horner, D.M., 1987, GRI geologic and economic appraisal of coalbed methane in the San Juan Basin, *in* Proceedings, 1987 Coalbed Methane Symposium: Tuscaloosa, University of Alabama, School of Mines and Energy Development, p. 119–125.
- Kelso, B.S., Goolsby, S.M., and Tremain, C.M., 1980, Deep coal bed methane potential of the San Juan River coal region, southwestern Colorado: Colorado Geological Survey Open-File Report 80-2, 56 p.
- Kelso, B.S., and Rushworth, P., 1982, Southern Ute/Department of Energy coalbed methane test wells: Colorado Geological Survey Open-File Report 82-4, 22 p.
- Kelso, B.S., and Wicks, D.E., 1988, A geologic analysis of the Fruitland Formation coal and coal-bed methane resources of the San Juan Basin, southwestern Colorado and northwestern New Mexico, *in* Fassett, J.E., ed., Geology and Coal-Bed Methane Resources of the Northern San Juan Basin, Colorado and New Mexico: Rocky Mountain Association of Geologists Guidebook, p. 69–79.
- Law, B.E., 1990, Vitrinite reflectance data from Cretaceous and Tertiary rocks, San Juan Basin, New Mexico and Colorado: U.S. Geological Survey Open-File Report 90-659, 18 p.
- Law, B.E., 1992, Thermal maturity patterns of Cretaceous and Tertiary rocks, San Juan Basin, Colorado and New Mexico: Geological Society of America Bulletin, v. 104, p. 192–207.
- Levine, J.R., 1993, Coalification: The evolution of coal as source rock and reservoir rock for oil and gas, *in* Law, B.E., and Rice, D.D., Hydrocarbons from Coal: American Association of Petroleum Geologists Studies in Geology 38, p. 39–77.
- Mavor, Matt, and Nelson, C.R., 1997, Coalbed reservoir gas-in-place analysis: Chicago, Ill., Gas Research Institute, GRI Report no. GRI-97/0263, 134 p.
- M'Gonigle, J.W., and Roberts, L.N.R., 1997, Coal geology and resources, *in* Van Loenen, R.E., and Gibbons, A.B., eds., Mineral Resource Potential and Geology of the San Juan National Forest, Colorado: U.S. Geological Survey Bulletin 2127, p. 101–115.
- Nickelson, H.B., 1988, One hundred years of coal mining in the San Juan Basin, New Mexico: New Mexico Bureau of Mines and Mineral Resources Bulletin 111, 227 p.
- North American Stratigraphic Code, 1983: The North American Commission on Stratigraphic Nomenclature: American Association of Petroleum Geologists Bulletin, v. 67, no. 5, p. 841–875.
- Nummedal, Dag, and Molenaar, C.M., 1995, Sequence stratigraphy of ramp-setting strand plain successions: The Gallup Sandstone, New Mexico, *in* Van Wagoner, J.C., and Bertram, G.T., eds., Sequence Stratigraphy of Foreland Basin Deposits: American Association of Petroleum Geologists Memoir 64, p. 277–310.
- Obradovich, J.D., 1993, A Cretaceous time scale, *in* Caldwell, W.G.E., and Kauffman, E.G., eds., Evolution of the Western Interior Basin: Geological Association of Canada, Special Paper 39, p. 379–396.
- Obradovich, J.D., and Hicks, J.F., 1999, A review of the isotopic calibration points for the geomagnetic polarity time scale in the interval 83 to 33 Ma (C34n to C13n): Denver, Colo., Geological Society of America 1999 Annual Meeting, Abstracts with Programs Volume, v. 31, no. 7, p. A-71.
- Obradovich, J.D., and Cobban, W.A., 1975, A time scale for the Late Cretaceous of the Western Interior of North America, *in* Caldwell, W.G.E., ed., The Cretaceous System in the Western Interior of North America: Geological Association of Canada, Special Paper 13, p. 31–54.
- Oil and Gas Journal, 1998, Multiwell Ojo Alamo development advancing in San Juan Basin: Oil and Gas Journal, April 27, 1998, p. 77.
- O'Sullivan, R.B., Mytton, J.W., Strobell, J.D., Jr., Scott, G.R., and Erpenbeck, M.F., 1986, Geologic map of the Tanner Lake quadrangle: U.S. Geological Survey Miscellaneous Field Studies Map MF-1864, scale 1:24,000.

- O'Sullivan, R.B., Scott, G.R., and Heller, J.S., 1979, Geologic map of the Bisti Trading Post quadrangle: U.S. Geological Survey Miscellaneous Field Studies Map MF-1075, scale 1:24,000.
- Pawlewicz, M.J., Nuccio, V.F., and Fassett, J.E., 1991, Vitrinite reflectance values of coal from drill-hole cuttings, San Juan Basin, New Mexico: U.S. Geological Survey Open-File Report 91-302, 10 p.
- Pike, W.S., Jr., 1947, Intertonguing marine and nonmarine Upper Cretaceous deposits of New Mexico, Arizona, and southwestern Colorado: Geological Society of America Memoir 24, 103 p.
- Rice, D.D., 1983, Relation of natural gas composition to thermal maturity and source rock type in San Juan Basin, northwestern New Mexico and southwestern Colorado: American Association of Petroleum Geologists Bulletin, v. 67, p. 1199–1218.
- Roberts, L.N.R., 1989, Results of 1988 coal exploratory drilling in the Fruitland Formation, western part of the Southern Ute Indian Reservation, La Plata County, Colorado: U.S. Geological Survey Open-File Report 89-487, 221 p.
- Roberts, L.N.R., 1991, Coal resources of the Fruitland Formation in part of the Ute Mountain Ute Indian Reservation, San Juan County, New Mexico: U.S. Geological Survey Bulletin 1938, 15 p.
- Roberts, L.N.R., and Kirschbaum, M.A., 1995, Paleogeography of the Late Cretaceous of the Western Interior of Middle North America—Coal distribution and sediment accumulation: U.S. Geological Survey Professional Paper 1561, 115 p.
- Roberts, L.N.R., and McCabe, P.J., 1992, Peat accumulation in coastal-plain mires: A model from coals of the Fruitland Formation (Upper Cretaceous) of southern Colorado, USA: International Journal of Coal Geology, v. 21, p. 115–138.
- Roberts, L.N.R., and Uptegrove, Jane, 1991, Coal geology and coal zone correlations in the Fruitland Formation, western part of the Southern Ute Indian Reservation, La Plata County, Colorado: U.S. Geological Survey Coal Investigations Map C-138, scale 1:24,000.
- Sandberg, D.T., 1986, Correlation of coal beds in the Fruitland Formation as interpreted from geophysical logs, east-central San Juan County, New Mexico: U.S. Geological Survey Miscellaneous Field Studies Map MF-1848.
- Sandberg, D.T., 1988a, Coal resources and coal-bed geometry, Fruitland Formation, Southern Ute Indian Reservation, Archuleta and La Plata Counties, Colorado, *in* Fassett, J.E., ed., Geology and Coal-Bed Methane Resources of the Northern San Juan Basin, Colorado and New Mexico: Rocky Mountain Association of Geologists Guidebook, p. 39–50.
- Sandberg, D.T., 1988b, Distribution of coal beds in the Fruitland Formation, Southern Ute Indian Reservation, Archuleta and La Plata Counties, southwestern Colorado: U.S. Geological Survey Open-File Report 88-230, 5 maps, scale 1:100,000.
- Sandberg, D.T., 1990, Coal resources of Upper Cretaceous Fruitland Formation in the Southern Ute Indian Reservation, southwestern Colorado: U.S. Geological Survey Professional Paper 1505-D, 24 p.
- Schneider, G.B., Weide, D.L., Mytton, J.W., and Scott, G.R., 1979, Geologic map of the Pueblo Bonito NW quadrangle: U.S. Geological Survey Miscellaneous Field Studies Map MF-1118, scale 1:24,000.
- Scott, A.R., Kaiser, W.R., and Ayers, W.B., Jr., 1994, Thermal maturity of Fruitland coals and composition of Fruitland Formation and Pictured Cliffs Sandstone gases, *in* Ayers, W.B., Jr., and Kaiser, W.R., eds., Coalbed Methane in the Upper Cretaceous Fruitland Formation, San Juan Basin, New Mexico and Colorado: New Mexico Bureau of Mines and Mineral Resources Bulletin, p. 165–186.
- Scott, G.R., O'Sullivan, R.B., and Mytton, J.W., 1979, Geologic map of the Alamo Mesa West quadrangle: U.S. Geological Survey Miscellaneous Field Studies Map MF-1074, scale 1:24,000.
- Semken, S.C., and McIntosh, W.C., 1997, $^{40}\text{Ar}/^{39}\text{Ar}$ age determinations for the Carrizo Mountains laccolith, Navajo Nation, Arizona, *in* Anderson, O.J. and others, eds., Mesozoic Geology and Paleontology of the Four Corners Region: New Mexico Geological Society Guidebook 48, p. 75–80.
- Shoemaker, J.W., Beaumont, E.C., and Kottowski, F.E., 1971, Strip-pable low-sulfur coal resources of the San Juan Basin in New Mexico and Colorado: New Mexico Bureau of Mines and Mineral Resources Memoir 25, 189 p.
- Shoemaker, J.W., and Holt, R.D., 1973, Coal resources of Southern Ute and Ute Mountain Ute Indian Reservations, Colorado and New Mexico: New Mexico State Bureau of Mines and Mineral Resources Circular 134, 22 p.
- Stach, E., Mackowsky, M.T., Taylor, G.H., Chandra, D., Teichmuller, M., and Teichmuller, R., 1982, Stach's text book of coal petrology (3rd ed.): Stuttgart, Germany, Borntraeger, 535 p.
- Strobell, J.D., O'Sullivan, R.B., Mytton, J.W., and Erpenbeck, M.F., 1985, Geologic map of the Pretty Rock quadrangle: U.S. Geological Survey Miscellaneous Field Studies Map MF-1788, scale 1:24,000.
- Thaden, R.E., and Zech, R.S., 1984, Preliminary structure contour map of the San Juan Basin: U.S. Geological Survey Miscellaneous Field studies Map MF-1673, scale 1:500,000.
- Turner, C.E., and Fishman, N.S., 1991, Jurassic Lake T'oo'dichi': A large alkaline, saline lake, Morrison Formation, eastern Colorado Plateau: Geological Society of America Bulletin, v. 104, p. 538–558.
- U.S. Geological Survey, 1946, Physical Divisions of the United States [prepared by Fenneman]: U.S. Geological Survey map.
- Whitehead, Neil H, III, 1993, SJ-1. Fruitland Formation, *in* Hjellming, Carol A., ed., Atlas of Major Rocky Mountain Gas Reservoirs: New Mexico Bureau of Mines and Mineral Resources, p. 119–122.
- Whyte, M.R., and Shoemaker, J.W., 1977, A geological appraisal of the deep coals of the Menefee Formation of the San Juan Basin, New Mexico, *in* Fassett, J.E., ed., Supplemental Articles to San Juan Basin III: New Mexico Geological Society 40th Annual Field Trip Guidebook, p. 41–48.
- Williams, G.D., and Stelk, C.R., 1975, Speculation on the Cretaceous paleogeography of North America, *in* Caldwell, W.G.E., ed., The Cretaceous System in the Western Interior of North America: Geological Association of Canada Special Paper 13, p. 1–20.
- Williamson, T.E., and Lucas, S.G., 1992, Stratigraphy and mammalian biostratigraphy of the Paleocene Nacimiento Formation, southern San Juan Basin, New Mexico, *in* Lucas, S.G., Kues, B.S., Williamson, T.E., and Hunt, A.P., eds., San Juan Basin IV: New Mexico Geological Society 43rd Annual Field Conference Guidebook, p. 265–296.

Wilson, R.W., and Jentgen, R.W., 1980, Coal test drilling for the De-na-zin Bisti area, San Juan County, New Mexico: U.S. Geological Survey Open-File Report 78-960, 87 p.

Wood, G.H., Jr., Kehn, T.M., Carter, M.D., and Culbertson, W.C., 1983, Coal resource classification system of the U.S. Geological Survey: U.S. Geological Survey Circular 891, 65 p.

Appendix 1—ArcView Files for Coal Assessment of the San Juan Basin, New Mexico and Colorado

The ArcView files used for the coal resource assessment of the San Juan Basin include geographic, geologic, coal-resource, and coal- and surface-ownership information—these files are presented as views in the ArcView project. The ArcView project and the digital files are stored on both discs of this CD-ROM set—Appendix 1 of chapter Q resides on both discs. Persons who do not have ArcView 3.1 may query the data by means of the ArcView Data Publisher on disc 1. Persons who do have ArcView 3.1 may utilize the full functionality of the software by accessing the data that reside on disc 2. An explanation of the ArcView project and data library—and how to get started using the software—is given by Biewick and Mercier (chap. D, this CD-ROM). Metadata for all digital files are also accessible through the ArcView project.

Appendix 2—Database for the Fruitland Formation Coal Assessment of the San Juan Basin, New Mexico and Colorado

This database was the basis for the net-coal isopach map (fig. 28); this map was used to determine Fruitland coal resources for the basin. The database contains location, lithologic, and stratigraphic data (including top and bottom depths of coal beds) from the StratiFact database. This file consists of ASCII format, DBF, and Excel spreadsheets on disc 2 of this CD-ROM.

Appendix 3—Figures and Tables from Fassett and Hinds (1971)

These illustrations, labeled figures A3-1 through A3-11 and tables A3-1 and A3-2 are adapted, with one exception, from stratigraphic and coal-quality data in Fassett and Hinds (1971). Data points, contour lines, and geologic information were copied from scanned images of the original maps and fitted to the San Juan Basin base map of this report. Line drawings were traced from the original scanned images. Figure A3-10 (not previously published) shows the distribution of sulfur percentages throughout the basin (sulfur data from table A3-2). Detailed discussions of these figures are in Fassett and Hinds (1971).

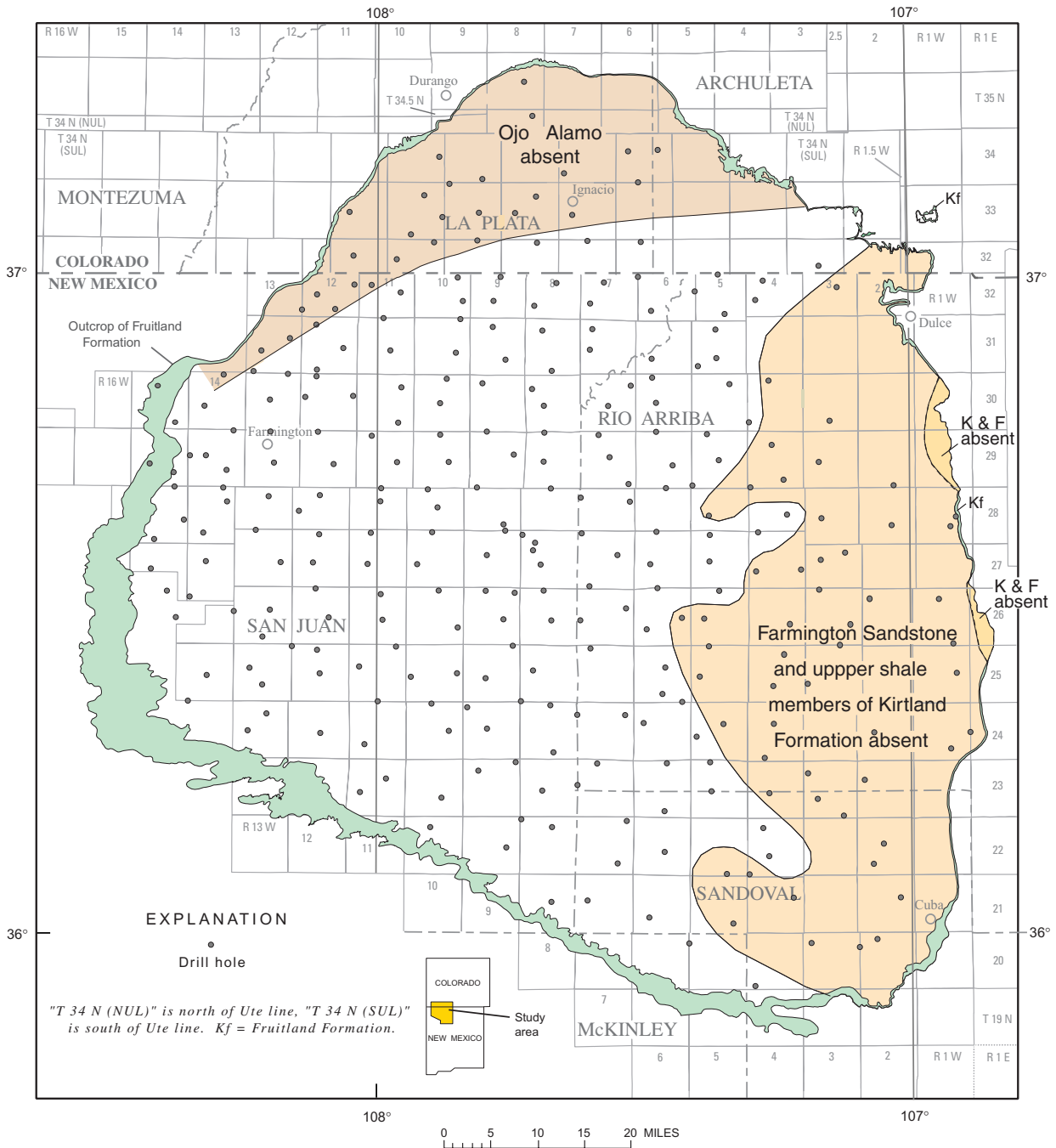


Figure A3-1. Map showing areas in the subsurface of the San Juan Basin where rock units of the Fruitland Formation, Kirtland Formation, and Ojo Alamo Sandstone are absent. All drill holes used for stratigraphic subsurface control are shown. K&F, Kirtland and Fruitland Formations. Map is modified from figure 9 of Fassett and Hinds (1971)

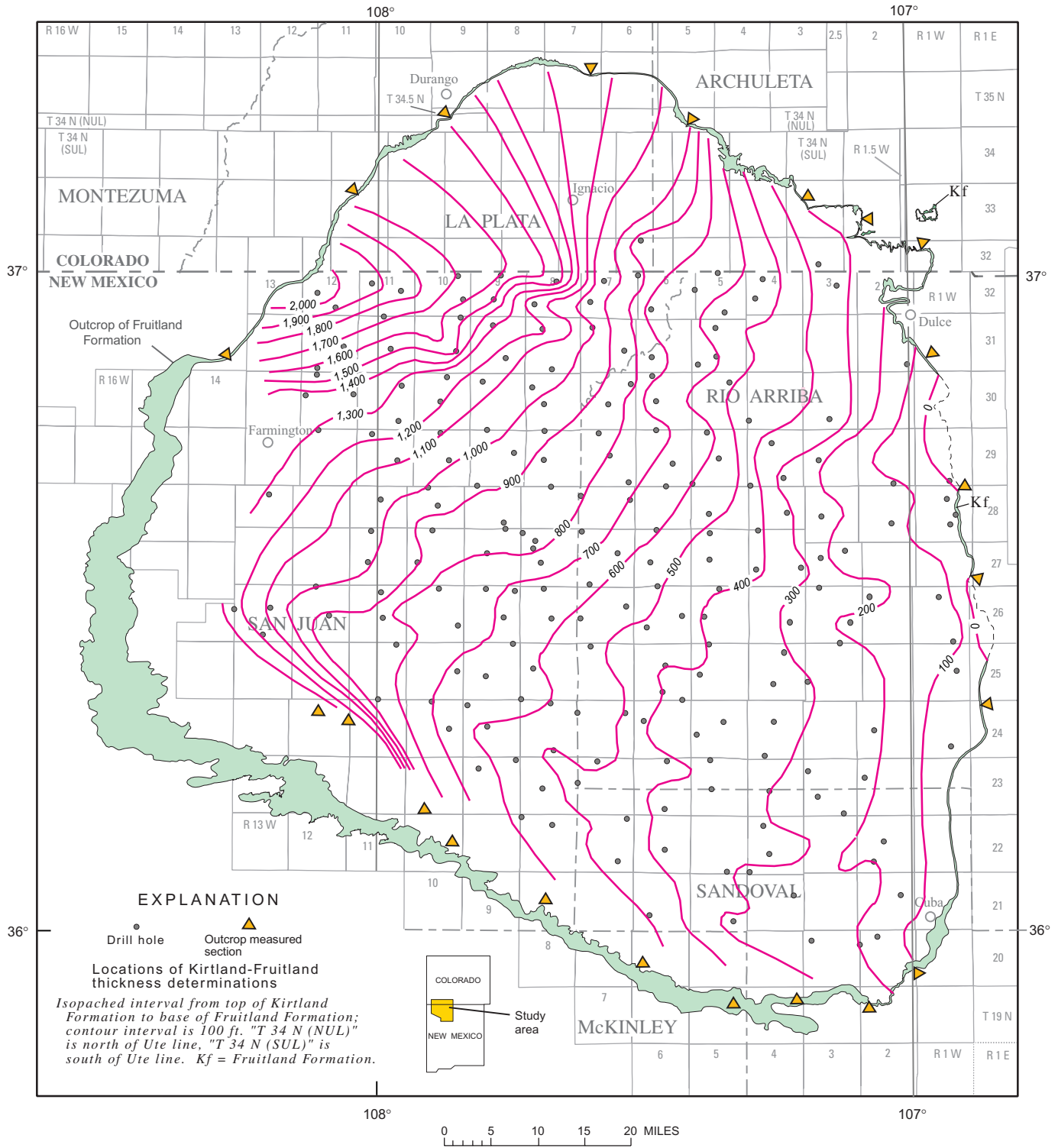


Figure A3-2. Isopach map of the Fruitland Formation and Kirtland Shale. Modified from figure 11 of Fassett and Hinds (1971).

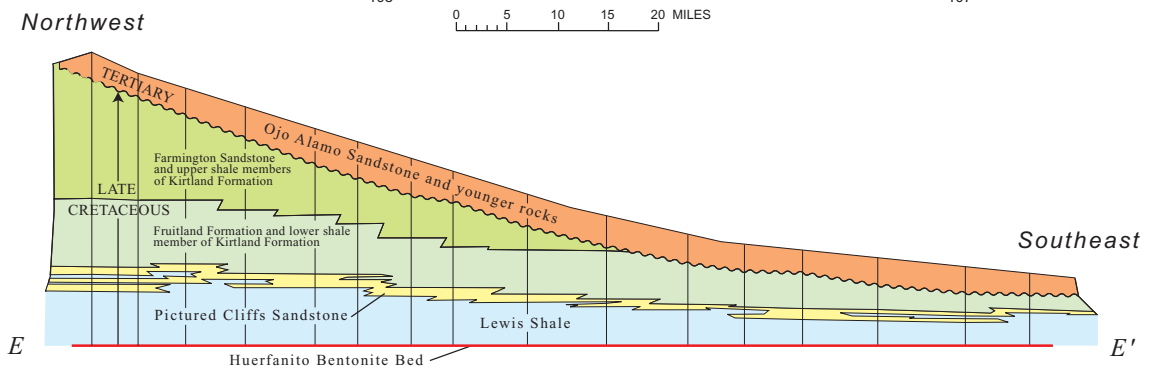
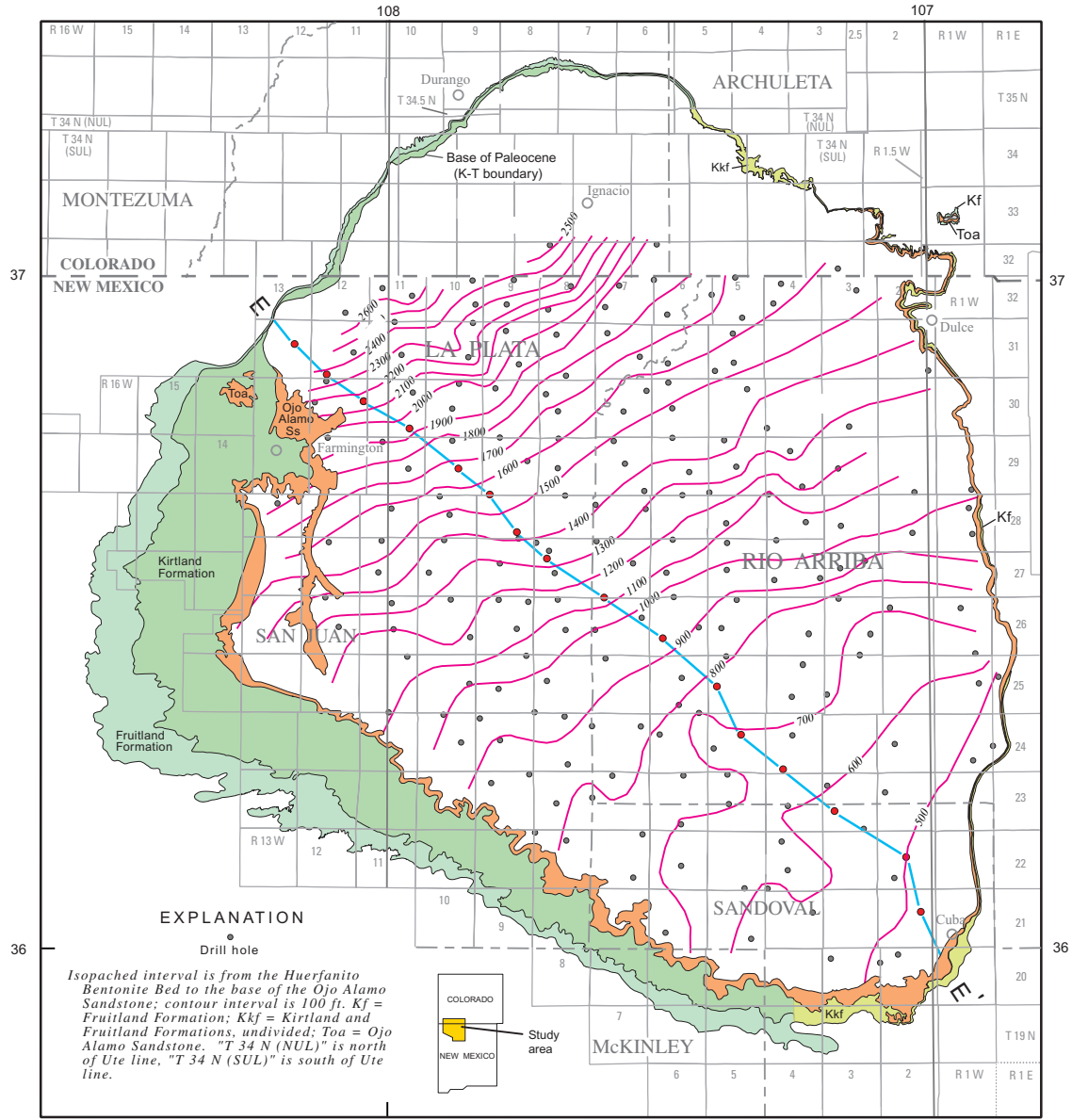
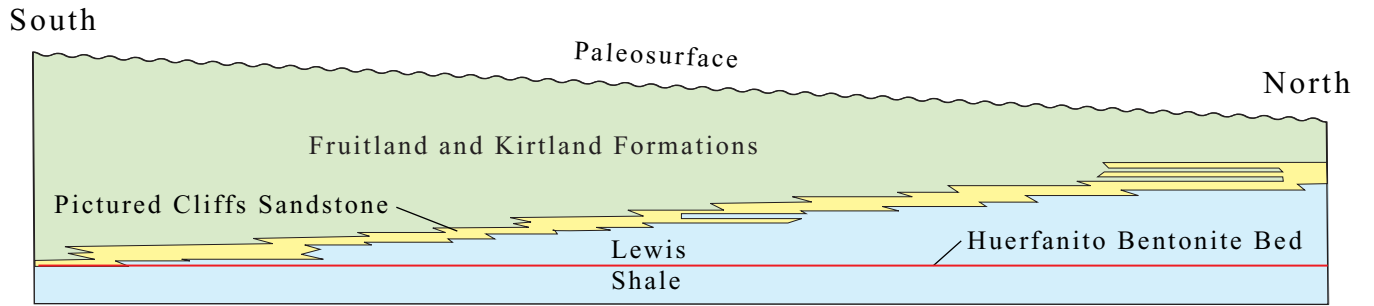
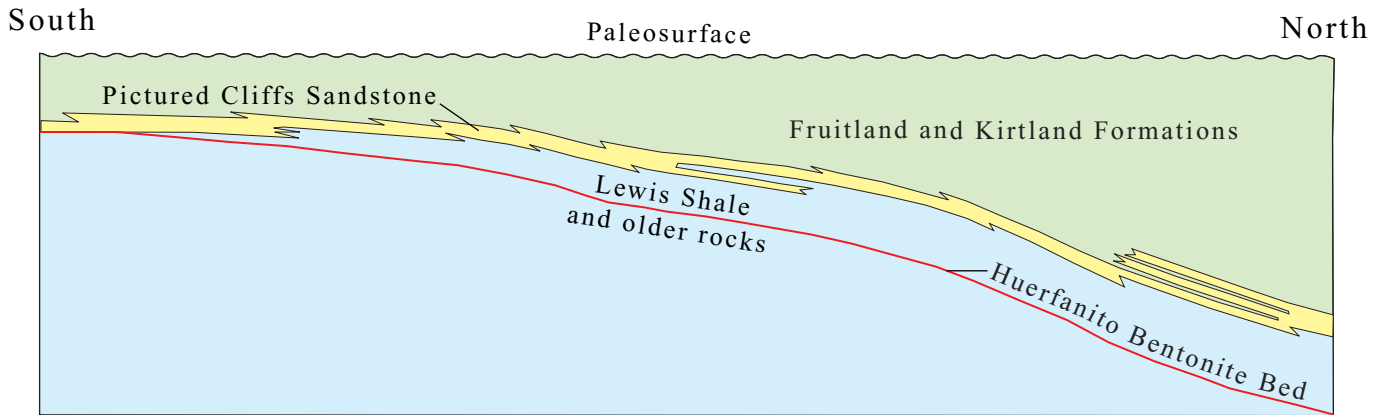


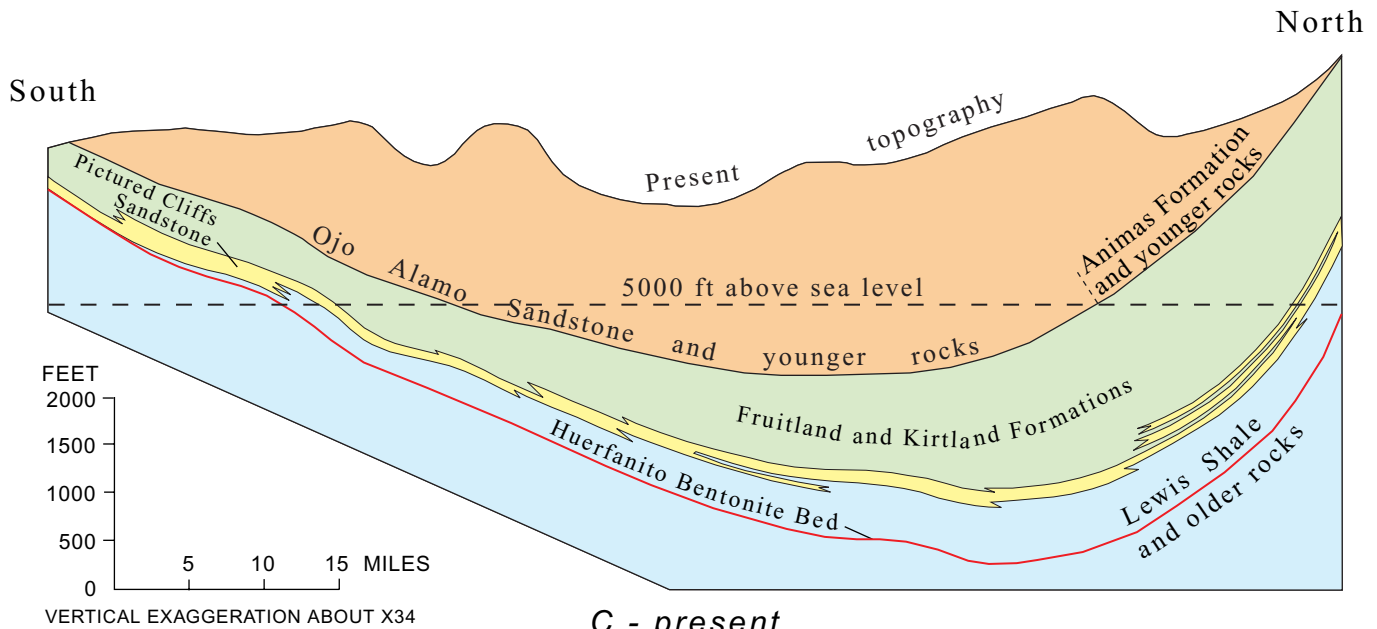
Figure A3-3. Isopach map of the interval between the Huerfanito Bentonite Bed of the Lewis Shale and the base of the Ojo Alamo Sandstone (modified from figure 13 of Fassett and Hinds, 1971). Kirtland Formation and Ojo Alamo Sandstone outcrops are from plate 1 of Fassett and Hinds. Stratigraphic cross section below map shows thinning of Kirtland and Fruitland Formations southeastward across San Juan Basin (modified from cross section E-E' on plate 2 of Fassett and Hinds (1971). Line of section is on map.



A - about 71 Ma, end of Campanian

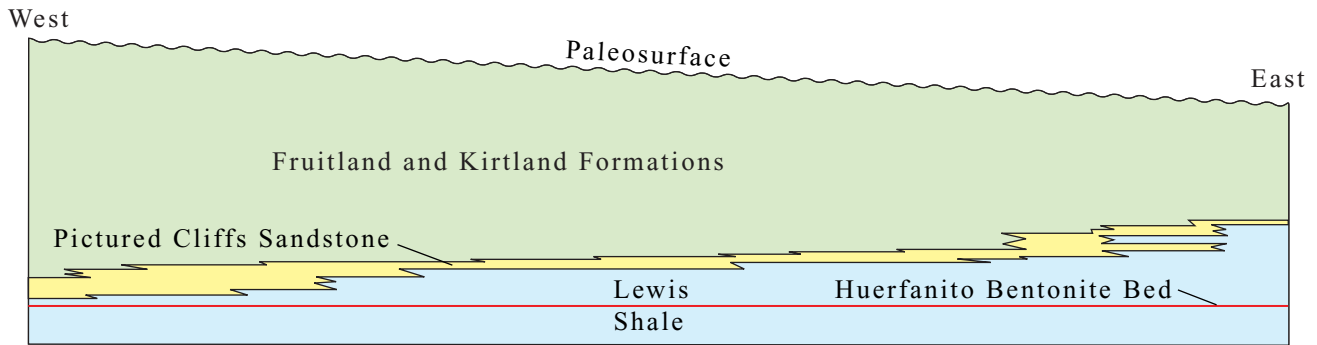


B - about 65 Ma, beginning of Paleocene

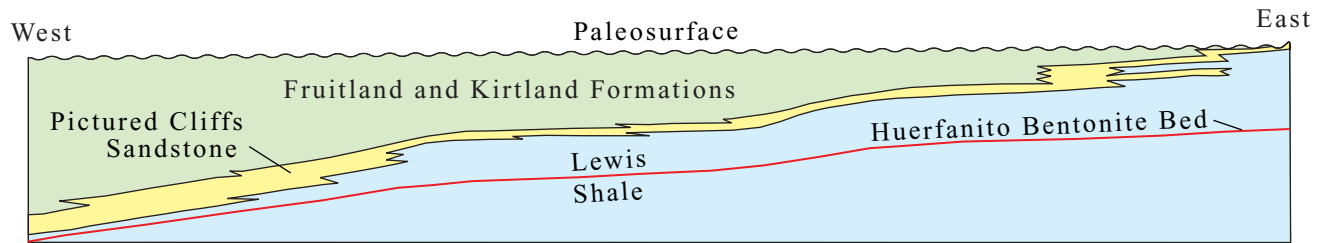


C - present

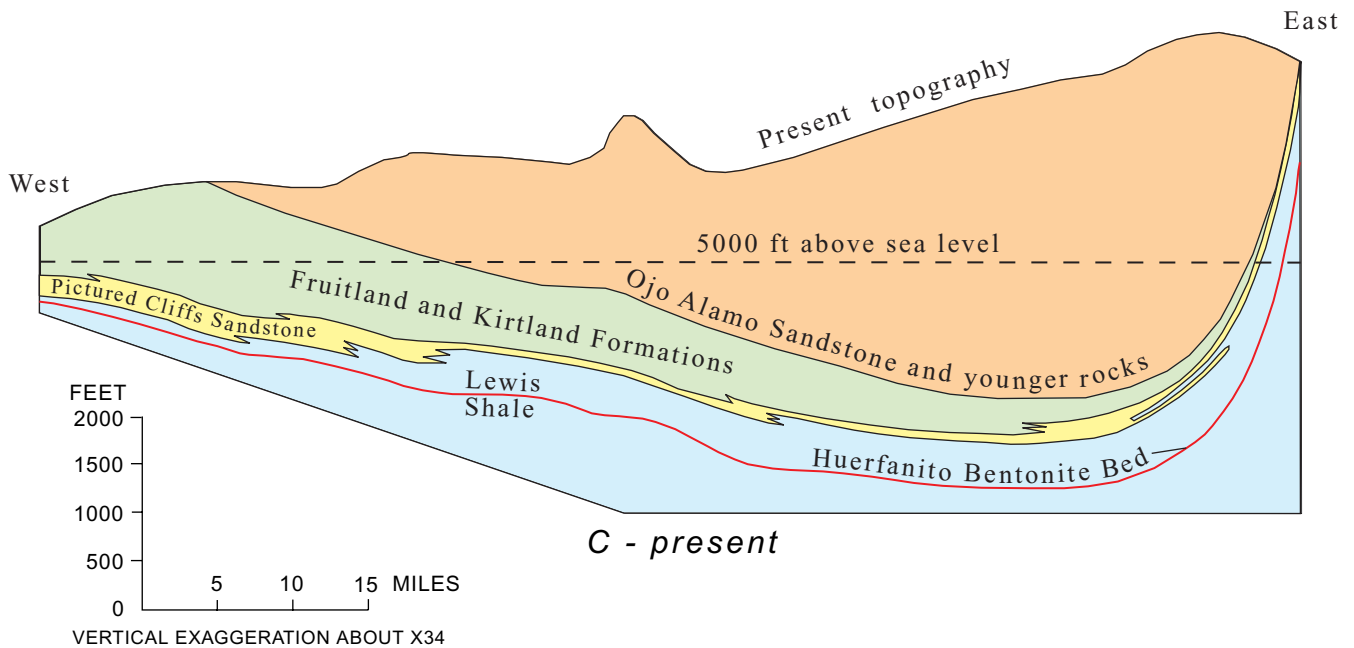
Figure A3-4. North-trending diagrammatic cross sections showing the structural evolution of the San Juan Basin from Late Cretaceous time to the present. *A*, shows the paleosurface at the time the Kirtland Formation was being deposited; datum is Huerfanito Bentonite Bed. *B*, shows an erosional paleosurface after the basin area was uplifted in the southeast and the Fruitland and Kirtland were beveled by erosion prior to deposition of the Ojo Alamo Sandstone; datum is paleosurface line. *C*, shows the present topography and structure of the basin; datum is mean sea level. Modified from figure 17 of Fassett and Hinds (1971).



A - about 71 Ma, end of Campanian



B - about 65 Ma, beginning of Paleocene



C - present

Figure A3-5. East-trending diagrammatic cross sections showing the structural evolution of the San Juan Basin from Late Cretaceous time to the present. *A*, shows the paleosurface at the time the Kirtland Formation was being deposited; datum is Huerfanito Bentonite Bed. *B*, shows an erosional paleosurface after the basin area was uplifted in the southeast and the Fruitland and Kirtland were beveled by erosion prior to deposition of the Ojo Alamo Sandstone; datum is paleosurface line. *C*, shows the present topography and structure of the basin; datum is mean sea level. Modified from figure 18 of Fassett and Hinds (1971).

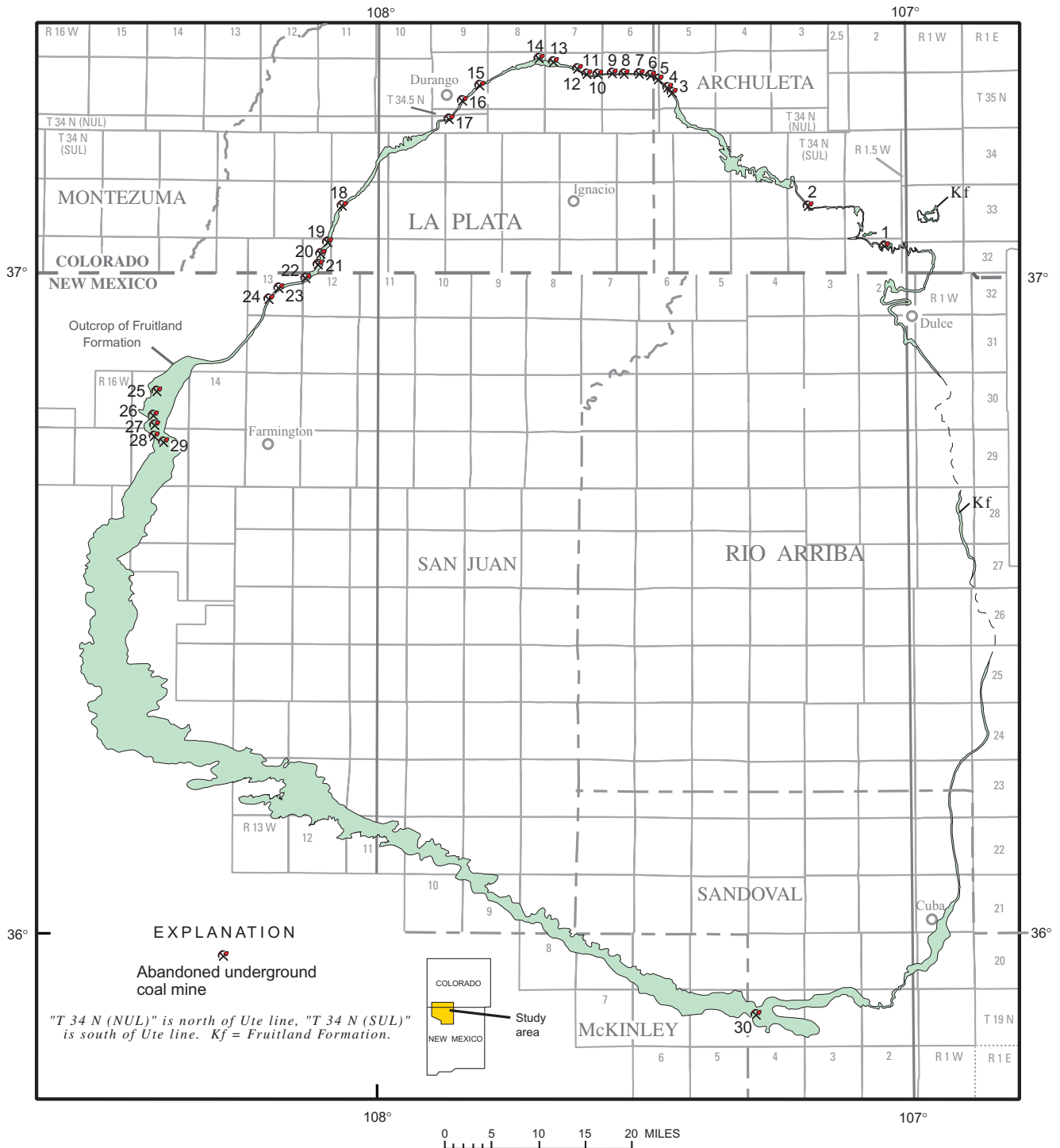


Figure A3-6. Map of San Juan Basin showing locations of small, underground, Fruitland Formation coal mines; all of these mines are now abandoned. Coal-mine numbers are keyed to table A3-1(below). Map is modified from figure 19 of Fassett and Hinds (1971).

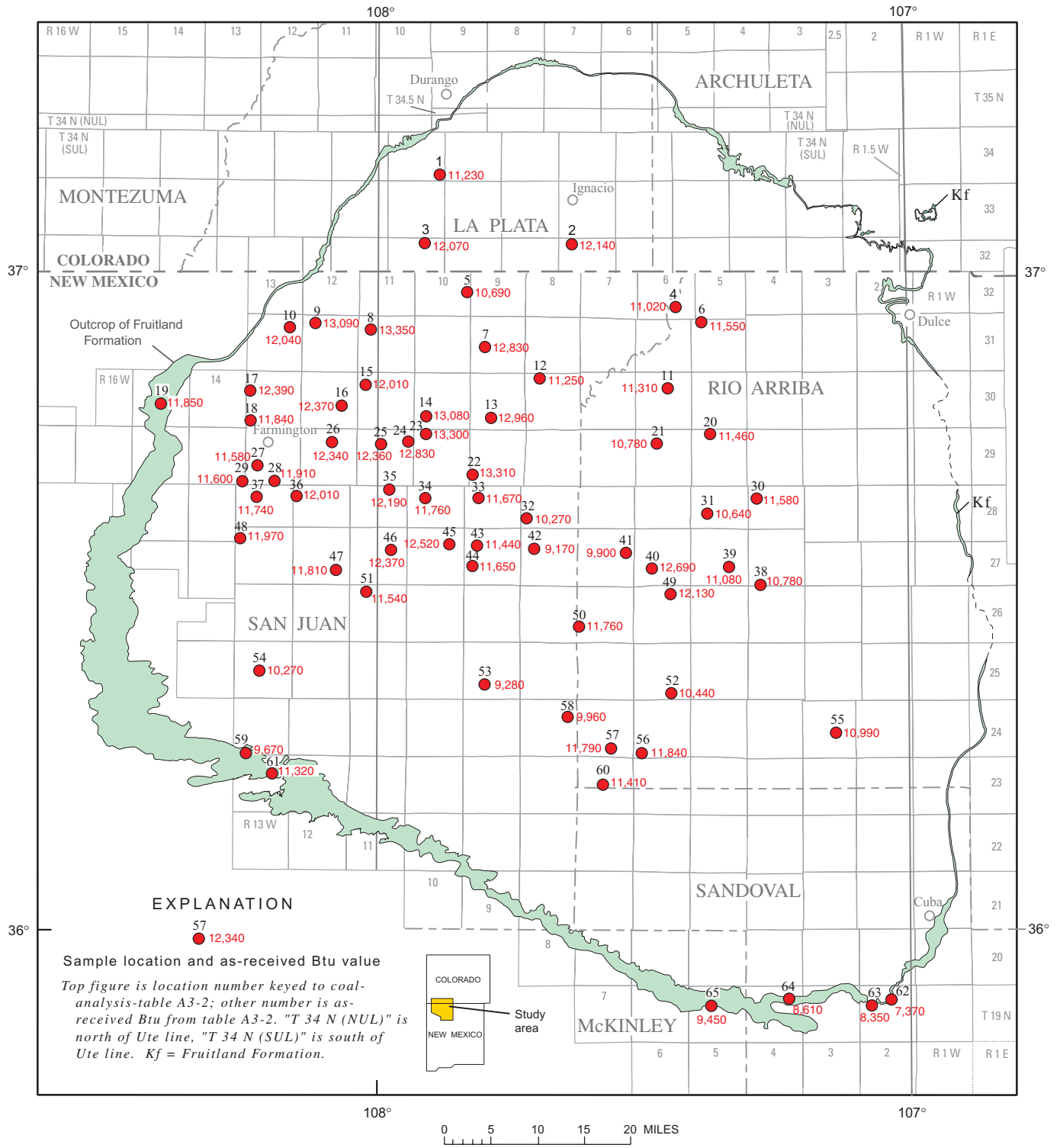


Figure A3-7. Map showing distribution of heating values (Btu) from analyses of Fruitland Formation coal beds in the San Juan Basin. Complete analyses are in table A3-2. Modified from figure 23 of Fassett and Hinds (1971).

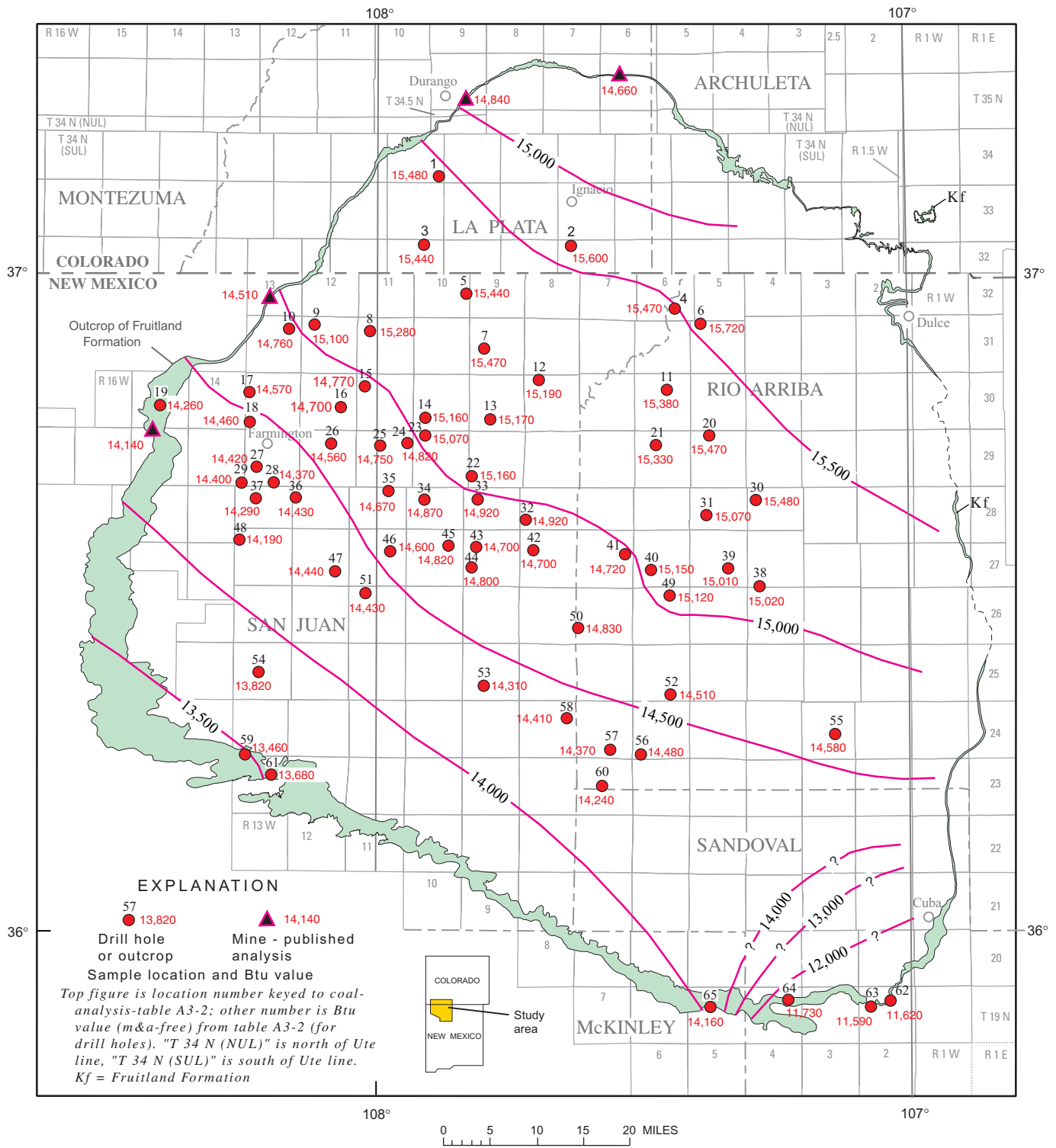


Figure A3-8. Map showing distribution of moisture-and-ash-free heating values (Btu) from analyses of Fruitland Formation coal beds in the San Juan Basin. Complete analyses are in table A3-2. Map is modified from figure 25 of Fassett and Hinds (1971). Contour interval is 500 Btu.

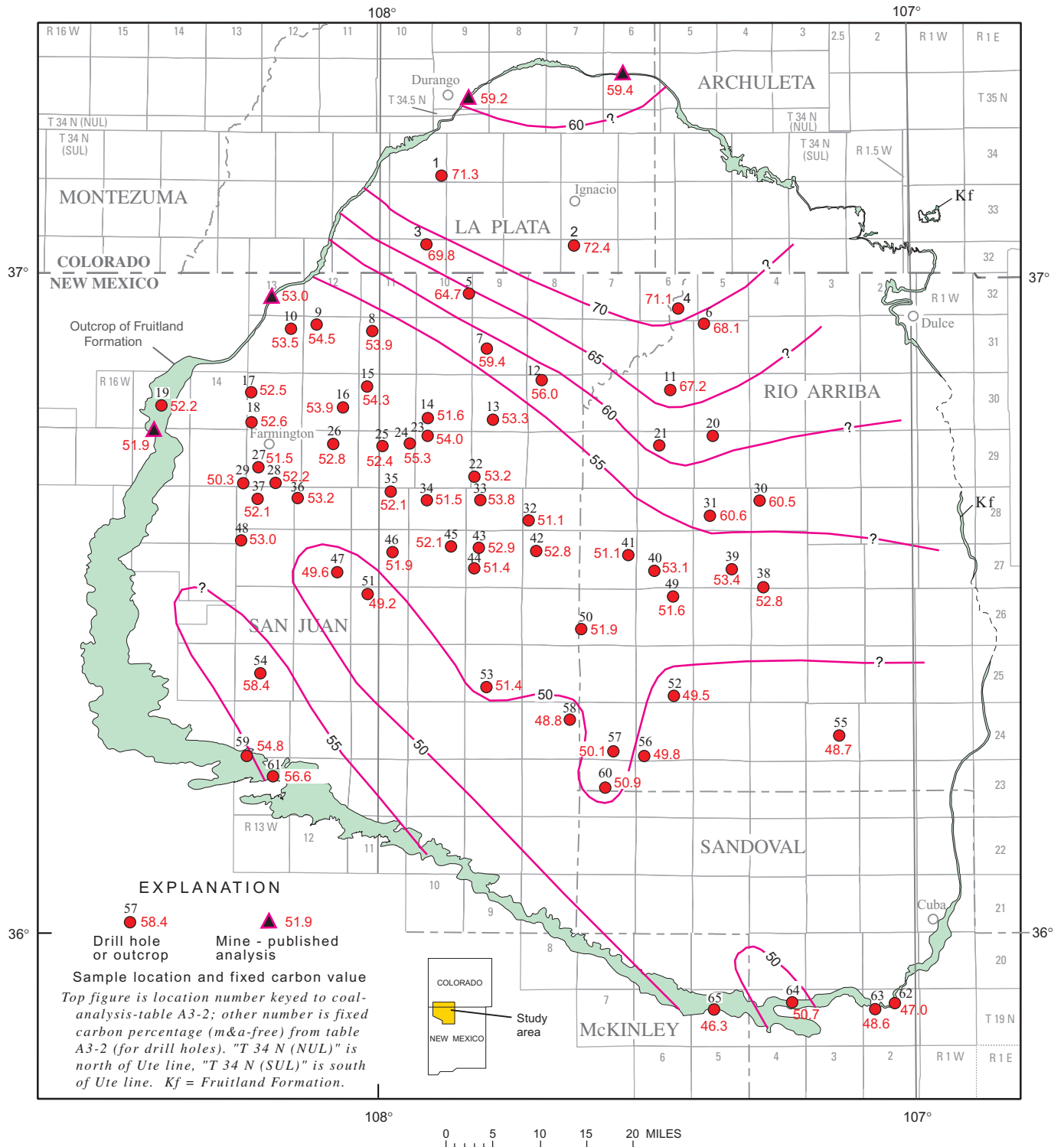


Figure A3-9. Map showing distribution of fixed-carbon values in percent for moisture-and-ash-free coal from analyses of Fruitland Formation coal beds in the San Juan Basin. Complete analyses are in table A3-2. Map is modified from figure 26 of Fassett and Hinds (1971). Contour interval is variable.

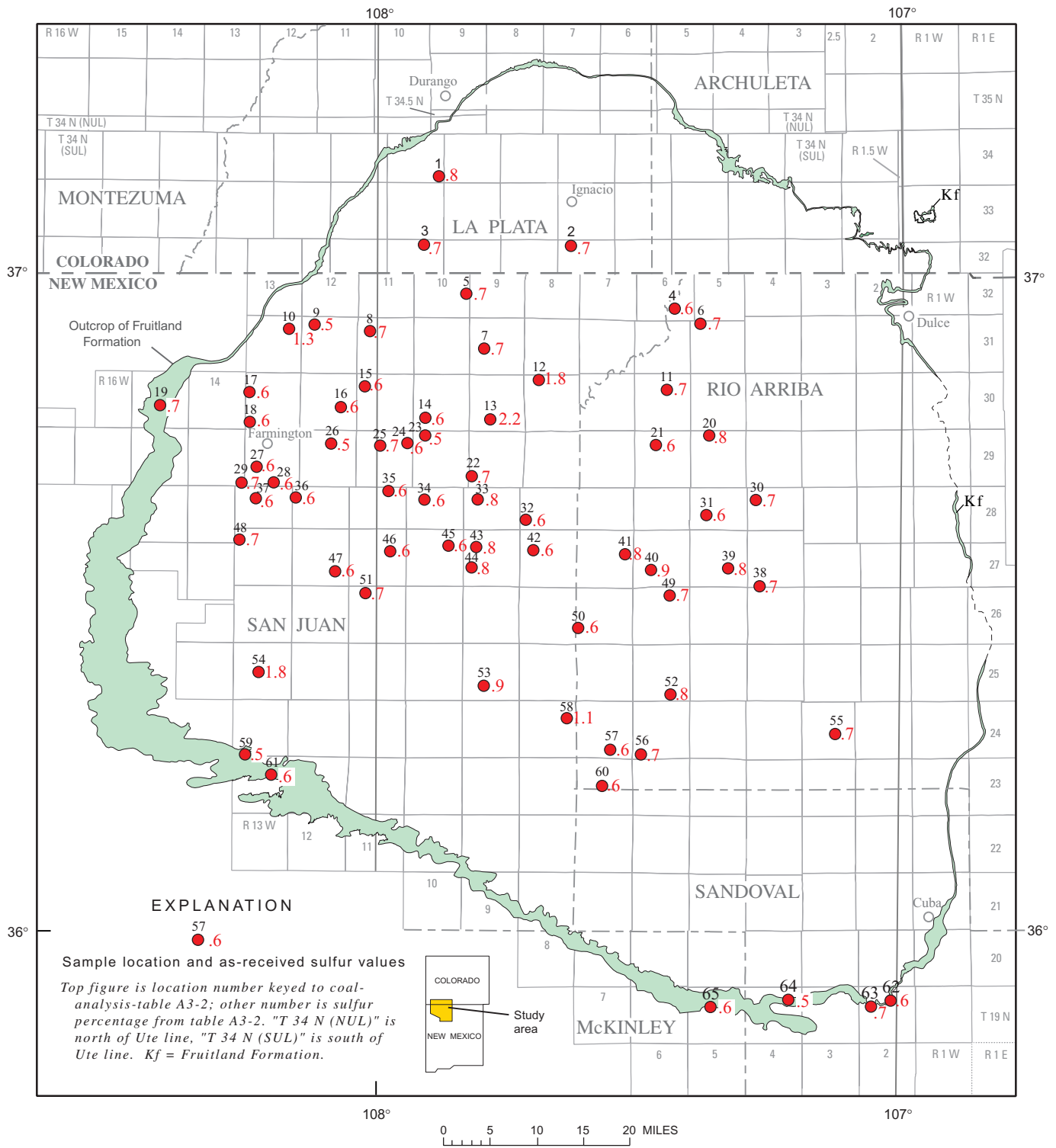


Figure A3-10. Map showing distribution of sulfur values from analyses of Fruitland Formation coal beds in the San Juan Basin. Complete analyses are in table A3-2.

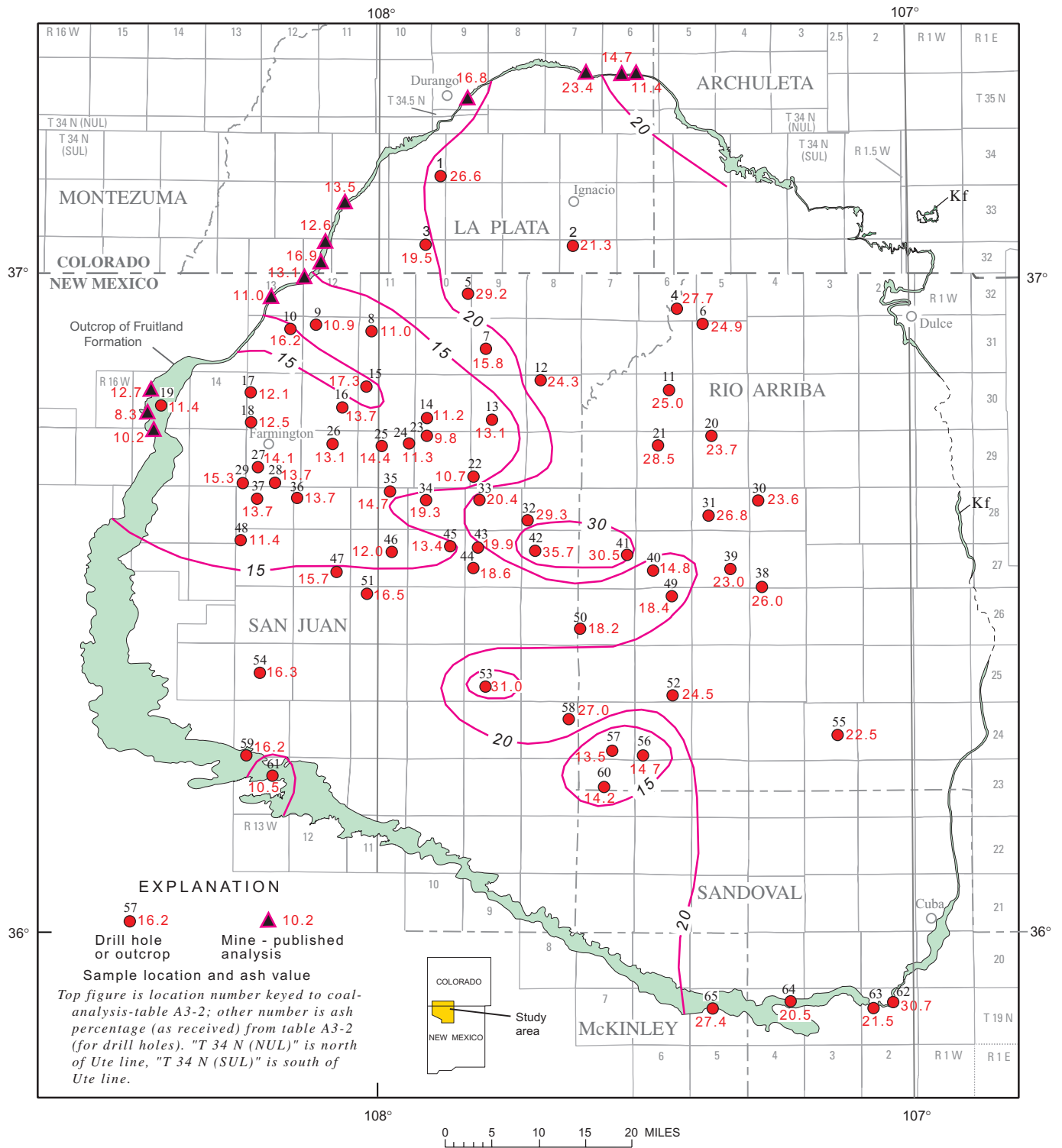


Figure A3-11. Map showing distribution of ash from analyses of Fruitland Formation coal beds in the San Juan Basin. Complete analyses are in table A3-2. Map is modified from figure 24 of Fassett and Hinds (1971). Contour interval is variable.

Table A3-1. Production and dates of operation of abandoned, underground Fruitland coal mines shown on figure A3-6.

[N.D.A., no data available. Modified from Fassett and Hinds (1971)]

Map no.	Name of mine	Period of operation	Production (short tons)	Map no.	Name of mine	Period of operation	Production (short tons)
1	Archuleta	N.D.A.	N.D.A.	16	La Plata	1893-1902	5,447
2	Talian	1913-1915	7,637	17	Unknown	N.D.A.	N.D.A.
3	Columbine	1938-1956	10,596	18	Mormon	N.D.A.	N.D.A.
4	Cooper	N.D.A.	N.D.A.	19	Fort Lewis	1943-1949	1,395
5	Triple S	1941-1951	5,348		Henderson	N.D.A.	N.D.A.
	Shamrock No. 1	1928-1936	3,916	20	Soda Spring	1928-1947	5,218
	Shamrock No. 2	1937-1941	2,398	21	Cinder Butte (Pruitt?)	N.D.A.	N.D.A.
6	Morning Glory	1930-1936	4,207	22	New Mexico (Kempton)	1928-1945	10,361
7	Palmer	N.D.A.	N.D.A.	23	Bill Thomas (Morgan)	1931-1947	7,521
8	Blue Jay	1935-1944	3,135	24	Jones	?-1918(?)	N.D.A.
9	Love	N.D.A.	N.D.A.	25	Prospect drift	N.D.A.	N.D.A.
10	Excelsior (3 shafts)	1927-1938	3,914	26	Marcelius (Caudell?)	1924-1938	10,318
11	Schutz (2 shafts)	N.D.A.	N.D.A.	27	Blanchard	N.D.A.	N.D.A.
12	Prospect pit	N.D.A.	N.D.A.	28	Black Diamond	1918-1933(?)	N.D.A.
13	Unknown	N.D.A.	N.D.A.		(Christenson), (3 mines?)	N.D.A.	N.D.A.
14	do	N.D.A.	N.D.A.	29	L. W. Hendrickson	1929-1930(?)	N.D.A.
15	do	N.D.A.	N.D.A.	30	Prospect drift	N.D.A.	N.D.A.

Table A3-2. Analyses of coal samples from the Fruitland Formation, San Juan Basin. (After table 4 of Fassett and Hinds, 1971.)

[Form of analyses: A, as-received; B, moisture free; C, moisture and ash free]

Locality number	USBM lab. no.	Well or source	Location			Approx. sample depth (ft)	Form of analysis	Proximate					Heating value (Btu)	Remarks
			Quarter section	T. N.	R. W.			Moisture	Volatile matter	Fixed carbon	Ash	Sulfur		
Colorado														
1	H-38041	El Paso Nat. Gas Bondad 34-10 No. 3X	36	34	10	2,406-2,438	A	0.9	20.8	51.7	26.6	0.8	11,230	
							B		21.0	52.2	26.8	0.8	11,330	
							C		28.7	71.3		1.1	15,480	
2	H-55350	Mobil Oil Schofield Auto 31X-5	NE 5	32	7	2,656-2,669	A	0.8	21.5	56.4	21.3	0.7	12,140	
							B		21.6	66.9	21.5	0.7	12,240	
							C		27.6	72.4		0.8	15,600	
3	H-46452	Atlantic Rein Southern Ute 32-10 No. 15-1	NE 4	15.32	10	2,825-2,890	A	2.3	23.6	54.6	19.6	0.7	12,070	
							B		24.2	55.9	19.9	0.7	12,360	
							C		30.2	69.8		0.9	15,440	
New Mexico														
4	H-33642	La Plata Gathering San Juan Unit 32-50 No. 2-27	SE 27	32	6	2,811-2,830	A	1.1	20.6	50.6	27.7	0.6	11,020	
							B		20.8	51.2	28.0	0.6	11,130	
							C		28.9	71.1		0.9	15,470	
5	H-55381	Delhi Taylor Wickens No.1	NE 24	32	10	3,370-3,400	A	1.6	24.4	44.9	29.2	0.7	10,690	
							B		24.8	45.5	29.7	0.7	10,860	
							C		35.3	64.7		1.0	15,440	
6	H-16696	El Paso Nat. Gas Rosa Unit No. 41	SW 5	31	5	3,124-3,136	A	1.6	23.5	50.0	24.9	0.7	11,550	
							B		23.8	50.9	25.3	0.7	11,740	
							C		31.9	68.1		1.0	15,720	
7	H-50012	Delhi Taylor Barrett No. 1	SW 20	31	9	3,230-3,255	A	1.3	33.7	49.2	15.8	0.7	12,830	
							B		34.1	49.9	16.0	0.7	13,000	
							C		40.6	59.4		0.9	15,470	
8	H-16777	El Paso Nat. Gas Case No.9	SW 8	31	11	2,710-2,740	A	1.7	40.3	47.0	11.0	0.7	13,350	
							B		41.0	47.9	11.1	0.7	13,580	
							C		46.1	53.9		0.8	15,280	
9	H-19884	Consolidated Oil & Gas Mitchell No.1-5	SW 5	31	12	2,215-3,000	A	2.4	39.4	47.3	10.9	0.5	13,090	
							B		40.4	48.5	11.1	0.5	13,410	
							C		45.5	54.5		0.6	15,100	
10	H-15141	Consolidated Oil & Gas Freeman No. 1-11	NE 11	31	13	1,776-1,782	A	2.3	37.9	43.6	16.2	1.3	12,040	
							B		38.8	44.7	16.5	1.3	12,320	
							C		46.5	53.5		1.6	14,760	
11	H-15142	El Paso Nat. Gas S.J.U. 30-6 No. 37	NE 10	30	6	3,100-3,105	A	1.5	24.1	49.4	25.0	0.7	11,310	
							B		24.5	50.1	25.4	0.7	11,480	
							C		32.8	67.2		0.0	15,380	
12	H-50079	Delhi Taylor Moore No.6	NE 5	30	8	2,800-3,028	A	1.7	32.6	41.4	24.3	1.8	11,250	
							B		33.2	42.1	24.7	1.8	11,440	
							C		44.0	56.0		2.4	15,190	

Table A3-2. Analyses of coal samples from the Fruitland Formation, San Juan Basin. (After table 4 of Fassett and Hinds, 1971)—*Continued.*

Locality number	USBM lab. no.	Well or source	Location			Approx. sample depth (ft)	Form of analysis	Proximate					Heating value (Btu)	Remarks
			Quarter section	T. N.	R. W.			Moisture	Volatile matter	Fixed carbon	Ash	Sulfur		
New Mexico—Continued														
13	H-35925	El Paso Nat. Gas Turner No.3	SE 28	30	9	2,385-2,390	A	1.5	39.9	45.5	13.1	2.2	12,960	
							B		40.5	46.2	13.3	2.2	13,150	
							C		46.7	53.3		2.5	15,170	
14(a)	H-19882	El Paso Nat. Gas Ludwick No. 20	SW 29	30	10	2,340-2,360	A	2.3	33.1	39.9	24.7	0.7	10,800	Uppermost of two samples from this location
							B		33.9	40.9	25.2	0.7	11,060	
							C		45.3	54.7		0.9	14,790	
14(b)	H-19883	El Paso Nat. Gas Ludwick No. 20	SW 29	30	10	2,505-2,515	A	2.6	41.7	44.5	11.2	0.6	13,080	Lowermost of two samples from this location
							B		42.9	45.6	11.5	0.6	13,420	
							C		48.4	51.6		0.7	15,160	
75	H-13062	Aztec Oil & Gas Ruby Jones No. 1	NE 7	30	11	2,020-2,030	A	1.4	37.2	44.1	17.3	0.6	12,010	
							B		37.7	44.8	17.5	0.6	12,180	
							C		45.7	54.3		0.7	14,770	
16	H-15140	Southwest Production Sullivan No. 1	NE 22	30	12	1,713-1,742	A	2.2	38.8	45.3	13.7	0.6	12,370	
							B		39.7	48.3	14.0	0.6	12,640	
							C		46.1	53.9		0.7	14,700	
17	H-16308	R & G Drilling Lunt No. 62	NW 18	30	13	1,425-1,440	A	2.8	40.4	44.7	12.1	0.6	12,390	
							B		41.6	45.9	12.5	0.6	12,750	
							C		47.5	52.5		0.7	14,570	
18	H-19399	Compass Exploration Federal No. 131-A	NE 31	30	13	1,070-1,080	A	5.7	38.8	43.0	12.5	0.6	11,840	
							B		41.2	45.5	13.3	0.6	12,540	
							C		47.4	52.6		0.7	14,460	
19	H-78945	N.M.P.S.C.C Core Hole No. 7	21	30	15	69-70	A	5.6	39.7	43.3	11.4	0.7	11,850	Sample of coal core, not floated, A is air-dried analysis
							B		42.0	46.0	12.0	0.7	12,540	
							C		47.8	52.2		0.8	14,260	
20	H-18102	El Paso Nat. Gas S.J. U. 295 No. 17	NE 5	29	5	3,175-3,200	A	2.2	29.3	44.8	23.7	0.8	11,460	
							B		30.0	45.8	24.2	0.8	11,720	
							C		39.5	60.5		1.1	15,470	
21	H-7560	El Paso Nat. Gas S.J. U. 29-6 No. 66	SW 9	29	6	3,575-3,580	A	1.2	27.7	42.6	28.5	0.6	10,780	
							B		28.0	43.1	28.9	0.6	10,910	
							C		39.4	60.6		0.8	15,330	
22	H-16310	Aztec Oil & Gas Cain No. 16-D	SW 30	29	9	1,985-2,005	A	1.6	41.1	46.6	10.7	0.7	13,310	
							B		41.7	47.5	10.8	0.7	13,520	
							C		46.8	53.3		0.7	15,160	
23(a)	H-27541	Aztec Oil & Gas Grenier "B" No. 3	SW 5	29	10	2,065-2,080	A	2.3	39.1	42.1	16.5	1.9	12,020	Uppermost of two samples from this location
							B		40.0	43.1	16.9	2.0	12,300	
							C		48.1	51.9		2.4	14,800	
23(b)	H-27540	Aztec Oil & Gas Grenier "B" No. 3	SW 5	29	10	2,150-2,160	A	2.0	40.6	47.6	9.8	0.5	13,300	Lowermost of two samples from this location
							B		41.4	48.6	10.0	0.5	13,560	
							C		46.0	54.0		0.6	15,070	

Table A3-2. Analyses of coal samples from the Fruitland Formation, San Juan Basin. (After table 4 of Fassett and Hinds, 1971)—*Continued.*

Locality number	USBM lab. no.	Well or source	Location			Approx. sample depth (ft)	Form of analysis	Proximate					Heating value (Btu)	Remarks
			Quarter section	T. N.	R. W.			Moisture	Volatile matter	Fixed carbon	Ash	Sulfur		
New Mexico—Continued														
24	H-13060	Tidewater N.M. Fed. No. 12-E	SE 12	29	11	2,065-2,070	A	2.1	38.7	47.9	11.3	0.6	12,830	
							B		39.5	48.9	11.6	0.6	13,100	
							C		44.7	55.3		0.7	14,820	
25	H-3028	International Oil Fogelson No. 1-9	NW 9	29	11	1,905-1,910	A	1.8	39.9	43.9	14.4	0.7	12,360	
							B		40.6	44.8	14.6	0.7	12,590	
							C		47.6	52.4		0.8	14,750	
26	H-3030	Tennessee Oil & Gas Cornell Gas Unit A No. 1	NW 10	29	12	1,740-1,750	A	2.1	40.0	44.8	13.1	0.5	12,340	
							B		40.9	45.7	13.4	0.5	12,600	
							C		47.2	52.8		0.6	14,560	
27	H-8360	Aztec Oil & Gas Hagood No. 21-G	SW 20	29	13	1,125-1,140	A	5.6	39.0	41.3	14.1	0.6	11,580	
							B		41.3	43.8	14.9	0.6	12,260	
							C		48.5	51.5		0.7	14,410	
28	H-4052	Aztec Oil & Gas Hagood No. 13-G	SE 34	29	13	1,635-1,640	A	3.5	39.6	43.2	13.7	0.5	11,910	
							B		41.0	44.8	14.2	0.6	12,330	
							C		47.8	51.2		0.6	14,370	
29	H-4051	Humble Oil & Gas Humble No. L-9	SE 36	29	14	1,490-1,495	A	4.1	40.0	40.6	15.3	0.7	11,600	
							B		41.7	42.3	16.0	0.7	12,100	
							C		49.7	50.3		0.9	14,400	
30	H-3855	El Paso Nat. Gas S.J.U. 28-4 No. 28	NE 19	28	4	4,115-1,120	A	1.6	31.1	43.7	23.6	0.7	11,580	
							B		31.6	44.4	24.0	0.7	11,770	
							C		41.6	58.4		0.9	15,480	
31	H-7224	El Paso Nat. Gas S.J.U. 28-5 No.50	SW 28	28	5	3,323-3,345	A	2.6	31.6	39.0	26.8	0.6	10,640	
							B		32.5	40.0	27.5	0.6	10,920	
							C		44.8	55.2		0.9	15,070	
32	H-13779	El Paso Nat. Gas Florence No. 10-C	NE 30	28	8	2,185-2,195	A	1.9	33.7	35.1	29.3	0.6	10,270	
							B		34.3	35.8	29.9	0.7	10,460	
							C		48.9	51.1		0.9	14,920	
33	H-13061	Aztec Oil & Gas Reid No. 23-D	SW 17	28	9	1,985-1,990	A	1.4	36.1	42.1	20.4	0.8	11,670	
							B		36.6	42.7	20.7	0.8	11,830	
							C		46.2	53.8		1.0	14,920	
34	H-5472	Aztec Oil & Gas Caine No.13	NW 16	28	10	1,842-1,853	A	1.6	38.4	40.7	19.3	0.6	11,760	
							B		39.0	41.4	19.6	0.6	11,950	
							C		48.5	51.5		0.8	14,870	
35	H-12704	Redfern & Herd Redfern & Herd No. 5	SW 10	28	11	1,490-1,500	A	2.1	39.8	43.4	14.7	0.6	12,190	
							B		40.7	44.3	15.0	0.6	12,460	
							C		47.9	52.1		0.7	14,670	
36	H-24567	Sunray Mid-Continent Gallegos No.122	NW 18	28	12	1,305-1,315	A	3.0	38.9	44.4	13.7	0.6	12,010	
							B		40.1	45.8	14.1	0.6	12,390	
							C		46.8	53.2		0.7	14,430	

Table A3-2. Analyses of coal samples from the Fruitland Formation, San Juan Basin. (After table 4 of Fassett and Hinds, 1971)—*Continued.*

Locality number	USBM lab. no.	Well or source	Location			Approx. sample depth (ft)	Form of analysis	Proximate					Heating value (Btu)	Remarks				
			Quarter section	T. N.	R. W.			Moisture	Volatile matter	Fixed carbon	Ash	Sulfur						
New Mexico—Continued																		
37	H-7225	Pan American Holder No. 7	NW 16	28	13	1,705-1,715	A	4.1	39.4	42.8	13.7	0.6	11,740					
							B							41.1	44.6	14.3	0.6	12,240
							C							47.9	52.1		0.7	14,290
38	H-18101	E1 Paso Nat. Gas S.J.U. 274 No. 30	SW 32	27	4	3,935-3,945	A	2.2	33.9	37.9	26.0	0.7	10,780					
							B							34.6	38.8	26.6	0.7	11,010
							C							47.2	52.8		0.9	15,020
39	H-33317	E Paso Nat. Gas S.J.U. 275 No. 74	SE 23	27	5	3,250-3,260	A	3.1	34.4	39.5	23.0	0.8	11,080					
							B							35.6	40.7	23.7	0.9	11,440
							C							46.6	53.4		1.1	15,010
40	H-33643	E1 Paso Nat. Gas Rincon Unit No. 171	SW 21	27	6	3,165-3,180	A	1.4	39.3	44.5	14.8	0.9	12,690					
							B							39.8	45.2	15.0	0.9	12,870
							C							46.9	53.1		1.1	15,150
41	H-35788	E1 Paso Nat. Gas Rincon Unit No. 177	SE 13	27	7	3,130-3,140	A	2.3	32.9	34.3	30.5	0.8	9,900					
							B							33.7	35.1	31.2	0.8	10,130
							C							48.9	51.1		1.2	14,720
42	H-21490	E1 Paso Nat. Gas Schwerdtfeger No. 20-A	NE 8	27	8	2,800-2,820	A	1.9	29.5	32.9	35.7	0.6	9,170					
							B							30.0	33.6	36.4	0.6	9,350
							C							47.2	52.8		1.0	14,700
43	H-12705	Aztec Oil & Gas Whitley No. 6-D	SW 8	27	9	2,215-2,230	A	2.2	36.7	41.2	19.9	0.8	11,440					
							B							37.5	42.1	20.4	0.8	11,700
							C							47.1	52.9		1.1	14,700
44	H-13063	Aztec Oil & Gas Hudson No. 5-D	NW 29	27	9	2,135-2,145	A	2.7	38.3	40.4	18.6	0.8	11,650					
							B							39.3	41.6	19.1	0.8	11,970
							C							48.6	51.4		1.0	14,800
45	H-15776	Aztec Oil & Gas Hanks No. 14-D	SW 12	27	10	1,900-1,905	A	2.2	40.4	44.0	13.4	0.6	12,520					
							B							41.3	45.1	13.6	0.6	12,790
							C							47.9	52.1		0.7	14,820
46	H-5021	British American Oil Fullerton No. 8	NE 14	27	11	1,920-1,930	A	3.3	40.8	43.9	12.0	0.6	12,370					
							B							42.2	45.4	12.4	0.6	12,790
							C							48.1	51.9		0.7	14,600
47	H-3031	Southwest Production Cambell No. 2	NE 26	27	12	1,900-1,910	A	2.6	41.2	40.5	15.7	0.6	11,810					
							B							42.3	41.6	16.1	0.6	12,120
							C							50.4	49.6		0.7	14,440
48	H-36175	Royal Development Ojo Amarillo No. 2	SW 6	27	13	1,214-1,245	A	4.3	39.7	44.6	11.4	0.7	11,970					
							B							41.4	46.7	11.9	0.7	12,500
							C							47.0	53.0		0.8	14,190
49	H-32698	Caulkins Oil State "A" MD No. 62	NE 12	26	6	3,184-3,200	A	1.3	38.9	41.4	18.4	0.7	12,130					
							B							39.4	41.9	18.7	0.7	12,290
							C							48.4	51.6		0.9	15,120

Table A3-2. Analyses of coal samples from the Fruitland Formation, San Juan Basin. (After table 4 of Fassett and Hinds, 1971)—*Continued.*

Locality number	USBM lab. no.	Well or source	Location			Approx. sample depth (ft)	Form of analysis	Proximate					Heating value (Btu)	Remarks
			Quarter section	T. N.	R. W.			Moisture	Volatile matter	Fixed carbon	Ash	Sulfur		
New Mexico—Continued														
50	H-5020	Kay Kimbell Leiberman No. 5	SW 19	26	7	2,105-2,150	A	2.5	38.1	41.2	18.2	0.6	11,760	
							B		39.1	42.2	18.7	0.6	12,060	
							C		48.1	51.9		0.8	14,830	
51	H-12706	Southwest Production Ted Henderson No. 1	NE 5	26	11	1,700-1,705	A	3.6	40.6	39.3	16.5	0.7	11,540	
							B		42.1	40.8	17.1	0.7	11,970	
							C		50.8	49.2		0.8	14,430	
52	H-37832	Merrion & Associates Federal No. 3-35	SW 35	25	6	2,455-2,465	A	3.6	36.3	35.6	24.5	0.8	10,440	
							B		37.7	36.9	25.4	0.8	10,830	
							C		50.5	49.5		1.1	14,510	
53	H-16695	Century Exploration Mobil Rudman No. 2	SW 21	25	9	1,620-1,625	A	4.2	31.5	33.3	31.0	0.9	9,280	
							B		32.8	34.8	32.4	0.9	9,680	
							C		48.6	51.4		1.4	14,310	
54	H-40806	Standard of Texas State No. 1	SW 16	25	13	1,156-1,208	A	9.5	30.9	43.3	16.3	1.8	10,270	Abnormal moisture may be due to inadequate drying of sample
							B		34.1	47.9	18.0	2.0	11,340	
							C		41.6	58.4		2.5	13,820	
55	H-32405	El Paso Nat. Gas Lindrith No. 42	NE 22	24	3	3,194-3,205	A	2.1	38.7	36.7	22.5	0.7	10,990	
							B		39.5	37.5	23.0	0.7	11,230	
							C		51.3	48.7		1.0	14,580	
56	H-22075	Val Reese & Assoc. Bobby "B" No. 2-31	NE 31	24	6	2,070-2,090	A	3.6	41.1	40.6	14.7	0.7	11,840	
							B		42.6	42.2	15.2	0.7	12,280	
							C		50.2	49.8		0.9	14,480	
57	H-31101	Val Reese & Assoc. Lybrook No. 7-27	NE 27	24	7	2,140-2,150	A	4.4	40.9	41.2	13.5	0.6	11,790	
							B		42.8	43.1	14.1	0.6	12,340	
							C		49.9	50.1		0.7	14,370	
58	H-5022	Dorfman Production Nancy Fed. No. 1	SE 12	24	8	2,525-2,535	A	3.9	35.4	33.7	27.0	1.1	9,960	
							B		36.8	35.1	28.1	1.1	10,370	
							C		51.2	48.8		1.5	14,410	
59	H-19885	N.M.P.S.C.C DH-32-1	NW 32	24	13	100-112	A	12.0	32.5	39.3	16.2	0.5	9,670	Coal core crushed and floated
							B		36.9	44.7	18.4	0.6	10,990	
							C		45.2	54.8		0.7	13,460	
60	H-16309	Val Reese & Assoc. Betty "B" No. 1-15	NW 15	23	7	2,180-2,195	A	5.7	39.3	40.8	14.2	0.6	11,410	
							B		41.7	43.3	15.0	0.7	12,100	
							C		49.1	50.9		0.8	14,240	
61	H-22722	N.M.P.S.C.C DH-3-2.	SW 3	23	13	42-44	A	6.7	35.9	46.9	10.5	0.6	11,320	Coal core not floated
							B		38.6	50.3	11.2	0.6	12,140	
							C		43.4	56.6		0.7	13,680	
62	I-2723	Fruitland outcrop	SW 3	19	2	Surface	A	5.9	33.6	29.8	30.7	0.6	7,370	Weathered coal from surface exposure.
							B		35.7	31.7	32.6	0.7	7,830	
							C		53.0	47.0		1.0	11,620	

Table A3-2. Analyses of coal samples from the Fruitland Formation, San Juan Basin. (After table 4 of Fassett and Hinds, 1971)—Continued.

Locality number	USBM lab. no.	Well or source	Location		Approx. sample depth (ft)	Form of analysis	Moisture			Proximate			Heating value (Btu)	Remarks
			Quarter section	T. N.			R. W.	Moisture	Volatile matter	Fixed carbon	Ash	Sulfur		
New Mexico—Continued														
63	I-2722	Fruitland outcrop	SE. 7	19	2	Surface	A	6.5	37.0	35.0	21.5	0.7	8,350	Weathered coal from surface
							B		39.6	37.4	23.0	0.7	8,930	exposure
							C		51.4	48.6		0.9	11,590	Weathered coal from surface
64	H-99246	Fruitland outcrop	NE 11	19	4	Surface	A	6.2	36.2	37.1	20.6	0.5	8,610	Weathered coal from surface
							B		38.6	39.6	21.8	0.5	9,170	exposure
							C		49.3	50.7		0.6	11,730	Sample from small prospect
65	I-53220	Pit sample	SE. 9	19	5	Surface	A	5.8	35.8	31.0	27.4	0.6	9,450	Sample from small prospect
							B		38.1	32.8	29.1	0.6	10,040	pit
							C		53.7	46.3		0.9	14,160	

Appendix 4—Table of Mean Vitrinite-Reflectance Values in Percent (R_m) for Fruitland Formation Coal Samples in the San Juan Basin

The data in this table were used to construct the thermal maturity map on figure 37. The database contains location and vitrinite-reflectance data, depths to samples, source of data, drill-hole names and elevations, and kinds of samples analyzed.

Table begins on next page.

Table A4-1. Mean vitrinite reflectance values (R_m) for coal samples from the Fruitland Formation.

[Sample localities shown on figure 37. NMBMMR, New Mexico Bureau of Mines and Mineral Resources; NA, not available]

Point ID	Well Name	Elev.	Depth	Sample	R_m (%)	Footage	Longitude	Latitude	Source	
New Mexico										
19-04-01-NE	NMBMMR coal test hole	6811	347	Core	0.39	NA	-107.20277	35.91229	Hoffman (1991)	
19-04-03-NE	NMBMMR coal test hole	6721	185	Core	0.42	NA	-107.24409	35.91044	Hoffman (1991)	
20-05-28-SW	NMBMMR coal test hole	6793	406	Core	0.47	NA	-107.37640	35.92853	Hoffman (1991)	
20-05-31-SW	NMBMMR coal test hole	6665	197	Core	0.45	NA	-107.41439	35.91421	Hoffman (1991)	
20-05-34-SW	NMBMMR coal test hole	6645	140	Core	0.42	NA	-107.35738	35.91601	Hoffman (1991)	
20-06-18-SW	NMBMMR coal test hole	6699	172	Core	0.47	NA	-107.51998	35.96116	Hoffman (1991)	
20-06-26-SW	NMBMMR coal test hole	6657	161	Core	0.46	NA	-107.44990	35.92983	Hoffman (1991)	
20-06-28-NW	NMBMMR coal test hole	6619	94	Core	0.51	NA	-107.48592	35.93641	Hoffman (1991)	
20-07-08-NW	NMBMMR coal test hole	6637	200	Core	0.45	NA	-107.60454	35.98371	Hoffman (1991)	
20-07-10-SE	NMBMMR coal test hole	6631	190	Core	0.44	NA	-107.55807	35.97343	Hoffman (1991)	
21-07-33-SW	NMBMMR coal test hole	6624	366	Core	0.43	NA	-107.58856	36.00572	Hoffman (1991)	
21-08-07-SW	NMBMMR coal test hole	6610	268	Core	0.44	NA	-107.72677	36.06377	Hoffman (1991)	
21-08-17-SW	NMBMMR coal test hole	6588	186	Core	0.46	NA	-107.70578	36.04771	Hoffman (1991)	
21-08-22-SE	NMBMMR coal test hole	6540	375	Core	0.45	NA	-107.66831	36.03134	Hoffman (1991)	
21-08-36-NW	NMBMMR coal test hole	6587	140	Core	0.42	NA	-107.64151	36.01228	Hoffman (1991)	
22-09-36-SW	NMBMMR coal test hole	6474	289	Core	0.49	NA	-107.74057	36.09576	Hoffman (1991)	
22-10-17-SE	NMBMMR coal test hole	6315	219	Core	0.49	NA	-107.91934	36.13936	Hoffman (1991)	
23-04-14-NE	Chase Oil Jicarilla Apache 47-34	7309	2845	Cuttings	0.51	310 FNL, 800 FEL	-107.21736	36.23052	Pawlewicz and others (1991)	
23-07-05-NW	Dugan-SAPP C 4	7087	2000	Cuttings	0.51	900 FNL, 1660 FWL	-107.59950	36.26120	Pawlewicz and others (1991)	
23-07-15-NW	BCO-Betty B 2	7294	1920	Cuttings	0.44	1850 FNL, 790 FWL	-107.56693	36.22940	Fassett and Nuccio (1990)	
23-07-16-SW	BCO-State J 4	7237	1820	Cuttings	0.49	1940 FNL, 2070 FWL	-107.58082	36.22924	Pawlewicz and others (1991)	
23-07-21-NE	BCO Fed B 7	NA	2110	Cuttings	0.47	790 FNL, 890 FEL	-107.57376	36.21767	Fassett and Nuccio (1990)	
23-07-29-NW	Yates Henry AGC Fed 1	6903	1534	Cuttings	0.46	860 FNL, 590 FWL	-107.60380	36.20261	Fassett and Nuccio (1990)	
23-09-24-NW	Yates Hurricane Federal 1	6758	1100	Cuttings	0.46	400 FNL, 900 FWL	-107.74529	36.21859	Fassett and Nuccio (1990)	
23-10-05-SE	Dugan Champ 5	6542	960	Cuttings	0.44	2150 FSL, 800 FEL	-107.91242	36.25423	Fassett and Nuccio (1990)	
23-11-01-NE	Dugan Flo-Jo 1	6555	990	Cuttings	0.47	660 FNL, 330 FEL	-107.94624	36.26057	Pawlewicz and others (1991)	
23-11-01-NW	Dugan Flo-Jo 2	6575	930	Cuttings	0.49	660 FNL, 1980 FWL	-107.95628	36.26086	Pawlewicz and others (1991)	
23-11-19-NE	NMBMMR coal test hole	6115	303	Core	0.47	NA	-108.03829	36.21821	Hoffman (1991)	
23-11-27-NE	NMBMMR coal test hole	6726	366	Core	0.42	NA	-107.98675	36.19881	Hoffman (1991)	
23-12-04-NW	NMBMMR coal test hole	6065	300	Core	0.42	NA	-108.12512	36.26250	Hoffman (1991)	
23-12-12-SW	NMBMMR coal test hole	6049	292	Core	0.46	NA	-108.06446	36.23563	Hoffman (1991)	
23-13-02-NW	NMBMMR coal test hole	6601	254	Core	0.46	NA	-108.19869	36.25712	Hoffman (1991)	
24-06-31-NW	BCO Federal Bobby B 3	6730	1826	Cuttings	0.48	1850 FNL, 930 FWL	-107.51465	36.27044	Pawlewicz and others (1991)	
24-09-32-SE	Yates Ristra AGW 1	6846	1145	Cuttings	0.45	2180 FSL, 2145 FEL	-107.80990	36.26932	Pawlewicz and others (1991)	
26-07-12-NE	UNOCAL Rincon Unit 270	6472	2740	Cuttings	0.59	1658 FNL, 2311 FEL	-107.52461	36.50216	Pawlewicz and others (1991)	
26-08-18-SW	Meridian Kah-Des-Pah 2	6193	1860	Cuttings	0.55	1430 FSL, 2210 FWL	-107.72382	36.48483	Pawlewicz and others (1991)	
27-06-16-NE	UNOCAL-Rincon Unit 257	6521	3180	Cuttings	0.61	2223 FNL, 1835 FEL	-107.46922	36.57527	Pawlewicz and others (1991)	
27-06-18-NE	UNOCAL-Rincon Unit 252	6545	3190	Cuttings	0.63	1640 FNL, 1605 FEL	-107.50418	36.57634	Pawlewicz and others (1991)	
27-06-18-SW	UNOCAL-Rincon Unit 239	6660	3101	Cuttings	0.65	1810 FSL, 1645 FWL	-107.51003	36.57211	Fassett and Nuccio (1990)	

Table A4-1. Mean vitrinite reflectance values (R_m) for coal samples from the Fruitland Formation—*Continued*.

Point ID	Well Name	Elev.	Depth	Sample	R_m (%)	Footage	Longitude	Latitude	Source	
New Mexico—Continued										
27-06-20-SW	UNOCAL-Rincon Unit 255	6490	3020	Cuttings	0.60	1185 FSL, 1840 FWL	-107.49297	36.55515	Pawlewicz and others (1991)	
27-06-21-SW	UNOCAL-Rincon Unit 240	6623	3190	Cuttings	0.64	1500 FSL, 1750 FWL	-107.47519	36.55666	Fassett and Nuccio (1990)	
27-06-22-SW	UNOCAL-Rincon Unit 241	6532	3135	Cuttings	0.61	1500 FSL, 990 FWL	-107.45975	36.55680	Fassett and Nuccio (1990)	
27-06-23-SW	UNOCAL-Rincon Unit 242	6622	3230	Cuttings	0.68	790 FSL, 1810 FWL	-107.43904	36.55509	Fassett and Nuccio (1990)	
27-07-13-NE	UNOCAL-Rincon Unit 276	6636	3200	Cuttings	0.68	1080 FNL, 1240 FEL	-107.51974	36.57851	Pawlewicz and others (1991)	
27-07-14-SW	Rincon Unit 279	6734	3231	Cuttings	0.60	1735 FSL, 1456 FWL	-107.54687	36.57227	Pawlewicz and others (1991)	
27-07-23-NE	UNOCAL-Rincon Unit 281	6628	3100	Cuttings	0.61	880 FNL, 830 FEL	-107.53824	36.56542	Pawlewicz and others (1991)	
27-07-27-SW	UNOCAL-Rincon Unit 287	6653	2900	Cuttings	0.62	1056 FSL, 1088 FWL	-107.56688	36.53988	Pawlewicz and others (1991)	
27-09-04-NE	Meridian Turner Hughes 272	6864	2940	Cuttings	0.61	790 FNL, 1330 FEL	-107.78506	36.60831	Pawlewicz and others (1991)	
27-09-19-SW	UNOCAL Lodewick 13	6505	2280	Cuttings	0.58	975 FSL, 1665 FWL	-107.83143	36.55602	Pawlewicz and others (1991)	
27-09-21-NE	Meridian Cleveland 220	6218	2060	Cuttings	0.61	850 FNL, 1470 FEL	-107.78872	36.56531	Pawlewicz and others (1991)	
27-10-11-SW	McKenzie Angel Peak 11K 2	6258	2135	Cuttings	0.60	1350 FSL, 1360 FWL	-107.86850	36.58603	Pawlewicz and others (1991)	
27-10-13-SW	McKenzie Angel Peak 13M 1	6140	1886	Cuttings	0.60	900 FSL, 1190 FWL	-107.85083	36.57020	Pawlewicz and others (1991)	
27-10-15-SW	McKenzie Angel Peak 15M 7	6121	1865	Cuttings	0.57	940 FSL, 800 FWL	-107.88814	36.57041	Pawlewicz and others (1991)	
27-10-17-SW	Meridian Rowley 155	6152	1916	Cuttings	0.53	1420 FSL, 1850 FWL	-107.92053	36.57196	Pawlewicz and others (1991)	
27-10-22-NE	Meridian Gordon 500	6189	2020	Cuttings	0.59	2500 FNL, 1400 FEL	-107.87777	36.56077	Pawlewicz and others (1991)	
27-11-16-SW	Marathon Schwerdtfeger 15C	6266	1938	Cuttings	0.53	1600 FSL, 1355 FWL	-108.01290	36.57233	Fassett and Nuccio (1990)	
28-04-18-SW	Meridian SJ 28-4 Unit 202	7533	4475	Cuttings	0.64	1450 FSL, 1030 FWL	-107.29613	36.65783	Pawlewicz and others (1991)	
28-05-15-NE	Meridian-SJ 28-5 Unit201	6717	3546	Cuttings	0.77	1040 FNL, 1100 FEL	-107.34083	36.66545	Fassett and Nuccio (1990)	
28-05-16-NE	Meridian-SJ 28-5 U 202	6605	3500	Cuttings	0.71	1850 FNL, 790 FEL	-107.35772	36.66329	Pawlewicz and others (1991)	
28-05-17-NE	Meridian-SJ 28-5 Unit203	6589	3440	Cuttings	0.75	1280 FNL, 1725 FEL	-107.37887	36.66487	Fassett and Nuccio (1990)	
28-05-18-NE	Meridian-SJ 28-5 U 204	6719	3587	Cuttings	0.75	790 FNL, 1185 FEL	-107.39493	36.66610	Pawlewicz and others (1991)	
28-06-10-SW	Meridian-SJ 28-5 U 401	6495	3345	Cuttings	0.67	1095 FSL, 2225 FWL	-107.45538	36.67166	Pawlewicz and others (1991)	
28-06-12-SW	Meridian-SJ 28-5 U 403	6498	3777	Cuttings	0.76	1540 FSL, 1980 FWL	-107.42010	36.67279	Fassett and Nuccio (1990)	
28-06-19-SW	Meridian-SJ 28-5 U 406	6625	3339	Cuttings	0.69	680 FSL, 1140 FWL	-107.51079	36.64137	Fassett and Nuccio (1990)	
28-08-12-SW	Meridian-Hardie D 800	6437	3010	Cuttings	0.68	790 FSL, 1850 FWL	-107.63452	36.67060	Pawlewicz and others (1991)	
28-08-26-NE	Meridian-Howell 800	5887	2300	Cuttings	0.65	1340 FNL, 1685 FEL	-107.64659	36.63538	Pawlewicz and others (1991)	
28-09-26-SW	Meridian Lackey "H" 709	5981	2170	Cuttings	0.62	790 FSL, 1450 FWL	-107.76138	36.62797	Pawlewicz and others (1991)	
28-09-30-SW	Meridian Hancock 713	6265	2362	Cuttings	0.62	980 FSL, 1920 FWL	-107.83070	36.62838	Pawlewicz and others (1991)	
28-10-25-SW	Meridian Omler 500	5838	1880	Cuttings	0.61	2335 FSL, 790 FWL	-107.85061	36.62969	Pawlewicz and others (1991)	
28-10-36-SW	Meridian Omler 501	5903	1922	Cuttings	0.61	1670 FSL, 1920 FWL	-107.85097	36.61565	Pawlewicz and others (1991)	
29-07-05-NE	Meridian-SJ 29-7 U 505	6151	2910	Cuttings	0.73	1050 FNL, 1690 FEL	-107.59084	36.75885	Pawlewicz and others (1991)	
29-07-16-NE	Meridian-SJ 29-7 U 509	6266	3030	Cuttings	0.73	795 FNL, 1090 FEL	-107.57069	36.73088	Pawlewicz and others (1991)	
29-07-18-SW	Meridian-SJ 29-7 U 511	6929	3624	Cuttings	0.64	910 FSL, 1055 FWL	-107.61478	36.72128	Pawlewicz and others (1991)	
29-07-19-NE	Meridian-SJ 29-7 U 512	6686	3370	Cuttings	0.74	1460 FNL, 2365 FEL	-107.61080	36.71458	Pawlewicz and others (1991)	
29-07-30-NW	Meridian-SJ 29-7 Unit513	6347	2930	Cuttings	0.70	790 FNL, 1450 FWL	-107.61362	36.70216	Fassett and Nuccio (1990)	
29-07-33-SE	Meridian-SJ 29-7 U 514	6240	2948	Cuttings	0.73	1190 FSL, 1655 FEL	-107.57216	36.67810	Pawlewicz and others (1991)	
29-07-36-NE	Meridian-SJ 29-7 U 515	6543	3198	Cuttings	0.71	1755 FNL, 1055 FEL	-107.51640	36.68456	Pawlewicz and others (1991)	
29-07-36-SW	Meridian-SJ 29-7 U 516	6833	3622	Cuttings	0.66	1720 FSL, 1540 FWL	-107.52566	36.67965	Pawlewicz and others (1991)	
29-08-01-NE	Meridian Howell "C" 200	6080	2790	Cuttings	0.79	800 FNL, 1350 FEL	-107.62285	36.75907	Pawlewicz and others (1991)	
29-08-02-NE	Meridian State Com 100	6296	3009	Cuttings	0.72	1300 FNL, 890 FEL	-107.63833	36.75673	Pawlewicz and others (1991)	

Table A4-1. Mean vitrinite reflectance values (R_m) for coal samples from the Fruitland Formation—*Continued*.

Point ID	Well Name	Elev.	Depth	Sample	R_m (%)	Footage	Longitude	Latitude	Source	
New Mexico—Continued										
29-08-05-NE	Meridian Sunray 210	6269	2850	Cuttings	0.73	1120 FNL, 1450 FEL	-107.69344	36.75792	Pawlewicz and others (1991)	
29-08-07-NE	Amoco Day B 12	6208	2836	Cuttings	0.72	1380 FNL, 1190 FEL	-107.72377	36.75651	Pawlewicz and others (1991)	
29-08-09-NW	Meridian Day Com 200	6468	3230	Cuttings	0.71	880 FNL, 790 FWL	-107.68555	36.74411	Pawlewicz and others (1991)	
29-08-10-SW	Meridian Roelofs "A" 200	6328	3000	Cuttings	0.66	790 FSL, 1655 FWL	-107.66526	36.73463	Pawlewicz and others (1991)	
29-08-12-SW	Meridian Vanderwart 200	6346	3020	Cuttings	0.73	790 FNL, 1155 FWL	-107.63160	36.73438	Pawlewicz and others (1991)	
29-08-14-NW	Meridian Roelofs "A" Com 201	6328	3016	Cuttings	0.69	790 FNL, 1090 FWL	-107.64957	36.72984	Pawlewicz and others (1991)	
29-08-17-SW	Meridian Day 201	6413	3020	Cuttings	0.68	1425 FSL, 1425 FWL	-107.70166	36.72181	Pawlewicz and others (1991)	
29-08-24-NW	Meridian Hardie "A" Com 210	6613	3228	Cuttings	0.72	1810 FNL, 1660 FWL	-107.73422	36.71298	Pawlewicz and others (1991)	
29-08-26-NW	Meridian Hardie "A" 211	6361	2960	Cuttings	0.68	790 FNL, 1840 FWL	-107.75296	36.70147	Pawlewicz and others (1991)	
29-09-01-NE	Meridian Riddle "A" 717	6394	2960	Cuttings	0.66	1560 FNL, 1545 FEL	-107.72494	36.75568	Pawlewicz and others (1991)	
29-09-13-NE	Meridian Feuille 718	6420	2860	Cuttings	0.66	920 FNL, 1145 FEL	-107.72551	36.72938	Pawlewicz and others (1991)	
29-09-14-SE	Amoco Shane Gas Com-A	6405	2959	Cuttings	0.70	1790 FSL, 1030 FEL	-107.74317	36.72282	Amoco	
29-09-21-SW	D.J. Simmons A. B. Geren No. 1	5624	2042	Cuttings	0.65	475 FSL, 1060 FWL	-107.78783	36.70486	Fassett and Nuccio (1990)	
29-09-22-SW	Meridian Grambling 720	5665	2106	Cuttings	0.67	1330 FSL, 1270 FWL	-107.77008	36.70736	Fassett and Nuccio (1990)	
29-09-23-SW	D.J. Simmons A. B. Geren No. 2	5903	2393	Cuttings	0.68	1505 FSL, 1755 FWL	-107.75027	36.70777	Fassett and Nuccio (1990)	
29-09-28-NE	Meridian Grambling 722	5627	1957	Cuttings	0.65	790 FNL, 1830 FEL	-107.78074	36.70149	Pawlewicz and others (1991)	
29-09-29-NE	D.J. Simmons A. B. Geren No. 6	5824	2195	Cuttings	0.66	965 FNL, 1690 FEL	-107.80575	36.69181	Fassett and Nuccio (1990)	
29-10-08-NE	Meridian Nye 290	5791	2161	Cuttings	0.64	790 FNL, 805 FEL	-107.90162	36.74498	Pawlewicz and others (1991)	
29-10-12-NE	Meridian Lackey "A" 292	5710	2060	Cuttings	0.64	1795 FNL, 1490 FEL	-107.83169	36.74160	Pawlewicz and others (1991)	
29-10-20-NE	Meridian Hubbell Com 296	5589	1740	Cuttings	0.62	1310 FNL, 2270 FEL	-107.90642	36.71467	Pawlewicz and others (1991)	
29-10-23-SW	Union Texas Albright 19	5595	1770	Cuttings	0.58	1010 FSL, 800 FWL	-107.85974	36.70744	Pawlewicz and others (1991)	
29-10-27-NE	Union Texas Albright 20	5502	1680	Cuttings	0.59	2205 FNL, 825 FEL	-107.86530	36.69840	Pawlewicz and others (1991)	
29-11-01-SW	Meridian Lloyd "B" 600	5865	2050	Cuttings	0.57	1450 FSL, 1085 FWL	-107.94744	36.75160	Pawlewicz and others (1991)	
29-11-05-NE	Fifield Com 800	5776	1800	Cuttings	0.62	1600 FNL, 790 FEL	-108.00810	36.75700	Pawlewicz and others (1991)	
29-11-27-NW	Manana Marian S 1	5421	1585	Cuttings	0.59	1547 FNL, 1583 FWL	-107.98192	36.69975	Fassett and Nuccio (1990)	
30-04-20-NE	Meridian-SJ 30-4 U 101	7556	4230	Cuttings	0.82	790 FNL, 1495 FEL	-107.27355	36.80200	Pawlewicz and others (1991)	
30-06-07-NE	Meridian-SJ 30-6 U 451	6282	1110	Cuttings	0.88	1515 FNL, 960 FEL	-107.49797	36.83018	Pawlewicz and others (1991)	
30-06-07-SW	Meridian-SJ 30-6 U 450	6365	3260	Cuttings	0.94	1530 FSL, 1830 FWL	-107.50644	36.82428	Pawlewicz and others (1991)	
30-06-08-NE	Meridian-SJ 30-6 U 430	6273	3080	Cuttings	0.93	2235 FNL, 1605 FEL	-107.48205	36.82805	Pawlewicz and others (1991)	
30-06-08-SW	San Juan 30-6 Unit 459	NA	3160	Cuttings	0.96	1490 FSL, 1188 FWL	-107.49056	36.82399	Pawlewicz and others (1991)	
30-06-10-NE	Meridian-SJ 30-6 U 432	6299	3085	Cuttings	0.95	800 FNL, 1840 FEL	-107.44658	36.83191	Pawlewicz and others (1991)	
30-06-11-NE	Meridian-SJ 30-6 U 437	6304	3090	Cuttings	10.30	1670 FSL, 845 FEL	-107.42525	36.82962	Pawlewicz and others (1991)	
30-06-11-SW	Meridian-SJ 30-7 U 433	6136	2850	Cuttings	0.94	1820 FSL, 1175 FWL	-107.43639	36.82474	Pawlewicz and others (1991)	
30-06-12-NE	Meridian-SJ 30-6 U 438	6220	3029	Cuttings	1.01	2045 FNL, 1015 FEL	-107.41027	36.82869	Pawlewicz and others (1991)	
30-06-12-SW	Meridian-SJ 30-6 U 434	6200	2980	Cuttings	0.88	900 FSL, 790 FWL	-107.41964	36.82233	Pawlewicz and others (1991)	
30-06-13-SW	Meridian-SJ 30-6 U 445	6164	2964	Cuttings	0.97	1450 FSL, 1025 FWL	-107.41890	36.80925	Pawlewicz and others (1991)	
30-06-14-NE	Meridian-SJ 30-6 U 442	6349	3152	Cuttings	1.02	790 FNL, 850 FEL	-107.42530	36.81758	Pawlewicz and others (1991)	
30-06-14-SW	Meridian-SJ 30-6 U 439	6377	3180	Cuttings	0.96	900 FSL, 975 FWL	-107.43709	36.80779	Pawlewicz and others (1991)	
30-06-15-NE	Meridian-SJ 30-6 U 436	6210	3020	Cuttings	0.93	1840 FNL, 1560 FEL	-107.44575	36.81459	Pawlewicz and others (1991)	
30-06-16-NE	Meridian-SJ 30-6 U 407	6302	3092	Cuttings	0.97	1540 FNL, 1175 FEL	-107.46268	36.81560	Fassett and Nuccio (1990)	
30-06-16-SW	Meridian-SJ 30-6 U 408	6560	3360	Cuttings	0.92	1660 FSL, 1275 FWL	-107.47213	36.81002	Pawlewicz and others (1991)	

Table A4-1. Mean vitrinite reflectance values (R_m) for coal samples from the Fruitland Formation—*Continued*.

Point ID	Well Name	Elev.	Depth	Sample	R_m (%)	Footage	Longitude	Latitude	Source	
New Mexico—Continued										
30-06-17-NE	Meridian-SJ 30-6 U 454	6293	3129	Cuttings	0.96	1190 FNL, 1090 FEL	-107.48030	36.81654	Pawlewicz and others (1991)	
30-06-17-SW	Meridian-SJ 30-6 U 453	6668	3590	Cuttings	0.96	1450 FSL, 1635 FWL	-107.48895	36.80957	Pawlewicz and others (1991)	
30-06-18-NE	Meridian-SJ 30-6 U 456	6394	3330	Cuttings	0.98	565 FNL, 735 FEL	-107.49723	36.81832	Pawlewicz and others (1991)	
30-06-18-SW	Meridian-SJ 30-6 U 455	6641	3470	Cuttings	0.94	1080 FSL, 1510 FWL	-107.50770	36.80849	Pawlewicz and others (1991)	
30-06-19-NE	Meridian-SJ 30-6 U 458	6370	3190	Cuttings	0.87	1470 FNL, 1180 FEL	-107.49869	36.80137	Pawlewicz and others (1991)	
30-06-19-SW	Meridian-SJ 30-6 U 457	6210	3010	Cuttings	0.94	915 FSL, 1170 FWL	-107.50877	36.79335	Pawlewicz and others (1991)	
30-06-21-NE	Meridian-SJ 30-6 U 470	6440	3350	Cuttings	0.93	1580 FNL, 1330 FEL	-107.46318	36.80096	Pawlewicz and others (1991)	
30-06-21-SW	San Juan 30-6 Unit 471	6330	2550	Cuttings	0.95	1820 FSL, 1430 FWL	-107.47160	36.79592	Pawlewicz and others (1991)	
30-06-22-NE	Meridian-SJ 30-6 U 472	6453	3240	Cuttings	0.96	790 FNL, 1305 FEL	-107.44499	36.80300	Pawlewicz and others (1991)	
30-06-22-SW	Meridian-SJ 30-6 U 473	6415	3210	Cuttings	0.91	1140 FSL, 960 FWL	-107.45534	36.79399	Pawlewicz and others (1991)	
30-06-26-NE	Meridian-SJ 30-6 U 410	6683	3490	Cuttings	0.95	1220 FNL, 910 FEL	-107.42573	36.78713	Pawlewicz and others (1991)	
30-06-27-NE	Meridian-SJ 30-6 U 474	6484	3325	Cuttings	0.90	1230 FNL, 1660 FEL	-107.44613	36.78722	Pawlewicz and others (1991)	
30-06-28-SW	Meridian-SJ 30-6 U 477	6286	3110	Cuttings	0.89	1230 FSL, 790 FWL	-107.47393	36.77974	Pawlewicz and others (1991)	
30-06-30-NE	Meridian-SJ 30-6 U 480	6270	3127	Cuttings	0.92	790 FNL, 1305 FEL	-107.49923	36.78851	Pawlewicz and others (1991)	
30-06-34-NE	Meridian-SJ 30-6 U 483	6512	3449	Cuttings	0.99	1330 FNL, 790 FEL	-107.44323	36.77243	Pawlewicz and others (1991)	
30-06-36-SW	Meridian-SJ 30-6 U 444	6543	3470	Cuttings	0.89	1450 FSL, 790 FWL	-107.42001	36.76565	Pawlewicz and others (1991)	
30-07-02-NE	Blackwood/Nichols NE Blanco 415	6407	3205	Cuttings	0.90	1540 FNL, 1480 FEL	-107.53581	36.84452	Pawlewicz and others (1991)	
30-07-03-NE	Blackwood/Nichols NE Blanco 485	6263	3080	Cuttings	0.88	1240 FNL, 1175 FEL	-107.55294	36.84551	Fassett and Nuccio (1990)	
30-07-04-SW	Blackwood/Nichols NE Blanco 421R	6224	3110	Cuttings	0.88	1070 FSL, 465 FWL	-107.58341	36.83746	Pawlewicz and others (1991)	
30-07-06-NE	Blackwood/Nichols NE Blanco 451	6206	3085	Cuttings	0.89	210 FNL, 1900 FEL	-107.61050	36.84202	Pawlewicz and others (1991)	
30-07-06-SW	Blackwood/Nichols NE Blanco Unit 453	6190	3090	Cuttings	0.83	930 FSL, 610 FWL	-107.61563	36.83715	Pawlewicz and others (1991)	
30-07-07-NE	Blackwood/Nichols NE Blanco Unit 432	6301	3125	Cuttings	0.85	195 FNL, 790 FEL	-107.60590	36.83394	Pawlewicz and others (1991)	
30-07-10-NE	Meridian NE-Blanco 411	6265	3151	Cuttings	0.91	1465 FNL, 1350 FEL	-107.55361	36.83033	Pawlewicz and others (1991)	
30-07-11-SW	Meridian-SJ 30-6 U 461	6300	3090	Cuttings	0.84	1185 FSL, 1095 FWL	-107.54512	36.82338	Pawlewicz and others (1991)	
30-07-13-SW	Meridian-SJ 30-6 U 401	6133	3350	Cuttings	0.81	790 FSL, 1800 FWL	-107.52469	36.80773	Pawlewicz and others (1991)	
30-07-14-NE	Meridian-SJ 30-6 U 464	6284	3080	Cuttings	0.87	1710 FNL, 1555 FEL	-107.53624	36.81518	Pawlewicz and others (1991)	
30-07-15-SE	Meridian-SJ 30-6 U 465	6249	2980	Cuttings	0.76	1530 FSL, 1845 FEL	-107.55518	36.80953	Pawlewicz and others (1991)	
30-07-16-NE	Meridian-Francis Creek S 100	6262	3040	Cuttings	0.78	2485 FNL, 790 FEL	-107.56948	36.81310	Pawlewicz and others (1991)	
30-07-20-NW	Blackwood/Nichols NE Blanco Unit 479	6328	3235	Cuttings	0.79	1166 FNL, 2315 FWL	-107.59501	36.80239	Pawlewicz and others (1991)	
30-07-21-SW	Blackwood/Nichols NE Blanco Unit 405	6736	3650	Cuttings	0.83	875 FSL, 1145 FWL	-107.58087	36.79330	Pawlewicz and others (1991)	
30-07-29-NE	Blackwood/Nichols NE Blanco Unit 477	6336	3165	Cuttings	0.76	1650 FNL, 1160 FEL	-107.58884	36.78632	Fassett and Nuccio (1990)	
30-07-34-NE	Meridian San Juan 30-6 Unit 426	6230	3070	Cuttings	0.81	1460 FSL, 1450 FWL	-107.56200	36.76592	Pawlewicz and others (1991)	
30-07-36-SW	Meridian San Juan 30-6 Unit 468	6317	3744	Cuttings	0.91	1895 FSL, 1465 FWL	-107.52577	36.76705	Fassett and Nuccio (1990)	
30-08-01-NE	Blackwood/Nichols NE Blanco Unit 465	6432	3250	Cuttings	0.84	1020 FNL, 780 FEL	-107.62031	36.84460	Pawlewicz and others (1991)	
30-08-04-NE	Amoco Moore A-8	6271	3106	Cuttings	0.82	1395 FNL, 1490 FEL	-107.67648	36.84324	Fassett and Nuccio (1990)	
30-08-04-SW	Meridian, Howell "A" 301	6239	3050	Cuttings	0.81	460 FSL, 1180 FWL	-107.68567	36.83415	Pawlewicz and others (1991)	
30-08-05-NE	Amoco Moore B-3	6283	3008	Cuttings	0.81	1290 FNL, 1220 FEL	-107.69359	36.84362	Fassett and Nuccio (1990)	
30-08-06-NE	Meridian Florance H-3	6095	2897	Cuttings	0.78	1480 FNL, 1025 FEL	-107.71074	36.84309	Pawlewicz and others (1991)	
30-08-07-NE	Amoco Howell com "C" 300	NA	2870	Cuttings	0.71	1660 FNL, 1320 FWL	-107.71838	36.82841	Pawlewicz and others (1991)	
30-08-08-SW	Amoco Moore C-3	6436	3156	Cuttings	0.73	1120 FSL, 1325 FWL	-107.70269	36.82096	Fassett and Nuccio (1990)	
30-08-09-SW	Amoco Moore Gas Com 1	5875	2663	Cuttings	0.79	1550 FSL, 1690 FWL	-107.68321	36.82274	Pawlewicz and others (1991)	

Table A4-1. Mean vitrinite reflectance values (R_m) for coal samples from the Fruitland Formation—*Continued*.

Point ID	Well Name	Elev.	Depth	Sample	R_m (%)	Footage	Longitude	Latitude	Source	
New Mexico—Continued										
30-08-10-NE	Amoco Howell Gas Com 1	6252	3109	Cuttings	0.81	890 FNL, 910 FEL	-107.65586	36.82948	Pawlewicz and others (1991)	
30-08-12-SW	Meridian NE Blanco Unit 437	6085	2995	Cuttings	0.81	1240 FSL, 1650 FWL	-107.62821	36.82038	Fassett and Nuccio (1990)	
30-08-14-SW	Amoco Florance I-3	6476	3334	Cuttings	0.80	1420 FSL, 1630 FWL	-107.64727	36.80781	Pawlewicz and others (1991)	
30-08-18-NE	Amoco Florance X-1	6415	3159	Cuttings	0.76	1015 FNL, 790 FEL	-107.70986	36.81497	Pawlewicz and others (1991)	
30-08-18-NW	Meridian Howell "C" Com 301	6290	3048	Cuttings	0.72	1660 FNL, 1320 FWL	-107.71804	36.81381	Pawlewicz and others (1991)	
30-08-21-NW	Meridian Howell "K" 303	5858	2610	Cuttings	0.71	1840 FNL, 995 FWL	-107.68631	36.79887	Pawlewicz and others (1991)	
30-08-22-NW	Meridian Howell "K" 302	5822	2645	Cuttings	0.76	2056 FNL, 1675 FWL	-107.66572	36.79831	Pawlewicz and others (1991)	
30-08-23-NE	Amoco Florance J-3	6396	3188	Cuttings	0.80	2200 FNL, 1630 FEL	-107.64118	36.79784	Pawlewicz and others (1991)	
30-08-25-SW	Amoco Florance K-3	6208	2920	Cuttings	0.75	1788 FSL, 790 FWL	-107.63272	36.78041	Fassett and Nuccio (1990)	
30-08-26-SW	Amoco Gartner Gas Com B-1	5927	2697	Cuttings	0.73	1443 FSL, 1154 FWL	-107.64936	36.77922	Pawlewicz and others (1991)	
30-08-27-SW	Amoco Gartner A-12	6155	2886	Cuttings	0.72	1920 FSL, 1060 FWL	-107.66784	36.78099	Pawlewicz and others (1991)	
30-08-28-SW	Amoco Gartner A-14	6287	2977	Cuttings	0.71	1830 FSL, 1810 FWL	-107.68317	36.78025	Fassett and Nuccio (1990)	
30-08-29-SW	Meridian Howell E-301	5933	2620	Cuttings	0.74	1140 FSL, 1850 FWL	-107.70025	36.77828	Pawlewicz and others (1991)	
30-08-31-SW	Meridian Howell M-300	6278	2929	Cuttings	0.65	1590 FSL, 875 FWL	-107.71668	36.76448	Pawlewicz and others (1991)	
30-08-32-SW	Meridian Beaver Lodge Com 320	5813	2400	Cuttings	0.69	1850 FSL, 790 FWL	-107.70394	36.76566	Fassett and Nuccio (1990)	
30-08-33-NE	Amoco Gartner A-15	6319	2958	Cuttings	0.72	1790 FNL, 840 FEL	-107.67416	36.77058	Pawlewicz and others (1991)	
30-08-34-SW	Amoco Florance A-1	6334	2941	Cuttings	0.72	1370 FSL, 1210 FWL	-107.66710	36.76540	Pawlewicz and others (1991)	
30-08-35-NE	Amoco Florance P-3	6070	2820	Cuttings	0.76	1970 FNL, 1670 FEL	-107.64116	36.76996	Pawlewicz and others (1991)	
30-08-36-SW	Meridian EPNG Com "D" 300	6004	2780	Cuttings	0.76	800 FNL, 950 FEL	-107.62121	36.77351	Pawlewicz and others (1991)	
30-09-01-NE	Amoco Pritchard A-10	6337	3125	Cuttings	0.74	1730 FNL, 1810 FEL	-107.72916	36.84221	Fassett and Nuccio (1990)	
30-09-02-SE	Meridian Turner "B" Com "A" 200	5946	2737	Cuttings	0.74	1000 FSL, 1545 FEL	-107.74615	36.83549	Pawlewicz and others (1991)	
30-09-03-NE	Amoco Florance L	6039	2879	Cuttings	0.79	2465 FNL, 1220 FEL	-107.76260	36.84042	Amoco	
30-09-03-NW	Meridian Riddle 250	6115	3042	Cuttings	0.70	795 FNL, 1040 FWL	-107.77270	36.84504	Pawlewicz and others (1991)	
30-09-05-NE	Amoco Florance M-3	6240	2969	Cuttings	0.69	1730 FNL, 1290 FEL	-107.79862	36.84222	Fassett and Nuccio (1990)	
30-09-05-NW	Meridian Woodriver 250	6300	2870	Cuttings	0.74	1710 FNL, 1495 FWL	-107.80688	36.84266	Pawlewicz and others (1991)	
30-09-06-SW	Meridian Quigley Com 250	6540	3280	Cuttings	0.76	1030 FSL, 850 FWL	-107.82349	36.83651	Pawlewicz and others (1991)	
30-09-07-NE	Meridian Pierce 250	6374	3086	Cuttings	0.74	1030 FNL, 1180 FEL	-107.81585	36.83005	Pawlewicz and others (1991)	
30-09-08-NE	Meridian Pierce Com 251	6239	2984	Cuttings	0.68	950 FNL, 1175 FEL	-107.79788	36.82994	Pawlewicz and others (1991)	
30-09-09-SW	Meridian Duff Com 260	6210	2840	Cuttings	0.68	790 FSL, 1785 FWL	-107.78760	36.82049	Pawlewicz and others (1991)	
30-09-10-SW	Amoco Florance Gas Com D-1	6192	2938	Cuttings	0.77	2160 FSL, 1260 FWL	-107.77170	36.82417	Pawlewicz and others (1991)	
30-09-11-NE	Meridian Lindsey Com 250	5853	2656	Cuttings	0.75	1190 FNL, 855 FEL	-107.74376	36.82947	Pawlewicz and others (1991)	
30-09-11-SW	Amoco Florance 114 FT 2	6035	2793	Cuttings	0.71	2390 FSL, 980 FWL	-107.75479	36.82474	Pawlewicz and others (1991)	
30-09-15-NW	Meridian Riddle "A" Com 201	6392	3120	Cuttings	0.72	935 FNL, 1480 FWL	-107.77089	36.81562	Pawlewicz and others (1991)	
30-09-21-SW	Meridian Florence Com 260	6052	2740	Cuttings	0.67	1200 FSL, 2100 FWL	-107.78666	36.79325	Pawlewicz and others (1991)	
30-09-22-SE	Amoco Florance AC 4	5878	2580	Cuttings	0.73	1550 FSL, 1120 FEL	-107.76212	36.79356	Amoco	
30-09-24-NE	Meridian Florance O-3	5810	2472	Cuttings	0.76	1845 FNL, 1560 FEL	-107.72712	36.79864	Pawlewicz and others (1991)	
30-09-28-NE	Meridian Turner 251	5845	2500	Cuttings	0.65	1450 FNL, 1150 FEL	-107.78010	36.78551	Pawlewicz and others (1991)	
30-09-28-NW	Meridian Mansfield Com 260	5896	2540	Cuttings	0.65	1490 FNL, 1100 FWL	-107.79023	36.78578	Pawlewicz and others (1991)	
30-09-29-SW	Meridian Mansfield Com 251	6066	2610	Cuttings	0.66	1130 FNL, 940 FWL	-107.80838	36.78676	Pawlewicz and others (1991)	
30-10-01-SW	Meridian Sunray "B" 201	6445	3150	Cuttings	0.65	1390 FSL, 1340 FWL	-107.83720	36.83736	Pawlewicz and others (1991)	
30-10-06-NW	Meridian Atlantic "C" 202	6033	2600	Cuttings	0.63	790 FNL, 805 FWL	-107.92909	36.84565	Pawlewicz and others (1991)	

Table A4-1. Mean vitrinite reflectance values (R_m) for coal samples from the Fruitland Formation—*Continued*.

Point ID	Well Name	Elev.	Depth	Sample	R_m (%)	Footage	Longitude	Latitude	Source	
New Mexico—Continued										
30-10-07-SW	Meridian Sunray "J" 210	6118	2930	Cuttings	0.61	790 FSL, 880 FWL	-107.92933	36.82099	Pawlewicz and others (1991)	
30-10-10-SE	Meridian San Juan 200	6487	2920	Cuttings	0.62	1120 FSL, 1145 FWL	-107.87509	36.82273	Pawlewicz and others (1991)	
30-10-12-NE	Meridian Grambling "C" 200	6341	3048	Cuttings	0.67	1180 FNL, 605 FEL	-107.82859	36.83031	Pawlewicz and others (1991)	
30-10-13-NE	Meridian Turner Federal 210	6366	3360	Cuttings	0.63	950 FNL, 1790 FEL	-107.83247	36.81636	Pawlewicz and others (1991)	
30-10-13-SW	Meridian Pierce "A" 210	6400	2993	Cuttings	0.65	1190 FSL, 1800 FWL	-107.83776	36.80783	Pawlewicz and others (1991)	
30-10-15-SW	Meridian Sunray "B" 215	6338	2820	Cuttings	0.66	800 FSL, 800 FWL	-107.87625	36.80630	Pawlewicz and others (1991)	
30-10-21-NE	Meridian Sunray "D" 225	6317	2790	Cuttings	0.63	1490 FNL, 1100 FEL	-107.88293	36.79982	Pawlewicz and others (1991)	
30-10-23-NE	Meridian Riddle "B" 223	6260	2840	Cuttings	0.54	1850 FNL, 830 FEL	-107.84696	36.79933	Pawlewicz and others (1991)	
30-10-25-NW	Meridian Florence "A" 210	6074	2510	Cuttings	0.63	845 FNL, 1590 FWL	-107.83884	36.78792	Pawlewicz and others (1991)	
30-10-28-SW	Amoco Stewart B-1	6223	2663	Cuttings	0.66	870 FSL, 1210 FWL	-107.89452	36.77801	Pawlewicz and others (1991)	
30-11-16-NE	Mesa Oper. Ltd FC State Com 16	5777	2140	Cuttings	0.60	1870 FNL, 1705 FEL	-107.99211	36.81377	Pawlewicz and others (1991)	
30-14-11-SE	Dugan Blazer 2	6045	1680	Cuttings	0.52	1190 FSL, 1500 FEL	-108.27370	36.82455	Fassett and Nuccio (1990)	
30-14-17-SW	Dugan Turks Toast	5625	1140	Cuttings	0.52	1850 FSL, 790 FWL	-108.33791	36.81203	Pawlewicz and others (1991)	
30-15-03-SW	NMBMMR coal test hole	5365	153	Core	0.59	NA	-108.41232	36.83658	Hoffman (1991)	
31-05-19-SE	Northwest Pipelineline Rosa Unit 204	6342	3195	Cuttings	1.19	1590 FSL, 1465 FEL	-107.39889	36.88230	Amoco	
31-05-29-NE	Meridian Rosa Unit 200	6388	3260	Cuttings	1.10	1265 FNL, 1475 FEL	-107.38105	36.87439	Pawlewicz and others (1991)	
31-06-11-SW	Meridian Rosa Unit 216	6273	3071	Cuttings	1.05	1500 FSL, 1705 FWL	-107.43468	36.91097	Pawlewicz and others (1991)	
31-06-21-SW	Meridian Rosa Unit 260	6350	3170	Cuttings	1.07	1040 FSL, 1310 FWL	-107.47232	36.88080	Pawlewicz and others (1991)	
31-06-22-NE	Meridian Rosa Unit 201	6250	3083	Cuttings	1.04	1640 FNL, 420 FEL	-107.44210	36.88803	Pawlewicz and others (1991)	
31-06-23-NE	Meridian Rosa Unit 213	6285	3127	Cuttings	0.97	1020 FNL, 1535 FEL	-107.42773	36.88963	Pawlewicz and others (1991)	
31-06-26-NE	Meridian Rosa Unit 211	6405	3232	Cuttings	1.08	2275 FNL, 1410 FEL	-107.42731	36.87163	Pawlewicz and others (1991)	
31-06-30-SW	Blackwood/Nichols NE Blanco Unit 495	6348	3260	Cuttings	0.92	1658 FSL, 957 FWL	-107.50958	36.86808	Pawlewicz and others (1991)	
31-07-01-SW	Blackwood/Nichols NE Blanco Unit 462	6571	3280	Cuttings	1.04	805 FSL, 1370 FWL	-107.52575	36.92364	Pawlewicz and others (1991)	
31-07-11-NE	Blackwood/Nichols NE Blanco Unit 440	6534	3160	Cuttings	0.96	1156 FNL, 903 FEL	-107.53364	36.91814	Pawlewicz and others (1991)	
31-07-13-NE	Blackwood/Nichols NE Blanco Unit 458	6519	3165	Cuttings	0.92	1135 FNL, 1125 FEL	-107.51624	36.90380	Pawlewicz and others (1991)	
31-07-15-NE	Blackwood/Nichols NE Blanco Unit 452	6553	3175	Cuttings	0.91	1785 FNL, 1770 FEL	-107.55432	36.90185	Pawlewicz and others (1991)	
31-07-15-SW	Blackwood/Nichols NE Blanco Unit 482	6548	3395	Cuttings	0.86	890 FSL, 790 FWL	-107.56372	36.89485	Pawlewicz and others (1991)	
31-07-16-NE	Blackwood/Nichols NE Blanco Unit 484	6540	3420	Cuttings	0.98	990 FNL, 790 FEL	-107.56914	36.90408	Pawlewicz and others (1991)	
31-07-20-NE	Blackwood/Nichols NE Blanco Unit 408	6460	3160	Cuttings	0.97	1035 FNL, 1305 FEL	-107.58910	36.88943	Pawlewicz and others (1991)	
31-07-22-SW	Blackwood/Nichols NE Blanco Unit 476	6464	3190	Cuttings	0.84	1200 FSL, 840 FWL	-107.56382	36.88128	Pawlewicz and others (1991)	
31-07-24-NE	Blackwood/Nichols NE Blanco Unit 428	6457	3155	Cuttings	0.89	1075 FNL, 790 FEL	-107.51534	36.88912	Pawlewicz and others (1991)	
31-07-25-NE	Blackwood/Nichols NE Blanco Unit 493	6297	3200	Cuttings	0.94	1477 FSL, 793 FEL	-107.51558	36.86748	Pawlewicz and others (1991)	
31-07-27-NE	Blackwood/Nichols NE Blanco Unit 470	6419	3210	Cuttings	0.88	1400 FNL, 960 FEL	-107.55224	36.87389	Pawlewicz and others (1991)	
31-07-29-NE	Blackwood/Nichols NE Blanco Unit 472	6451	3333	Cuttings	0.97	1330 FNL, 1330 FEL	-107.58946	36.87405	Pawlewicz and others (1991)	
31-07-29-SW	Blackwood/Nichols NE Blanco Unit 412	6303	3175	Cuttings	0.92	840 FSL, 1725 FWL	-107.59708	36.86584	Pawlewicz and others (1991)	
31-07-30-NE	Blackwood/Nichols NE Blanco Unit 414	6390	3275	Cuttings	0.96	2330 FNL, 150 FEL	-107.60351	36.87134	Pawlewicz and others (1991)	
31-07-32-NE	Blackwood/Nichols NE Blanco Unit 448	6388	3165	Cuttings	0.78	1515 FNL, 1340 FEL	-107.58948	36.85916	Pawlewicz and others (1991)	
31-07-32-SW	Blackwood/Nichols NE Blanco Unit 450	6363	3240	Cuttings	0.95	795 FSL, 2010 FWL	-107.59612	36.85124	Pawlewicz and others (1991)	
31-07-33-SW	Blackwood/Nichols NE Blanco Unit 446	6316	3190	Cuttings	0.92	2045 FSL, 1395 FWL	-107.58015	36.85478	Pawlewicz and others (1991)	
31-07-34-NW	Blackwood/Nichols NE Blanco Unit 404	6297	3153	Cuttings	1.03	1730 FNL, 260 FWL	-107.56596	36.85860	Amoco	
31-07-36-NE	Meridian NE-Blanco,483	6220	3142	Cuttings	0.99	1750 FNL, 2045 FEL	-107.51988	36.85855	Pawlewicz and others (1991)	

Table A4-1. Mean vitrinite reflectance values (R_m) for coal samples from the Fruitland Formation—*Continued*.

Point ID	Well Name	Elev.	Depth	Sample	R_m (%)	Footage	Longitude	Latitude	Source	
New Mexico—Continued										
31-07-36-SW	Meridian NE-Blanco,481	6483	3390	Cuttings	0.87	1005 FSL, 1835 FWL	-107.52446	36.85176	Pawlewicz and others (1991)	
31-08-19-NW	Union Texas Quinn 2A	6404	3150	Cuttings	0.77	1690 FNL, 1520 FWL	-107.71677	36.88572	Fassett and Nuccio (1990)	
31-08-22-NW	Northwest Pipelineline SK 32-8 Unit 7A	6528	3110	Cuttings	0.84	880 FNL, 870 FWL	-107.66816	36.88738	Amoco	
31-08-25-NE	Blackwood/Nichols NE Blanco Unit 471	6415	3280	Cuttings	0.94	1315 FNL, 1710 FEL	-107.62372	36.87212	Pawlewicz and others (1991)	
31-08-25-SW	Blackwood/Nichols NE Blanco Unit 445	6404	3275	Cuttings	0.94	990 FSL, 815 FWL	-107.63255	36.86422	Pawlewicz and others (1991)	
31-08-27-SW	Meridian Hale 350	6326	3170	Cuttings	0.88	815 FSL, 1180 FWL	-107.66712	36.86383	Pawlewicz and others (1991)	
31-08-28-NE	Amoco Kernaghan B-5	6332	3184	Cuttings	0.93	1210 FNL, 1115 FEL	-107.67422	36.87186	Fassett and Nuccio (1990)	
31-08-28-NW	Meridian Howell "D" 350	6509	3393	Cuttings	0.87	1450 FNL, 790 FWL	-107.68574	36.87153	Pawlewicz and others (1991)	
31-08-29-NE	Amoco Kernaghan B-6	6581	3426	Cuttings	0.82	1280 FNL, 1800 FEL	-107.69465	36.87190	Pawlewicz and others (1991)	
31-08-29-SW	Meridian Howell "D" 351	6508	3330	Cuttings	0.75	1180 FSL, 1840 FWL	-107.70087	36.86520	Pawlewicz and others (1991)	
31-08-30-NE	Amoco Kernaghan B-7	6554	3367	Cuttings	0.83	1440 FNL, 1040 FEL	-107.71002	36.87183	Fassett and Nuccio (1990)	
31-08-31-NE	Meridian Howell "D" 352	6350	3192	Cuttings	0.76	1165 FNL, 1000 FEL	-107.71088	36.85856	Pawlewicz and others (1991)	
31-08-31-SW	Amoco Dawson Gas Com 1	6328	3117	Cuttings	0.80	1210 FSL, 660 FWL	-107.72078	36.85055	Amoco	
31-08-33-SW	Amoco Kernaghan B-8	6407	3224	Cuttings	0.90	1140 FSL, 1700 FWL	-107.68350	36.85037	Fassett and Nuccio (1990)	
31-08-34-NE	Meridian Hale 353	6242	3128	Cuttings	0.83	620 FNL, 2360 FEL	-107.66168	36.85965	Pawlewicz and others (1991)	
31-09-02-NE	Meridian San Juan 32-9 Unit 201	6469	3210	Cuttings	0.90	2275 FNL, 885 FEL	-107.74277	36.92760	Pawlewicz and others (1991)	
31-09-08-NE	Amoco San Juan 32-9 105	6767	3488	Cuttings	0.83	1400 FNL, 790 FEL	-107.79712	36.91566	Pawlewicz and others (1991)	
31-09-19-SW	Amoco Barrett Gas Com A	6676	3439	Cuttings	0.73	1810 FSL, 925 FWL	-107.82301	36.88153	Amoco	
31-09-21-NW	Meridian Sunray "G" 251	6475	3330	Cuttings	0.79	830 FNL, 1165 FWL	-107.78967	36.88824	Pawlewicz and others (1991)	
31-09-21-SE	Meridian Sunray "G" 250	6167	3020	Cuttings	0.78	800 FSL, 1175 FEL	-107.78059	36.87834	Pawlewicz and others (1991)	
31-09-22-SW	Amoco Riddle B-1 2	6283	3052	Cuttings	0.79	1980 FSL, 1095 FWL	-107.77239	36.88174	Pawlewicz and others (1991)	
31-09-25-SW	Amoco Trigg Fed Gas Com C	5998	2801	Cuttings	0.81	2240 FSL, 865 FWL	-107.73761	36.86770	Amoco	
31-09-27-NE	Amoco Schwerdtfeger Gas Com	6237	3049	Cuttings	0.84	1760 FNL, 1910 FEL	-107.76471	36.87132	Amoco	
31-09-27-SW	Amoco Pritchard B-5	6211	3013	Cuttings	0.76	1840 FSL, 1175 FWL	-107.77213	36.86674	Fassett and Nuccio (1990)	
31-09-27-SW	Amoco Schwerdtfeger A-3	6085	2897	Cuttings	0.80	1120 FSL, 810 FWL	-107.77329	36.86475	Fassett and Nuccio (1990)	
31-09-28-SW	San Juan Production Sheets	6150	2957	Cuttings	0.78	990 FSL, 1650 FWL	-107.78732	36.86413	Amoco	
31-09-28-SW	Meridian Sheets 250	6172	2993	Cuttings	0.72	1135 FSL, 1840 FEL	-107.78242	36.86461	Pawlewicz and others (1991)	
31-09-30-NE	Amoco Riddle Gas Com 1B1	6392	3037	Cuttings	0.72	2380 FNL, 1370 FEL	-107.81640	36.86964	Amoco	
31-09-34-SW	Amoco Pritchard B 5	6211	3000	Cuttings	0.80	1840 FSL, 1175 FWL	-107.77221	36.85232	Amoco	
31-10-02-NE	Meridian San Juan 32-9 Unit 209	6321	2900	Cuttings	0.74	1545 FNL, 1640 FEL	-107.84924	36.92971	Pawlewicz and others (1991)	
31-10-02-SW	Meridian San Juan 32-9 Unit 210	6148	2973	Cuttings	0.82	900 FSL, 1500 FWL	-107.85554	36.92230	Pawlewicz and others (1991)	
31-10-04-NE	Amoco Wood Gas Com-A	5833	2372	Cuttings	0.74	1155 FNL, 1745 FEL	-107.88373	36.93109	Amoco	
31-10-21-NE	Meridian Lambe Com 200	6153	2909	Cuttings	0.71	915 FNL, 1330 FEL	-107.88257	36.88804	Fassett and Nuccio (1990)	
31-10-23-NE	Meridian Atlantic (D Com) 205	6370	3140	Cuttings	0.75	1190 FNL, 1450 FEL	-107.84710	36.88750	Fassett and Nuccio (1990)	
31-10-29-NE	Meridian Atlantic "A" 211	5992	2510	Cuttings	0.64	1450 FNL, 1850 FEL	-107.90218	36.87227	Pawlewicz and others (1991)	
31-10-29-SW	Meridian Atlantic "A" 210	6041	2710	Cuttings	0.62	1450 FSL, 1530 FWL	-107.90861	36.86618	Pawlewicz and others (1991)	
31-10-31-NE	Meridian Atlantic "C" 215	6056	2689	Cuttings	0.67	1580 FNL, 1460 FEL	-107.91877	36.85762	Pawlewicz and others (1991)	
31-10-34-NW	Tenneco Atlantic 1E	6215	2810	Cuttings	0.71	1030 FNL, 840 FWL	-107.87512	36.85902	Amoco - GRI	
31-10-35-NE	Meridian Atlantic "C" 200	6420	3155	Cuttings	0.68	1450 FNL, 1545 FEL	-107.84759	36.85829	Pawlewicz and others (1991)	
31-11-01-NE	Amoco Mudge A 55	6058	2780	Cuttings	0.70	1410 FNL, 1610 FEL	-107.93754	36.93049	Amoco	
31-11-04-NE	Amoco Neal A 24	6163	2442	Cuttings	0.65	2050 FNL, 820 FEL	-107.98887	36.92815	Amoco	

Table A4-1. Mean vitrinite reflectance values (R_m) for coal samples from the Fruitland Formation—*Continued*.

Point ID	Well Name	Elev.	Depth	Sample	R_m (%)	Footage	Longitude	Latitude	Source	
New Mexico—Continued										
31-11-05-NE	Amoco Case B 19	6417	3055	Cuttings	0.71	880 FNL, 1560 FEL	-108.00803	36.93164	Amoco	
31-11-05-SW	Amoco Case A 18	6197	2635	Cuttings	0.66	1270 FSL, 1625 FWL	-108.01555	36.92349	Amoco	
31-11-06-NE	Meridian Grenier 100	6522	2980	Cuttings	0.64	1640 FNL, 1790 FEL	-108.02609	36.92966	Pawlewicz and others (1991)	
31-11-07-SW	Southland Royaltyty Grenier 101	6218	2590	Cuttings	0.67	1925 FSL, 1830 FWL	-108.03602	36.90904	Pawlewicz and others (1991)	
31-11-17-SW	Amoco Case B-1	6168	2730	Cuttings	0.70	1250 FSL, 1370 FWL	-108.01705	36.89498	Pawlewicz and others (1991)	
31-11-18-SW	Southland Royaltyty Grenier 102	6090	2630	Cuttings	0.69	1865 FSL, 1330 FWL	-108.03505	36.89706	Pawlewicz and others (1991)	
31-11-20	Meridian Grenier 103	6035	2550	Cuttings	0.66	2135 FSL, 1290 FWL	-108.01726	36.88313	Fassett and Nuccio (1990)	
31-11-24-SE	H. F. Petroleumtiegrew Ruple Pool Unit 1-X	5771	2620	Cuttings	0.66	654 FSL, 1980 FEL	-107.93885	36.87819	Amoco	
31-11-27-SE	Meridian Calloway 1-A	5686	2248	Cuttings	0.66	1175 FSL, 1470 FEL	-107.97370	36.86552	Pawlewicz and others (1991)	
31-11-30-NW	Tenneco Heaton 1-E A	5913	2310	Cuttings	0.60	790 FNL, 1520 FWL	-108.03482	36.87526	Amoco	
31-11-36-SE	Grt. West. D.Pubco State Com A-1	6061	2373	Cuttings	0.62	1690 FSL, 935 FEL	-107.93507	36.85240	Fassett and Nuccio (1990)	
31-12-09-NW	Tenneco Newberry 2-E A	6140	2380	Cuttings	0.67	560 FNL, 1720 FWL	-108.10320	36.91931	Amoco	
31-12-09-SE	El Paso Newberry 8-A	6193	2459	Cuttings	0.63	1030 FSL, 1625 FEL	-108.09686	36.90886	Amoco	
31-12-11-NE	Southland Royaltyty Davis 504	6322	2720	Cuttings	0.70	1065 FNL, 1475 FEL	-108.06031	36.91726	Amoco	
31-12-11-NE	Southland Royaltyty Davis 504	6322	2720	Cuttings	0.70	1065 FNL, 1475 FEL	-108.06018	36.91710	Pawlewicz and others (1991)	
31-12-11-SE	Southern Union Davis	NA	2780	Cuttings	0.65	990 FSL, 990 FEL	-108.05949	36.90861	Amoco	
31-12-12-SW	Meridian Davis 502	6264	2808	Cuttings	0.67	2085 FSL, 1330 FWL	-108.05118	36.91183	Pawlewicz and others (1991)	
31-12-14-NE	Southland Royalty Harper Com 100	6228	2550	Cuttings	0.65	1915 FNL, 1625 FEL	-108.06248	36.90064	Pawlewicz and others (1991)	
31-12-19-SW	Colorado Western Govt-South Union	5903	2270	Cuttings	0.57	1090 FSL, 1090 FWL	-108.14232	36.88080	Amoco	
31-13-02-NE	Quinoco Chavez H 2-2	5748	1999	Cuttings	0.70	2440 FNL, 828 FEL	-108.16596	36.92960	Pawlewicz and others (1991)	
31-13-02-SW	Quinoco Jaquez K 2-2	5720	2033	Cuttings	0.56	2270 FSL, 1765 FWL	-108.17492	36.92798	Pawlewicz and others (1991)	
31-14-27-SE	Wintershall Corp Ute MinUte 27	NA	635	Cuttings	0.58	995 FSL, 1055 FEL	-108.29274	36.86552	Amoco	
32-02-25-SW	Outcrop	NA		Outcrop	0.64	2084 FSL, 2328 FWL	-106.99570	36.95662	Amoco	
32-03-22-SE	Stanolind O&G Jicarilla Apache	6988	1092	Cuttings	0.80	3830 FSL, 840 FEL	-107.13128	36.97630	Amoco	
32-03-23-NW	Pan American Petroleumroleum Pagosa	NA	3612	Cuttings	1.38	1030 FNL, 1190 FWL	-107.12430	36.97717	Amoco	
32-04-14-NW	McHugh Carracas Mesa 14	6273	2888	Cuttings	1.31	1100 FNL, 1100 FWL	-107.22860	36.99088	Amoco	
32-04-15-NE	Nassau Carracas Unit 15 B- 7	6548	3364	Cuttings	1.24	1650 FNL, 1850 FEL	-107.23876	36.98929	Fassett and Nuccio (1990)	
32-04-17-SE	Nassau Carracas Unit 17 B- 15	6883	4200	Cuttings	1.30	650 FSL, 2070 FEL	-107.27519	36.98104	Fassett and Nuccio (1990)	
32-04-18-SE	Nassau Carracas Unit 18 B-15	7329	4128	Cuttings	1.27	580 FSL, 1710 FEL	-107.29190	36.98081	Fassett and Nuccio (1990)	
32-04-18-SW	Nassau Carracas U 18 B-13	7432	4160	Cuttings	1.14	790 FSL, 900 FWL	-107.30052	36.98150	Fassett and Nuccio (1990)	
32-04-19-NE	Nassau Carracas U 19 B-1	7353	4115	Cuttings	1.27	750 FNL, 400 FEL	-107.28732	36.97725	Fassett and Nuccio (1990)	
32-04-20-NW	Nassau Carracas U 20B 3	7400	4137	Cuttings	1.28	1170 FSL, 1480 FWL	-107.28086	36.96971	Fassett and Nuccio (1990)	
32-04-21-NW	Nassau Carracas U 21B 5	7346	4300	Cuttings	1.27	1655 FNL, 1185 FWL	-107.26397	36.97479	Fassett and Nuccio (1990)	
32-04-26-SE	Nassau Carracas U 26B 16	7048	4003	Cuttings	1.26	790 FSL, 790 FEL	-107.21691	36.95271	Fassett and Nuccio (1990)	
32-04-26-SW	Nassau Resource Carracas Unit PC 26B 13	NA	4001	Cuttings	1.33	1100 FSL, 790 FSL	-107.22856	36.95341	Amoco	
32-04-27-NW	Nassau Carracas U 27B 5	7253	4285	Cuttings	1.22	1740 FNL, 800 FWL	-107.24720	36.95999	Fassett and Nuccio (1990)	
32-04-28-NW	Nassau Carracas U 28B 5	7333	4045	Cuttings	1.30	1850 FNL, 790 FWL	-107.26533	36.95979	Fassett and Nuccio (1990)	
32-04-30-NE	Nassau Carracas U 30B 8	7212	3947	Cuttings	1.21	2240 FNL, 620 FEL	-107.28815	36.95860	Fassett and Nuccio (1990)	
32-04-32-NW	Nassau Carracas U 32B 5	7203	4125	Cuttings	1.24	1630 FNL, 790 FWL	-107.28337	36.94584	Fassett and Nuccio (1990)	
32-04-34-NE	Nassau Carracas U 34B 2	7284	4178	Cuttings	1.23	790 FNL, 1850 FEL	-107.23844	36.94832	Fassett and Nuccio (1990)	
32-04-35-SE	Nassau Carracas U 35B 9	6993	3934	Cuttings	1.24	1850 FSL, 790 FEL	-107.21695	36.94119	Fassett and Nuccio (1990)	

Table A4-1. Mean vitrinite reflectance values (R_m) for coal samples from the Fruitland Formation—*Continued*.

Point ID	Well Name	Elev.	Depth	Sample	R_m (%)	Footage	Longitude	Latitude	Source	
New Mexico—Continued										
32-04-36-SE	Nassau Carracas U 36B 15	7033	4006	Cuttings	1.23	1190 FSL, 1850 FEL	-107.20258	36.93942	Fassett and Nuccio (1990)	
32-05-11-SE	Nassau Carracas U 11A 9	7519	4255	Cuttings	1.28	1675 FSL, 1190 FEL	-107.32567	36.99193	Fassett and Nuccio (1990)	
32-05-13-SW	Nassau Carracas U 13A 14	7418	4128	Cuttings	1.24	800 FSL, 1760 FWL	-107.31546	36.97522	Fassett and Nuccio (1990)	
32-05-14-NE	Nassau Carracas U 14A 1	7393	3966	Cuttings	1.20	1000 FNL, 680 FEL	-107.32383	36.98462	Fassett and Nuccio (1990)	
32-05-14-SW	Nassau Carracas Unit 14 A 13	7269	3824	Cuttings	1.26	230 FSL, 380 FWL	-107.33841	36.97354	Fassett and Nuccio (1990)	
32-05-17-NE	Amoco Seibel Gas Unit B	6114	2624	Cuttings	1.41	1850 FNL, 770 FEL	-107.37912	36.98218	Amoco	
32-05-21-SE	Nassau Carracas U 21A 15	7043	3714	Cuttings	1.17	790 FSL, 1850 FEL	-107.36418	36.96048	Fassett and Nuccio (1990)	
32-05-22-SE	Nassau Carracas Unit 22 A 16	7065	3781	Cuttings	1.18	790 FSL, 790 FEL	-107.34244	36.96065	Fassett and Nuccio (1990)	
32-05-22-SW	Nassau Carracas U 22A 13	7034	3730	Cuttings	1.18	620 FSL, 540 FWL	-107.35597	36.96014	Fassett and Nuccio (1990)	
32-05-23-NE	Nassau Carracas U 23A 2	7424	3960	Cuttings	1.08	1190 FNL, 1850 FEL	-107.32789	36.96954	Fassett and Nuccio (1990)	
32-05-23-SW	Nassau Carracas Unit 23 A 12	7185	3940	Cuttings	1.22	1650 FSL, 1190 FWL	-107.33565	36.96314	Fassett and Nuccio (1990)	
32-05-24-NW	Nassau Resource Carracas Unit PC 24A	7327	3954	Cuttings	1.24	790 FNL, 1140 FWL	-107.31765	36.97069	Amoco	
32-05-26-NE	Nassau Carracas U 26A 2	7215	3970	Cuttings	1.21	790 FNL, 1450 FEL	-107.32657	36.95627	Fassett and Nuccio (1990)	
32-05-27-NE	Nassau Carracas U 27A 8	7188	3882	Cuttings	1.18	1480 FNL, 990 FEL	-107.34317	36.95440	Fassett and Nuccio (1990)	
32-05-27-SW	Nassau Resource Carracas Unit 27A	6843	3582	Cuttings	1.27	970 FSL, 1580 FWL	-107.35235	36.94663	Amoco	
32-05-28-SW	Meridian Quint Mesa C 100	7160	3905	Cuttings	1.14	2360 FSL, 1740 FWL	-107.37034	36.95059	Pawlewicz and others (1991)	
32-05-33-SE	Schalk John E USA-62	6303	2200	Cuttings	1.15	1190 FSL, 890 FEL	-107.36088	36.93268	Amoco	
32-05-35-NE	Nassau Carracas U 35A 8	6922	3673	Cuttings	1.17	1500 FNL, 1020 FEL	-107.32503	36.93977	Fassett and Nuccio (1990)	
32-06-07-NE	Meridian Allison Unit 133	6236	2760	Cuttings	1.19	790 FNL, 2490 FEL	-107.49912	36.99756	Pawlewicz and others (1991)	
32-06-10-NE	Pacific NW Pipelineline San Juan 32-5 Unit	6194	2660	Cuttings	1.30	990 FNL, 990 FEL	-107.43905	36.99727	Amoco	
32-06-16-SW	Meridian Allison Unit 100	6137	2781	Cuttings	1.25	1780 FSL, 1540 FWL	-107.46702	36.97829	Pawlewicz and others (1991)	
32-06-17-SW	Meridian Allison Unit 101	6596	3210	Cuttings	1.03	1840 FSL, 1190 FWL	-107.48678	36.97838	Pawlewicz and others (1991)	
32-06-18-NE	Meridian Allison Unit 111	6507	3060	Cuttings	1.17	2480 FNL, 1450 FEL	-107.49580	36.98102	Pawlewicz and others (1991)	
32-06-18-SW	Meridian Allison Unit 112	6517	3128	Cuttings	1.19	1850 FSL, 1190 FEL	-107.50432	36.97824	Pawlewicz and others (1991)	
32-06-19-NE	Meridian Allison Unit 114	6513	3150	Cuttings	1.20	1240 FNL, 1120 FEL	-107.49480	36.96979	Pawlewicz and others (1991)	
32-06-19-NW	Meridian Allison Unit 136	6681	3260	Cuttings	1.17	2360 FNL, 925 FWL	-107.50514	36.96659	Pawlewicz and others (1991)	
32-06-20-NW	Meridian Allison Unit 116	6385	2960	Cuttings	1.26	1850 FNL, 880 FWL	-107.48784	36.96820	Pawlewicz and others (1991)	
32-06-20-SW	Meridian Allison Unit 115	6522	3169	Cuttings	1.19	2400 FSL, 1975 FWL	-107.48413	36.96523	Pawlewicz and others (1991)	
32-06-21-NE	Meridian EPNG A 100	6385	3076	Cuttings	1.23	2030 FNL, 1905 FEL	-107.45856	36.96982	Pawlewicz and others (1991)	
32-06-21-SW	Meridian Allison Unit 117	6482	3161	Cuttings	1.15	930 FSL, 1540 FWL	-107.46700	36.96127	Pawlewicz and others (1991)	
32-06-23-NE	Meridian-SJ 32-5 U,101	6416	3112	Cuttings	1.18	2325 FNL, 1010 FEL	-107.42125	36.96683	Pawlewicz and others (1991)	
32-06-23-SW	Meridian-SJ 32-5 U,100	6331	4369	Cuttings	1.12	1765 FSL, 1485 FWL	-107.43073	36.96364	Pawlewicz and others (1991)	
32-06-24-SW	Meridian-SJ 32-5 U,102	6369	3000	Cuttings	1.18	1820 FSL, 1635 FWL	-107.41202	36.96375	Pawlewicz and others (1991)	
32-06-25-SW	Meridian-SJ 32-5 U,104	6411	3121	Cuttings	1.19	540 FSL, 985 FWL	-107.41434	36.94576	Pawlewicz and others (1991)	
32-06-26-NE	Meridian-SJ 32-5 U,107	6353	3080	Cuttings	1.15	2045 FNL, 645 NEL	-107.41997	36.95293	Pawlewicz and others (1991)	
32-06-27-NE	Meridian-SJ 32-5 U 108	6428	3158	Cuttings	1.24	2100 FNL, 100 FEL	-107.43630	36.95319	Fassett and Nuccio (1990)	
32-06-28-NE	Meridian EPNG "B" 100	6463	3100	Cuttings	1.17	1015 FNL, 2485 FEL	-107.46258	36.95563	Pawlewicz and others (1991)	
32-06-29-NE	Meridian Allison Unit 102	6507	3200	Cuttings	1.16	860 FNL, 1950 FEL	-107.47909	36.95619	Pawlewicz and others (1991)	
32-06-29-SW	Meridian Allison Unit 119	6381	3077	Cuttings	1.16	1595 FSL, 1765 FWL	-107.48488	36.94820	Pawlewicz and others (1991)	
32-06-30-NE	Meridian Allison Unit 120	6404	3087	Cuttings	1.15	1070 FNL, 1100 FEL	-107.49475	36.95556	Pawlewicz and others (1991)	
32-06-30-SW	Meridian Allison Unit 121	6576	3087	Cuttings	1.08	1780 FSL, 930 FWL	-107.50540	36.94886	Pawlewicz and others (1991)	

Table A4-1. Mean vitrinite reflectance values (R_m) for coal samples from the Fruitland Formation—*Continued*.

Point ID	Well Name	Elev.	Depth	Sample	R_m (%)	Footage	Longitude	Latitude	Source	
New Mexico—Continued										
32-07-09-SE	Meridian Allison Unit 123	6586	3240	Cuttings	1.22	1015 FSL, 1850 FEL	-107.56946	36.9903	Pawlewicz and others (1991)	
32-07-12-SW	Meridian Allison Unit 125	6542	3158	Cuttings	1.15	790 FSL, 1595 FWL	-107.52109	36.98972	Pawlewicz and others (1991)	
32-07-14-NE	Meridian Allison Unit 126	6636	3275	Cuttings	1.25	1900 FNL, 1765 FEL	-107.53276	36.98217	Pawlewicz and others (1991)	
32-07-14-SW	Meridian Allison Unit 127	6829	3458	Cuttings	1.09	1080 FSL, 790 FWL	-107.54293	36.97604	Pawlewicz and others (1991)	
32-07-15-NW	Meridian Allison Unit 107	6600	3080	Cuttings	1.07	941 FNL, 1510 FWL	-107.55811	36.98496	Pawlewicz and others (1991)	
32-07-22-NE	Pacific NW Pipelineline San Juan 32-7 Unit	NA	3230	Cuttings	1.10	1650 FNL, 1650 FEL	-107.55133	36.96844	Amoco	
32-07-23-SE	Meridian Allison Unit 108	6549	3266	Cuttings	1.15	841 FSL, 790 FWL	-107.54273	36.96089	Pawlewicz and others (1991)	
32-07-25-NE	Meridian Allison Unit 132	6472	3168	Cuttings	1.12	1460 FNL, 790 FEL	-107.51119	36.95447	Pawlewicz and others (1991)	
32-07-25-SW	Meridian Burnt Mesa 101	6603	3339	Cuttings	1.14	1175 FSL, 1500 FWL	-107.52156	36.94736	Pawlewicz and others (1991)	
32-07-26-SW	Meridian Burnt Mesa 100	6734	3433	Cuttings	1.06	1164 FSL, 790 FWL	-107.54230	36.94735	Pawlewicz and others (1991)	
32-07-36-NE	NW Pipelineline San Juan 32-7 204	6472	3188	Cuttings	1.03	815 FNL, 2005 FEL	-107.51551	36.94156	Pawlewicz and others (1991)	
32-08-08-SE	Southland Royalty Trail Canyon 101	6730	3350	Cuttings	1.07	1850 FSL, 850 FEL	-107.69020	36.99660	Pawlewicz and others (1991)	
32-08-12-NE	Meridian Reese Mesa 104	7103	3760	Cuttings	1.19	840 FNL, 1465 FEL	-107.62162	36.99760	Pawlewicz and others (1991)	
32-08-13-NW	Southland Royalty Reese Mesa 100	7100	3950	Cuttings	1.15	1450 FNL, 805 FWL	-107.63153	36.97972	Amoco	
32-08-13-NW	Meridian Reese Mesa 100	7100	3961	Cuttings	1.15	1450 FNL, 805 FWL	-107.63145	36.98635	Pawlewicz and others (1991)	
32-08-20-SW	Pacific NW Pipelineline San Juan32-8 Unit	NA	3700	Cuttings	1.07	1600 FSL, 1150 FWL	-107.70225	36.96718	Amoco	
32-08-32-SE	Meridian Rattlesnake Canyon 102	6550	3440	Cuttings	0.93	1185 FSL, 1185 FEL	-107.69252	36.93645	Pawlewicz and others (1991)	
32-09-36-NE	Meridian San Juan 32-9 Unit 228	6592	3380	Cuttings	0.94	1160 FNL, 1350 FEL	-107.72642	36.94354	Pawlewicz and others (1991)	
32-10-11-NE	Meridian Carter Ute 100	6659	3270	Cuttings	1.09	1180 FNL, 1450 FEL	-107.84650	36.99815	Pawlewicz and others (1991)	
32-10-16-NE	Meridian Burroughs Com "A" 100	6367	3099	Cuttings	0.98	2025 FNL, 1625 FEL	-107.88338	36.98664	Pawlewicz and others (1991)	
32-10-16-SW	Meridian EPNG Com "C" 100	6767	3425	Cuttings	0.86	1850 FSL, 1487 FWL	-107.89029	36.98295	Pawlewicz and others (1991)	
32-10-17-SW	Amoco Decker Gas Com A	6115	2853	Cuttings	0.91	1550 FSL, 960 FWL	-107.91060	36.98202	Amoco	
32-10-20-SE	Meridian Oil Payne 6	6334	3109	Cuttings	0.83	1667 FSL, 805 FEL	-107.89817	36.96789	Amoco	
32-10-23-SE	Meridian Carter Ute 104	6650	3263	Cuttings	0.97	945 FSL, 720 FEL	-107.64790	36.96706	Pawlewicz and others (1991)	
32-10-24-NE	Amoco San Juan 32-9 Unit 104	6813	3263	Cuttings	0.97	1430 FNL, 1450 FEL	-107.83082	36.97299	Amoco	
32-10-27-SW	Amoco Keys Gas Com G 1	5952	2728	Cuttings	0.88	1480 FSL, 1620 FWL	-107.87207	36.95307	Amoco	
32-10-28-NE	Amoco Holmberg Gas Com C 1	6043	2824	Cuttings	0.97	1255 FNL, 1450 FEL	-107.88258	36.96002	Amoco	
32-10-29-NE	El Paso Scott 21	6058	2952	Cuttings	0.82	1760 FNL, 1860 FEL	-107.90197	36.95854	Amoco	
32-10-32-NE	Amoco State Gas Com-BW	5919	2690	Cuttings	0.91	790 FNL, 1480 FEL	-107.90800	36.96017	Amoco	
32-10-32-SW	Amoco State Gas Com-BX	6087	2848	Cuttings	0.79	1490 FSL, 1790 FWL	-107.90784	36.93852	Amoco	
32-10-33-NE	Amoco Ealum Gas Com C 1	5998	2562	Cuttings	0.86	1645 FNL, 1615 FEL	-107.88319	36.94444	Amoco	
32-10-33-NW	Amoco Cahn Gas Com 1	6012	2807	Cuttings	0.80	1030 FNL, 1600 FWL	-107.89037	36.94600	Amoco	
32-11-07-SW	Grt. West. Dr. J. E. Decker 10	6481	2937	Cuttings	0.71	1690 FSL, 1775 FWL	-108.03095	36.99683	Pawlewicz and others (1991)	
32-11-08-SW	Grt. West. Dr. Decker-11	6619	3135	Cuttings	0.77	910 FSL, 955 FWL	-108.01630	36.99491	Pawlewicz and others (1991)	
32-11-09-NW	Union Texas Petroleumroleum Ute 39	NA	2590	Cuttings	0.77	1195 FNL, 1750 FWL	-107.99610	36.99655	Fassett and Nuccio (1990)	
32-11-12-NW	Union Texas Petroleumroleum Ute 34	NA	2900	Cuttings	0.87	2470 FNL, 2260 FWL	-107.94200	36.99322	Fassett and Nuccio (1990)	
32-11-12-SE	Union Texas Petroleumroleum Ute 33	NA	3080	Cuttings	0.84	2210 FSL, 1220 FEL	-107.93606	36.99832	Fassett and Nuccio (1990)	
32-11-13-SW	Amoco Barnes B 21	6223	2926	Cuttings	0.76	1250 FSL, 800 FWL	-107.94687	36.98128	Amoco	
32-11-14-SW	Meridian Primo Mudge 100	NA	3090	Cuttings	0.79	1120 FSL, 1450 FWL	-107.96198	36.98068	Amoco	
32-11-16-NW	Northwest Pipelineline Cox Canyon Unit	NA	3572	Cuttings	0.75	890 FNL, 1525 FWL	-107.99684	36.98967	Amoco	
32-11-22-SW	Amoco Barnes Gas Com B 1	6475	3172	Cuttings	0.74	1180 FSL, 1390 FWL	-107.97930	36.96599	Amoco	

Table A4-1. Mean vitrinite reflectance values (R_m) for coal samples from the Fruitland Formation—*Continued*.

Point ID	Well Name	Elev.	Depth	Sample	R_m (%)	Footage	Longitude	Latitude	Source	
New Mexico—Continued										
32-11-23-NE	Amoco Barnes GC A-1	6251	2903	Cuttings	0.77	1090 FNL, 1530 FEL	-107.95487	36.97475	Pawlewicz and others (1991)	
32-11-23-SW	Amoco Barnes Gas Com C 1	6334	3059	Cuttings	0.76	1660 FSL, 1330 FWL	-107.96227	36.96758	Amoco	
32-11-24-SW	Meridian Primo Mudge 100	6348	3090	Cuttings	0.79	1120 FSL, 1450 FWL	-107.94480	36.96646	Fassett and Nuccio (1990)	
32-11-25-SW	Amoco Fields A 21	6325	3067	Cuttings	0.78	1330 FSL, 1150 FWL	-107.94626	36.95260	Amoco	
32-11-26-NE	Amoco Barnes Gas Com E E	6366	3086	Cuttings	0.83	1010 FNL, 1470 FEL	-107.95503	36.96049	Amoco	
32-11-26-NW	Tenneco Barnes	NA	3150	Cuttings	0.76	1520 FNL, 1490 FWL	-107.96188	36.95882	Amoco	
32-11-27-NE	Amoco Barnes A 20	6463	3122	Cuttings	0.76	1230 FNL, 800 FEL	-107.96972	36.95946	Amoco	
32-11-28-NE	Amoco Fields A 19	6287	2970	Cuttings	0.73	1940 FNL, 1180 FEL	-107.98841	36.95737	Amoco	
32-11-30-SE	Nassau Bettin' on Bisti 30 9	NA	1210	Cuttings	0.43	1980 FSL, 660 FEL	-108.02135	36.95414	Pawlewicz and others (1991)	
32-11-33-NE	Amoco Neal A 21	6132	2791	Cuttings	0.66	2305 FNL, 1120 FEL	-107.98882	36.94195	Amoco	
32-11-33-SW	Amoco Neal A-1	6181	2857	Cuttings	0.70	2140 FSL, 910 FWL	-107.99903	36.93992	Pawlewicz and others (1991)	
32-11-34-NE	Amoco Fields A 23	6149	2840	Cuttings	0.72	1580 FNL, 2270 FEL	-107.97548	36.94401	Amoco	
32-11-35-NE	Amoco Storey Gas Com B 1	6340	3056	Cuttings	0.73	1040 FNL, 1400 FEL	-107.95516	36.94596	Amoco	
32-12-08-SW	NMBMMR coal test hole	5958	205	Core	0.52	NA	-108.12056	36.99523	Hoffman (1991)	
32-12-12-SW	Great Western Dr. J. E. Decker 9	6252	2649	Cuttings	0.75	1506 FSL, 938 FWL	-108.05150	36.99788	Fassett and Nuccio (1990)	
32-12-14-SE	Outcrop Prewitt mine	NA	Surface	Outcrop	0.58	624 FSL, 1618 FEL	-108.10833	37.00969	Law (1990)	
32-12-21-NW	Aztec Culpepper-Martin 102	NA	2127	Cuttings	0.65	990 FNL, 1650 FWL	-108.10293	36.97612	Amoco	
32-12-25-NE	Amoco Moore GC B-1	6423	2740	Cuttings	0.61	1570 FNL, 1030 FEL	-108.04042	36.9594	Pawlewicz and others (1991)	
32-12-27-NE	Amoco Moore D	6189	2557	Cuttings	0.67	1180 FNL, 1570 FEL	-108.07821	36.96106	Amoco	
32-12-28-SW	Meridian Culpepper Martin 103	5790	2350	Cuttings	0.65	1335 FSL, 1845 FWL	-108.10228	36.95349	Pawlewicz and others (1991)	
32-13-13-SW	NMBMMR coal test hole	6050	293	Core	0.54	NA	-108.14842	36.98517	Hoffman (1991)	
32-13-14-SE	NMBMMR coal test hole	6072	152	Core	0.52	NA	-108.17045	36.98026	Hoffman (1991)	
32-13-28-SW	NMBMMR coal test hole	6032	387	Core	0.54	NA	-108.21223	36.95578	Hoffman (1991)	
Colorado										
32c-03-22-NE	Stanolind, S. Ute 1	7188	1950	Cuttings	0.79	NE NW NE	-107.15954	37.01003	Law (1990)	
32c-05-08-SE	Amoco Seibel Gas Unit A 1	6153	2702	Cuttings	1.44	690 FSL, 860 FEL	-107.40877	37.02717	Amoco	
32c-06-02-SE	Tiffany Gas Glover 1	6490	3084	Cuttings	1.22	1650 FSL, 990 FEL	-107.46337	37.04379	Amoco	
32c-06-15-NW	Pac. NW Pipeline. Arboles 32-6	6197	2640	Cuttings	1.29	1525 FNL, 1525 FWL	-107.49076	37.0204	Law (1990)	
32c-06-19-NW	Meridian Oil Allison Unit 136	6681	3250	Cuttings	1.17	2360 FNL, 925 FWL	-107.54677	37.00325	Amoco	
32c-06-20-NW	Meridian Oil Allison Unit 116	6385	2940	Cuttings	1.26	1850 FNL, 880 FWL	-107.52919	37.00459	Amoco	
32c-07-04-SE	Mobil Oil Colorado 32-7 10-2	NA	2554	Cuttings	1.11	1476 FSL, 895 FEL	-107.60759	37.04278	Amoco	
32c-07-14-SW	Bakke W E Oil Ute	NA	3180	Cuttings	1.02	1000 FSL, 1000 FWL	-107.58283	37.01268	Amoco	
32c-07-16-NW	Sohio S. Ute 15-16	6373	3450	Cuttings	1.23	1167 FNL, 1024 FWL	-107.61899	37.02101	Law (1990)	
32c-07-16-SW	Bakke W E Oil Southern Ute	NA	2040	Cuttings	1.03	1265 FSL, 990 FWL	-107.61921	37.01328	Amoco	
32c-10-02-NE	NCRA S. Ute 2-3	NA	2888	Cuttings	1.13	1035 FNL, 1280 FEL	-107.89780	37.05027	Law (1990)	
32c-10-03-SE	Ladd Cox Canyon 2-3	6602	3105	Core	1.05	1600 FSL, 1600 FEL	-107.91660	37.0433	Law (1990)	
32c-10-05-SW	Amoco SO Ute Tribal XX PLA 9	7281	3780	Cuttings	1.00	1650 FSL, 2360 FWL	-107.95739	37.04366	Amoco	
32c-10-07-SE	Amoco Southern Ute Tribal J	6649	3195	Cuttings	1.05	1470 FSL, 1990 FEL	-107.97229	37.02877	Amoco	
32c-10-10-NE	Pac. NW Pipeline. NW Cedar Hill 8-10	6411	3010	Cuttings	1.12	SE NW SE	-107.91664	37.03611	Law (1990)	
32c-10-11-NE	Meridian Oil Carter Ute 100	6659	3270	Cuttings	1.09	1180 FNL, 1450 FEL	-107.89827	37.03540	Amoco	

Table A4-1. Mean vitrinite reflectance values (R_m) for coal samples from the Fruitland Formation—*Continued*.

Point ID	Well Name	Elev.	Depth	Sample	R_m (%)	Footage	Longitude	Latitude	Source	
Colorado—Continued										
32c-10-12-NE	Amoco MH Montgomery GU APLA-9 1	6219	2779	Cuttings	1.09	1610 FNL, 1040 FEL	-107.87902	37.03404	Amoco	
32c-10-12-NE	Pacific NW Pipelineline NW Cedar Hill 7-12	6025	2600	Cuttings	1.15	NE NE NE	-107.87662	37.03755	Law (1990)	
32c-10-15-SW	Amoco Southern Ute 32-10 15-3	6466	3118	Cuttings	0.94	1610 FSL, 1390 FWL	-107.92425	37.01448	Amoco	
32c-10-16-SW	Amoco Southern Ute 32-10 16.2	6364	3027	Cuttings	0.88	1765 FSL, 1990 FWL	-107.94054	37.01499	Amoco	
32c-10-17-SW	Amoco GRI Observation	NA	3151	Cuttings	0.90	1880 FSL, 1530 FWL	-107.96015	37.01547	Amoco	
32c-10-18-NW	Amoco Southern Ute Tribal H 1	6583	3118	Cuttings	1.02	830 FNL, 1040 FWL	-107.97989	37.02247	Amoco	
32c-10-19-NW	Amoco Clark/Cummins GU A PLA-9 1	6553	3241	Cuttings	0.89	2250 FNL, 1420 FWL	-107.97852	37.00415	Amoco	
32c-10-20-NE	Amoco Hendrickson GU B PLA-9 1	6638	3258	Cuttings	0.90	2240 FNL, 1580 FWL	-107.95296	37.00404	Amoco	
32c-10-20-NW	Amoco Hendrickson GU A PLA-9 1	6481	3113	Cuttings	0.88	2590 FNL, 1490 FWL	-107.96031	37.00313	Amoco	
32c-10-22-NW	Amoco JB Gardner GU APLA-9 1	6255	2929	Cuttings	0.95	2150 FNL, 1120 FWL	-107.92546	37.00412	Amoco	
32c-10-22-SW	Pacific NW Pipeline NW Cedar Hill 32-10	NA	2980	Cuttings	0.93	1190 FSL, 1190 FWL	-107.92525	37.00328	Amoco	
32c-10-23-NW	Amoco Robin Frazier GU APLA-9 1	6320	2985	Cuttings	0.98	1000 FNL, 990 FWL	-107.90739	37.00731	Amoco	
32c-10-23-SE	Meridian Oil Inc Carter Ute 104	6650	3240	Cuttings	0.97	945 FSL, 720 FEL	-107.89586	37.00269	Amoco	
32c-11-07-NE	Amax O&G Southern Ute 5-7	6204	1448	Cuttings	0.80	1020 FNL, 1050 FEL	-108.07748	37.03668	Amoco	
32c-11-07SE	Ladd S. Ute 1-7	6150	1690	Cuttings	0.74	1320 FSL, 1260 FEL	-108.07823	37.02866	Law (1990)	
32c-11-09-NW	Union Texas Petroleum Ute	NA	2590	Cuttings	0.77	1195 FNL, 1750 FWL	-108.04978	37.03609	Amoco	
32c-11-12-NW	Union Texas Petroleum Ute	NA	2900	Cuttings	0.87	2470 FNL, 2260 FWL	-107.99391	37.03242	Amoco	
32c-11-12-SE	Union Texas Petroleum Ute	NA	3080	Cuttings	0.84	2210 FSL, 1220 FEL	-107.98768	37.03088	Amoco	
32c-12-12-NW	Outcrop	NA	0	Outcrop	0.70	961 FSL, 1000 FWL	-108.10621	37.03679	Amoco	
33-02-32-NE	Outcrop-coal mine	NA	Surface	Outcrop	0.64	1266 FNL, 2282 FEL	-108.15638	36.97805	Law (1990)	
33-03-16-SW	Outcrop Cat Creek Gap	NA	Surface	Outcrop	0.64	372 FSL, 1527 FWL	-107.08975	37.06405	Law (1990)	
33-05-10-NW	Amoco Canderlaria	NA	2750	Cuttings	1.42	600 FNL, 2285 FWL	-107.38034	37.12490	Amoco	
33-06-03-NW	Amoco Southern Ute Tribal-B	7441		Cuttings	1.42	1020 FNL, 990 FWL	-107.49263	37.13753	Amoco	
33-06-17-NW	Perlman William Southern Ute 17-2	6750		Cuttings	1.60	1240 FNL, 1560 FWL	-107.52682	37.10770	Amoco	
33-06-18-NE	Perlman Baird 18-2	6698	3170	Core	1.41	1490 FNL, 1000 FEL	-107.53565	37.10709	Law (1990)	
33-06-20-SW	Perlman Hott 20-2	6610	3130	Core	1.49	1500 FSL, 1360 FWL	-107.52737	37.08633	Law (1990)	
33-06-21-SE	Amoco Southern Ute Tribal C 4	6926		Cuttings	1.55	1000 FSL, 1120 FEL	-107.49999	37.08540	Amoco	
33-06-21-SW	Amoco Southern Ute Tribal C 1	6722		Cuttings	1.55	1190 FSL, 990 FWL	-107.51053	37.08578	Amoco	
33-06-29-NW	Amoco HOTT Unit 2	6566	3104	Cuttings	1.51	1150 FNL, 1755 FWL	-107.52604	37.07904	Amoco - GRI	
33-06-33-NW	Amoco Southern Ute Gas Unit AA 1	6806	2732	Cuttings	1.25	830 FNL, 810 FWL	-107.51118	37.06563	Amoco - GRI	
33-07-17-NW	Stanolind Ute 6-B	6515	2740	Cuttings	1.23	2310 FWL, 2310 FNL	-107.63257	37.10495	Law (1990)	
33-07-20-SW	Amoco S Ute Gas Unit AA 1	6607	2723	Cuttings	1.31	1650 FSL, 1630 FWL	-107.63510	37.08695	Amoco	
33-07-21-NW	Amoco Southern Ute Gas 3	6383	2402	Cuttings	1.31	1070 FNL, 1650 FWL	-107.61686	37.09374	Amoco	
33-07-28-NW	Amoco Salvador Gas Unit A 1	6364	2452	Cuttings	1.28	1060 FNL, 1150 FWL	-107.61858	37.07929	Amoco	
33-07-30-NW	Amoco Simms Gas Unit E 1	6491	2738	Cuttings	1.41	820 FNL, 1630 FWL	-107.65298	37.08000	Amoco	
33-07-34-SE	Pac. NW Pipeline. Ignacio 3-34	6623	2890	Cuttings	1.26	1450 FSL, 1190 FEL	-107.59053	37.05717	Law (1990)	
33-08-01-SW	Pac. NW Pipeline. Ignacio 2-1	6644	2740	Cuttings	1.28	1850 FSL, 1320 FWL	-107.67229	37.13098	Law (1990)	
33-08-07-NW	Amerada Fassett 1	6658	2850	Cuttings	1.29	990 FNL, 1650 FWL	-107.76237	37.12278	Law (1990)	
33-08-10-NE	Amoco Ford Gas Unit A 1	6664		Cuttings	1.43	1150 FNL, 1100 FEL	-107.69882	37.12257	Amoco	
33-08-16-NW	Amerada Herrera 1	6692	2890	Cuttings	1.16	1320 FNL, 1320 FWL	-107.72673	37.10762	Law (1990)	
33-08-23-NE	Amoco Pan American Fee	NA	2950	Cuttings	1.40	1090 FNL, 1020 FEL	-107.68033	37.09374	Amoco	

Table A4-1. Mean vitrinite reflectance values (R_m) for coal samples from the Fruitland Formation—*Continued*.

Point ID	Well Name	Elev.	Depth	Sample	R_m (%)	Footage	Longitude	Latitude	Source	
Colorado—Continued										
33-09-04-SE	Amoco John Barnes Gas Unit A PLA-6 1	6280	2664	Cuttings	1.32	1210 FSL, 1460 FEL	-107.82665	37.12899	Amoco	
33-09-06-SE	Amoco Clovis Gas Unit A 1	6473	2722	Cuttings	1.28	435 FSL, 1880 FEL	-107.86379	37.12683	Amoco	
33-09-07-NE	Amoco Lyle Short Gas Unit A 1	6467	2805	Cuttings	1.42	1630 FNL, 1590 FEL	-107.86280	37.12114	Amoco	
33-09-07-SE	Pac. NW Pipeline. Bondad 17-7	6453	2490	Cuttings	1.09	1420 FSL, 1100 FEL	-107.86120	37.11502	Law (1990)	
33-09-08-NW	Amoco Clovis Gas Unit B	6460	2721	Cuttings	1.36	2506 FNL, 115 FWL	-107.85695	37.11870	Amoco	
33-09-13-NW	Pac. NW Pipeline. Bondad 7-13	6678	2930	Cuttings	1.36	1070 FNL, 1340 FWL	-107.78135	37.10808	Law (1990)	
33-09-16-SE	NCRA Southern Ute 504 7-16	6670	3070	Cuttings	1.32	2200 FSL, 900 FEL	-107.82490	37.10272	Amoco	
33-09-16-SE	NCRA S. Ute Unit 504 2-16	6692	3158	Cuttings	1.34	880 FSL, 1280 FEL	-107.82618	37.09912	Law (1990)	
33-09-18-SE	Amoco Roy Eshelman Gas Unit PLA-6	6411	2842	Cuttings	1.21	1640 FSL, 1400 FEL	-107.86230	37.10103	Amoco	
33-09-19-SE	Amoco Raymond Koon Gas Unit A PLA-6 1	6357	2899	Cuttings	1.28	2270 FSL, 1450 FEL	-107.86253	37.08827	Amoco	
33-10-01-SE	Meridian Bondad 33-10 Com 104	6263	2980	Cuttings	1.13	1400 FSL, 1135 FEL	-107.87938	37.12950	Pawlewicz and others (1991)	
33-10-03-SE	Amoco Frank Davis Gas Unit A PLA-6 1	6392	2615	Cuttings	1.09	1610 FSL, 2010 FEL	-107.91859	37.13012	Amoco	
33-10-08-NW	Enervest Black Ridge SU 8-2	NA	3151	Cuttings	1.13	1545 FNL, 1360 FWL	-107.96126	37.12155	EnerVest SJ Op.	
33-10-11-SE	Amoco Presentacion Medina Gas Unit 1	6213	2561	Cuttings	1.22	1010 FSL, 1620 FEL	-107.89926	37.11378	Amoco	
33-10-13-SE	Amoco S Ute Tribal Gas Unit QQ PLA-6 1	6175	2603	Cuttings	1.21	1560 FSL, 1530 FEL	-107.88078	37.10078	Amoco	
33-10-14-NW	Amoco Thomas Jacques Gas Unit A PLA-6 1	6323	2694	Cuttings	1.21	1650 FNL, 1070 FWL	-107.90798	37.10654	Amoco	
33-10-15-SE	Amoco Thomas Jacques Gas Unit B PLA-6 1	6319	2638	Cuttings	1.15	1640 FSL, 1290 FEL	-107.91608	37.10129	Amoco	
33-10-17-NE	Emerald Gas Operating Black Ridge 17-2	7588	2842	Cuttings	1.10	845 FNL, 1705 FEL	-107.95361	37.10908	Pawlewicz and others (1991)	
33-10-17-SE	Enervest Black Ridge SU 17-1 (Dev)	NA	3191	Cuttings	1.15	1126 FSL, 1338 FEL	-107.95226	37.10005	EnerVest SJ Op.	
33-10-23-NW	Amoco Thomas Jacques Gas Unit F 1	6254	2721	Cuttings	1.17	990 FNL, 1110 FWL	-107.90776	37.09399	Amoco	
33-10-25-SE	Amoco MF Sharp Gas Unit A PLA-6 1	6088	2536	Cuttings	1.18	1210 FSL, 990 FEL	-107.87891	37.07076	Amoco	
33-10-25-SW	Amoco Sharp Gas Unit	NA		Cuttings	1.07	1510 FSL, 1440 FWL	-107.88860	37.07138	Amoco	
33-10-28-NW	Amoco Southern Ute 28-3, 33-10 PLA-6	NA	3145	Cuttings	1.06	1070 FNL, 2180 FWL	-107.94019	37.07942	Amoco	
33-10-30-NW	Palo Petroleum Eldridge 30-1	6680	3185	Cuttings	1.06	1774 FNL, 1017 FWL	-107.98024	37.07805	Amoco	
33-10-31-NW	Palo Petroleum Eldridge 31-1	6564	3096	Cuttings	1.08	990 FNL, 1002 FWL	-107.98022	37.06577	Amoco	
33-10-33-SE	Amoco Cyrus Johnson Gas Unit A PLA 6	6569	3192	Cuttings	1.16	1410 FSL, 1280 FEL	-107.93379	37.05719	Amoco	
33-10-34-NW	Pac. NW Pipeline. Bondad 2-34	6575	2685	Cuttings	1.03	1650 FNL, 990 FWL	-107.92600	37.06321	Law (1990)	
33-10-35-SE	NCRA S. Ute Unit 503 4-35	6288	2852	Cuttings	1.16	1315 FSL, 1880 FEL	-107.89995	37.05673	Law (1990)	
33-11-12-200	Meridian Ute 200	7060	3470	Cuttings	1.02	725 FSL, 1165 FEL	-107.98793	37.11363	Pawlewicz and others (1991)	
33-11-12-NW	Meridian Ute 201	7004	3275	Cuttings	0.91	2030 FNL, 1790 FWL	-107.99558	37.12066	Pawlewicz and others (1991)	
33-11-13-SE	Palo Petroleum Southern Ute 13 1	6777	3435	Cuttings	1.01	1274 FSL, 1538 FEL	-107.98910	37.10097	Amoco	
33-11-14-NW	Palo Petroleum Southern Ute 14 1	7104	3442	Cuttings	1.01	1805 FNL, 1791 FWL	-108.01402	37.10674	Amoco	
33-11-14-SE	Palo Petroleum Southern Ute 14 2	6820	3264	Cuttings	1.08	1300 FSL, 1350 FEL	-108.00693	37.10104	Amoco	
33-11-20-NE	Enervest Valencia Canyon SU 20-4	6678	1408	Cuttings	0.79	1597 FNL, 330 FEL	-108.05723	37.09251	EnerVest SJ Op.	
33-11-20-SE	Enervest Valencia Canyon SU 20-1	6596	1450	Cuttings	0.79	1083 FSL, 1098 FEL	-108.05979	37.08557	EnerVest SJ Op.	
33-11-23-NW	Palo Petroleum Southern Ute 23 1	6782	3218	Cuttings	1.03	1596 FNL, 1507 FWL	-108.01505	37.09287	Amoco	
33-11-23-SE	Palo Petroleum Southern Ute 23 2	6669	3140	Cuttings	1.01	1377 FSL, 2613 FEL	-108.01111	37.08675	Amoco	
33-11-24-NW	Palo Petroleum Southern Ute 24 1	6665	3124	Cuttings	1.04	890 FNL, 1390 FWL	-107.99742	37.09506	Amoco	
33-11-27-SE	MonSanto Ute 1	6736	3120	Cuttings	0.92	1650 FEL, 1650 FSL	-108.02570	37.07286	Law (1990)	
33-11-29-NW	Enervest Valencia Canyon SU 29-2	6523	1291	Cuttings	0.76	1818 FNL, 2500 FWL	-108.06528	37.07766	EnerVest SJ Op.	
33-11-29-SE	Enervest Valencia Canyon SU 29-1	6443	1963	Cuttings	0.73	740 FSL, 845 FEL	-108.05887	37.07010	EnerVest SJ Op.	

Table A4-1. Mean vitrinite reflectance values (R_m) for coal samples from the Fruitland Formation—*Continued*.

Point ID	Well Name	Elev.	Depth	Sample	R_m (%)	Footage	Longitude	Latitude	Source	
Colorado—Continued										
33-11-30-NE	Enervest Valencia Canyon SU 30-4	6471	422	Cuttings	0.68	1841 FNL, 775 FEL	-108.07658	37.07761	EnerVest SJ Op.	
33-11-31-NE	Enervest Valencia Canyon SU 31-4	6280	621	Cuttings	0.70	1167 FNL, 1204 FEL	-108.07810	37.06506	EnerVest SJ Op.	
33-11-31-SE	Enervest Valencia Canyon SU 31-1	6366	956	Cuttings	0.71	2019 FSL, 1324 FEL	-108.07842	37.05950	EnerVest SJ Op.	
33-11-32-NW	Enervest Valencia Canyon SU 32-2	6352	1415	Cuttings	0.75	2005 FNL, 1320 FWL	-108.06936	37.06262	EnerVest SJ Op.	
33-11-32-SE	Enervest Valencia Canyon SU 32-1	6320	1950	Cuttings	0.74	1157 FSL, 2474 FEL	-108.06432	37.05690	EnerVest SJ Op.	
33-11-33-NW	Meridian Southern Ute 300	6435	2480	Cuttings	0.73	1850 FNL, 1255 FWL	-108.05155	37.06299	EnerVest SJ Op.	
33-11-34-NW	Palo Petroleum Southern Ute 34 1R	NA	3091	Cuttings	0.93	1304 FNL, 1542 FWL	-108.03261	37.06458	Amoco	
33-11-35-SE	Palo Petroleum Southern Ute 35 1	6432	2870	Cuttings	0.97	1465 FSL, 1782 FEL	-108.00815	37.05763	Amoco	
33-11-36-SE	Palo Petroleum Eldridge 36 2	6459	3000	Cuttings	1.01	1168 FSL, 1029 FEL	-107.98709	37.05690	Amoco	
34n-05-09-NE	Outcrop Yellow Jacket	NA	Surface	Outcrop	0.79	1395 FNL, 1170 FEL	-107.42036	37.23394	Law (1990)	
34n-06-18-NW	Amoco Beaver Creek Gas Unit B 1	6819	2190	Cuttings	1.24	1470 FNL, 1650 FWL	-107.57199	37.21742	Amoco	
34n-07-01-SE	Amoco Taliaferro Trust Gas Unit A 1	7055	1666	Cuttings	1.02	1740 FSL, 1640 FEL	-107.58359	37.24090	Amoco	
34n-07-06-SW	Natomas North Gearhart 1-6	7123		Cuttings	1.20	1485 FSL, 1935 FWL	-107.68009	37.24076	Amoco	
34n-07-15-NW	M. Anderson Sitton&Gray 1	6825	2340	Cuttings	1.27	C NE NW	-107.62443	37.2209	Law (1990)	
34n-08-02-SE	Pan American Keyes	NA	2202	Cuttings	1.42	1980 FSL, 720 FEL	-107.70712	37.24213	Amoco - GRI	
34n-08-10-SW	Perlman William Mayfield 1-10U	6862		Cuttings	1.57	1125 FSL, 1325GEL	-107.73670	37.22547	Amoco - GRI	
34n-08-18-SE	Fuelco Sun-Tyner Lunt 1	6778	2720	Cuttings	1.46	1783 FSL, 1946 FEL	-107.78415	37.21981	Law (1990)	
34n-09-04-NW	Outcrop	NA	0	Outcrop	0.80	2153 FNL, 2097 FEL	-107.86366	37.23891	Amoco	
34s-04-30-NE	Outcrop Chimney Rock Mine	NA	Surface	Outcrop	0.86	2150 FNL, 2120 FEL	-107.32296	37.16369	Law (1990)	
34s-05-32-SE	Amoco Pargin Mountain Unit 3	6653	3109	Cuttings	1.66	740 FSL, 2360 FEL	-107.41442	37.14313	Amoco	
34s-05-35-SW	Amoco Bull Creek Federal A 1	6376	2032	Cuttings	1.49	640 FSL, 1360 FWL	-107.36549	37.14270	Amoco	
34s-06-14-NE	Amoco Pargin Mounatin Unit 2	8730	5166	Cuttings	1.59	550 FNL, 1600 FEL	-107.46553	37.19684	Amoco	
34s-06-14-NE	Lecada Natural Federal	NA		Cuttings	1.63	1450 FNL, 1120 FEL	-107.46384	37.19438	Amoco	
34s-06-19-SE	Amoco Boone Gas Unit 1	6909	2874	Cuttings	1.40	1090 FSL, 1850 FEL	-107.53840	37.17207	Amoco	
34s-06-20-NW	Natomas Smith 1-20	7058	2900	Cuttings	1.28	1470 FNL, 990 FWL	-107.52849	37.17946	Law (1990)	
34s-07-20-NW	Amoco HN Pearson A 1	6804	2783	Cuttings	1.34	1650 FNL, 1080 FWL	-107.63678	37.17926	Amoco	
34s-07-21-NE	Perlman S. Ute 21-1	6825	2220	Core	1.28	990 FNL, 990 FEL	-107.60762	37.18116	Law (1990)	
34s-07-23-SE	Perlman S. Ute 23-1	6731	2311	Core	1.30	1550 FSL, 18440 FEL	-107.57418	37.17346	Law (1990)	
34s-07-25-NW	Amoco Gary Beebe Gas Unit A 1	6739	2783	Cuttings	1.36	1010 FNL, 1210 FWL	-107.56368	37.16633	Amoco	
34s-08-11-SW	Perlman William Mayfield 1-11U	6883		Cuttings	1.60	1440 FSL, 1210 FWL	-107.69084	37.20248	Amoco	
34s-08-20-SW	Perlman William McCaw 20-1	6709		Cuttings	1.56	860 FSL, 550 FWL	-107.74784	37.17149	Amoco	
34s-08-25-SE	S Ute Dpt Energy Oxford 1	NA	2819	Core	1.37	2142 FSL, 542 FEL	-107.66048	37.16064	Kelso and Rushworth (1982)	
34s-08-25-SW	S Ute Dpt Energy Oxford 2	6706	2840	Cuttings	1.44	1120 FSL, 2450 FWL	-107.66840	37.15790	Kelso and Rushworth (1982)	
34s-08-36-SE	Amoco Southern Ute Tribal	NA	2794	Cuttings	1.40	1120 FSL, 1650 FEL	-107.66435	37.14343	Amoco	
34s-09-12-Se	Tenneco Larson 1-12	6927	2311	Core	1.34	1550 FSL, 1400 FEL	-107.77259	37.20269	Law (1990)	
34s-09-13-NE	Tenneco Fassett 2-13	6848	2504	Core	1.54	1650 FNL, 1850 FEL	-107.77423	37.19384	Law (1990)	
34s-09-15-NW	Amoco Linder Gas Unit A 1	NA	2664	Cuttings	1.30	1407 FNL, 1976 FWL	-107.81420	37.19445	Amoco	
34s-09-16-SE	Amoco McMahan Gas Unit A 1	6841	2701	Cuttings	1.50	1030 FSL, 2020 FEL	-107.82797	37.18652	Amoco	
34s-09-19-NE	Amoco Weasel Skin Gas Unit 1	6638	2484	Cuttings	1.33	380 FNL, 160 FEL	-107.85790	37.18282	Amoco	
34s-09-21-NE	Amoco Simon Land and Cattle 21U-1R Unit 1	6801	2756	Cuttings	1.37	1250 FNL, 1180 FEL	-107.82510	37.18027	Amoco	
34s-09-22-SE	Amoco Roger D. Kelly Gas Unit 1	6778	2771	Cuttings	1.49	1600 FSL, 1325 FEL	-107.80894	37.17369	Amoco	

Table A4-1. Mean vitrinite reflectance values (R_m) for coal samples from the Fruitland Formation—*Continued*.

Point ID	Well Name	Elev.	Depth	Sample	R_m (%)	Footage	Longitude	Latitude	Source
Colorado—Continued									
34s-09-26-NW	Amoco Cugnini Gas Unit A 1	6764	2956	Cuttings	1.55	1490 FNL, 910 FWL	-107.80112	37.16515	Amoco
34s-09-27-NW	Greenbrier & Mendota Simon 1	6787	2805	Cuttings	1.24	W1/2 NW NW	-107.81993	37.16743	Law (1990)
34s-09-36-NW	Amoco Federal Land Bank Unit C 1	6697	3033	Cuttings	1.64	1030 FNL, 1530 FWL	-107.78099	37.15179	Amoco
34s-10-11U-SE	Enervest Indian Creek SU 11U-1	6891	2207	Cuttings	0.99	946 FSL, 1559 FEL	-107.89884	37.20025	EnerVest SJ Op.
34s-10-12U-NW	Enervest Indian Creek SU 12U-2	6696	2163	Cuttings	1.05	1562 FNL, 1906 FWL	-107.88682	37.20777	EnerVest SJ Op.
34s-10-12U-SE	Enervest Indian Creek Wheeler 12U-1	6574	2412	Cuttings	1.15	1150 FSL, 2298 FEL	-107.88330	37.20089	EnerVest SJ Op.
34s-10-13-NW	Enervest Indian Creek Wheeler 13-2	6539	2552	Cuttings	1.17	1792 FNL, 2464 FWL	-107.88494	37.19277	EnerVest SJ Op.
34s-10-13-SE	Enervest Indian Creek SU 13-1	6285	2386	Cuttings	1.22	943 FSL, 1646 FEL	-107.88100	37.18615	EnerVest SJ Op.
34s-10-14-NW	Enervest Indian Creek SU 14-2	6923	2510	Cuttings	1.02	1456 FNL, 1797 FWL	-107.90526	37.19384	EnerVest SJ Op.
34s-10-14-SE	Enervest Indian Creek SU 14-1	6646	2626	Cuttings	1.14	1681 FSL, 1626 FEL	-107.89908	37.18824	EnerVest SJ Op.
34s-10-15-NE	Enervest 44 Canyon SU 15-4	6835	1513	Cuttings	0.90	1340 FNL, 1053 FEL	-107.91511	37.19422	EnerVest SJ Op.
34s-10-15-SE	Enervest 44 Canyon Wheeler 15-1	6632	2397	Cuttings	1.05	1003 FSL, 1774 FEL	-107.91760	37.18636	EnerVest SJ Op.
34s-10-16-SE	Enervest 44 Canyon Wheeler 16-1	NA	1367	Cuttings	0.81	646 FSL, 857 FEL	-107.93256	37.18523	EnerVest SJ Op.
34s-10-21-SE	Enervest 44 Canyon McCulloch 21-2	6803	2847	Cuttings	0.98	1097 FSL, 1321 FEL	-107.93415	37.17208	EnerVest SJ Op.
34s-10-22-NW	Enervest Indian Creek Wheeler 22-2	6790	2831	Cuttings	1.10	1758 FNL, 1187 FWL	-107.92548	37.17866	EnerVest SJ Op.
34s-10-22-SE	Enervest Indian Creek Wheeler 22-3	NA	2774	Cuttings	1.15	1000 FSL, 1573 FEL	-107.91683	37.17200	EnerVest SJ Op.
34s-10-23-NW	Enervest Indian Creek Wheeler 23-2	6607	2770	Cuttings	1.10	1070 FNL, 1758 FWL	-107.90538	37.18072	EnerVest SJ Op.
34s-10-24-NW	Enervest Indian Creek SU 24-2	6380	2490	Cuttings	1.16	2180 FNL, 1548 FWL	-107.88823	37.17762	EnerVest SJ Op.
34s-10-28-NW	Enervest 44 Canyon McCulloch 28-2	6927	3196	Cuttings	1.14	1557 FWL, 1856 FNL	-107.94240	37.16384	EnerVest SJ Op.
34s-10-36-NE	McKenzie Methane Southern Ute-Mobil 36-1	6247	2441	Cuttings	1.34	1445 FNL, 1130 FEL	-107.87928	37.15074	Amoco
34s-11-36-SE	Enervest Bridge Timber SU 36-1	7662	4048	Cuttings	1.07	1413 FSL, 1206 FEL	-107.98826	37.14418	Pawlewicz and others (1991)
35-06-14-N1/2	Outcrop	NA	Surface	Outcrop	0.57	1856 FNL, 2332 FEL	-107.49555	37.30275	Law (1990)
35-06-16-NE	Outcrop	NA	0	Outcrop	0.80	1234 FNL, 1612 FEL	-107.52930	37.30449	Amoco
35-06-30-SE	Amoco Parry Gas Company Gas Unit B 1	7089	1455	Cuttings	0.96	2350 FSL, 430 FEL	-107.56160	37.27168	Amoco
35-06-32-NW	Natomas Jones 1-32	7107	1730	Cuttings	0.92	1735 FL, 1320 FNL	-107.55409	37.26151	Law (1990)
35-06-34-NW	Amoco Sauls Creek 1	7259	2331	Cuttings	1.13	900 FNL, 1410 FWL	-107.51894	37.26250	Amoco
35-07-08-N1/2	Outcrop	NA	Surface	Outcrop	0.56	1964 FNL, 2362 FEL	-107.65777	37.3178	Law (1990)
35-07-14-NW	Outcrop	NA	0	Outcrop	0.81	2016 FNL, 1416 FWL	-107.60881	37.30286	Amoco
35-07-15-SE	Amoco Gurr Federal Gas Unit 1	7271	1032	Cuttings	0.90	1130 FSL, 1060 FEL	-107.61744	37.29717	Amoco - GRI
35-07-19-NW	Amoco Wilbourn Federal Gas Unit 1	7692	1898	Cuttings	1.15	1080 FNL, 2070 FWL	-107.67935	37.29176	Amoco
35-07-22-NE	Amoco Huntington Gas Unit A 1	7379	1595	Cuttings	1.06	2380 FNL, 1905 FEL	-107.62027	37.28749	Amoco
35-07-23-SW	Amoco Cibrad Gas Unit A 1	7178	1454	Cuttings	1.04	770 FSL, 880 FWL	-107.61057	37.28182	Amoco
35-07-31-SE	Amoco Gearhart Gas Unit A 1	7257	2219	Cuttings	1.49	950 FSL, 730 FEL	-107.67046	37.25387	Amoco
35-07-35-NW	Amoco Robert Dulin Gas Unit 1	7024	1602	Cuttings	1.13	1630 FNL, 205 FWL	-107.61295	37.26063	Amoco
35-08-36-SE	Amoco State of Colorado AV 1	7197	2004	Cuttings	1.35	1780 FSL, 2010 FEL	-107.69357	37.25627	Amoco
35-08-36-SW	M. Anderson State 1	7288	2123	Cuttings	1.23	676 FSL, 662 FWL	-107.70248	37.25324	Law (1990)
35-09-24-NE	Outcrop	NA	0	Outcrop	0.66	1425 FNL, 1436 FEL	-107.80010	37.29042	Amoco
35-09-27-SW	Outcrop	NA	0	Outcrop	0.80	1150 FSL, 2006 FWL	-107.84067	37.26718	Amoco
35-09-35-SE	Enervest 44 Canyon Day-V-Ranch 35-2	6988	2110	Cuttings	1.24	535 FSL, 2476 FEL	-107.82184	37.25264	EnerVest SJ Op.
35-09-36-SE	Fuel ResourceS State 36-2	7110	2400	Cuttings	1.29	683 FSL, 1643 FEL	-107.80078	37.25338	Amoco
35-09-36-SE	Natomas State 1-36	7115	2400	Cuttings	1.29	905 FSL, 1825 FEL	-107.80142	37.25398	Law (1990)

Appendix 5—Isostatic-Residual-Gravity Anomaly Map of the San Juan Basin Area (from Heywood, 1992)

The Heywood (1992) map is a scanned image of the original illustration. The overlay of vitrinite-reflectance contour lines, dikes, and sills are from figure 37.

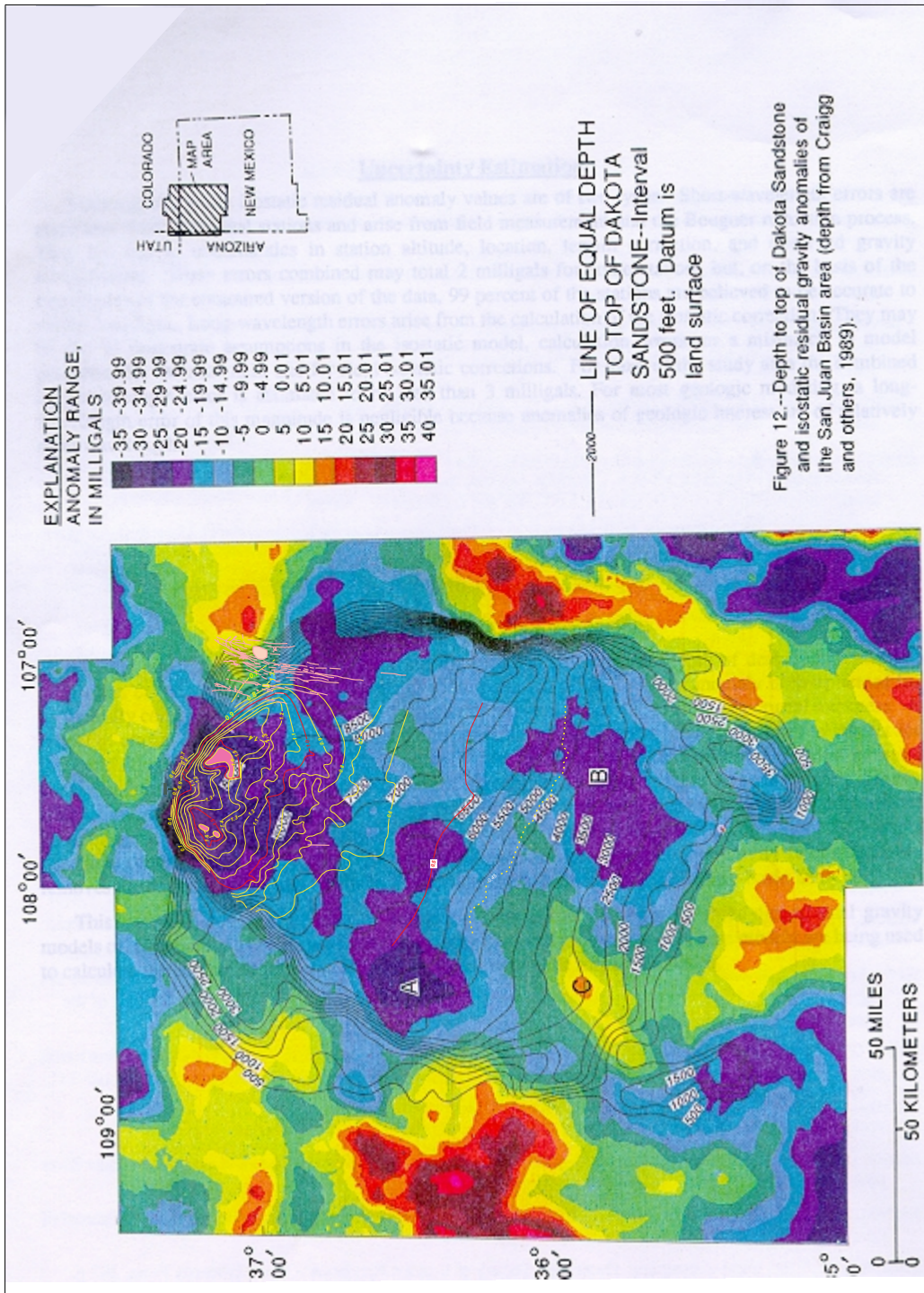


Figure A5-1. Isostatic residual gravity anomalies of the San Juan Basin area (modified from figure 12 of Heywood, 1992). Overlay of vitrinite-reflectance contour lines and dikes and sills from figure 37.

Appendix 6—Tables and Figures for Fruitland Formation Coal Resources in Various Categories for the San Juan Basin

Five tables labeled A6-1 through A6-5 contain coal resources in millions of short tons by quadrangle, township, surface ownership, coal ownership, and overburden categories, respectively. Four figures labeled A6-1 through A6-4 show 7½-minute quadrangles, surface ownership, coal ownership, and distribution of Fruitland coal in standard USGS categories, respectively.

Table A6-1. Estimated Fruitland Formation coal resources (in millions of short tons) in five overburden categories by 7.5' quadrangle and State in beds 1.2 ft thick or greater, San Juan Basin, Colorado and New Mexico.

[Quadrangle areas are shown on figure A5-1. Coal tonnages are rounded to two significant figures. Totals may not add due to independent rounding]

Quadrangle	Overburden (ft)					Grand total
	0-500	500-1000	1000-2000	2000-3000	>3000	
Colorado						
Abode Downs Ranch	0.91	0.0	0.93	0.0	0.0	1.8
Allison	0.0	0.0	0.0	1200	1600	2700
Baldy Mountain	180	140	180	150	15	670
Basin Mountain	550	240	600	1700	560	3700
Bayfield	0.0	0.0	280	2300	660	3300
Bondad Hill	0.0	0.0	0.0	1100	3200	4300
Carracas	0.0	0.0	240	1100	860	2200
Chimney Rock	220	280	500	75	0.0	1100
Durango East	120	84	380	260	0.0	840
Gem Village	0.0	0.0	0.0	3000	4.8	3000
Ignacio	0.0	0.0	0.0	770	2700	3400
Kline	86	60	100	43	0.0	290
La Plata	0.56	0.0	0.0	0.0	0.0	0.56
Loma Linda	40	43	140	4100	69	4300
Lonetree Canyon	53	19	1.3	0.0	0.0	73
Long Mountain	0.0	0.0	0.0	1400	3800	5200
Ludwig Mountain	150	140	860	370	5.5	1500
Pagosa Junction	250	200	320	220	0.0	980
Pargin Mountain	110	91	260	700	2000	3100
Pinkerton Mesa	390	240	700	1700	780	3800
Redmesa	3.9	0.0	0.0	0.0	0.0	3.9
Rules Hill	250	160	820	690	0.0	1900
Tiffany	0.0	0.0	0.0	1400	1800	3200
Trujillo	190	1.7	0.0	0.0	0.0	190
Colorado totals	2600	1700	5400	22000	18000	50000
New Mexico						
Abode Downs Ranch	12	39	300	1800	870	3000
Alamo Mesa East	350	1200	360	0.0	0.0	2000
Alamo Mesa West	900	1100	350	0.0	0.0	2300
Anastacio Spring	0.0	0.0	0.0	67	3800	3900
Archuleta	0.0	0.0	0.0	2500	1300	3800
Arroyo Chijuillita	0.0	0.3	89	150	0.0	240
Aztec	0.0	0.0	27	2100	210	2400
Bancos Mesa	0.0	0.0	0.0	28	1700	1700
Bancos Mesa Nw	0.0	0.0	0.0	680	1600	2300
Billy Rice Canyon	0.0	0.0	0.0	520	1600	2100
Bisti Trading Post	530	880	0.59	0.0	0.0	1400
Bixler Ranch	0.0	0.0	0.0	0.0	1000	1000
Blanco	0.0	0.0	1000	2600	49	3600

Table A6-1. Estimated Fruitland Formation coal resources (in millions of short tons) in five overburden categories by 7.5' quadrangle and State in beds 1.2 ft thick or greater, San Juan Basin, Colorado and New Mexico—*Continued*.

Quadrangle	Overburden (ft)					Grand total
	0-500	500-1000	1000-2000	2000-3000	>3000	
New Mexico—Continued						
Blanco Trading Post	0.0	0.0	1500	0.0	0.0	1500
Bloomfield	0.0	0.0	1600	410	0.0	2000
Burnham Trading Post	970	40	0.0	0.0	0.0	1000
Burnt Mesa	0.0	0.0	0.0	160	2800	3000
Canada Ojitos	0.0	0.0	0.0	0.79	240	240
Carracas Canyon	0.0	1.9	52	190	750	990
Carson Trading Post	0.0	0.0	1700	0.0	0.0	1700
Cedar Canyon	6	7.5	25	69	200	310
Cedar Hill	0.0	0.0	0.0	1900	1300	3100
Cement Lake	0.0	0.0	0.0	0.0	2000	2000
Cordova Canyon	87	51	100	61	28	330
Counselor	0.0	0.0	370	240	0.0	610
Crow Mesa East	0.0	0.0	52	940	0.0	990
Crow Mesa West	0.0	0.0	610	360	0.0	970
Cuba	0.0	0.0	27	1	0.0	28
Cutter Canyon	0.0	0.0	2.7	2300	840	3100
Deer Mesa	0.0	26	370	0.13	0.0	400
Delgadito Mesa	0.0	0.0	0.0	550	3800	4300
Dulce	9.2	6.6	2.5	0.0	0.0	18
East Fork Kutz Canyon	0.0	0.0	1700	530	0.0	2300
Espinosa Ranch	0.0	0.0	0.0	0.0	2100	2100
Farmington North	0.0	5.4	1800	530	0.0	2300
Farmington South	0.0	51	1500	0.0	0.0	1600
Fire Rock Well	910	840	0.0	0.0	0.0	1800
Five Lakes Canyon NE	0.0	0.0	0.0	580	500	1100
Five Lakes Canyon NW	0.0	0.0	5.3	470	290	760
Flora Vista	0.0	0.0	1000	1200	0.0	2200
Fourmile Canyon	0.0	0.0	0.0	0.0	3000	3000
Fresno Canyon	0.0	0.0	320	2400	89	2900
Fruitland	1100	86	0.0	0.0	0.0	1100
Gallegos Trading Post	0.0	0.0	1900	0.0	0.0	1900
Gobernador	0.0	0.0	0.0	0.0	2700	2700
Gomez Ranch	0.0	0.0	0.0	270	3100	3300
Gonzales Mesa	0.0	0.0	0.0	1800	480	2300
Gould Pass	0.0	0.0	0.0	1600	1300	2900
Horn Canyon	0.0	0.0	1600	3.9	0.0	1600
Huerfanito Peak	0.0	0.0	230	2500	0.0	2700
Huerfano Trading Post	0.0	0.0	630	970	0.0	1600
Huerfano Trading Post NW	0.0	0.0	1400	180	0.0	1600
Huerfano Trading Post SW	0.0	760	1300	0.0	0.0	2100
Hugh Lake	0.0	0.0	1500	0.0	0.0	1500
John Mills Lake	0.0	0.0	2.6	57	600	660
Johnson Trading Post	95	96	51	0.0	0.0	240
Kimbeto	260	1500	230	0.0	0.0	2000
Kirtland	130	690	240	0.0	0.0	1100
Kirtland SE	0.0	270	1300	0.0	0.0	1600
Kirtland SW	1000	870	0.94	0.0	0.0	1900
La Plata	190	190	550	1700	0.0	2700
Laguna Gurule	0.0	0.06	0.73	35	950	990
Lapis Point	0.0	0.0	0.0	550	2300	2800

Table A6-1. Estimated Fruitland Formation coal resources (in millions of short tons) in five overburden categories by 7.5' quadrangle and State in beds 1.2 ft thick or greater, San Juan Basin, Colorado and New Mexico—*Continued*.

Quadrangle	Overburden (ft)					Grand total
	0-500	500-1000	1000-2000	2000-3000	>3000	
New Mexico—Continued						
Leandro Canyon	0.0	0.0	0.0	0.0	1900	1900
Leavry Canyon	0.0	0.0	0.0	0.0	810	810
Lindrith	0.0	0.0	0.0	180	2000	2200
Los Indios Canyon	0.0	0.0	0.0	0.0	1.8	1.8
Lybrook	0.0	2.6	480	180	0.0	660
Lybrook NW	0.0	470	680	2.1	0.0	1100
Lybrook SE	140	950	100	0.0	0.0	1200
Mesa Portales	65	25	14	0.0	0.0	100
Moncisco Wash	0.0	0.65	2900	0.0	0.0	2900
Mule Dam	0.0	290	340	0.0	0.0	630
Navajo Dam	0.0	0.0	0.0	710	3600	4300
Newcomb NE	620	0.0	0.0	0.0	0.0	620
Newcomb SE	190	0.0	0.0	0.0	0.0	190
Ojito	0.0	0.0	0.0	0.0	2100	2100
Ojo Encino Mesa	350	64	4.1	0.0	0.0	420
Otero Store	0.0	0.0	0.0	1400	200	1600
Pine Lake	0.0	0.0	0.0	0.0	2800	2800
Pretty Rock	1400	7.4	0.0	0.0	0.0	1400
Pueblo Alto Trading Post	570	13	0.0	0.0	0.0	580
Pueblo Bonito	130	0.0	0.0	0.0	0.0	130
Pueblo Bonito NW	1500	1000	0.82	0.0	0.0	2500
Pueblo Pintado	61	0.0	0.0	0.0	0.0	61
Purgatory Canyon	25	3.3	0.0	0.0	0.0	29
Regina	0.0	0.12	15	73	110	190
Rincon Marquez	1.2	0.0	0.0	0.0	0.0	1.2
Santos Peak	0.0	0.0	0.0	250	3900	4100
Sargent Ranch	440	63	0.0	0.0	0.0	500
Schmitz Ranch	0.0	0.0	0.0	0.0	2900	2900
Smouse Mesa	0.0	0.0	0.0	2300	0.0	2300
Star Lake	760	250	0.0	0.0	0.0	1000
Tafoya Canyon	0.0	0.0	9.6	1000	0.0	1000
Tancosa Windmill	0.0	0.0	460	630	0.0	1100
Tank Mountain	0.0	0.0	0.0	400	3000	3400
Tanner Lake	580	0.0	0.0	0.0	0.0	580
Taylor Ranch	0.0	0.0	100	180	0.0	280
The Hogack North	0.36	0.0	0.0	0.0	0.0	0.36
The Hogback South	640	0.0	0.0	0.0	0.0	640
The Pillar	0.0	690	1800	0.0	0.0	2500
The Pillar 3 NE	60	0.0	0.0	0.0	0.0	60
The Pillar NW	1000	820	50	0.0	0.0	1900
Thompson Mesa	0.0	0.0	550	1600	0.0	2200
Tinian	47	0.0	0.0	0.0	0.0	47
Turley	0.0	0.0	0.0	2000	1400	3400
Vigas Canyon	0.0	0.0	0.0	0.0	3700	3700
Waterflow	500	100	0.0	0.0	0.0	600
Wirt Canyon	35	17	20	14	42	130
Wolf Stand	62	0.0	0.0	0.0	0.0	62
Youngs Lake	200	680	1100	0.0	0.0	2000
New Mexico totals	16000	14000	34000	44000	70000	180000
Grand totals	19000	16000	40000	66000	88000	230000

Table A6-2. Estimated Fruitland Formation coal resources (in millions of short tons) in five overburden categories by township and State in beds 1.2 ft thick or greater, San Juan Basin, Colorado and New Mexico.

[Township boundaries are shown on most of the San Juan Basin maps in this report. Coal tonnages are rounded to two significant figures. Totals may not add due to independent rounding. Note: T34N R3W(s): (s) is south of Ute line (fig. 28)]

Township	Overburden (ft)					Grand total
	0-500	500-1000	1000-2000	2000-3000	>3000	
Colorado						
T32N 1W	0.01	0.0	0.0	0.0	0.0	0.01
T32N 1.5W	0.85	0.0	0.0	0.0	0.0	0.85
T32N 2W	110	0.0	0.0	0.0	0.0	110
T32N 3W	57	55	160	67	0.0	340
T32N 4W	0.0	0.0	1.1	570	180	750
T32N 5W	0.0	0.0	0.0	680	230	910
T32N 6W	0.0	0.0	0.0	740	260	1000
T32N 7W	0.0	0.0	0.0	4.8	1200	1200
T32N 8W	0.0	0.0	0.0	0.0	1600	1600
T32N 9W	0.0	0.0	0.0	240	1500	1800
T32N 10W	0.0	0.0	0.0	180	1700	1900
T32N 11W	6	51	330	1200	300	1900
T32N 12W	200	62	32	0.0	0.0	290
T33N 2W	53	0.0	0.0	0.0	0.0	53
T33N 3W	230	81	68	0.0	0.0	380
T33N 4W	22	120	470	410	170	1200
T33N 5W	0.0	0.0	76	480	1100	1600
T33N 6W	0.0	0.0	0.0	20	1900	1900
T33N 7W	0.0	0.0	0.0	1800	240	2100
T33N 8W	0.0	0.0	0.0	640	1100	1700
T33N 9W	0.0	0.0	0.0	1400	1200	2500
T33N 10W	0.0	0.0	0.0	1400	1900	3300
T33N 11W	200	150	390	700	990	2400
T33N 12W	12	0.0	0.0	0.0	0.0	12
T34N 3W(s)	6.4	0.0	0.0	0.0	0.0	6.4
T34N 4W(s)	130	110	38	0.0	0.0	280
T34N 5W ¹	210	230	500	540	520	2000
T34N 6W ¹	0.0	0.0	140	920	1600	2700
T34N 7W ¹	0.0	0.0	150	2200	3.3	2300
T34N 8W ¹	0.0	0.0	0.0	2700	0.0	2700
T34N 9W ¹	84	70	160	2600	68	3000
T34N 10W(s)	400	150	490	1200	320	2600
T34N 11W(s)	150	80	120	99	1.9	440
T34.5N 9W	16	13	25	69	0.0	120
T35N 5W	120	75	52	17	0.0	260
T35N 6W	170	150	520	490	19	1300
T35N 7W	130	130	840	390	0.0	1500
T35N 8W	220	120	700	390	0.0	1400
T35N 9W	57	46	93	110	0.0	310
Colorado totals	2600	1700	5400	22000	18000	50000
New Mexico						
T19N R2W	17	0.0	0.0	0.0	0.0	17
T19N R3W	57	0.0	0.0	0.0	0.0	57
T19N R4W	180	0.0	0.0	0.0	0.0	180
T19N R5W	340	0.0	0.0	0.0	0.0	340
T19N R6W	190	0.0	0.0	0.0	0.0	190

Table A6-2. Estimated Fruitland Formation coal resources (in millions of short tons) in five overburden categories by township and State in beds 1.2 ft thick or greater, San Juan Basin, Colorado and New Mexico—*Continued*.

Township	Overburden (ft)					Grand total
	0-500	500-1000	1000-2000	2000-3000	>3000	
New Mexico—Continued						
T20N R2W	26	12	4.6	0.0	0.0	43
T20N R3W	33	77	43	0.0	0.0	150
T20N R4W	41	57	16	0.0	0.0	110
T20N R5W	180	88	0.0	0.0	0.0	270
T20N R6W	440	210	0.0	0.0	0.0	650
T20N R7W	450	1.9	0.0	0.0	0.0	450
T20N R8W	60	0.0	0.0	0.0	0.0	60
T21N R1W	0.0	0.0	2.5	0.0	0.0	2.5
T21N R2W	0.0	0.42	68	35	0.0	100
T21N R3W	0.0	0.0	68	63	0.0	130
T21N R4W	0.0	4.4	120	11	0.0	140
T21N R5W	0.0	38	210	0.0	0.0	250
T21N R6W	0.0	410	110	0.0	0.0	510
T21N R7W	140	710	12	0.0	0.0	860
T21N R8W	810	320	0.0	0.0	0.0	1100
T21N R9W	220	0.0	0.0	0.0	0.0	220
T21N R10W	8.5	0.0	0.0	0.0	0.0	8.5
T22N R1W	0.0	0.0	29	27	0.0	56
T22N R2W	0.0	0.0	11	250	1.8	260
T22N R3W	0.0	0.0	0.0	270	0.0	270
T22N R4W	0.0	0.0	160	66	0.0	230
T22N R5W	0.0	0.0	510	0.0	0.0	510
T22N R6W	0.0	0.0	290	6.4	0.0	300
T22N R7W	0.0	110	250	0.0	0.0	360
T22N R8W	6	790	150	0.0	0.0	940
T22N R9W	250	620	0.0	0.0	0.0	870
T22N R10W	1000	57	0.0	0.0	0.0	1100
T22N R11W	510	0.0	0.0	0.0	0.0	510
T22N R12W	72	0.0	0.0	0.0	0.0	72
T22N R13W	6.8	0.0	0.0	0.0	0.0	6.8
T23N R1W	0.0	0.18	1.8	20	100	120
T23N R2W	0.0	0.0	0.0	420	550	980
T23N R3W	0.0	0.0	0.0	170	420	590
T23N R4W	0.0	0.0	7.3	630	94	730
T23N R5W	0.0	0.0	180	330	0.0	510
T23N R6W	0.0	0.0	100	280	0.0	380
T23N R7W	0.0	0.0	250	180	0.0	430
T23N R8W	0.0	33	550	2.4	0.0	590
T23N R9W	0.0	680	360	0.0	0.0	1000
T23N R10W	100	1200	120	0.0	0.0	1500
T23N R11W	1200	450	0.0	0.0	0.0	1700
T23N R12W	1000	0.0	0.0	0.0	0.0	1000
T23N R13W	370	0.0	0.0	0.0	0.0	370
T24N R1W	0.0	0.0	0.09	27	570	600
T24N R2W	0.0	0.0	0.0	140	1100	1200
T24N R3W	0.0	0.0	0.0	180	1100	1300
T24N R4W	0.0	0.0	0.0	880	230	1100
T24N R5W	0.0	0.0	0.0	760	0.0	760
T24N R6W	0.0	0.0	11	490	0.0	500
T24N R7W	0.0	0.0	27	500	0.0	530

Table A6-2. Estimated Fruitland Formation coal resources (in millions of short tons) in five overburden categories by township and State in beds 1.2 ft thick or greater, San Juan Basin, Colorado and New Mexico—*Continued*.

Township	Overburden (ft)					Grand total
	0-500	500-1000	1000-2000	2000-3000	>3000	
New Mexico—Continued						
T24N R8W	0.0	0.0	320	190	0.0	510
T24N R9W	0.0	0.0	770	0.0	0.0	770
T24N R10W	0.0	96	890	0.0	0.0	990
T24N R11W	5.7	920	330	0.0	0.0	1300
T24N R12W	440	960	1.4	0.0	0.0	1400
T24N R13W	480	660	0.0	0.0	0.0	1100
T25N R1W	0.0	0.0	0.0	6.8	380	390
T25N R2W	0.0	0.0	0.0	0.0	1400	1400
T25N R3W	0.0	0.0	0.0	0.0	1500	1500
T25N R4W	0.0	0.0	0.0	54	1300	1400
T25N R5W	0.0	0.0	0.0	1000	360	1400
T25N R6W	0.0	0.0	0.0	870	0.0	870
T25N R7W	0.0	0.0	0.0	1000	0.0	1000
T25N R8W	0.0	0.0	240	800	0.0	1000
T25N R9W	0.0	0.0	730	130	0.0	860
T25N R10W	0.0	0.0	1100	93	0.0	1200
T25N R11W	0.0	0.47	840	0.0	0.0	840
T25N R12W	0.0	87	1200	0.0	0.0	1200
T25N R13W	0.0	270	1600	0.0	0.0	1900
T25N R14W	4.8	950	410	0.0	0.0	1400
T26N R1W	0.0	0.0	0.0	0.0	7.5	7.5
T26N R2W	0.0	0.0	0.0	0.0	350	350
T26N R3W	0.0	0.0	0.0	0.0	1800	1800
T26N R4W	0.0	0.0	0.0	0.0	2100	2100
T26N R5W	0.0	0.0	0.0	500	1700	2200
T26N R6W	0.0	0.0	0.0	1100	520	1600
T26N R7W	0.0	0.0	0.0	1700	0.0	1700
T26N R8W	0.0	0.0	180	1300	0.0	1500
T26N R9W	0.0	0.0	410	850	0.0	1300
T26N R10W	0.0	0.0	240	660	0.0	890
T26N R11W	0.0	0.0	1200	3.7	0.0	1200
T26N R12W	0.0	0.0	1300	0.0	0.0	1300
T26N R13W	0.0	0.0	1600	0.0	0.0	1600
T26N R14W	0.0	100	670	0.0	0.0	770
T27N R2W	0.0	0.0	0.0	0.0	62	62
T27N R3W	0.0	0.0	0.0	0.0	1100	1100
T27N R4W	0.0	0.0	0.0	0.0	1800	1800
T27N R5W	0.0	0.0	0.0	0.0	2300	2300
T27N R6W	0.0	0.0	0.0	170	2400	2600
T27N R7W	0.0	0.0	0.0	740	910	1700
T27N R8W	0.0	0.0	49	1700	69	1800
T27N R9W	0.0	0.0	130	1400	0.0	1600
T27N R10W	0.0	0.0	750	840	0.0	1600
T27N R11W	0.0	0.0	1400	66	0.0	1400
T27N R12W	0.0	0.0	910	0.0	0.0	910
T27N R13W	0.0	0.0	790	0.0	0.0	790
T27N R14W	0.0	18	900	0.0	0.0	920
T27N R15W	130	480	83	0.0	0.0	680
T27N R16W	320	0.0	0.0	0.0	0.0	320
T28N R1W	0.0	0.0	0.0	5.4	33	39

Table A6-2. Estimated Fruitland Formation coal resources (in millions of short tons) in five overburden categories by township and State in beds 1.2 ft thick or greater, San Juan Basin, Colorado and New Mexico—*Continued*.

Township	Overburden (ft)					Grand total
	0-500	500-1000	1000-2000	2000-3000	>3000	
New Mexico—Continued						
T28N R2W	0.0	0.0	0.0	0.0	810	810
T28N R3W	0.0	0.0	0.0	0.0	1600	1600
T28N R4W	0.0	0.0	0.0	0.0	1100	1100
T28N R5W	0.0	0.0	0.0	0.0	1900	1900
T28N R6W	0.0	0.0	0.0	16	1400	1500
T28N R7W	0.0	0.0	0.0	730	1000	1800
T28N R8W	0.0	0.0	0.0	1200	44	1200
T28N R9W	0.0	0.0	43	1400	49	1500
T28N R10W	0.0	0.0	920	440	0.0	1400
T28N R11W	0.0	0.0	800	0.0	0.0	800
T28N R12W	0.0	0.0	490	0.0	0.0	490
T28N R13W	0.0	0.0	450	0.0	0.0	450
T28N R14W	0.0	240	200	0.0	0.0	430
T28N R15W	680	320	0.0	0.0	0.0	1000
T28N R16W	240	0.0	0.0	0.0	0.0	240
T29N R1W	7.1	13	32	73	59	180
T29N R2W	0.0	0.0	0.0	0.0	820	820
T29N R3W	0.0	0.0	0.0	0.0	910	910
T29N R4W	0.0	0.0	0.0	0.0	1000	1000
T29N R5W	0.0	0.0	0.0	0.0	1300	1300
T29N R6W	0.0	0.0	0.0	0.0	2000	2000
T29N R7W	0.0	0.0	0.0	13	2600	2600
T29N R8W	0.0	0.0	0.0	980	960	1900
T29N R9W	0.0	0.0	150	1800	38	2000
T29N R10W	0.0	0.0	1100	630	0.0	1700
T29N R11W	0.0	0.0	610	96	0.0	700
T29N R12W	0.0	0.0	1300	0.0	0.0	1300
T29N R13W	0.0	54	990	0.0	0.0	1000
T29N R14W	63	550	180	0.0	0.0	800
T29N R15W	690	75	0.0	0.0	0.0	770
T29N R16W	0.24	0.0	0.0	0.0	0.0	0.24
T30N R1W	72	31	55	22	1.1	180
T30N R2W	0.0	0.0	19	68	420	510
T30N R3W	0.0	0.0	0.0	0.0	280	280
T30N R4W	0.0	0.0	0.0	0.0	1100	1100
T30N R5W	0.0	0.0	0.0	43	1300	1300
T30N R6W	0.0	0.0	0.0	240	2200	2400
T30N R7W	0.0	0.0	0.0	420	2200	2600
T30N R8W	0.0	0.0	0.0	1500	630	2100
T30N R9W	0.0	0.0	0.0	1600	180	1800
T30N R10W	0.0	0.0	0.0	950	750	1700
T30N R11W	0.0	0.0	170	1500	0.0	1600
T30N R12W	0.0	0.0	810	440	0.0	1200
T30N R13W	0.0	0.0	1200	130	0.0	1300
T30N R14W	11	310	1000	0.0	0.0	1300
T30N R15W	390	260	0.18	0.0	0.0	650
T31N R1W	18	15	2.1	0.0	0.0	35
T31N R2W	15	10	32	31	110	200
T31N R3W	0.0	0.0	0.0	0.0	110	110
T31N R4W	0.0	0.0	0.0	0.0	950	950

Table A6-2. Estimated Fruitland Formation coal resources (in millions of short tons) in five overburden categories by township and State in beds 1.2 ft thick or greater, San Juan Basin, Colorado and New Mexico—*Continued*.

Township	Overburden (ft)					Grand total
	0-500	500-1000	1000-2000	2000-3000	>3000	
New Mexico—Continued						
T31N R5W	0.0	0.0	0.0	25	1000	1100
T31N R6W	0.0	0.0	0.0	140	950	1100
T31N R7W	0.0	0.0	0.0	310	1500	1800
T31N R8W	0.0	0.0	0.0	140	2500	2700
T31N R9W	0.0	0.0	0.0	360	2000	2300
T31N R10W	0.0	0.0	0.0	1000	750	1800
T31N R11W	0.0	0.0	0.0	1200	88	1300
T31N R12W	0.0	0.0	0.0	1300	14	1400
T31N R13W	37	62	470	1000	0.0	1600
T32N R2W	11	1	0.0	0.0	0.0	12
T32N R3W	15	14	61	110	57	250
T32N R4W	0.0	0.0	0.0	98	620	720
T32N R5W	0.0	0.0	0.0	5	940	940
T32N R6W	0.0	0.0	0.0	550	700	1200
T32N R7W	0.0	0.0	0.0	41	1400	1500
T32N R8W	0.0	0.0	0.0	0.0	1500	1500
T32N R9W	0.0	0.0	0.0	0.0	1200	1200
T32N R10W	0.0	0.0	0.0	770	990	1800
T32N R11W	0.0	0.0	0.0	250	1500	1700
T32N R12W	55	79	420	870	210	1600
T32N R13W	110	93	190	540	0.0	940
Unsurveyed ²	4400	1600	400	0.0	0.0	6400
N. Mex. totals	16000	14000	34000	44000	70000	180000
Grand totals	19000	16000	40000	66000	88000	230000

¹ T34N is present as two tiers of townships; one north and one south of the Ute line (fig. 28). Coal tonnages shown for each of these five townships are totals for the two townships.

² Unsurveyed areas are not bounded by official township boundaries and are all Tribal lands.

Table A6-3. Estimated Fruitland Formation coal resources (in millions of short tons) in five overburden categories by surface ownership and by State in beds 1.2 ft thick or greater, San Juan Basin, Colorado and New Mexico.

[Surface ownership is shown on figure A5-2. Non-Federal surface includes State, private, and Tribal land. Coal tonnages are rounded to two significant figures. Totals may not add due to independent rounding]

State	Surface owner	Overburden (ft)					Grand totals
		0-500	500-1000	1000-2000	2000-3000	>3000	
Colorado	Federal	520	360	700	1800	2200	5500
	Non-Federal	2100	1300	4700	21000	16000	44000
Colorado totals		2600	1700	5400	22000	18000	50000
New Mexico	Federal	4600	6000	12000	28000	39000	89000
	Non-Federal	11000	8200	23000	16000	31000	89000
New Mexico totals		16000	14000	34000	44000	70000	180000
Grand Total		19000	16000	40000	66000	88000	230000

Table A6-4. Estimated Fruitland Formation coal resources (in millions of short tons) in five overburden categories by coal ownership and State in beds 1.2 ft thick or greater, San Juan Basin, Colorado and New Mexico.

[Coal ownership is shown on figure A5-3. Non-Federal surface includes State, private, and Tribal land. Coal tonnages rounded to two significant figures. Totals may not add due to independent rounding]

State	Coal Ownership	Overburden (ft)					Grand totals
		0-500	500-1000	1000-2000	2000-3000	>3000	
Colorado	Federal	1100	680	1800	11000	6200	21000
	Non-Federal	1500	1000	3500	12000	12000	29000
Colorado totals		2600	1700	5400	22000	18000	50000
New Mexico	Federal	6400	7700	18000	31000	48000	110000
	Non-Federal	9500	6400	16000	14000	21000	67000
New Mexico totals		16000	14000	34000	44000	70000	180000
Grand Total		19000	16000	40000	66000	88000	230000

Table A6-5. Estimated Fruitland Formation coal resources (in millions of short tons) in beds 1.2 ft thick or greater, San Juan Basin, Colorado and New Mexico.

[Resources are given in five overburden categories; five thickness categories; and by county, State, and reliability category. Distribution of coal resources by net-thickness categories is shown on figure A5-4. Coal tonnages rounded to two significant figures. Totals may not add due to independent rounding]

County	Reliability	0-500 ft overburden					0-500 total	500-1000 ft overburden					500-1000 total	1000-2000 ft overburden					1000-2000 total
		Net-coal thickness category						Net-coal thickness category						Net-coal thickness category					
		1.2-2.3	2.3-3.5	3.5-7.0	7.0-14.0	>14.0		1.2-2.3	2.3-3.5	3.5-7.0	7.0-14.0	>14.0		1.2-2.3	2.3-3.5	3.5-7.0	7.0-14.0	>14.0	
Colorado																			
Archuleta	Identified	0	0	5.8	100	250	360	0	0	0	98	300	400	0	0	0	100	930	1000
	Hypothetical	7.5	11	88	130	380	610	0	0	0	1.2	290	290	0	0	0	0	390	390
	Archuleta total	7.5	11	93	230	630	970	0	0	0	99	590	690	0	0	0	100	1300	1400
La Plata	Identified	0	0	0	0	1600	1600	0	0	0	0	1000	1000	0	0	0	0	3900	3900
	Hypothetical	0	0	0	0	16	16	0	0	0	0	1.3	1.3	0	0	0	0	0.0	0.0
	La Plata total	0	0	0	0	1600	1600	0	0	0	0	1000	1000	0	0	0	0	3900	3900
	Colorado total	7.5	11	93	230	2200	2600	0	0	0	99	1600	1700	0	0	0	100	5300	5400
New Mexico																			
McKinley	Identified	1.3	8	33	440	1200	1700	16	25	23	69	170	300	0	0	0	0	0	0
	Hypothetical	0	0	0	0.21	5	5.2	0	0	0	0	0	0	0	0	0	0	0	0
	McKinley total	1.3	8	33	440	1200	1700	16	25	23	69	170	300	0	0	0	0	0	0
Rio Arriba	Identified	1.7	3.9	17	18	0	41	1	0.7	4.9	21	0.0	28	3.6	4.2	28	210	18	260
	Hypothetical	2.5	4.2	35	54	0	96	1.2	1.7	13	42	0.0	57	0.59	1.2	20	96	0	120
	Rio Arriba total	4.3	8.1	52	72	0	140	2.2	2.4	18	63	0.0	85	4.2	5.4	48	300	18	380
San Juan	Identified	0	0	12	530	7800	8400	0	0	0	320	9000	9300	0	0	35	1900	29000	31000
	Hypothetical	0	0	33	610	4600	5300	0	0	0	17	3000	3100	0	0	0.49	48	740	790
	San Juan total	0	0	44	1100	12000	14000	0	0	0	340	12000	12000	0	0	35	1900	30000	32000
Sandoval	Identified	65	52	92	48	140	400	33	64	100	350	870	1400	48	160	680	1000	330	2200
	Hypothetical	2.9	6.3	0	83	0	93	0	0	0	0.04	0	0.04	12	34	17	2.5	0	66
	Sandoval total	68	58	92	130	140	490	33	64	100	350	870	1400	60	190	700	1000	330	2300
	New Mexico total	74	74	220	1800	14000	16000	51	91	140	820	13000	14000	64	200	780	3200	30000	34000
	Grand total	81	85	310	2000	16000	19000	51	91	140	920	15000	16000	64	200	780	3300	35000	40000

Table A6-5. Estimated Fruitland Formation coal resources (in millions of short tons) in beds 1.2 ft thick or greater, San Juan Basin, Colorado and New Mexico—*Continued.*

County	Reliability	2000-3000 ft overburden Net-coal thickness category					2000-3000 total	>3000 ft overburden Net-coal thickness category					>3000 total	Grand total
		1.2-2.3	2.3-3.5	3.5-7.0	7.0-14.0	>14.0		1.2-2.3	2.3-3.5	3.5-7.0	7.0-14.0	>14.0		
Colorado														
Archuleta	Identified	0	0	0	0	2500	2500	0	0	0	0	2500	2500	6800
	Hypothetical	0	0	0	0	660	660	0	0	0	0	1100	1100	3000
Archuleta total		0	0	0	0	3100	3100	0	0	0	0	3600	3600	9800
La Plata	Identified	0	0	0	0	19000	19000	0	0	0	0	14000	14000	40000
	Hypothetical	0	0	0	0	0	0	0	0	0	0	0	0	18
La Plata total		0	0	0	0	19000	19000	0	0	0	0	14000	14000	40000
Colorado total		0	0	0	0	22000	22000	0	0	0	0	18000	18000	50000
New Mexico														
Mc Kinley	Identified	0	0	0	0	0	0	0	0	0	0	0	0	2000
	Hypothetical	0	0	0	0	0	0	0	0	0	0	0	0	5.2
Mc Kinley total		0	0	0	0	0	0	0	0	0	0	0	0	2000
Rio Arriba	Identified	7.7	13	140	1300	12000	13000	16	32	200	1400	50000	52000	65000
	Hypothetical	1.2	2.5	19	150	1.1	180	4.6	7.8	40	260	790	1100	1500
Rio Arriba total		9	15	160	1500	12000	13000	21	40	240	1700	51000	53000	66000
San Juan	Identified	0	0	0	340	29000	29000	0	0	0	8.1	17000	17000	95000
	Hypothetical	0	0	0	0	7.2	7.2	0	0	0	0	42	42	9200
San Juan total		0	0	0	340	29000	29000	0	0	0	8.1	17000	17000	100000
Sandoval	Identified	16	89	400	740	460	1700	0.23	0.75	6	67	170	250	6000
	Hypothetical	0	7.3	5.9	0	0	13	0	0	0	0	0	0	170
Sandoval total		16	96	400	740	460	1700	0.23	0.75	6	67	170	250	6200
New Mexico total		25	110	570	2600	41000	44000	21	40	250	1700	68000	70000	180000
Grand total		25	110	570	2600	63000	66000	21	40	250	1700	86000	88000	230000

Q128 Geologic Assessment of Coal in the Colorado Plateau: Arizona, Colorado, New Mexico, and Utah

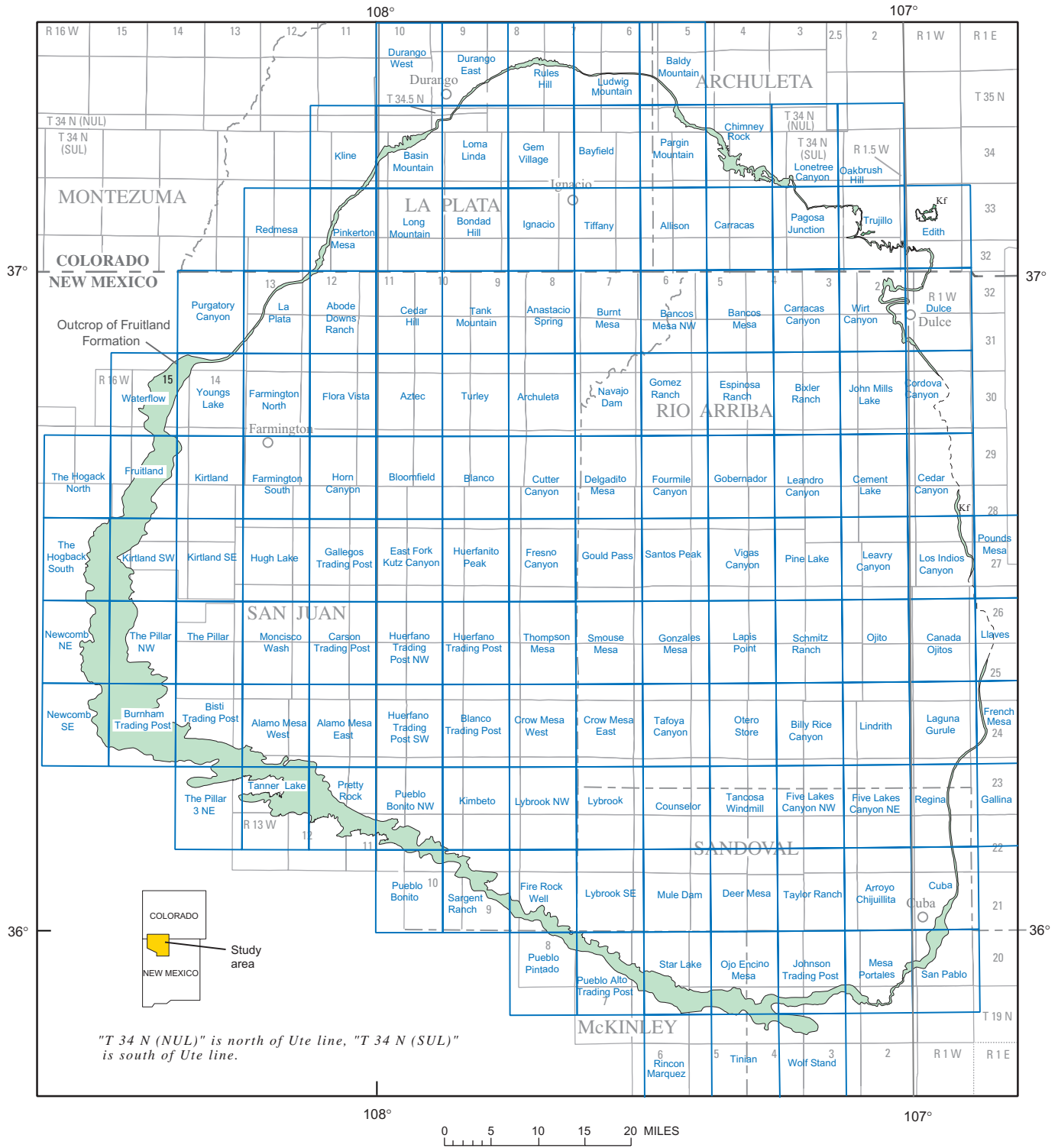


Figure A6-1. Map showing 7 1/2-minute topographic quadrangles in the San Juan Basin.

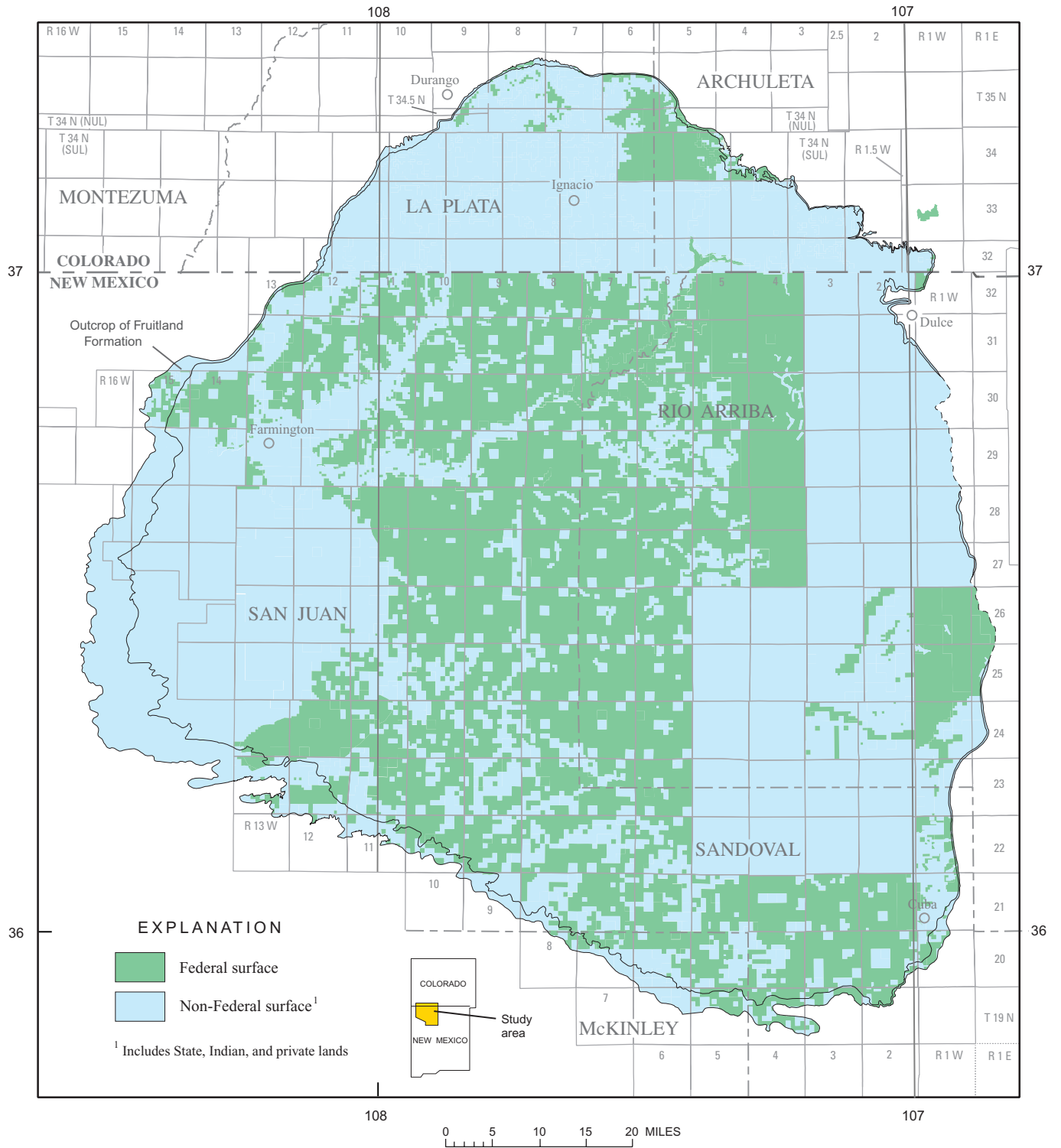


Figure A6-2. Map showing Federal and non-Federal surface ownership for the San Juan Basin.

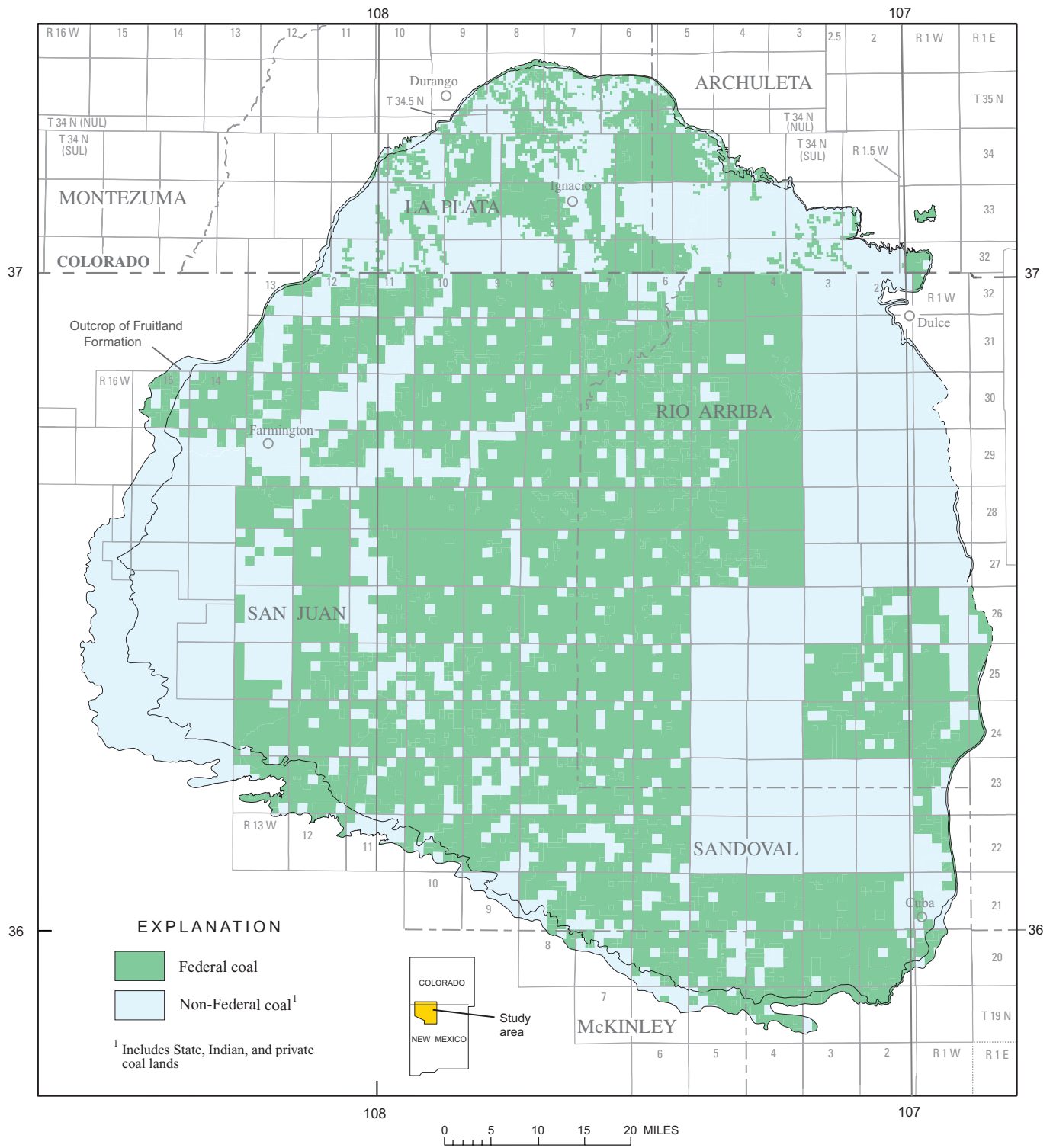


Figure A6-3. Map showing coal ownership in the San Juan Basin.

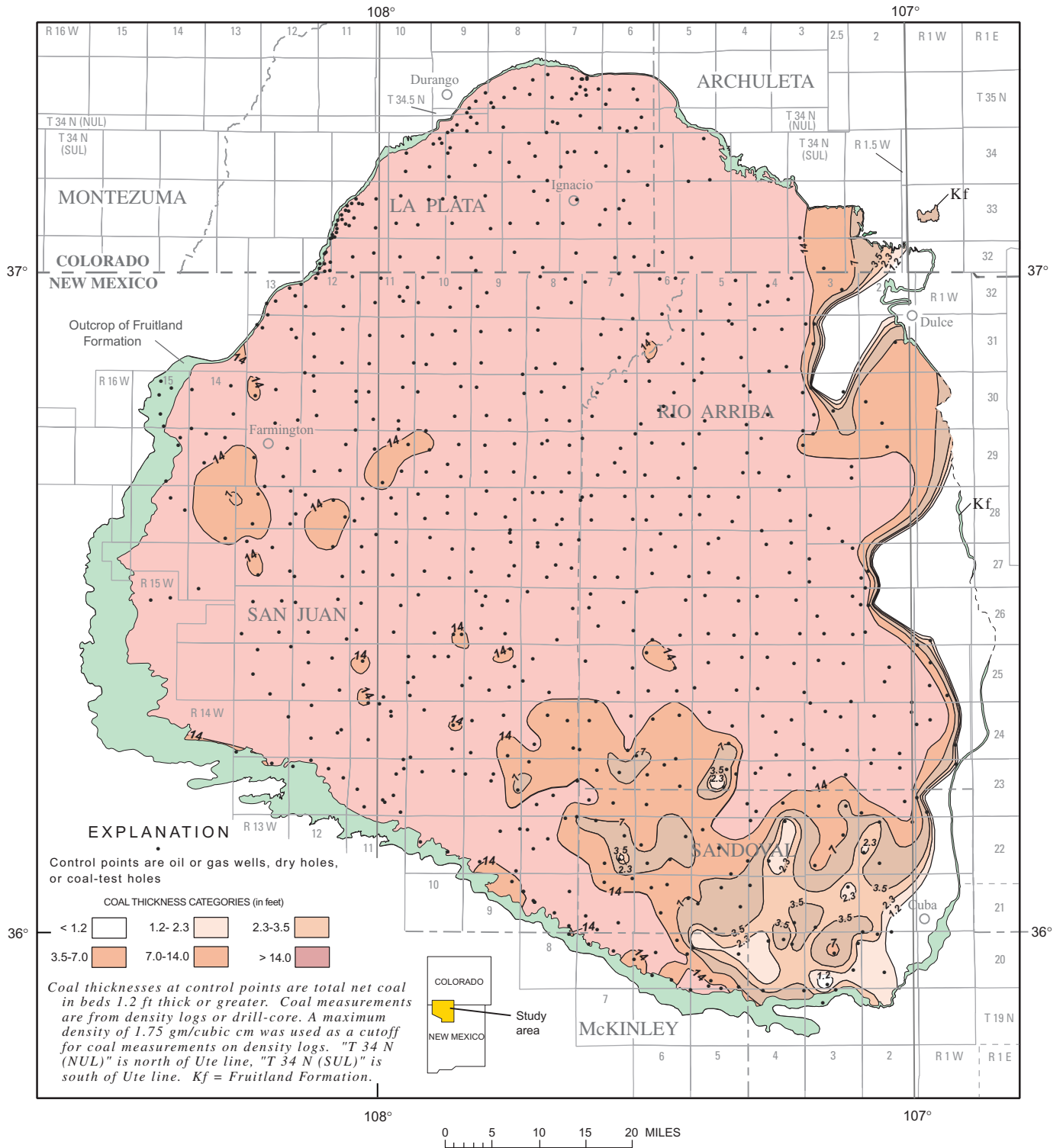


Figure A6-4. Map showing distribution of net Fruitland coal in standard USGS thicknesses categories in the San Juan Basin.

